John J. Hughes · Jan Válek
Caspar J. W. P. Groot *Editors*

Historic Mortars

Advances in Research and Practical Conservation

Springer

Historic Mortars

John J. Hughes · Jan Válek
Caspar J. W. P. Groot
Editors

Historic Mortars

Advances in Research and Practical Conservation

Springer

Editors
John J. Hughes
School of Engineering and Computing
University of the West of Scotland
Paisley
Scotland, UK

Jan Válek
The Czech Academy of Sciences
Institute of Theoretical and Applied Mechanics
Prague
Czech Republic

Caspar J. W. P. Groot
Technical University of Delft
Delft
The Netherlands

ISBN 978-3-319-91604-0 ISBN 978-3-319-91606-4 (eBook)
https://doi.org/10.1007/978-3-319-91606-4

Library of Congress Control Number: 2018941234

Printed on acid-free paper

This Springer imprint is published by the registered company Springer International Publishing AG part of Springer Nature
The registered company address is: Gewerbestrasse 11, 6330 Cham, Switzerland

Preface

The characterisation of mortars found in historic masonry structures, and the design of compatible repair and replacement materials, that maintain the authenticity and integrity of heritage assets, is a perennial topic in the conservation of the built cultural heritage. It is a recurring theme worthy of continued research, which the current series of Historic Mortars Conferences, begun in 2008 in Lisbon,[1] was established to address.

The papers contained herein were chosen from those first presented at the third Historic Mortars Conference in Glasgow in 2013. This book contains a state of the art in three thematic areas related to the place of mortar materials, in their diversity, in historic structures. This volume is a companion to the earlier "Historic Mortars: Characterisation, Assessment and Repair" (Válek et al. 2012), related to the second Historic Mortars Conference held in Prague in 2010.

The content covers aspects of mortar characterisation, the development of new materials, the historical contexts of mortar production and more theoretical and experimental materials developments. A developing focus in mortar studies is that on the occurrence, nature and conservation potential of historic hydraulic materials, such as Roman cements and early Portland cement. In part, this represents an expanding and more nuanced understanding of materials used in the past that challenges the assumptions of "best practice" of recent decades. Studies of processes for small-scale binder production sit alongside characterisation studies that bring forward increasing details of the compositions and performances of historic

[1] Perhaps, the earliest dedicated mortars conference was held in Rome in 1981. Then, there was Paisley in 1999 and Delft in 2005, and these latter two events related to the activities of the RILEM TCs on Historic Mortars (TC-COM and TC-RHM). More recently, there have been HMC 08 (Lisbon), 10 (Prague), 13 (Glasgow) and 16 (Santorini).

materials. This has relevance today, as we study materials with life cycles beyond the comprehension of most contemporary designers and builders. Hopefully, this research will shed light on the possibilities for improved sustainability derived from historically inspired materials use.

Paisley, Scotland, UK — John J. Hughes
Prague, Czech Republic — Jan Válek
Delft, The Netherlands — Caspar J. W. P. Groot
April 2018

Reference

Válek, J., Hughes, J. J & Groot, C. J. W. P. (Eds.). (2012). *Historic mortars: Characterisation, assessment and repair*, Springer. http://dx.doi.org/10.1007/978-94-007-4635-0, ISBN 978-94-007-4634-3

Contents

Part I
Characterisation of Historic Materials

How to Identify a Natural Cement: Case Study of the Vassy Church, France

M. Bouichou, E. Marie-Victoire, A. Texier and T. Blondiaux

Abstract Natural or Roman cements were the first modern cements to be industrially produced at the beginning of the 19th century in Europe. Used equally by engineers for their hydraulic properties, and by architects for their aesthetic qualities, they were massively employed for façade decoration or as cast-stone elements for masonries. This cultural heritage, even if it is abundant, is relatively unknown and needs now to be clearly identified and restored. Because of lack of knowledge and data on these cements, they are often identified as Portland cement or hydraulic lime, or hydraulic lime mixed with gypsum or Portland cement. Furthermore, heterogeneous calcination and varied quarried stone, which strongly modify their properties, make their characterizations more difficult. This paper presents a case study of the Vassy Church, with a focus on the binder identification of mortars. The Vassy church, built in 1859 by Gariel, a Vassy cement producer, is located in Burgundy, France. On the church, ochre-coloured mortars, were used either indoors, outdoors, as renders, as pointing mortars, as "run in situ" mortars, applied on stone or brick. Different types of mixes were employed, from rich to poor mortars. The testing protocol of those analysis firstly consisted of clinker grain analysis on polished sections (with and without Borax etching) by optical (OM) and scanning electron microscopy (SEM) observations, coupled with EDS analysis. Secondly, hydrated phases were characterised on mortar fractures, through SEM observations coupled with EDS analysis. Finally, crystallised phases were identified by XRD analysis of the binder in powder samples. Results of these analysis show

M. Bouichou (✉) · E. Marie-Victoire · A. Texier
Laboratoire de recherche des Monuments Historiques, Ministère de la Culture,
Sorbonne universités, CRC-LRMH, CNRS-USR 3224, Champs-sur-Marne, France
e-mail: myriam.bouichou@culture.gouv.fr

E. Marie-Victoire
e-mail: elisabeth.marie-victoire@culture.gouv.fr

A. Texier
e-mail: annick.texier@culture.gouv.fr

T. Blondiaux
Bureau d'étude Brizot-Masse, Paris, France
e-mail: t.blondiaux@brizot-masse.fr

J. J. Hughes et al. (eds.), *Historic Mortars*,
https://doi.org/10.1007/978-3-319-91606-4_1

several clinker morphologies and compositions, and different types of hydrates phases, according to the carbonation state. The presence of Gehlenite in very significative proportion, and C–A–S–H phases as a matrix in all of the samples, the absence of portlandite and the strong presence of ettringite in non-carbonated areas clearly indicate that the binder used to manufacture the cement mortars of the Vassy church was a natural cement, with a high sulfate and aluminate content. Furthermore, the coexistence of unburnt, burnt and over-burnt anhydrous grains reveal a production by a heterogeneous firing process. These results show important differences in terms of microstructure between natural cements and the other common hydraulic binders like Portland cement or lime.

Keywords Natural cements · Clinkers · Ettringite · Vaterite

1 Introduction

Natural cements were the earliest binders to be industrially produced. From the beginning of the 19th century, they were fabricated by extracting a single limestone, containing clay, and by burning it at a low temperature in vertical kilns. Starting in England, the production of these cements expanded throughout Europe: to France, Austria, Poland and Russia (Hughes et al. 2007a; Weber et al. 2007a). Because of the diversity of limestones used and the manufacturing processes, natural cements present different chemical compositions and properties (Gosselin et al. 2009; Weber et al. 2007b).

In architecture, natural cements were used for façade decoration, for mouldings cast or run in situ in the mortar (Hughes et al. 2007b; Weber et al. 2007b), and rendering, but also as cast-stone elements for masonries (Cailleux et al. 2005, 2006). They were also used, thanks to their hydraulic properties, by engineers for maritime works, railways, and water and gas networks.

The identification of these materials and their characterisation is an essential preliminary step toward their restoration. Relatively unknown, these binders are often confused with Portland cement or hydraulic lime. In France, natural cement mortars were also identified as gypsum-lime mortar, as French natural cements containing sulfates. This paper presents a case study of the Vassy Church, in the town of Etaules located in Burgundy, where Vassy cement was produced. Vassy cement is known for its use as a restoration material in several cathedrals during the 19th century (Gosselin et al. 2009). This study aimed to characterise and identify the binder in mortars used in the construction of the Vassy Church, in order to be able to advise on compatible restoration mortars.

2 Visual Assesment and Sampling

The Vassy-lès-Avallon church was built between 1859 and 1862 by the architect Tircuit, at the initiative of the Gariel family, producers of the Vassy cement. Indoors, the walls are covered with an ochre mortar, with a white paint finish (Fig. 1). The arches and the foundations which are made of stone, are coated with an ochre mortar up to the intersecting ribs. Some elements, such as the columns, are also covered with an ochre mortar that can be made out under the white paint. There is no evidence of the implement technology used such as with run-in situ mortar making, or molding marks.

This fourteenth century Gothic style church (Fig. 2) is 45 m long and has three naves and five spans. Its bell tower is completed by a spire. The structure and the tower were primarily constructed from brick masonry, covered with a render. The bricks are joined with an ochre mortar. Some elements, like the bell tower, the door and the pinnacles are made of stone. The columns which decorate the tower are also

Fig. 1 Vassy church, indoors

made of stone, but covered with a run-in situ ochre mortar (Fig. 3). Under the balustrade at the base of the spire, a slab made of pieces of stone coated with an ochre mortar surmounts a run-in situ mortar cornice (Fig. 4). The pointing mortars of both the cut stone masonry and the stone hook of the spire, are made of an ochre mortar, with a high binder content. The bell tower is decorated with a clock, with roman numerals and decorations made of mosaics, with ochre mortar between the pieces of mosaics.

The worst deterioration was observed on the façades that are the most exposed to wind and rain, that is to say, the northern and the western façades. These degradations essentially consisted of an erosion of the mortar skin, and in cracking and pattern-cracking of the rendering mortars, specially noticeable in the areas of the most exposed to the wind and rain. Underneath the balustrade at the base of the spire, an abundant spalling of the cement slab was also visible, probably linked to a waterproofing problem of the lead sheet protection.

Three ocher-couloured mortars sampled from the bell tower were analyzed:

– M1: a low-binder-content render mortar covering the brick walls;

Fig. 2 Vassy church façade (photo Thierry Leynet)

Fig. 3 Stone columns covered with an ochre run-in situ mortar

Fig. 4 Stone hook and cornice made of an ochre run-in situ mortar

- M2: a rich-binder-content render mortar called, which was used to set the stone hooks in the spire. It should be noted that no metallic reinforcement was observed;
- M3: and a mortar from a run-in situ element, named M3.

3 Mortars Analysis

3.1 Analysis Protocol

Several methods of analysis were applied to the sampled specimens in order to characterise the different types of mortars present in the building, focusing on the identification of the binders that were used.

Phenolphthalein tests were undertaken to assess the carbonation depth of the mortars, bearing in mind that only the presence of non carbonated areas in hydraulic mortars allows the recognition of the original hydrated phases in hydraulic binders.

Crystalline phases of the sampled mortars were identified using X-ray diffraction The residual anhydrous binder grains were identified using polished sections using optical microscopy (OM), before and after borax attack to reveal the chemical compositions of clinker phases (Campbell 1999) and using scanning electron microscopy (SEM) coupled to elemental analysis (EDS). Finally, the hydrated phases of the mortars, were observed by SEM + EDS on freshly broken samples.

3.2 Macroscopic Observations and Phenolphthalein Tests

The three samples were light-ochre coloured. The M1 render mortar had a high aggregate-content, when the rich-binder-content M2 mortar was very compact and only contained a few aggregates. The M3 run-in situ mortar very much looked like the the render mortar M1, but was exhibiting a white crust on its outer surface (Fig. 5).

Concerning the measured depths of carbonation, only a few areas were not carbonated in mortars M1 and M2, from a depth of 3 cm to the surface. However, carbonation fronts were completely discontinuous. Finally, white fine crystallizations were noticed in pores, in non-carbonated areas (Fig. 6).

3.3 The Crystallised Phases: X-Ray Diffraction (XRD)

The X-ray diffraction analysis (Table 1) lead to the determination of the nature of the binder used in the different mortars. The presence of gehlenite and wollastonite (anhydrous phases typical of a moderate firing of natural cements), the absence of

Fig. 5 M3 mortar with white crust on its outer surface

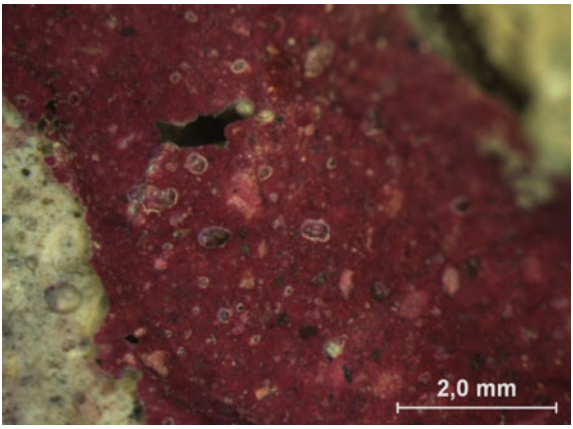

Fig. 6 M2 mortar, pink surface after phenolptaleine tests, white crystallisations in pores

Table 1 Synthesis of the XRD diffractograms obtained on the different samples

	Mortar M1		Binder-Rich mortar M2		Molding mortar M3	Mortar M3 crust
Carbonation	Yes	No	Yes	No	Yes	
Calcite	+++ +	+++	+++	+++	++++	+
Vaterite	+	++	+++ +	+	+	Ø
Ettringite	Ø	+++	++	+++ +	Ø	Ø
Gypsum	Ø	+++	++	+	+++	++++
Monocarboaluminate	Ø	Ø	++	+++	Ø	Ø
Hydrocalumite	Ø	Ø	+	++	Ø	Ø
Quartz	+++ +	+++ +	+++	+++	++++	++
Feldspar	+++	+++	Ø	Ø	+++	Ø
Gehlenite	++	++	+++	+++	++	Ø
Wollastonite	Ø	+	++	++	Ø	Ø

Very significant presence ++++ , significant presence +++, average presence ++, traces +, absence Ø

portlandite in the non-carbonated samples and the presence of gypsum in small amounts (in relation to the calcite amount), indicated that the binders used in mortars M1, M2 and M3 were natural cements. The white crust on M3 mortar outer surface is Gypsum.

3.4 Identification of the Anhydrous Grains

As a reminder, in the cement field, a particular notation is used to designate the components: C = CaO, SiO_2 = S, Al_2O_3 = A, Fe_2O_3 = F, CO_2 = C (Taylor 1997).

Four types of anhydrous grains were encountered on the polished sections of the rich-binder-content M2 mortar, and therefore containing a high amount of residual anhydrous grains.

The first type of grain was large and well crystallized, with small round beige C_2S crystals enclosed in a very bright single-phase matrix (Fig. 7). After borax attack, some crystals turned to brown while others remained beige, revealing differences in the C_2S crystallographic structures (Fig. 7). The SEM observations of type 1 grains, coupled with EDS confirmed the presence of C_2S (Fig. 8). While some crystals showed parallel striations and others did not, they all exhibited the same elemental chemical composition. The matrix phase was composed of Ca, Al, Si and Fe, indicating a mixture of brownmillerite (C_4AF) and gehlenite (C_2AS).

The second type of grain was well crystallized, with large beige C_2S crystals enclosed in a bright white and gray two-phases matrix (Fig. 9). After borax attack, some crystals turned to brown while others remained beige. The SEM observations of type 2 grains coupled with EDS, confirmed the presence of C_2S. Again, while some crystals showed parallel striations and others did not, they all showed the same elemental chemical composition. The dark matrix phase was composed of Ca, Al, Si, which corresponds to gehlenite (C_2AS) (Fig. 10). The lighter grey-coloured matrix phase was a mixture of brownmillerite (C_4AF) and gehlenite (C_2AS) (Fig. 10).

The third type of grain was large and well crystallized, with large beige crystals enclosed in a clear white single-phase matrix. After borax attack, all the crystals turned to blue (Fig. 11), suggesting the presence of C_3S with an occasional brown coloration of these C_3S crystals.

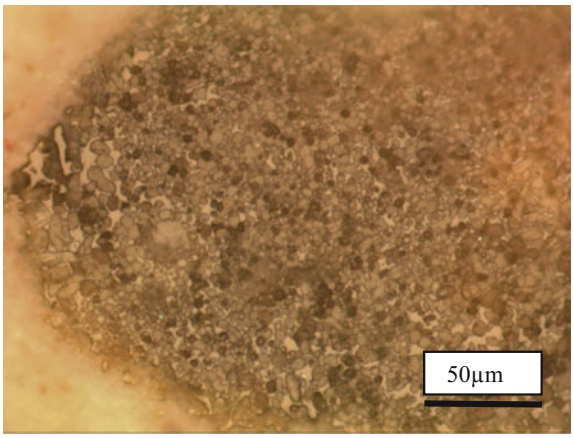

Fig. 7 OM view using polarized light (Z × 500) after borax attack, type 1 clinker grain, M2 mortar. Small round beige and brown C_2S crystals

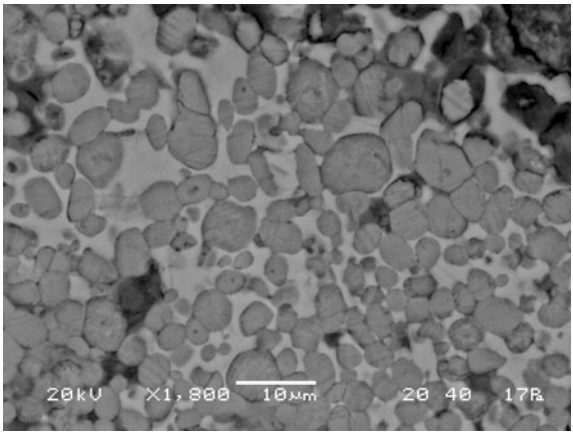

Fig. 8 BSE-SEM view (Z × 1800), type 1 clinker grain details, M2 mortar. Some C_2S crystals showed parallel striations and others did not

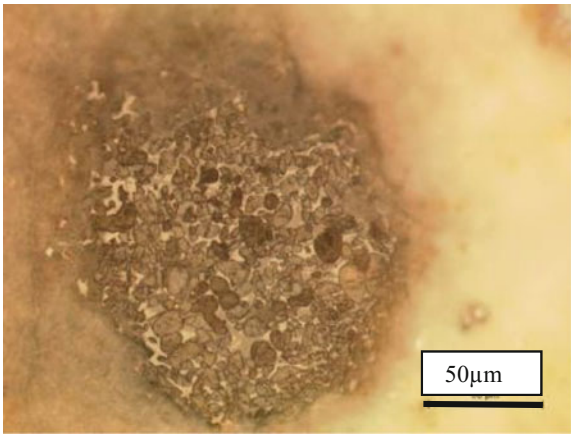

Fig. 9 OM view using polarized light (Z × 500), type 2 clinker grain, M2 mortar

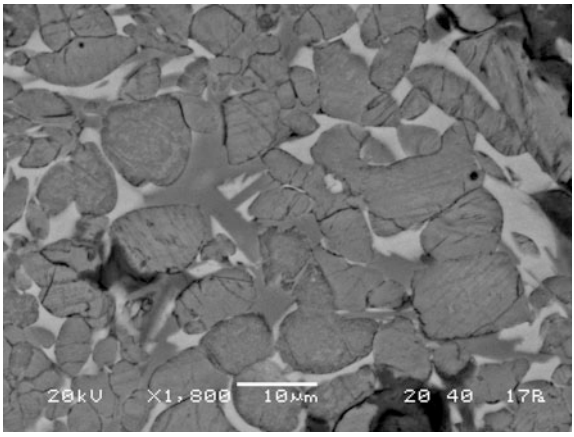

Fig. 10 BSE-SEM view (Z × 1800), details of type 2 clinker grain, M2 mortar

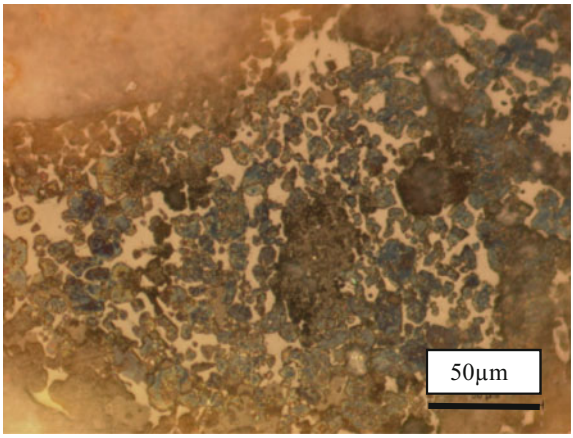

Fig. 11 OM view, using polarized light (Z × 500) after borax attack, type 3 clinker grain, M2 mortar. The blue colour reveals the presence of C_3S with an occasional brown coloration of these C_3S crystals

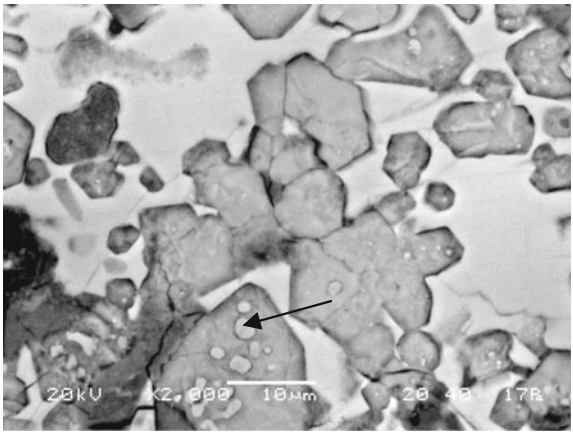

Fig. 12 BSE-SEM view (Z × 2000), details of type 3 clinker grain, M2 mortar. The crystals observed within the C_3S (corresponding to the brown coloration) were C_2S (pointer)

The SEM observations of the type 3 grains, coupled with EDS, confirmed the presence of C_3S (Fig. 12). The crystals observed within the C_3S (corresponding to the brown coloration) were C_2S (pointer—Fig. 12). The matrix phase was mainly composed of Ca, Al, Fe, which corresponds to a mixture of brownmillerite (C_4AF) and tri-calcium aluminate (C_3A).

The fourth type of grain was very poorly-crystallized (Fig. 13). It was composed of residual quartz grains in a matrix with a high content of Si, Ca and Al (Fig. 14). It should be noted that the Ca and Al content of the quartz grains was higher towards the outer part of the grains (pointer—Fig. 14).

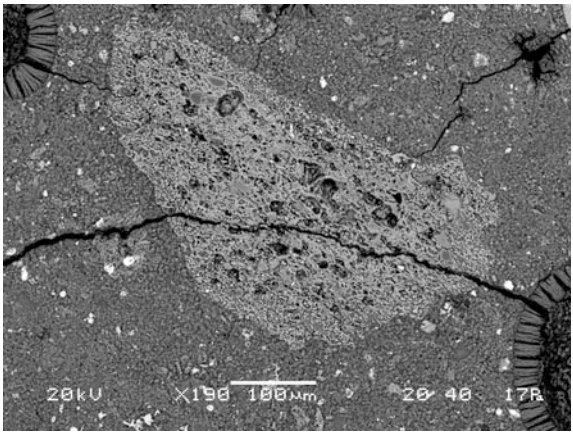

Fig. 13 BSE-SEM view (Z × 190), type 4 clinker grain, M2 mortar. Poorly crystallized anhydrous grain

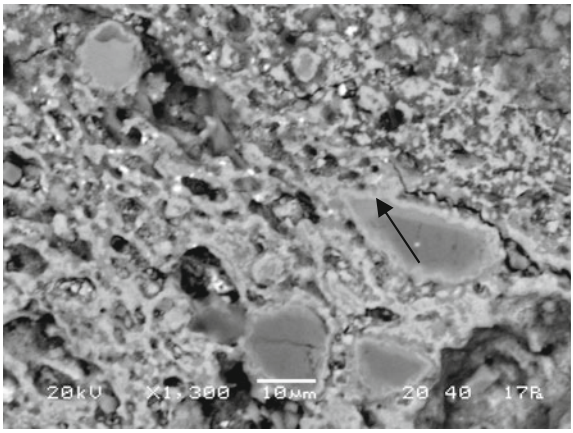

Fig. 14 BSE-SEM view (Z × 600), details of type 4 clinker grain, M2 mortar. Residual quartz grains with Ca and Al contents higher in the outer parts

3.5 Hydrated Phases

Observations in non-carbonated areas were undertaken on the M2 rich-binder-content mortar sample. In non-carbonated areas, the binder phase was mainly composed of hydrated calcium-silico-aluminates (C–A–S–H), with variable sulfur concentrations depending on the area, but sometimes equivalent to that of aluminum. This compact binder phase was generally poorly crystallized (Fig. 15).

In some areas, small crystals were observed, which did not, however, reveal major differences in chemical composition (higher carbon concentration, presence of potassium).

Ettringite, or tri-sulfo-calcium-aluminates, were also observed with different shapes:

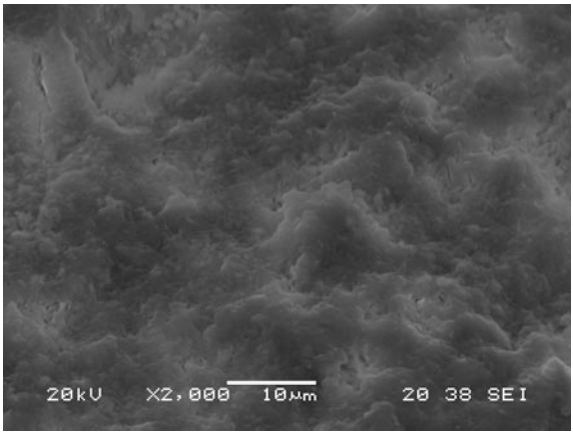

Fig. 15 SEM view (Z × 2000) of M2 mortar, non-carbonated poorly-crystallized binder matrix

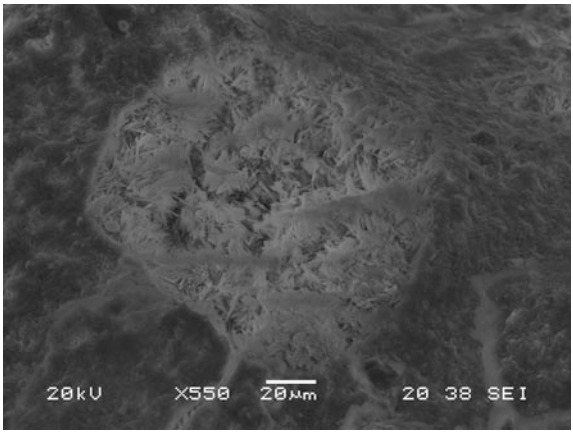

Fig. 16 SEM view (Z × 550) of a pore in non-carbonated mortar M2, acicular ettringite

– abundant acicular ettringite crystallization, completely filling up the pores (Fig. 16);
– less well-crystallized ettringite along the edges of the pores, where crystals were agglutinating in a compact mass;
– and small thin ettringite needles in the bottom of the pore.

The cement paste in carbonated areas was compact with occasional large pores. It consisted of a carbonated binding matrix, mainly made of calcium carbonates, originating from the carbonation of calcium silico-aluminates, of ettringite and calcium aluminate, leading to the formation of calcite, vaterite and amorphous carbonates. In mortar M2, the binding matrix was mainly composed of numerous and large trigonal calcium carbonate crystals (Fig. 17). They did not have the typical facies of calcite (rhombohedral), nor of vaterite, which usually crystallizes

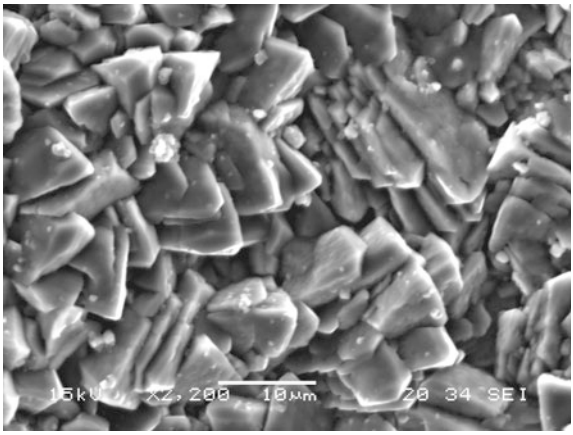

Fig. 17 SE-SEM view (Z x 2200) of M2 mortar, details of presumably vaterite crystals

as thickset needles. However, the shape of the vaterite crystallization strongly depends on the pH and the water intake (Tai and Chen 1998), and the results of X-ray diffraction showed that this was the main phase in carbonated areas. It is very likely that these crystals were a special type of vaterite.

Rhomboedral calcite crystals were also observed, coming from the carbonation of hydrated calcium silico-aluminate phases with a high silicon content. Indeed, the carbonation of this phase, which produces calcite, depletes it of its calcium and thus increases its proportion of silicon.

Finally, amorphous calcium carbonates were filling the pores and crevices of the cement paste (Fig. 18). Surprisingly, needle-shaped ettringite crystals in the pores and crevices of the concrete, as well as tablet-shaped calcium aluminate were observed in the carbonated M2 mortar (Fig. 19).

In the mortars M1 (poor mortar) and M3 (run-in situ mortar), tablet-shaped gypsum and massive gypsum (pointer—Fig. 20) crystallizations were observed in

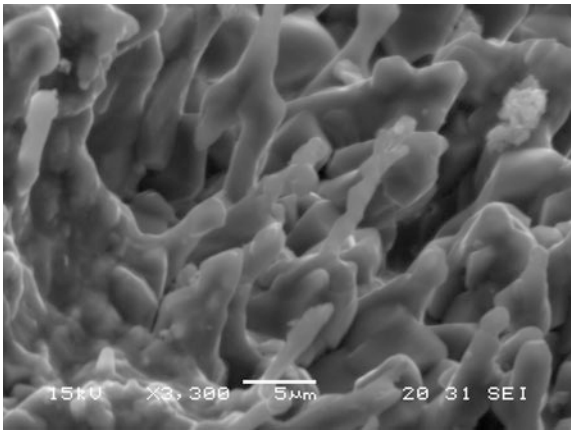

Fig. 18 SEM view (Z × 3300) of M2 mortar, amorphous calcium carbonates

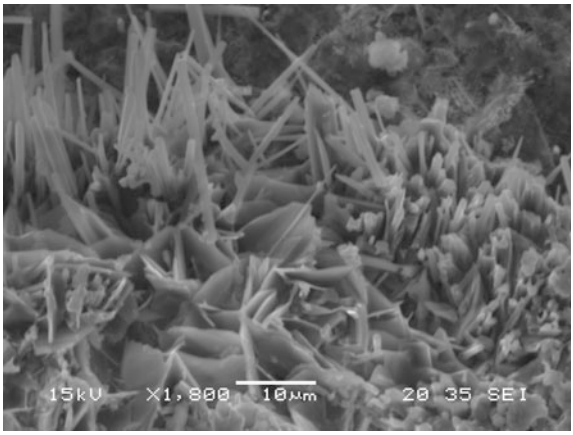

Fig. 19 SE-SEM view (Z × 1800) of the M2 mortar, ettringite and tablet-shaped calcium aluminate at the bottom of the pore

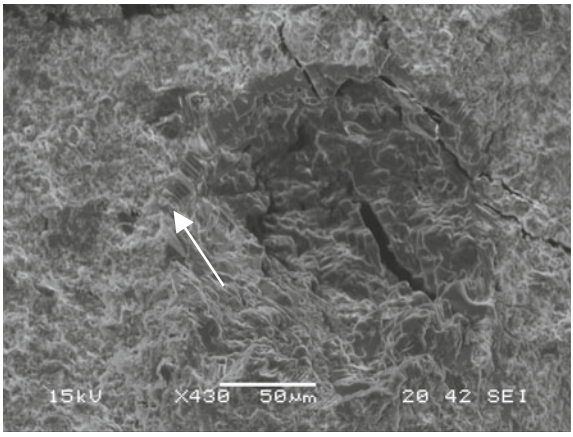

Fig. 20 SEM view (Z × 430) of the M3 mortar, pore covered with a layer of massive gypsum

the pores, gypsum being one of the by-products of the carbonation reaction of ettringite. It should be noted that during carbonation, ettringite decomposes into calcite, gypsum and alumina gel (Nishikawa et al. 1992).

4 Conclusion

In the Vassy church, ochre-coloured mortars were used both inside and outside, for rendering, pointing mortar or run-in situ mortar purposes. They were applied onto stone and brick. Different types of mixtures were used, from rich-binder-content mortars (almost a cement paste) to poor-binder-content mortars. The main degradation observed outdoors are a generalized erosion phenomenon, pattern cracking and localized spalling under a defective lead sheet protection.

The presence of gehlenite and C–A–S–H phases as a matrix in all of the samples, the absence of portlandite and the strong presence of ettringite in non-carbonated areas clearly indicated that the binder used to manufacture the cement mortars of the Vassy church was a natural cement, with a high sulfate and aluminate content, produced by a heterogeneous firing process.

Indeed, residual anhydrous clinker grains were characterized on polished sections and 4 types were distinguished. The most frequently observed grains were compounds of C_2S crystals surrounded by a two-phase C_2AS and C_4AF binding matrix (type 2 grains). After borax attack of these type-2 grains, C_2S crystals turned to brown while others remained beige. However, no chemical difference between these C_2S crystals was brought to light through EDS analyzes. On the type-3 grains, C_3S crystals (which turned to blue after a borax etching) were identified, whereas the type-4 grains were poorly crystalline and composed of silica grains with reaction rings and a CSA phase. Moreover, gehlenite was identified through XRD in all of the samples and wollastonite was detected in the sample with the highest cement content.

The coexistence of these four types of grain, and the presence of gehlenite and wollastonite which is typical of a moderate temperature firing (<1100 °C), could be explained by a very heterogeneous firing or by a mixture of unburnt, burnt and over-burnt materials (which is frequently mentioned in ancient documents, for special uses).

In terms of hydrated phases, XRD analyses and SEM observations revealed a significant presence of high sulfur content compounds: only gypsum in the carbonated samples and ettringite and gypsum in the non-carbonated samples. Ettringite was thus encountered in the pores in non-carbonated areas. The crystals had the shape of long well-crystallized needles. This ettringite may be primary, which means that it could be a normal product resulting from the hydration of the cement (Cailleux et al. 2005; Sommain 2008). It may also be secondary, resulting from the reaction of external or internal sulfates with the hydration products of the cement. Aluminate phases, such as hydrocalumite (C_4AH_{13}) and mono-carbonate calcium aluminates (C_4ACH_{11}) were also identified through XRD in non-carbonated samples, but portlandite was never detected. SEM observations of the cement matrix in non-carbonated areas indicated that it was composed of a C–A–S–H type amorphous phase, with traces of Fe, Mg and S. In carbonated areas, the binding matrix was made of calcium carbonates, probably mainly vaterite for the rich-binder-content mortar M2 and calcite for the lower-binder-content M1 and M3 mortars. Amorphous calcium carbonates were observed on all of the mortars using SEM.

As all of the analyzed mortars had particularly high sulfate contents, in order to be compatible, repair mortars will have to be resistant to sulfates. The binder to be used will therefore have to meet the following requirements:

– a low aluminate content to avoid the formation of expansive secondary ettringite, which could cause swelling and cracking of the repair mortar,

– and a low alkali content, to prevent the formation of alkali salts such as sodium sulfate (thenardite, mirabilite), potassium-calcium sulfate (syngenite), or tripotassium natrium sulfate (aphthitalite), which are expansive and deleterious salts.

Thus, current Portland cements present alkali and aluminate contents that are incompatible with these criteria. Contrarily, natural cements, which are still produced today, because their hydration leads to the formation of small amounts of portlandite, which does not cause the formation of expansive ettringite (Sommain 2008; Gosselin and Scrivener 2010), show a good sulfate resistance. In addition, their color and texture are similar to those of Vassy mortars, so they represent an interesting restoration material. However, some of the existing natural cements exhibit a significant alkali concentration, which constitutes a potential risk of deterioration. Preliminary compatibility tests are therefore necessary.

Acknowledgements This study was initiated within the frame of the Rocare project (EU 226898) financially supported by the European Commission (FP7-ENV-2008-1 program).

References

Cailleux, E., Marie-Victoire, E., & Sommain, D. (2005). Microstructural and weathering mechanisms of natural cements used in the 19th century in the French Rhône-Alpes region. In *Proceedings on the International Workshop on: Repair Mortars for Historic Masonry*, *Delft*. 26th–28th January 2005.

Cailleux, E., Marie-Victoire, E., & Sommain, D. (2006). Study of natural cements from the French Rhône-Alpes region. In *Proceedings of the International Conference on Heritage, Weathering and Conservation*, *Madrid* (vol. I, pp. 77–84). 21–24 June 2006.

Campbell, D. H. (1999). *Microscopical examination and interpretation of portland cement and clinker* (2nd ed., p. 201). New York: Portland cement association.

Gosselin, C., & Scrivener, K. L. (2010). Hydratation of natural cement used for architectural restoration. In IHMC 2010: *Proceedings of the 2nd Historic mortars conference and RILEM TC 203-RHM repair mortars for historic masonry, final workshop* (pp. 927–936). 22–24 September 2010, Prague, Czech Republic.

Gosselin, C., Martinet, G., Royer, A., & Vergès-Belmin, V. (2009). Natural cement and monumental restoration: The case of Bourges cathedral. *Materials and Structures, no, 42,* 749–763.

Hughes, D., Swann, S., & Gardner, A. (2007, March). Roman cement—Part one: Its ORIGINS and properties. *Journal of Architectural Construction*, 21–36

Hughes, D., Swann, S., & Gardner, A. (2007, November). Roman cement—Part two: Stucco and decorative elements, a conservation strategy. *Journal of Architectural Construction*, 41–58.

Nishikawa, T., Suzuki, K., & Ito, S. (1992). Decomposition of synthesized ettringite by carbonation. *Cement and Concrete Research, 22,* 6–14.

Tai, C.Y., & Chen, F. B. (1998, August). Polymorphism of $CaCO_3$ precipitated in a constant-composition environment. *American Institute of Chemical Engineers Journal*, *44* (8), 1790–1798. ISSN 0001-1541.

Sommain, D. (2008). La durabilité des bétons de ciment prompt naturel, in La durabilité des bétons sous la dir. de JP. OLLIVIER et A. VICHOT, Presses de l'Ecole Nationale des Ponts et Chaussées, 825–840.

Taylor, H. F. W. (1997). Cement chemistry. London: T. Telford, cop.
Weber, J., Gadermayr, N., Kozlowski, R., Mucha, D., Hughes, D., Jaglin, D., & Schwarz, W. (2007). Microstructure and mineral composition of Roman cements produce at defined calcination conditions. *Materials Characterization*, 1217–1228.
Weber, J., Gadermayrh, N., Bayer, K., Hughes, D., Kozlowski, R., Stillhammerova, M., Ullrich, D., & Vyskocilova, R. (2007). Roman Cement Mortars in Europe's architectural heritage of the 19th century. *Journal of ASTM International*, *4*(8), 15.

Methods of Microscopy to Identify and Characterise Hydraulic Binders in Historic Mortars—A Methodological Approach

J. Weber, T. Köberle and F. Pintér

Abstract The contribution focuses on microscopic techniques for use in the identification and characterisation of historic mortars, with the assumption that the key information to understanding historic mortar is contained in the binder. While bulk chemical or gross phase analytical tools may provide preliminary information on the binder type used, imaging methods such as light and electron microscopy offer a more detailed assessment due to the possibility to study simultaneously mineral compounds, textures and microstructures of reacted and unreacted binder components, as well as their interaction with the other constituents of a mortar. This holds not only for traditional air lime based mortar systems, but most specifically also for all those containing cementitious compounds. The use of standard techniques of polarising light microscopy (PLM) and scanning electron microscopy (SEM) on thin sections to identify the binder constituents of hydraulic mortars is discussed. Residual cement grains indicative of high temperatures of formation (typical in Portland cement mortars) can be observed and classified by reflecting light PLM on polished sections eventually supported by staining techniques, even if present in only small amounts. On the contrary, natural or Roman cement mortars, in which the binder was calcined at low temperature, require the use of thin section PLM with transmitted light, possibly complemented by SEM-techniques. For hydraulic lime mortars, either of the above approaches can be optimal, depending on whether they were naturally or artificially mixed. The contribution presents a

J. Weber (✉)
Institute of Arts and Technology, Section of Conservation Sciences,
University of Applied Arts Vienna, Salzgries 14/1, 1013 Vienna, Austria
e-mail: johannes.weber@uni-ak.ac.at

T. Köberle
Geologie-Denkmalpflege-Bauforschung, Nordstrasse 39, 01099 Dresden, Germany
e-mail: TKoeberle@gmx.de

F. Pintér
Scientific Laboratory, Federal Monuments Authority Austria,
Arsenal 15/4, 1030 Vienna, Austria
e-mail: farkas.pinter@bda.at

J. J. Hughes et al. (eds.), *Historic Mortars*,
https://doi.org/10.1007/978-3-319-91606-4_2

few examples of mortars made from each of the above binders and addresses additional observations, e.g. the leaching of the matrix by weathering agents.

Keywords Historic mortar · Hydraulic binder · Unhydrated residuals
Optical microscopy · SEM

1 Introduction

When dealing with mortars sampled from historic structures, there are many qualities that are of interest to the material analyst, such as physico-mechanical performance, microstructure, the petrographic or granulometric composition of the aggregate, and/or the types and causes of alteration of the mortar over time. In virtually all cases, however, one piece of information is considered key for any kind of mortar characterisation: namely the type of binder used to prepare the mortar. Understanding the binder greatly helps archeologists and conservation scientists to make sound decisions when searching for compatible materials to restore, repair and/or replace parts of a building. Additionally, it greatly enhances our understanding of the history of technology. It is usually the binder that lends its name to a mortar, be it lime, pozzolanic, hydraulic or cement based.

Identifying a mortar's binder can be simple to the experienced eye, particularly when examined in the context of a group of mortars whose properties are well understood, but even the most experienced researcher can have unexpected difficulties—a situation met by the authors on a nearly daily basis. As pointed out by several authors (St John et al. 1998; Elsen 2006; Krotzer and Walsh 2009; Ingham 2010), investigating binders petrographically, i.e. by employing imaging methods such as polarising light or scanning electron microscopy (Winter 2009), may yield much information about the binder's nature and mode of production.

Within this scope, the concept that "the key to binder identification lies in the unreacted residuals" (Walsh 2008) holds particularly for hydraulic binders.

Whether or not there is a sufficient unreacted portion of binder left in a mortar is not a matter of age, but rather of the fineness of to which it has been milled and the quality of reactions achieved during the manufacturing process—both factors are likely to be observable in historic mortars from before the First World War. The most widely used hydraulic binders of the 19th and early 20th centuries comprised cements calcined below sintering, usually called Roman cements (RC), natural hydraulic limes (NHL), and cements produced by sintering, called Portland cements (PC). The history of their production is generally known (e.g. Blezard 2003), though many details still need to be researched or have remained unpublished to date. These products were far less subject to quality regulation at this time than they are now that European norms define clear standards for composition and performance of commercial building limes and cements. Thus, the quality varied from one product to the other within certain limits, as did the process of production. Considering also the frequent practice of blending of various binders to prepare a

mortar on any particular project, the value of precise determination of the constituents of a historic mortar in terms of its binder becomes clear. The optimal method of this is careful and skilled assessment of the unhydrated binder residuals. Instrumental bulk analyses such as X-ray diffraction or chemical binder analysis are less capable of tracing all types of constituents relative to imaging analytical tools.

Microscopy is frequently used by three groups of professionals from the field of mortar research—conservation scientists on the one hand, and cement respectively concrete experts on the other. However because these groups are searching for different information, they utilise different approaches. Cement chemists usually are interested in the composition and microstructure of clinker sampled from the production process and use incident light microscopy in the bright field mode, eventually supported by etching and staining the polished section and using scanning electron microscopy (SEM) combined with X-ray diffraction (XRD). Concrete experts are mostly interested in the composition and causes of alteration of the sample over time. Such analyses are traditionally carried out on thin sections in transmitted polarised light and/or on polished sections by using SEM. Conservation scientists typically are trained in incident light microscopy employing the dark field mode, where stratigraphical features and paints can be better visualised. Eventually complementing this work with petrographic thin-section microscopy or SEM, many conservation microscopists are not well aware of the additional possibilities offered by the light microscope when switched from dark to bright field mode of observation. It is hence the aim of this contribution to demonstrate by a few examples the added value achieved by employing the full range of observation techniques offered by a petrographic microscope in combination with a scanning electron microscope.

2 Samples and Methods of Microscopy

2.1 Sample Preparation

In principle two types of microscopic sections can be produced from a mortar sample: either petrographic thin sections, usually covered by a glass slip, or polished cross sections. Neither type can be used for every mode of observation in a light or scanning electron microscope, so compromises have to be made taking account of the most appropriate technique to analyse the material.

The ideal case would be to produce both a thin and a cross section from adjacent parts of a sample, a rather expensive approach which moreover requires sufficiently large samples. A drawback to this approach is that a unique phenomenon seen in one section might not be visible in the other, depriving the operator the possibility to verify certain observations and their interpretation by another method. In this case, even the combination of all available techniques may not reveal a sample's true nature.

Probably the best choice is to produce polished thin sections, which allow for all light microscopy and SEM work to be done on the same section. PLM observations under incident light in the dark field mode yield images different from those from polished cross sections. This is caused by a part of the light passing through the material reflecting off its lower surface, thus creating images similar to the ones obtained by transmitted light under crossed polars. Another factor to consider is the necessity to sputter the section surface for SEM at high vacuum. The drawback to this is that this process is is not fully reversible thus the sample should have been carefully analysed and documented by PLM before sputtering. A possible solution would be to sputter just a part of the section

Whether polished or not, thin sections require great skill to prepare. A surprising number of bad thin sections are produced which greatly reduces the quality of information obtainable. The same holds for the method of impregnating the sample with a resin, which must penetrate the pore space to the highest possible extent. It is important to add a dye to the resin in order to get a good contrast between pore space and solid components. The yellowish UV-fluorescent dye mainly used for concrete petrography is less appropriate for conventional microscopy than the blue dye which gives better contrast.

2.2 Low Power Stereo Microscopy

Stereomicroscopes are usually designed for 3-dimensional images of uneven samples. They can also be used in a beneficial way to study plane microscopic sections utilizing a range of low magnifications, about 5 to 100x, which cannot be easily achieved with most polarising microscopes. Any mortar analysis on thin and/or polished sections should start with low power observation of the binder and aggregates to establish the major microstructural features of a mortar.

Modern stereomicroscopes provide not only incident light but also transmitted light facilities. If equipped with polarizers, they may offer a wide range of observation modes for thin sections. Some of them are rarely used by microscopists, e.g. using incident light on thin sections impregnated with dyed resin. If laid on a sheet of white paper, residuals of cement are usually easily visible by their brownish colour. Without a reflective white background, they would have probably remained undetected. Using the usual method of observation with transmitted light (Fig. 1a, b), the aggregate can be identified and phenomena like the full carbonation of the cementitious binder can be assessed. The high amount of unhydrated cement particles is only visible in the incident light mode provided that the section is placed on a white background (Fig. 1c).

Roman cement mortars can be identified equally well at low magnifications as their binders contain residual compounds that are larger than the clinker of historic PCs. To clearly distinguish them from aggregate takes some experience; the frequent zoning of the binder related nodules can be helpful. Figure 2a, b illustrates this with an example of a RC mortar, where even the high degree of leaching by

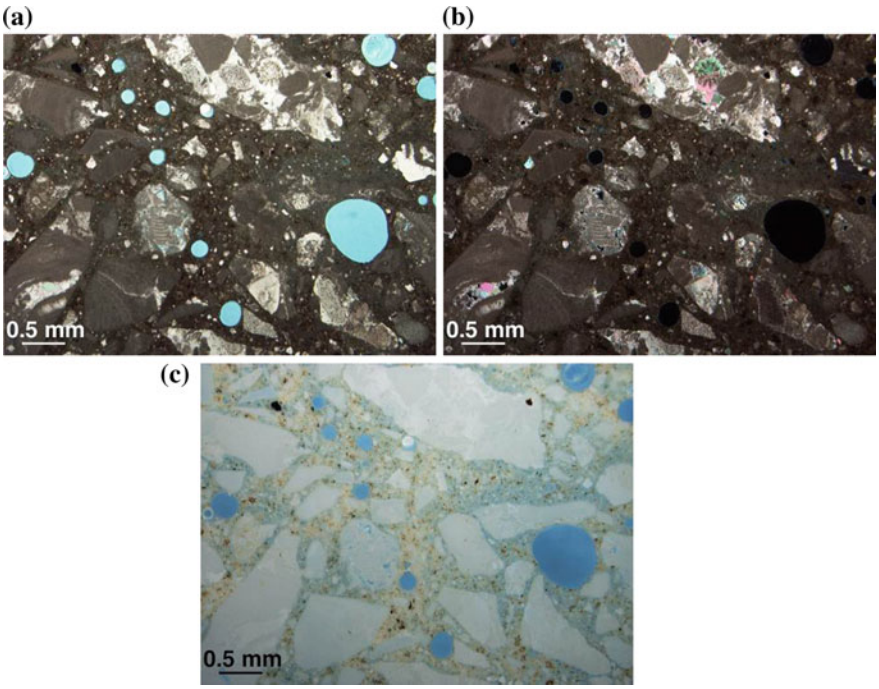

Fig. 1 Polished thin section of a 1910 White-PC mortar with limestone aggregate under the stereo-microscope; **a** transmitted light parallel polars, **b** crossed polars, **c** incident light. The PC clinker residuals are well visible in the incident light mode as brownish spots in the binder

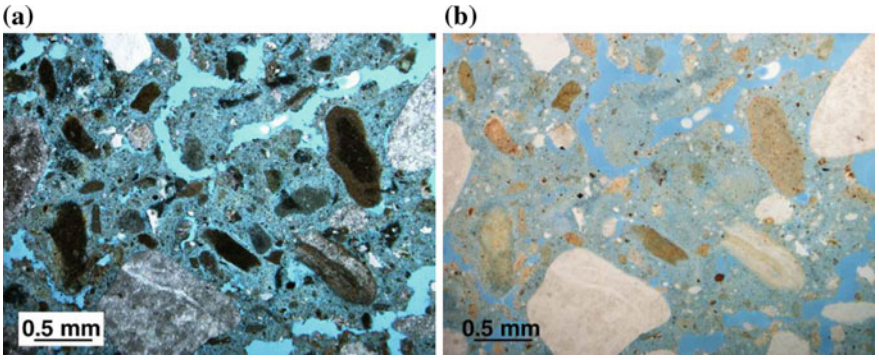

Fig. 2 Polished thin section of a 1870 RC bedding mortar under the stereomicroscope; **a** transmitted light parallel polars, **b** incident light. The RC residual nodules exhibit strong zoning which is best visible in transmitted light with parallel polars (**a**). The mortar is strongly leached and decayed by the action of percolating water

weathering has left the distinctive nodules unaltered. As shown below, however, an attempt to characterise these lumps more precisely by polarising microscopy may fail.

2.3 Polarising Microscopy

When equipped with facilities for light transmission and reflection, a polarising microscope is a versatile tool to study many details at magnifications up to about 1000 times. For our purposes this includes a more precise determination of the residual clinker in terms of crystal size and shape, phase identity and mutual relationships between the different phases. The usual mode of observation is under reflective light in the bright field, producing images of grey values according to the reflection coefficient of a phase. Traditionally used by cement chemists, this method provides quick access to several useful pieces of information about the type of cement used for a mortar, in particular when PC mortars are investigated. Figure 3a, b illustrates the advantage of reflective over transmitted light, especially when the clinker grains are small. However when studying coarse unhydrated clinker grains composed of large crystals, which are frequently found in historic PC mortars, it is worthwhile to have produced a polished thin section in order to observe the clinker also under transmitted light where additional optical parameters such as the interference colours become visible (Fig. 4a, b). Thus, by simply switching between transmitted light at parallel or crossed polars one can use the full range of facilities offered by the polarising microscope on one single preparation.

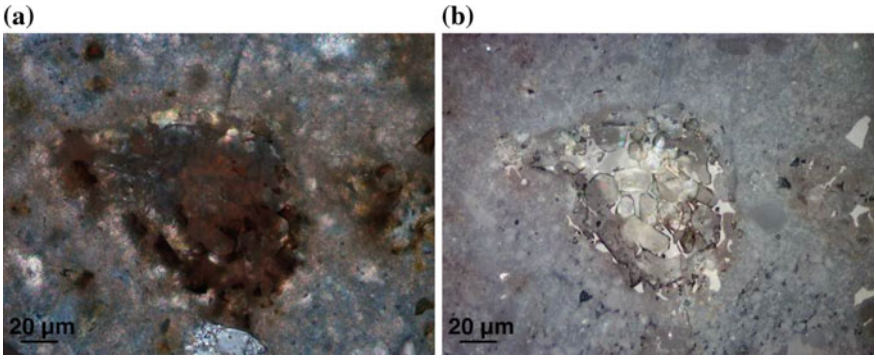

Fig. 3 Polished thin section of the White-PC mortar from Fig. 1; residual clinker grain under the polarising microscope, **a** transmitted light parallel polars, **b** reflective light, bright field. Angular alite, spherical belite and an interstitial phase mainly composed of aluminate while high reflecting ferrite occur only in small amounts; carbonation has led to the formation of a compact rim of carbonate, visible by its birefringence (**a**), while the calcium silicates are strongly depleted in calcium

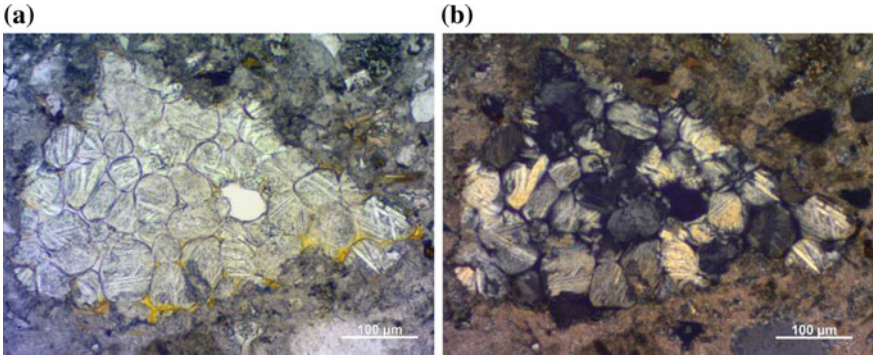

Fig. 4 Polished thin section of a 1879 PC pointing mortar; residual clinker grain under the polarising microscope, **a** transmitted light parallel polars, **b** crossed polars. Coarse belite crystals which can be clearly identified by their shape, interference colour and intersecting sets of twinning lamellae

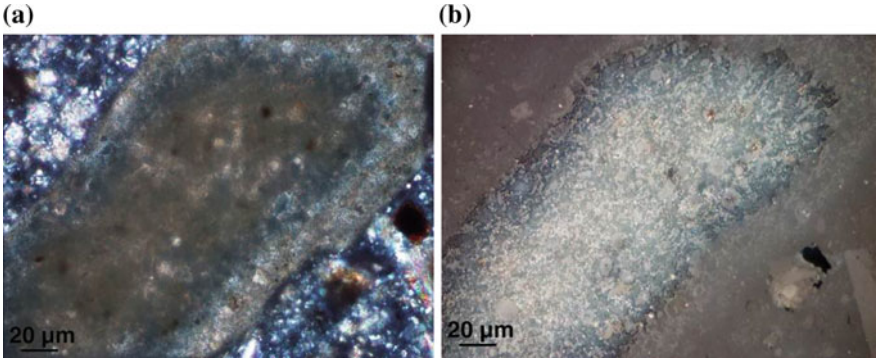

Fig. 5 Polished thin section of the RC mortar from Fig. 2; detail of a residual nodule under the polarising microscope, **a** transmitted light parallel polars, **b** reflective light, bright field. While the nodule as such is indicative for the RC nature of the sample, its fine grained texture makes it difficult to identify any of the phases by this method

In contrast to PC mortars, the polarising microscope is less convenient to study the precise phase composition of RC mortar residual structures, since these nodules are typically composed of very fine grained clinker phases of less well defined stoichiometry and hence less significant optical parameters (Fig. 5a, b). In this case the use of SEM is more promising.

A large range of methods to etch and/or stain polished thin sections by the use of different chemicals are used (see e.g. Gille et al. 1965; Campbell 1999) to allow for a clearer identification of clinker phases and to reveal microstructural details of individual crystals. Hydrofluoric acid, borax, salicylic acid, potassium hydroxide/sucrose, and nitric acid in ethanol (Nital) are just some of the most commonly employed etching agents, each of them having unique benefits for the identification

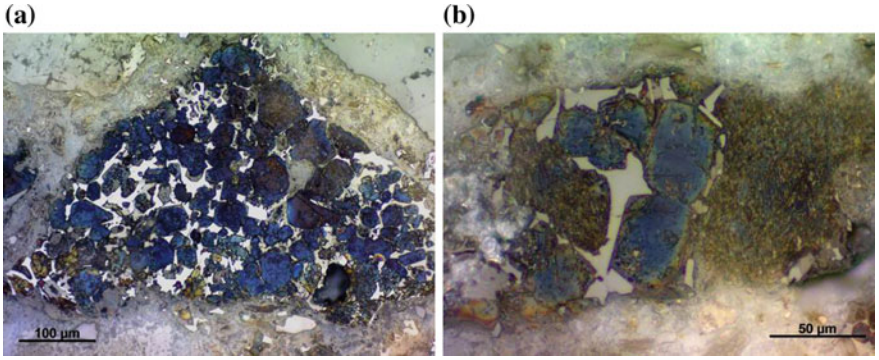

Fig. 6 Polished section of the PC mortar from Fig. 4; residual clinker grains under reflective light. Caused by etching with Nital, alite is easily detectable by its blue colour, while belite has turned brownish and the interstitial phases ferrite and aluminate have remained unaltered. The variety of alite sizes can be considered characteristic of historic PC, indicating an inhomogeneous raw feed and/or firing conditions

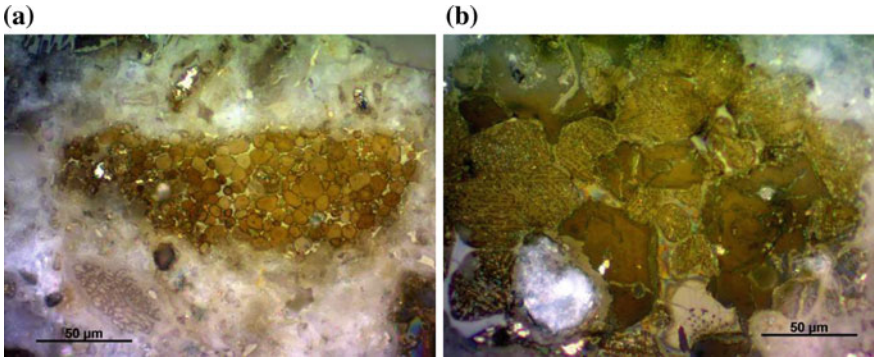

Fig. 7 Polished section of the PC mortar from Fig. 6; residual belite clinker grains under reflective light, etching with Nital. Similar to alite (Fig. 6), belite is of varying crystal size, the internal structure made visible by the etching allows conclusions to be drawn on the calcination process. Thus, the structurally uniform crystals have probably formed by conversion from the coarse belites with intersecting twinning lamellae, a process indicative of the use of a shaft kiln

of certain phases and visualisation of internal microstructures. The full range of possibilities has probably not yet been exploited for historic PC mortars; the use of Nital as illustrated in Fig. 6a, b and Fig. 7a, b serves just as an example.

2.4 Scanning Electron Microscopy

Despite all benefits offered by the techniques of light microscopy, the microscopist may have good reasons to decide to use SEM as additional tool to study the binders in a historic mortar sample (Winter 2012). It is clear that the instrument needs to be equipped with a good back-scattered electron detector and a X-ray analytical device (EDS) in order to make the desired observations. If it can be operated in the low vacuum mode, the operator should first try to study the section without coating it with a conductible layer of carbon This is especially true of a polished thin section since it would be altered by carbon-coating which is not fully reversible. Things to keep in mind when working under low vacuum are that the image resolution is lower and that the chemical spot analysis by EDS is less precise and confined than it would be in the high vacuum mode, due to the interaction between electrons and air molecules in the chamber.

SEM investigations are useful not only to study the unhydrated portion of the binder, but also can be employed to improve knowledge of the reacted part, which is usually of much finer grain size and hence less understandable by light microscopy than clinker residues. EDS-analysis of the hydrated binder may yield unpredicted results as to its nature: a mortar rich in residual cement may show very low amounts of silica in its hydrate binder, or on the contrary, it may lack calcium

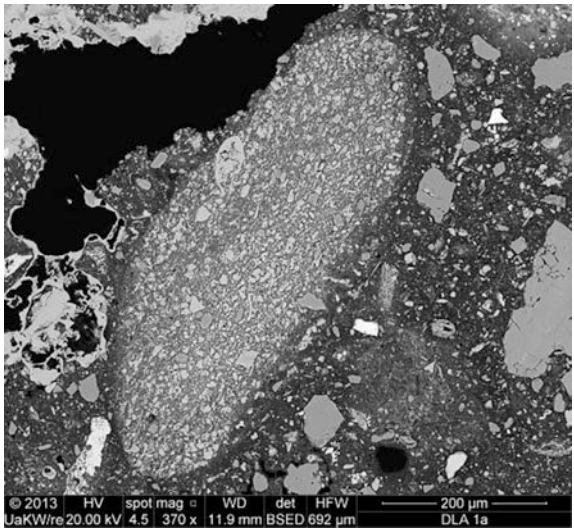

Fig. 8 Polished section of the RC mortar from Figs. 2 and 5; SEM/BSE image of an underfired residual nodule of the type shown in Fig. 5. The tiny mineral phases contained in the particle are quartz and calcite, unreacted minerals inherited from the raw feed marl. The surrounding binder is strongly depleted in calcium ions due to leaching effects which have caused calcite precipitates along the pore—visible on the top left. In fact, due to these alterations it cannot be excluded that we deal with a NHL instead of a RC mortar

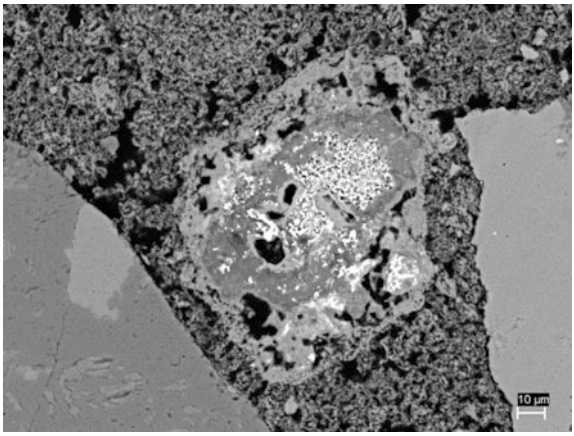

Fig. 9 Polished section of a 1899 NHL mortar; SEM/BSE image of an underfired residual nodule of the type shown in Fig. 5. The residual particle contains non-stoichiometric calcium silicates in compositions between CS and C_2S and aluminate ferrites (bright). The surrounding binder matrix is mostly lime

ions, as in the example shown in Fig. 8. While the first case would indicate a mixture of lime and cement with very low reactivity, possibly due to cement grains that are either overly coarse or of an inappropriate composition, the latter case is usually due to strong leaching effects caused by weathering.

With unhydrated residues, the advantage of high resolution imaging and elemental analysis offered by the SEM is of special benefit for small and/or non-ideally reacted phases as they occur in RC and NHL mortars. This is especially true of analysing RC mortars rich in "underfired" nodules, i.e. residual grains which did not calcine sufficiently to form reactive clinker phases (Gadermayr et al. 2013) (Fig. 8). Additionally the well fired portion of RC nodules frequently contains phases below the resolution of a polarising microscope or non-crystalline solid solution phases which can not be identified by their optical parameters (Fig. 9). In these cases using the SEM can be beneficial.

3 Conclusions

Historic cementitious or highly hydraulic mortar binders are chemically less well defined than modern ones. Their characterisation in mortar samples therefore requires a thorough analysis of the unhydrated residual particles in their structural context, a task which can be best accomplished by the use of microscopic means, possibly combined with chemical point analysis. Generally one can profit from the use of different modes of observation preferably performed on the same sample section. Within that frame, reflective light microscopy proves useful for mortars containing different amounts of PC, while PLM in transmitted light is advantageous for all types of hydraulic mortars. In all cases SEM techniques can provide significant additional insight.

In general the quality of sample preparation requires the highest possible standard. Polished thin sections are probably the best choice since they allow for the full range of microscopy on one sample.

Acknowledgements We would like to thank Anthony Baragona for English language editing.

References

Blezard, R.G. (2003). The history of calcareous cements. In: P.C. Hewlett (Ed.), *Lea's chemistry of cement and concrete*, fourth ed., Elsevier, Oxford, 1–23.

Campbell, D. (1999). *Microscopical examination and interpretation of portland cement and clinker* (2nd ed., p. 201). Skokie (IL): Portland Cement Association. ISBN 0-89312-084-7.

Elsen, J. (2006). Microscopy of historic mortars—A review. *Cement and Concrete Research, 36,* 1416–1424.

Gadermayr, N., Pintér, F., & Weber, J. (2013). Identification of 19th century Roman cements by the phase composition of clinker residues in historic mortars. In *Proceedings of the 12th International Congress on the Deterioration and Conservation of Stone*, New York, 22–26 October, 2012 (In press).

Gille, F., Dreizler, I., Grade, K., Krämer, H., & Woermann, E. (1965). *Mikroskopie des Zementklinkers* (p. 75). Bilderatlas: Association of the German Cement Industry, Beton-Verlag, Düsseldorf, West Germany.

Ingham, J. (2010). Geomaterials under the microscope (colour guide), Wiley, ISBN-10-1840761326.

Krotzer, D. S., & Walsh, J. J. (2009). Analyzing mortars and stuccos at the college of Charleston: A comprehensive approach. *APT Bulletin: Journal of Preservation Technology, 40*(1), 37–44.

St John, D. A., Poole, A. W., & Sims, I. (1998). *Concrete petrography—A handbook of investigative techniques* (p. 474). London-Sydney-Auckland: Arnold.

Walsh, J. J. (2008). Petrography: Distinguishing natural cement from other binders in historical masonry construction using forensic microscopy techniques. In M. P. Edison (Ed.), *Natural Cement* (pp. 20–31). American Society for Testing and Materials. ISBN 978-0-8031-3423-2.

Winter, B. N. (2009). *Understanding cement—An introduction to cement production, cement hydration deleterious processes in concrete* (p. 182). Rendlesham, Woodbridge, Suffolk UK: Electronically published by the WHD Microanalysis Consultants Ltd.

Winter, B. N. (2012). *Scanning electron microscopy of cement and concrete* (p. 192). Rendlesham, Woodbridge, Suffolk UK: WHD Microanalysis Consultants Ltd.

Composition and Application of Cimorné Finish: An Interwar Cement Render Decorated with Coloured Opalescent Glass Granules

Liesbeth Dekeyser, Laurent Fontaine, Ann Verdonck and Hilde De Clercq

Abstract A Walloon entrepreneur developed and patented *Cimorné* cement render at the beginning of the 1930s in Braine-l'Alleud (south of Brussels, Belgium). This peculiar façade finish consists of a pigmented multilayer cement mortar onto which opalescent and mass coloured glass granules were projected. Cimorné became popular in the interwar period and was available in a variety of (very bright) colours, depending on the global hue of the added opalescent glass granules. Local craftsmen developed in their characteristic manner application techniques, mixing the mortar of the cimorné render, based on a Portland cement mortar, on-site. Minor information is available about the cimorné technique, a regional applied finish of which the characteristics, formula and application method were mainly orally transmitted between craftsmen. Hence, knowledge about the cement mortar, its cement-sand ratio, granulometry, etc. is crucial and prior to durable repair and restoration campaigns. Interviews with retired plasterers revealed relevant information about the original formula, preparation on-site and application method. The information related to the cimorné craftsmanship was compared to data found in archival records, patents and interwar plastering and masonry manuals on the one hand and to results from laboratory analyses of mortar samples lifted on-site on the

L. Dekeyser (✉) · A. Verdonck
Department of Architectural Engineering,
Vrije Universiteit Brussel, Brussels, Belgium
e-mail: liesbeth.dekeyser@vub.ac.be

A. Verdonck
e-mail: ann.verdonck@vub.ac.be

L. Fontaine · H. De Clercq
Monument Laboratory, Royal Institute for Cultural Heritage (KIK-IRPA), Brussels, Belgium
e-mail: laurent.fontaine@kikirpa.be

H. De Clercq
e-mail: hilde.declercq@kikirpa.be

J. J. Hughes et al. (eds.), *Historic Mortars*,
https://doi.org/10.1007/978-3-319-91606-4_3

other hand. The overall results form the basis for restoration trials, which will be carried out on-site, in order to enable future durable and sustainable repair interventions of this peculiar Art Deco cement render.

Keywords Cement render · Interwar period · Opalescent glass
Mason manuals · Laboratory analyses

1 Cimorné Render and the Reconstruction of Its Formula

The second half of the nineteenth century was characterized by the development and application of Portland cement renders on several buildings. Initially cement façades were appreciated because of their resemblance to blue stone, but only after some decades this perception changed drastically in favour of more coloured façades (Van der Heiden 2010). Grey cement finishes were considered unattractive and transformed into white stone-like plasters or more coloured ones by the addition of alkali-resistant pigments like metal oxides. But pigments washed out and the colours faded over time. Around 1928, Pierre Pétroons (1897–1969) came up with the creation of a coloured and textured finish, based on the projection of opalescent coloured glass particles onto a Portland cement mortar render. The cimorné finish was born. Etymologically, cimorné is the combination of two French words *ciment* and *orné* literally meaning 'decorated cement'. This suggests the principle of cimorné: a decorative façade finish composed of a cement render with opalescent glass granules projected onto it. Portland cement and Marbrite opalescent glass were both manufactured in the province of Hainaut (Walloon Region, Belgium) and thus easily accessible for Pétroons, whose company was located in Braine-l'Alleud.

Pétroons launched his cimorné finish at the *World's Fair* of 1931 in Liège (Belgium) and patented it later on in Belgium, UK and France (Dekeyser et al. 2012). According to these patents, cimorné was commercialised as being 'rainproof', requiring 'little or no maintenance' (AAM 1932). Both renovated cottages and new villas were decorated with cimorné render in a variety of colours and patterns (Fig. 1). Despite the fact that cimorné was applied all over Belgium, this craftsmanship was a rather local custom and its formula and application technique were passed on between contractors.

An information letter from the cimorné company addressed to contractors and architects explained the cimorné technique and states, cited, '…once the cement render is executed, a technician is at your disposal to teach the projection technique during one or two days…' ('*...après cimentagé executé, un téchnicien est à sa disposition pour l'apprentissage de la projection, pendant un ou deux jours...*').

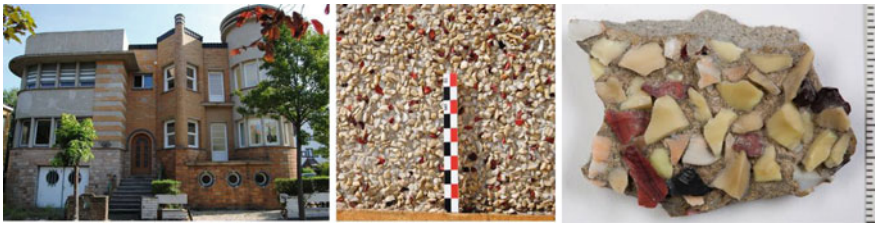

Fig. 1 Façade with grey cimorné zones (De Panne, Arch. L. Legein, 1936)—detailed picture of this cimorné finish with white, beige, yellow, black and dark red glass fragments—picture of the onsite lifted sample M1 (KIK-IRPA)

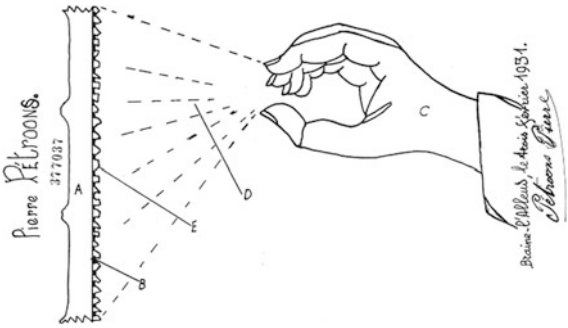

Fig. 2 Patent 377037 applied by Pierre Pétroons and demonstrates a manual projection method in order to apply the opalescent glass fragments onto the wet cement mortar (Patent BE377037, General State Archives, Brussels)

In order to facilitate the application and therefore the choice of this type of cladding, Pierre Pétroons sent his staff to architects and entrepreneurs to show the manual projection method (Fig. 2). Hence, written or iconographical data about the constituents or composition of the cement mortar are lacking. To compensate for this lacuna, retired plasterers were interviewed and their testimonies became of primary importance for the reconstruction of the cimorné formula and application method.

Despite the development of ready-mix plasters in the 1930s local entrepreneurs, consisting of masons as well as plasterers, mixed their cimorné mortar on-site, based on their personal experience and valid knowledge published in handbooks. The mason and plasterer manuals illustrate e.g. how to built a scaffolding, how to prepare a façade for rendering, how to apply mortars, which tools to use, different compositions for various purposes, etc. French, Belgian and Dutch manuals from the first decades of the twentieth century were consulted to expand the knowledge of application techniques and formulas of cement mortars. Although none of them mentions cimorné finish, decorative plasters based on Portland cement mortar in general are well described. These were compared to data resulting from testimonies of former practitioners and to results of laboratory analyses.

2 Plasterer and Mason Manuals

Regional available materials like Marbrite glass that was manufactured and commercialised by the S. A. Verreries de Fauquez in Braine-le-Comte (Belgium) and cement possibly coming from a cement factory in Hainaut (Stenvert 2010), were used to create cimorné finish. Being probably applied only in Belgium and the North of France, manuals published in both countries were searched. Although no sources of applications of cimorné façades in The Netherlands were found, some important manuals written by Van der Kloes, Oosterhof and Poptie were consulted (Table 1). The consulted manuals are related to a restricted publication period, the 1920s and 1930s, as cimorné was mainly applied in the period from 1932 until 1938. Thirteen manuals were found and thus selected for further research: lime-cement mortars were omitted and only data concerning cement mortars was selected. An overview of data found in different French, Dutch and Belgian manuals of the 1920s and 1930s related to the composition of cement mortars for outside use are summarized in Table 1.

The Dutch architect Van der Kloes (1845–1935) stated that the application of plaster is situated in between the expertise of the plasterer and this of the mason. He was the author of some important manuals about building materials in general, more specific about Portland cement mortars and their characteristics. Portland cement adheres well and possesses strong hydraulic properties. The supplement of gypsum to a Portland cement mortar must be avoided, since it was considered to be 'a depraved admixture' by Van der Kloes (1923, p. 144). Lime-cement mortars were created by the addition of lime, making the mortar cheaper, easier to apply and thus very popular in use. Too much lime added to cement was considered as reducing the watertightness and favouring shrinkage of the mortar. A mixture of 1 part cement, 1 part lime and 3 parts sand guaranteed a waterproof character (Van der Kloes 1908, p. 143). Mortars for exterior use were generally a mixture of 1 part cement to 3 parts sand. In general Portland cement was quite difficult to smear, but this 1:1:3 composition was quite easily applied according to Van der Kloes. It created a dull, sandy and unsightly look, but remained free of shrinkage and thus also crazing could be limited. At that time cement mortars were chosen over lime-cement mortars. All manuals mention Portland cement as being a 'miracle' product. Cement mortars were preferred for outside finishes and used to cover up entire façades as well as only plinths or details.

In general, a cement-sand ratio of 1 to 3 parts is advised for outside use in most of the manuals. Some of them prescribe a 'fat mortar' consisting of 1 part cement to 2 parts sand or even 1:1 proportions (Hanouille 1934; Chaplet 1938). Like Van der Kloes mentioned, this mixture is just enough waterproof. Hardly anything was documented about additives or retarders, which were often added on a trial-and-error basis. Moreover, this kind of information remained secret and was part of the mysteries of craftsmanship of the 1930s. To unveil these mysteries, former plasterers were interviewed.

Table 1 Overview of data found in different French, Dutch and Belgian manuals of the 1920s and 1930s related to the compositions of cement mortars for outside use

Manual	p.	Remarks	Trass	Lime	Cement	Sand	Water
Van Der Kloes, J.A., *Onze bouwmaterialen, deel III, Mortels en beton,* L.J. Veen, Amsterdam, 1908	143			1 part	1 part	3 parts	
Van Der Kloes, J.A., *Handleiding Voor Den Metselaar*, E.J. Brill, Leiden, 1923	150 150 240	To plaster For bricklaying For exterior use			1 part 1 part 1 part	2 parts 3 parts 3 parts	
Champly, R., *Béton armé enduits et agglomérés,* Desforges, Girardot et cie, Paris, 1931	15	For exterior use			100 kg	200 kg	
Poirson, *Encyclopéde Roret, Chaux, ciments, platre*, Paris, 1931	239	Cement mortar for coating			500–600 kg	1 m^3	
Oosterhof, *handboek voor den stucadoor,* van mantgem & de does, Amsterdam, 1932	58		½–1 part		1 part	3–5 parts	
Hannouille E., *Pour le Maçon et le Plâtrier*, Dunod, Paris, 1934	35 35 37	Renders Vertical rendering, very fat mortar		1 part/	/ 1 part 1 part	2 parts 2 parts 1 parts	0.4 l
Merciot, A., *Manuel du cimentier,* libr. Garnier frères, Paris, 1934	71 71	Exterior use Humid conditions			350–500 kg 660–800 kg	1 m^3 1 m^3	
Chaplet, A., *Pour le cimentier,* Dunod, Paris, 1938	24				1400 kg	1000 l	410 l
Nachtergal, A., *constructions civiles, matériaux de construction,* Rowart, Bruxelles, 1938	141				300–500 kg	1 m^3	
Poptie, *Handboek voor den stucadoor deel 1,* technische uitgeverij H. Stam, 1950	121	Rendering layer (1 cm thick)			1 part	3 parts	
Poptie, *Handboek voor den stucadoor deel 2,* technische uitgeverij H. Stam, 1950	19	Rendering layer			1 part	3 parts	

(continued)

Table 1 (continued)

Manual	p.	Remarks	Trass	Lime	Cement	Sand	Water
Beausoleil, O., *Les livres jaunes, n°2, maçonnerie, platre, ciment, carrelage,* La librairie du Midi, Bruxelles, 1966	22	Rendering layer Top layer			1 part 1 part	3 parts 2 parts	
Geldof, G.P., Stukadoren, technische uitgeverij H. Stam N.V., 1969	3 5 8 124	Rendering Rendering layer Float layer		1 1	1 part 1 part 1 part 1 part 2 parts	3 parts 5 parts 3 parts 3 parts 9 parts	

3 Testimonies of Former Plasterers

Recently, architects, owners and heritage agencies are confronted with a crucial need for information on how to conserve and restore cimorné plasters subject to several types of degradation phenomena. Hence, recently a growing interest in this local cimorné craftsmanship is noticed. Because of the limited knowledge found in the manuals and the lack of information about cimorné as a decorative finish, other sources had to be sought. The cimorné technique was mainly orally transmitted between Pierre Pétroons and other contractors. Retired plasterer Laurent Pays, who, in 2011, is 85 years old, carried out some demonstrations of the cimorné technique (Fig. 3). He was contacted and interviewed. Since his father was a former business partner of Pierre Pétroons, his testimony was very valuable for this study. Other retired plasterers were found via a call for information in local journals. In total, three retired plasterers communicated their experience with cimorné, its formula

Fig. 3 Left: Laurent Pays (middle) and his team carrying out a cimorné finish in the 1960s. Right: Laurent Pays has reached the age of 85 and demonstrated his technique in 2011

and application method. Each of them worked in a different region: the company of Gilbert Schoonheydt and his father was established in Halle, Romano Tondat and his father in Eeklo and Laurent Pays in Braine-l'Alleud.

According to their customs, the applied Portland mortar was composed of two or three rendering layers, depending on the condition of the masonry or concrete support. The rendering layer consisted of 1 part grey Portland cement and 2 parts sand. In contrast to the 1:3 composition described in the manuals, a 'fat mortar' was used and a top layer of about three to four millimetres was applied on the rewetted rendering layer. The cement to sand proportion of the top layer is 2:1 and thus not consistent with the previous results. Occasionally dry pigments were added to this top layer in order to create a suitable matrix for imbedding the projected coloured glass particles. This cement-rich layer must be sticky enough to favour the adhesion of the glass fragments that will be later on thrown into the wet mortar. So the formula of the top layer was chosen according to its adherence properties. To avoid quick drying of the top layer and consequently to extend the operating time for the projection of the glass particles, a commercial water retaining product named 'Pollux' was added to the rendering layer. (Interview and workshop Laurent Pays, 20.12.2012) The addition of water retaining products to the rendering groundlayer was however not recommended by Geldof, who suggested adding waterproof agents only to the top layer (Geldof 1969, p. 124). According to his book 'stukadoren', the rendering groundlayer of decorative plasters needed uniform and minor 'suction' properties to avoid differences in structure, texture and colour of the top layer. When the water repellent was added to the rendering layer, it 'burned' in case of extreme heat or sunlight (ultra-violet).

Occasionally Pays used linseed oil soap to improve the workability, but not retarders. The top layer was coloured by means of dry pigments added to the white cement and sand mixed in a 2:1 proportion. Chaplet described in 1938 'ciment blanc' (white cement) commercialised like 'hermine' and 'glyptolithe' (Chaplet 1938, p. 7). In contrast to Portland cement, a white cement based on white clay hardens rather quickly (Hanouille 1934, p. 27). He also mentioned the use of a small amount (<2%) of gypsum (plâtre) to enhance and sugar (like honey, dextrin, sucrose, lactose) to reduce the hardening time (p. 48) and discusses the coloration technique of mortars (p. 62). Laurent Pays himself applied pigments of *Stoopen &Meeûs* and *Bleu d'Outremer* (in Belgium also known as 'blauwselfabriek'), two Belgian companies situated near Antwerp and Ghent.

4 Results of Laboratory Analyses

To complete the data of manuals and oral testimonies, samples were lifted on-site and transmitted for further laboratory analysis (Table 2). Prior to the chemical and mineralogical analyses, the cimorné mortar samples were prepared according to a specific sample preparation method. Thin sections of mortar samples were prepared for further petrographical investigation to examine the type and characteristics of

the binder, aggregate and additives of the mortar sample. The yellow dye added to the resin used for the preparation of the thin section enables the analysis of the pore structure. Further, mortar specimens were imbedded in an inert epoxy resin and polished down to 1 μm grade using diamond pastes prior to the investigation with the optical microscope and SEM-EDX. At first the mortar samples were visually inspected under an optical microscope (ZEISS, Axioplan, reflection) to detect the number of layers, the homogeneity, impurities, etc. Subsequently the same samples, coated with a gold layer, were examined by SEM-EDX in order to examine the structure on a micro-level. The energy dispersive X-ray spectroscopy (EDX) enables the analysis of the constituting elements. Since the silicon content can be regarded as an indication for the hydraulicity of the binder, EDX analyses were performed to determine the average weight percentage of SiO_2 (silica) in relation to the total amount of SiO_2 and CaO. Finally, a chemical analysis was conducted to define the cement/sand ratio by pouring the mortar sample in a hydrochloric acid solution to dissolve the binder. In total, 5 samples of cimorné mortar lifted from the façades of different buildings have been investigated. The properties of the cement layers of the cimorné mortar are presented in Table 2.

From the results presented in Table 2 the use of cement as binding agent, with a silica content varying between 21.1 and 30 wt%, is noticed for both the rendering and the top layers. According to the colour, grey cement was used for the rendering layer while a lighter cement (probably white cement), appearing pale grey, was used for the top layer (the brownish hue of the three first cimorné samples in Table 2 can be explained by the addition of a small amount of iron as revealed by EDX analyses). The laboratory results are thus in agreement with Pays's testimony. The sand consists of quartz grains of which the size ranges from 80 μm to 1.73 mm (M6). The first three samples in Table 2 originate from Art Deco houses in De Panne, located South-East of the Belgian coast line, and contain a coarse quartz sand as aggregate with some lithics (sandstone, limestone and flintstone), as well as feldspar and glauconite grains (Figs. 4 and 5). The aggregate of the Pétroons' house sample on the other hand appears to be very pure quartz and only medium coarse. This villa was built around 1935 and covered with cimorné according to the 's-tandards' of cimorné's inventor. In the Molenbeek (Brussels) sample again a coarse quartz sand is found but with a different composition since only feldspar grains can be identified.

The cement:sand volume ratio for the rendering layer can be generalized to 1:1, although the abovementioned sources reveal a 1:2 proportion. Chaplet and Hannouille mentioned this proportion for a 'vertical rendering' and 'very fat mortar' (Table 1). The cement:sand ratio of the top layer (without the glass fragments) can hardly be precisely determined because of its limited thickness. The cement content is estimated as 3 to 6 times the sand content. The cement content determined analytically is hence considerably higher than the 2:1 ratio applied by Laurent Pays. Again a very fat mortar was applied in order to create a sticky surface onto which the projected glass would properly stick.

Table 2 Properties of the cement layers of the cimorné mortars

Code	Provenance	Layer	Colour	Thickness (mm)	Binder	Sand (type and maximum grain size)	Binder/sand-volume ratio
M1	House, Corner Dumontlaan-Visserslaan, De Panne	Rendering	Grey	3	Cement	Coarse, quartz, 1.38 mm	5:4
	(1937)	Top	Brown	2	Cement	Coarse, quartz 1.17 mm	11:2
M2	House, Visserslaan 28, De Panne	Rendering	Grey	8	Cement	Coarse, quartz 0.93 mm	1:1
	(1936)	Top	Brown	2	Cement	Coarse, quartz 1.32 mm	7:2
M3	House, Corner Dumontlaan-Visserslaan, De Panne	Rendering	Grey	3	Cement	Medium, quartz 0.90 mm	7:6
	(1937)	Top	Brown	2	Cement	Fine, quartz 0.39 mm	14:3
M5	Pétroons' house, Braine-l'Alleud	Rendering	Grey	3	Cement	Medium, quartz 0.52 mm	4:3
	(1935)	Top	Pale grey	2	Cement	Medium, quartz 0.52 mm	13:3
M6	House, Molenbeek (Brussels)	Rendering	Grey	15	Cement	Coarse, quartz 1.73 mm	1:1
	(1937)	Top	Grey	2	Cement	Coarse, quartz 1.13 mm	7:2

Fig. 4 Samples M1, M2, M3, M5, M6. (KIK-IRPA)

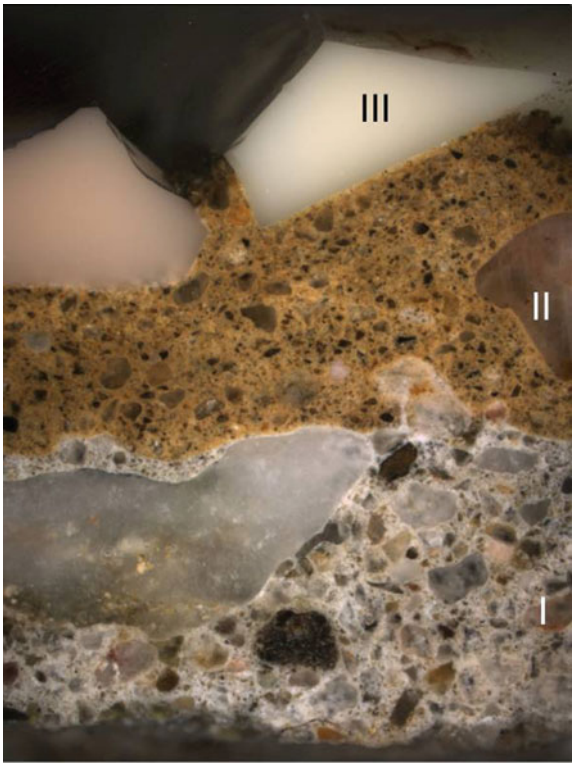

Fig. 5 Optical microscopic captured image of cimorné sample M1 with rendering layer (I), brownish top layer (II) and white opalescent glass fragments (III) (KIK-IRPA)

5 Restoration Challenges: Beyond Cimorné Formulas

Little information about the cimorné's formula was available. In an attempt to reconstruct this formula, a range of crucial sources was consulted and manuals of the interwar period were searched for instructions about the used binder and aggregates. They remain vague and only mention some cement-sand ratios. Because of its local development and application, cimorné is not included in these manuals. Hence guidelines for decorative plasters in general were listed. Former craftsmen were interrogated about their experiences with cimorné and the overall applied mixtures. Only three of them were traced and interviewed. Furthermore, contractors had their characteristic trade secrets and habits. Since cimorné technique was orally transmitted and passed on from father to son, a general formula does not

exist and cannot be searched for. However, the results of laboratory analyses confirmed the use of a cement-sand mortar (grey cement for the rendering layer and probably white cement for the top layer, the latter being sometimes coloured) and indicated the use of a medium to coarse quartz sand. Presumably contractors opted for raw materials that were easily available and built up their know-how based on experimenting and trial-and-error processes.

The obtained results are not exact, but provide insight into the composition of cimorné façades. Reconstructing the cimorné formula is only a minor step towards future restoration of this peculiar façade finish. The damage pathologies need to be mapped and further monitored in order to succeed in the conservation and restauration of damaged cimorné façades. The application methodology for the reparation of the cimorné plaster is crucial to contribute to a durable and sustainable restoration strategy. Therefore demonstrations and a workshop where Laurent Pays showed and transmitted his know-how to a team of restorers were organised. Once the original formula, the application technique and the damage patterns are known, on-site restoration trials will be carried out. Since marbrite glass production stopped in the 1960s, hardly any marbrite glass is left and thus a substitute material need to be defined. Further research and on-site test strips are essential, not only to reconstruct cimorné's formula, but to define correct restoration strategies for cimorné finish.

Acknowledgements The authors would like to thank Laurent Pays, Romano Tondat, Gilbert Schoonheydt, Françoise Lombaers and Claire Fontaine.

References

Appel aux cimenteurs ou granitistes Entrepreneurs bien entendu, archival records Archives d'architecture Moderne, Brussels.

Brevet cimorné, bureau à Braine-l'Alleud, archival records Archives d'architecture Moderne, Brussels (1932).

Chaplet, A. (1938). Pour le cimentier. Dunod, 189p.

Dekeyser, L., Verdonck, A., De Clercq, H., & Wouters, H. (2012). Marbrite Fauquez opalescent and mass coloured glass: History, production and composition. In J. Jasienko (Ed.), *Proceedings of the International Conference on Structural Analyses of Historical Constructions* (pp. 1106–1113). Wroclaw: University of Wroclaw.

Fontaine, L. (2011). Decoratieve bepleisteringen, materiaalanalysen, report of laboratory analyses. Royal Institute for Cultural Heritage.

Geldof, G. P. (1969). *Stukadoren*, Technische uitgeverij H. Stam N.V (239p)

Hanouille, E. (1934). Pour le maçon et le plâtrier, Dunod (180p).

Stenvert, R. (2010). Mooier voor minder: cementlagen en betonafwerking, in Stuc, Kunst en Techniek, E. F. Koldeweij (Ed.), Waanders uitgeverij, ISBN 9789040086502 (pp. 412–425).

Van der Heiden, P. C. (2010). Portlandcementpleister: geen kleur is ook een kleur, in Stuc, Kunst en Techniek, E. F. Koldeweij (Ed.), Waanders uitgeverij, ISBN 9789040086502 (pp. 392–405) Waanders uitgeverij, ISBN 9789040086502.

Van der Kloes, J. A., (1908). Onze bouwmaterialen, deel III: Mortels en beton, L.J. Veen (275p).

Van der Kloes, J. A. (1923). Handleiding voor den metselaar, E.J. Brill (291p).

Historic Renders and Their Weathering at the Temple Wat Mahathat, UNESCO World Heritage Site of Ayutthaya, Thailand

H. Siedel, E. Wendler and B. Ullrich

Abstract Investigations of renders on buildings of the temple Wat Mahathat in Ayutthaya showed that two different types of mortars have been applied. The original mortars from the period before 1767 are lime mortars, whereas hydraulic mortars were obviously used for restoration and stabilisation of the ruins in the 20th century. The use of organic additives like starch from boiled rice for historic mortar production is suspected, but could not be proved by analytical means. The analysis of probable additives is made more difficult due to microbiological activity in tropical climate which might heave lead to enzymatical decomposition of the primary organic compounds. The porosity and the hardness of renders, analysed in situ by easily applicable, non- or less-destructive investigations like Karsten tube measurements and drilling resistance, reflect a wide range of different weathering states. Therefore, appropriate restoration measures must be planned in detail for every part of the buildings; an overall treatment with water repellents cannot be recommended. The formation of peculiar, alveolar-like structures on some renders is caused by hardening of the surfaces along cracks due to intensified transport of dissolved components.

Keywords Rendered brickwork · Lime mortars · Hydraulic mortars
Organic additives · Weathering

H. Siedel (✉) · B. Ullrich
TU Dresden, Institute of Geotechnical Engineering, Dresden, Germany
e-mail: Heiner.Siedel@tu-dresden.de

B. Ullrich
e-mail: Bernd.Ullrich@tu-dresden.de

E. Wendler
Munich Stone Conservation Laboratories, Munich, Germany
e-mail: e.wendler@t-online.de

J. J. Hughes et al. (eds.), *Historic Mortars*,
https://doi.org/10.1007/978-3-319-91606-4_4

1 Introduction

The temple Wat Mahathat, a former royal monastery, is one of some historic temple complexes at the site of the old capital of Thailand, Ayutthaya, which was destroyed by Burmese invaders in 1767 and fell into ruins after the capital was moved to Bangkok. Ayutthaya is situated about 70 km north of Bangkok. The entire site which became part of the UNESCO World Heritage in 1991 is located on the banks of the Lop Buri River. An oxbow of this river offered a natural defence to the old capital on the north, west and south, whereas a canal on the east across the neck of land made the city an island and completed its defences as early as in the 14th century (Van Beek and Invernizzi Tettoni 1999). The buildings and walls of Wat Mahathat erected between the 14th and the 18th century are made of bricks covered with renders and plasters, and ornamented with stucco. The complex of the temple consisted of a central prang (sanctuary), i.e. a tall building with rounded top, ringed by open courtyards, enclosed by a wall and smaller prangs, a construction scheme which goes back to the older Khmer style architecture (Van Beek and Invernizzi Tettoni 1999). A large ubosot (the congregation and ordination hall of a monastery, reserved solely for the monks) and some vihans (assembly halls for monks and laity) can still be recognised by remnants of bases and walls. The rebuilt, second central prang from 1633 which had a height of about 50 metres collapsed again in 1911. Today only its base has remained. Little is known neither about the history of the site since the destruction nor about younger restoration measures from the 19th and 20th century, respectively. In 1956 the Fine Arts Department of Thailand undertook excavations around the central prang. Although in ruins today, the temple is still one of the most impressive places in historic Ayutthaya and attracts thousands of visitors every year. A field campaign at Wat Mahathat aimed at the characterisation of the remnants of renders on the walls of the buildings and of the enclosure. Furthermore, the weathering state of the remnants is characterised.

2 Setting and Sampling Strategy

At first sight, the remnants of renders exposed on the brick walls show visibly different states of weathering or preservation, respectively. Some of them seem to be weak with rough, sandy surfaces. Others are rough, but stable and stained by thin black surface layers, whereas another group shows dense, smooth and sometimes glossy surfaces. The thickness of the renders reaches from some millimetres up to some centimetres; the thicker ones were applied in at least two layers. Since the possibility to take samples was limited at the Heritage site, representative, visually different types of mortars were sampled at six points selected together with Thai experts from the Fine Arts Department and the Silpakorn University Bangkok (Table 1; Fig. 1). Unfortunately, the samples could not be assigned to certain construction or restoration periods, because detailed knowledge about the construction history and also about younger restoration measures is still lacking. Most

Table 1 Locations of sampling and in situ measurements and the investigated mortars

Sampling place	Description	Mortar	Peculiarities
MHT1	East side of the inner enclosure wall, near the SE corner; render	Light grey to brownish mortar; brick in the aggregate; lime lumps (MHT1/S2 and S3)	Different weathering states from smooth ("polished") to rough, back-weathered surface; cracks, in places alveolar-like structures
MHT2	Fragment of the southern wall of the ubosot (congregation and ordination hall), east of the inner enclosure; render	Light grey mortar; lime lumps, brick in aggregate; rarely shell fragments (MHT2/S6)	Stained black on the rough surface
MHT3	Architectural fragment with pillar bases from the central prang, render/ stucco with ornaments, three layers (ca. 5 cm thick)	Light grey mortar with lime lumps (sample from the outermost, 2 cm thick layer = MHT3/S7)	Black stained, rough surface
MHT4	Isolated architectural fragment fallen from the central prang, with thick render (at least five layers on brick)	Outermost grey render mortar with smooth, dense surface (MHT4/S8)	Partly stained black
MHT5	Render from a niche of the smaller prang outside the enclo-sure wall at the SW corner	Light grey mortar in two layers (MHT5/S10)	Rough on the surface; limestone pieces in the aggregate
MHT6	South side of the inner enclosure wall, near the SE corner; render	Light grey to brownish mortar (samples: MHT 6/ S12 = smooth render; / S13 = joint mortar); brick in the aggregate; lime lumps	Different weathering states from smooth ("polished") to rough, back-weathered surface; cracks, in places alveolar-like structures

likely the original renders belong to the last rebuilding period in the 17th and 18th century. The selected samples cover the range of different mortars that can be found today at Wat Mahathat and their weathering behaviour in tropical climate. Non-destructive and less-destructive in situ measurements (capillary water uptake with Karsten tube and drilling resistance) completed the investigation programme. Bearing in mind that in South East Asia and India there is an old tradition of using organic additives like molasses (from sugar cane) or water from boiled rice in making plasters, renders and stucco (Sirirat 1999; Chandra 2003), laboratory investigations were carried out to detect eventual small amounts of such additives. Moreover, special attention was drawn to the alveolar-like weathering structures on the walls of the inner enclosure.

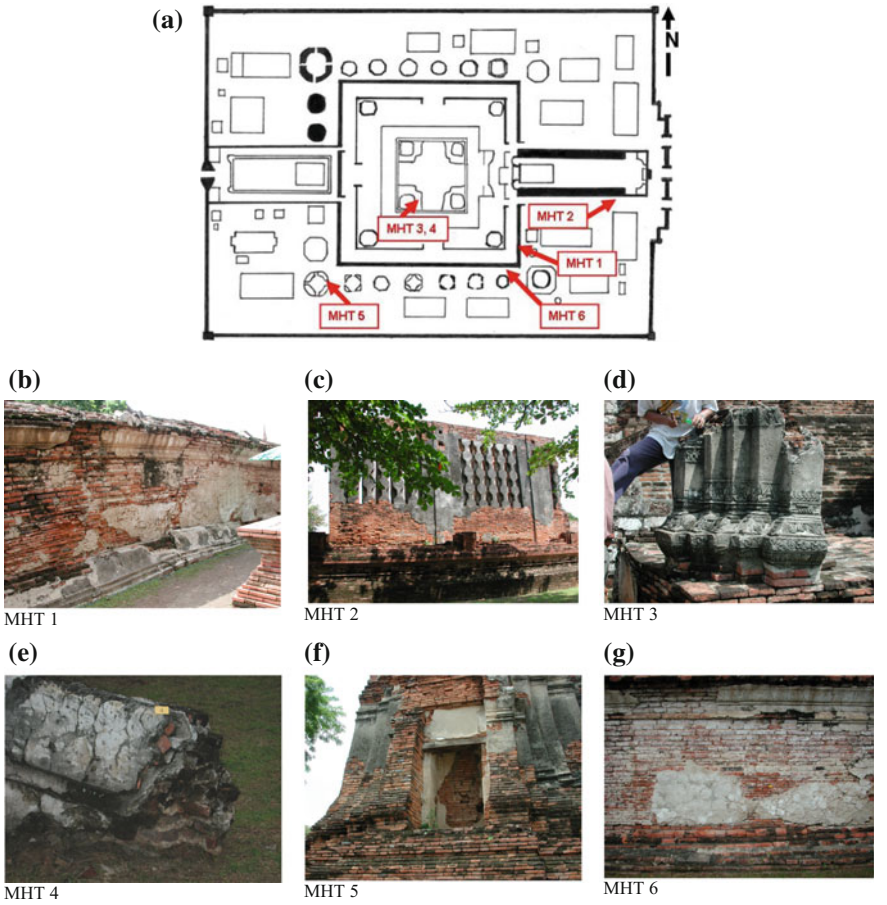

Fig. 1 **a**–**g**: Sketch map of Wat Mahathat (**a**) and documentation of places (**b**–**g**) where material samples were taken and in situ measurements were carried out (cf. Table 1)

3 Methods

Capillary water uptake per time was measured at various points on the surface of renders in situ by Karsten tube. In case of normal capillary suction (without water transport parallel to the surface or to the depth due to cracks), a w-value [kg/m^2 h$^{0.5}$] comparable to the C-value according to DIN EN 1925 can be calculated from the obtained curves (Snethlage and Wendler 1989; Siedel and Siegesmund 2014).

Drilling resistance (DR) (Wendler and Sattler 1996; Siedel and Siegesmund 2014) was measured with a "Durabo" apparatus to test the hardness of renders with high resolution from the surface to the depth. Since the diameter of the drill bit is only 3 mm, the method can be considered to be a 'less-destructive' investigation.

The binders of all samples were concentrated by carefully grinding them in an agate mortar and segregating coarse aggregate by sieving. These were characterised for their constituent phases by analysis with X-ray diffraction (XRD) and combined differential thermal analysis (DTA) and thermogravimetric analysis (TG). After thermal analyses with up to 1000 °C heat treatment, they were characterised by XRD again. XRD was performed with Siemens D5000 equipment ($Co_{K\alpha}$, 40 kV, 30 mA, 5–80°, step 0.02°, step time 4 s), DTA/TG with a Netzsch STA 409 PG (in static air, temperature range 25–1000 °C, heating rate 10 K/min). Polished thin sections and rough, broken mortar pieces of selected samples were additionally studied with optical and scanning electronic microscope (SEM). For investigations under SEM analysis was conducted using a Zeiss EVO 50 coupled with a ROENTEC detector XFlash 3001 for standardless elemental analysis by energy-dispersive spectroscopy (EDS). The respective samples were coated with Au/Pd.

Portions of the powdered mortar specimen (some 200 mg) were dispersed in 3 ml of distilled water in an ultrasonic bath for 10 min and then heated up to 80 °C in a water bath for a further two hours. After centrifugation at 4800 U/min for 5 min, the pH and the amount of nitrate in the filtrate have been measured. Then, small portions of the clear solution were analysed qualitatively for starch by a iodine/potassium iodide solution. The clear liquid was evaporated on a glass plate, and FTIR spectra were taken from the deposits (ATR technique, JASCO FTIR spectrometer 4100).

Since starch from rice was the most probable organic component to be expected, a reference sample was produced using pure quartz sand and pure calcium hydroxide (proportion 2:1). A mortar from these components has been prepared using the water from boiled rice. For completion of the mortar curing (carbonation), the specimen was wetted with distilled water once a week for three month. The p_H dropped towards neutral within an outermost 3 mm layer showing that calcium carbonate formation was completed in this zone.

To hydrolyse possible traces of oils/fats or proteins, the remainder from the water extraction was treated with 2 N hydrochloric acid and, after completion of the CO_2 formation from the carbonates, extracted with chloroform (trichloromethane). After removal of the solvent by evaporation on glass plates, FTIR spectra have been taken from deposits (if present).

4 Results

4.1 Phase Analysis of the Binders

The results of phase analyses are given in Table 2; typical DTA/TG patterns are displayed in Fig. 2. According to the results of phase analysis of the binders, all samples could be assigned to one of two groups: pure or slightly hydraulic lime

Table 2 Results of phase analysis of the binders

Sample no.[b]	Calcite (XRD)[a]	Calcite (DTA)	Exothermic reaction 320–340 °C (DTA), weight loss TG (%)	XRD after DTA (1000 °C)
MHT 1/S2 I and II	++/++	++/++	1.03/1.23	Lime, little larnite
MHT 1/S3 II	+	+	1.79	Wollastonite, little lime
MHT 2/S6 I and II	+/++	+/++	1.78/1.57	Lime
MHT 3/S7 I	++	++	1.69	Lime, little larnite
MHT 4/S8 I	+	+	1.65	Wollastonite, no lime
MHT 5/S10 I and II	+/+	+/+	1.38/1.21	Wollastonite, no lime
MHT 6/S12	+	+	1.01	Wollastonite, no lime
MHT 6/S13 joint	++	++	1.13	Lime, little larnite

Quartz and feldspar from the aggregate occurred in all samples and are not mentioned in the table
[a]assessed by relative peak height [b]Roman numerals: I—near surface; II—behind surface

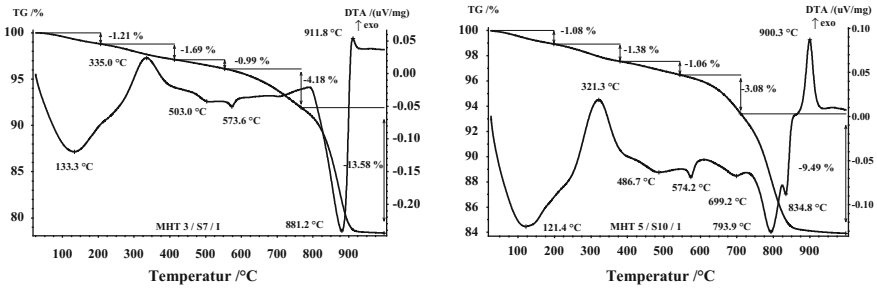

Fig. 2 Typical DTA/TG diagrams of mortars from Ayutthaya: MHT 3/S7 I (lime mortar/stucco, left) and MHT 5/S10 I (hydraulic mortar, right)

mortars (MHT 1/S2, MHT 2/S6, MHT 3/S7, and the joint mortar MHT 6/S13) and hydraulic mortars (MHT 1/S3, MHT 4/S8, MHT 5/S10 and MHT 6/S12). At least some of the latter seem to be modern cement mortars with little calcite, which might have been produced by carbonation of the surface layer. They are regarded as materials of younger restoration measures from the 20th century, which are not well documented at Wat Mahathat. EDS analyses of binder areas in a thin section of MHT 6/S12 under the SEM showed high contents of SiO_2 beside CaO (in a relation of about 1:2). The formation of a wollastonite phase ($CaSiO_3$) and no or little lime (CaO) after 1000 °C heat treatment suggests a remarkable content of reactive SiO_2 in the binder, whereas the mortars with high calcite contents form high lime

contents and sometimes traces of larnite (Ca_2SiO_4=C_2S) after heat treatment. The latter might be due to low contents of hydraulic phases (e.g. formed by reaction of brick fragments in aggregate or minor clay contents in the sand).

Obviously, the stucco with ornaments from a fragment of the central prang, the blackened render fragments on the brickwork of buildings as well as the analysed joint mortar are lime mortars. Hydraulic mortars, presumably younger additives, occur in some places on the walls of the inner enclosure, on a fragment of the central prang and in the niche of a smaller prang outside the inner enclosure.

Figure 3 shows the relation of the weight losses according to TG at temperatures between 200 and 600 °C (mainly assigned to hydraulic phases which cannot be clearly distinguished in thermal analysis due to their continuous weight loss over a wide range of temperatures, cf. Fig. 2) and >600 °C (assigned to carbonate phases; Moropoulou et al. 1995, 2005) for all investigated samples. The weight loss between 200 and 600 °C used for calculation was corrected by subtracting the weight loss assigned to ignition of organic matter, indicated by an exothermic reaction in DTA (see below). The results, which are in good accordance with the results of XRD analysis (cf. Table 2), allow to distinguish between the pure lime mortars (samples MHT 2/S6 I and II, green), weakly hydraulic limes (MHT1/S2 I and II, MHT 3/S7 I, MHT 6/S13 joint, red) and hydraulic limes (blue).

Some mortars (MHT 1/S3, MHT 2/S6, MHT 3/S7, MHT 4/S8) show a remarkable exothermic reaction in the DTA, connected with weight loss in the TG in the temperature range between 200 and 400 °C (Table 2). This might be due to the ignition of organic matter at these temperatures. The respective mortars show blackened surfaces (MHT 2/S6, MHT 3/S7 and MHT 4/S8) or green staining underneath the surface (MHT 1/S3, Fig. 4) due to microbiological activity.

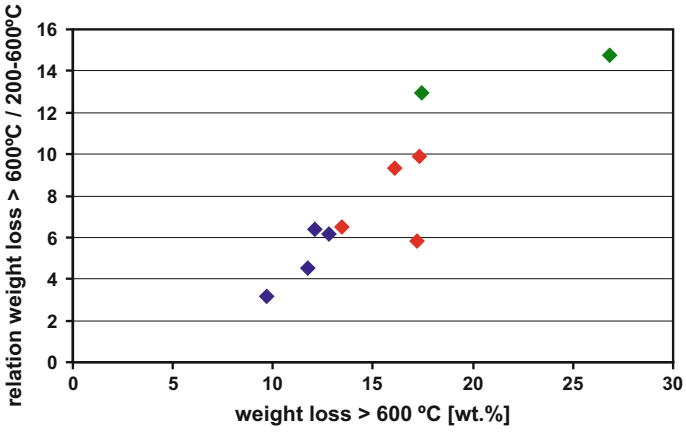

Fig. 3 Weight losses in TG indicating carbonate phases vs. those indicating hydraulic phases (Moropoulou et al. 1995, 2005) for the investigated samples. Green: pure lime mortars (MHT2/S6); red: slightly hydraulic mortars (MHT 1/S2, MHT 3/S7 and MHT 6/S13), blue: hydraulic mortars (MHT 1/S3, MHT 4/S8, MHT 5/S10 and MHT 6/S12) (Color figure online)

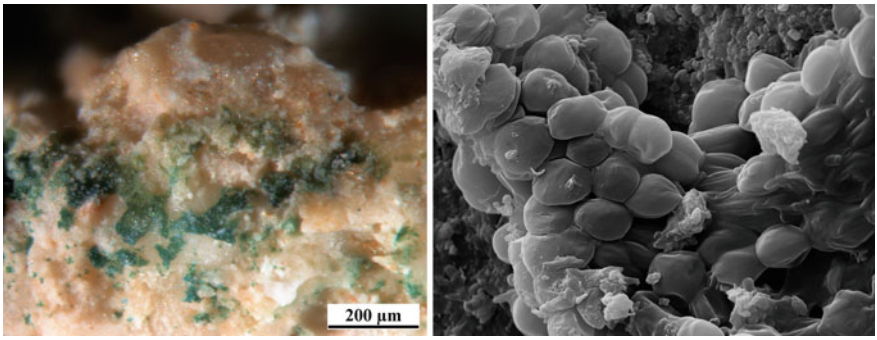

Fig. 4 Organic matter in the surface zone of mortar MHT 1/S3 in higher magnitude under the optical microscope (left) and SEM (right; right figure margin = 20 µm). EDS analyses of the structures in the SEM micrograph showed very high carbon contents

4.2 Investigations into Organic Additives

Because of the tradition of mortar making with organic additives in Thailand and taking into account the results of the phase analysis from Table 2, additional laboratory analyses were made on selected samples to extract and determine potential organic compounds. The main criterion chosen was the content of lime (as a marker for original historic mortar material).

As can be seen from Table 3, starch is not present in the investigated samples of the monument. However, it is most probable to assume that it has been decomposed after centuries with the help of microorganisms which might be rather active under tropical conditions. Two of the mortars contain significant amounts of nitrate which might be a product resulting from protein decomposition.

As expected from Table 3, the FTIR spectrum of sample MHT 1/S3 II does not fit to the vibration bands of starch extracts (Fig. 5a). However, C–H-vibrations at some 2900 cm^{-1} can be clearly recognized. Comparing with the spectrum of gum arabic (Fig. 5b), there is a much better correlation though there are some deviations in the fingerprint region due to contaminations with clay and lime. Identical (gum) spectra have been obtained with samples MHT 1/S2 II and MHT 3/S7 I. Some of the samples contained small amounts of oils, and the joint mortar sample MHT 3/S7 I even showed some trace of a nitrogen-organic compound (but no protein could be found).

4.3 Surface Hardness and Water Uptake of Mortars

Mortars with different weathering states were investigated with respect to their surface hardness and capillarity suction. These parameters are essential for the planning of conservation measures: hard surfaces do not need to be strengthened,

Table 3 Results of qualitative analysis of organic additives, supported by pH and nitrate content (wt%) of the aqueous extractions as well as by FTIR analysis (n.d. = not determined)

Sample no.	Starch	Gums	Oils/ protein	p_H	NO_3^- (%)	Comments
MHT 1/S2 II	–	+	±	6.5	<0.1	
MHT 1/S3 II	–	+	++	n. d.	n.d.	carboxylic acids[b]
MHT 2/S6 II	–	–	+	6.0	1.2	carboxylic acids[b]
MHT 3/S7 I	–	+	±	6.0	<0.1	
MHT 6/S13	–	–	?[d]	6.0	1.0	N-containing organic comp[c]
Reference[a]	+	–	–	6.0	–	

[a]Artificial lime mortar admixed with water from rice boiling
[b]after acid hydrolysis in $CHCl_3$-extraction. [c,d]after acid hydrolysis in water-extraction
[d]chemical composition not detectable by FTIR

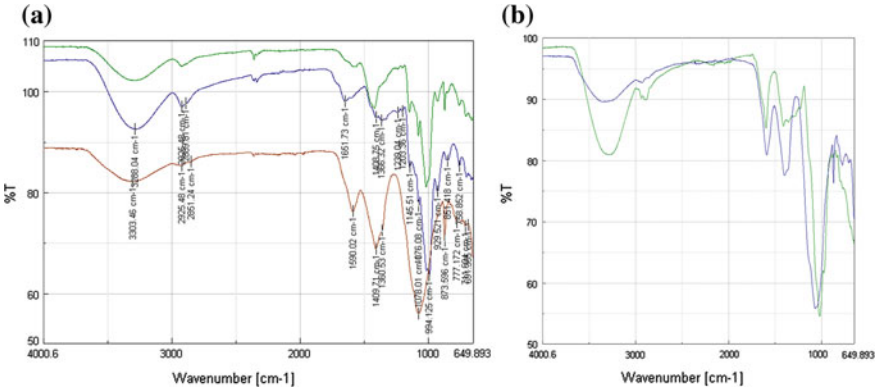

Fig. 5 **a** FTIR-Spectra from: hot water extractions of starch-containing reference mortar (green) and of sample MHT 1/S3 II (brown); water from boiling rice (blue); **b** FTIR-Spectra from hot water extractions of: sample MHT 1/S3 II (blue) and gum arabic (green) (Color figure online)

and the rates of capillary water absorption give information about the possibility to apply liquid consolidants or water repellent agents. However, the use of the latter is only useful if the uptake of rain water is certainly known to be the predominant factor of weathering.

Especially at the inner enclosure wall (MHT 1, MHT 6), humidity measurements show a high degree of moisture immediately below the render surface, which may lead to a transport and enrichment of dissolved components towards the surface (along the gradient of evaporation).

Dense mortars showing low capillary water uptake can be found in visibly intact areas with smooth, "polished" surfaces (on the enclosure wall, MHT 1 and 6, and on the fragment from the central prang, MHT 4, see Fig. 6). These renders normally consist of two layers: as confirmed by DR measurements, the polished surface is

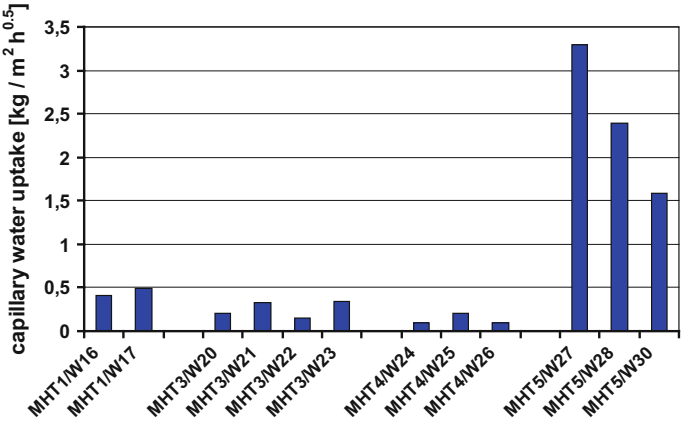

Fig. 6 Capillary water uptake (w values) calculated from Karsten tube measurements. The values displayed for area MHT 1 are also representative for area MHT 6

very hard due to sinter formation, while the interface between the two layers shows a low strength (insufficient contact), and in many cases, the outermost layer is already missing. In these cases, a hardened zone can also be found on top of these secondary surfaces, due to further transport of dissolved electrolytes (lime, silica) and deposition in the surface structure. Generally, the contact between the render and the brick underneath is rather poor in many cases.

Mortars with rough but stable surface and black staining may show a high capillary water uptake (MHT 2). Water absorption coefficients (w-values) for area MHT 2 could not be calculated due to irregular behaviour of the water uptake (influenced by water transport along cracks or parallel to surface), therefore results for this area are not displayed in Fig. 6. On the other hand, similar surfaces may have reduced capillarity (MHT 3), possibly due to "sealing" of the pores with organic matter.

All in all, the measured capillary water uptake scatters between 0.1 and 3.5 kg/m^2 $h^{0.5}$ (Fig. 6). The highest values were measured at a very soft render on the smaller prang (MHT 5), which is a poor hydraulic mortar with high portion of aggregates in a sheltered position inside a niche. In many cases, the results obtained from Karsten tube measurements suggest different pathways of water transport besides regular capillary water uptake, i.e. transport along cracks or parallel to the surface.

4.4 Patterns of Differential Erosion

Bizarre weathering structures frequently occur on the walls of the inner enclosure (MHT 1 and 6, Fig. 7). Similar patterns are also known from other places and are

Fig. 7 Alveolar weathering of renders on the enclosure wall (MHT 1, left, and detail from MHT 6, right). As can be seen on the right, the ridges are often preserved along cracks

often explained as a result of the formation of Liesegang patterns during the carbonation process (Rodriguez-Navarro et al. 2002) and subsequent differential erosion (Delgado Rodrigues 2016; Rodriguez-Navarro 2012; Dotter 2010). On the other hand, they are similar to those called "alveolar weathering" or "honeycomb weathering" on natural stones (e.g. Siedel 2010) with small "walls" or ridges that in parts still represent the original surface, surrounding deep, back-weathered "holes" between them. Although salts are often a driving force in the formation of alveolar structures in natural stone, no efflorescence or other activity of soluble salts could be detected in case of the renders in Ayutthaya. Most of the ridges are flanking a system of connected cracks in the mortar surface which might have already developed during shrinking of the thick render layers at an early stage of setting. Ridges along a directly connected network of shrinkage cracks in renders were also observed by Delgado Rodrigues (2016), who interpreted these structures as the result of higher weathering resistance of the respective areas due to intensified carbonation, facilitated by better access of CO_2 from air. However, the typical concentric, ring-shaped wall structures within the "cells" surrounded by the above mentioned ridges with cracks are lacking in Wat Mahatat. These patterns, called "flos tectorii" in Italian literature, might be assigned to differential erosion of "Liesegang rings" with higher or lower concentrated carbonated binder (Delgado Rodrigues 2016). In contrast, in the renders described here irregular shaped "isles" and "holes" within the cells marked by the surrounding system of cracks can be found. Measurements of DR topography of a weathered render surface show hardened surfaces on the ridges (and on the smooth surface of the visibly intact outer render layer), whereas the surfaces at the bottom of the adjoining holes are softer (Fig. 8a). Microscopic investigations on a thin section of a ridge structure displayed thin layers of silica coating the surfaces along the crack between the two flanks of the ridge (Fig. 8b). This indicates an intensified capillary transport of dissolved matter ($Ca(OH)_2$/lime, soluble silica) from the mortar to the evaporation zones along the cracks (arrows in Fig. 8a) and also on even surfaces in the neighbouring areas. As shown by Karsten tube measurements (cf. Fig. 6), the latter

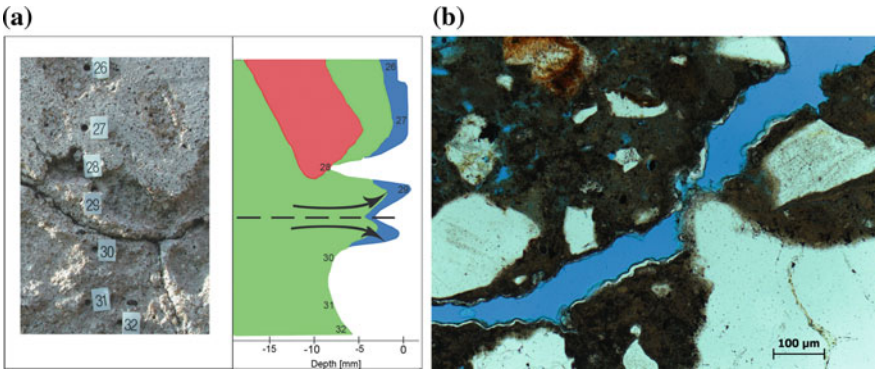

Fig. 8 **a** Drilling resistance measurements no. 26 to 32 along the surface topography of a render structure. Blue: very hard material on the surface of the outermost render layer (26, 27) as well as on the flanks of the cracks (29). Red: very soft zone between the two render layers = zone of detachment. Green: normal strength of the inner render layer. Dashed line: crack. Arrows: transport of electrolytes (Ca^{2+}, OH^- and mobile silica?) towards the surface zone, reinforcing the flanks by deposition of minerals. **b** Thin section across a ridge with two flanks and a crack in between at higher magnitude. The edges of the crack show a light, thin layer of silica (as chemically analysed by EDS in SEM) (Color figure online)

are dense, which is in good accordance with the higher DR measured near the surface. The intensive wetting of walls and ground during the rainy season in tropical climate provides enough water for intensive capillary transport of soluble components to the evaporation surfaces during the drying process in the dry season. Selective hardening of the border zones flanking the crack areas might thus lead to their better resistance against surface weathering. At the same time, the zones beneath the render surface next to the hardened zones along the cracks are depleted in binder, thus loosing contact to the underlying material when stressed by hygrothermic changes. It seems worth to be mentioned that the areas showing these deterioration patterns are mainly situated near the bottom of the walls, where the moisture is continuously rising from the ground into the wall even in the dry season. The transport rate of dissolved matter through the render near the ground is higher compared to that on the upper parts of the wall. Observations and measurements at the walls of Wat Mahathat lead to the assumption, that the driving force for the formation of differential erosion in the renders in our case is capillary transport, migration and precipitation of dissolved $Ca(OH)_2$ or lime, respectively.

5 Discussion and Conclusions

The investigation of representative samples from renders of the temple Wat Mahathat in Ayutthaya showed different types of mortars. Lime renders (some of them slightly hydraulic), often blackened on the surface due to microbiological

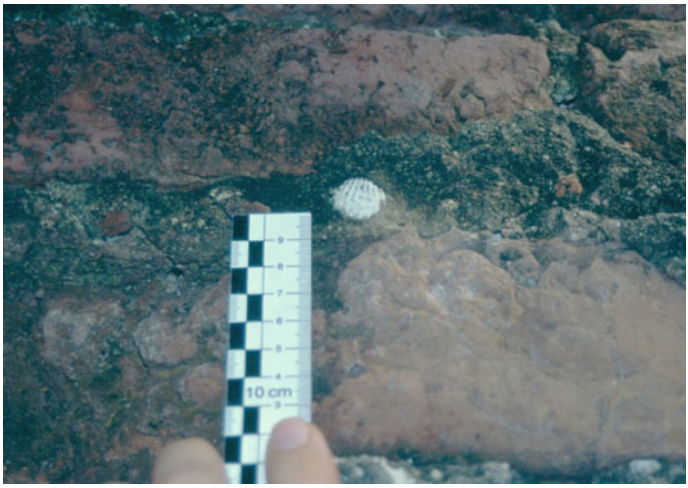

Fig. 9 Shell in a joint mortar in area MHT 2

activity, can be found on ruins of the halls and prangs and in some places on the enclosure walls. Samples taken from the enclosure walls, a niche of a smaller prang as well as on a brickwork fragment from the central prang turned out to be hydraulic mortars. They might be assigned to younger restoration measures from the 20th century, whereas the lime renders are most likely original historic mortars. The limestone for lime production might have come from a deposit of Permian, purely calcitic limestones at the Pasak River, north-east of the town Saraburi, which is the nearest outcrop of limestones in the surroundings of Ayutthaya (40 km away). Remnants of shells in some renders and joints (Fig. 9) indicate that a use of lime deposits from the sea (Gulf of Siam) is also possible. The location of Ayutthaya at the confluence of big rivers, the Pasak and the Chao Phya, might have facilitated the transport of lime from these sources to the site.

TG analysis clearly showed the presence of 1–2% of organic matter. Although the use of organic additives during ancient mortar production in Thailand is likely, analytical approaches carried out to prove this hypothesis were not successful. Small amounts of starch in a reference mortar made with water from rice boiling could be easily detected, whereas the same test was negative on the historic samples. It has to be taken into account, however, that intensive rain and microbiological activity in tropical climate have most probably lead to enzymatic decomposition of the primary organic compounds within some hundred years. Other organic components like oils, gums or even N-containing compounds could be identified, but these may also come from biochemical conversion of precursors, from a present biocolonization itself or even from material input of younger restoration measures.

The weathering state of the renders is different with respect to their drilling resistance and porosity (i.e. capillary water uptake). Therefore, decisions about

appropriate restoration measures for certain parts of the buildings should be made step-by-step on the basis of easy, non- or less-destructive measurements (Karsten tube, DR). An overall hydrophobic treatment of the entire surface of buildings cannot be recommended because of the very different capillary suctions of the material surfaces and due to the risk of moisture infiltration through cracks which would even lead to severe damage.

The peculiar structures of differential erosion found on some surfaces of renders on the inner enclosure wall can be explained by local depletion and enrichment of binder contents due to dissolution, capillary transport and deposition of binder compounds. The strong wetting-drying cycles in tropical climate might have intensified this process. More detailed research is needed to completely understand the formation of inhomogeneities in the renders and the mechanism of their different weathering.

Acknowledgements Thanks are due to the Deutsche Forschungsgemeinschaft and the National Research Council of Thailand for financial support of the field campaign of H.S. and E.W. in Ayutthaya. Special thanks to Chompunut Prasartset (Silpakorn University, Bangkok), Malatee Taiyaqupt and Pongsak Pongprayoon (Chulalongkorn University, Bangkok), Sumalee Sirirat (The Fine Arts Department of Thailand) and all other Thai colleagues who helped with organisation, sampling and information. Thanks also to Ute Steinhäusser for the FTIR investigations and to John J. Hughes for critical comments which helped to improve the manuscript.

References

Chandra, S. (Ed.). (2003). *History of architecture and ancient building materials in India*. New Delhi: Tech Books International.

Delgado Rodrigues, J. (2016). Liesegang rings in differential deterioration patterns of lime mortar. *Journal of Cultural Heritage, 21,* 819–822.

DIN EN 1925. (1999). Natural stone test methods—Determination of water absorption coefficient capillarity, Deutsches Institut für Normung e.V., Berlin, 6pp (in German).

Dotter, K. R. (2010). Historic lime mortars: Potential effects of local climate on the evolution of binder morphology and composition. *Geological Society London Special Publications, 331,* 119–126.

Moropoulou, A., Bakolas, A., & Anagnostopoulou, S. (2005). Composite materials in ancient structures. *Cement & Concrete Composites, 27,* 295–300.

Moropoulou, A., Bakolas, A., & Bisbikou, K. (1995). Characterization of ancient, Byzantine and later historic mortars by thermal and X-ray diffraction techniques. *Thermochimica Acta, 269* (270), 779–795.

Rodriguez-Navarro, C. (2012). Binders in historical buildings: Traditional lime in conservation. In J. M. Herrero & M. Vendrell (Eds.), *International Seminar on Archeometry and Cultural Heritage: the Contribution of Mineralogy* (Vol. 09, pp. 91–112). Bilbao: Seminarios de la Sociedad Española de Mineralogia.

Rodriguez-Navarro, C., Cazalla, O., Elert, K., & Sebastian, E. (2002). Liesegang pattern development in carbonating traditional lime mortars. *Proceedings of the Royal Society London A, 458,* 2261–2273.

Siedel, H. (2010). Alveolar weathering of Cretaceous building sandstones on monuments in Saxony, Germany. *Geological Society London Special Publications, 333,* 11–24.

Siedel, H., & Siegesmund, S. (2014). Characterization of stone deterioration on buildings. In S. Siegesmund & R. Snethlage (Eds.), *Stone in Architecture. Properties, Durability* (pp. 347–410). Berlin, Heidelberg: Springer, ISBN 978-3-642-45154-6.

Sirirat, S. (1999). Conservation treatments of Stucco in Thailand. In *Conservation of Monuments in Thailand I, Proceedings of the First Seminar on Thai-Japanese Cooperation in Conservation of Monuments in Thailand* (pp. 102–107). The Fine Arts Department, Thailand and Tokyo National Research Institute of Cultural Properties, Japan.

Snethlage, R., & Wendler, E. (1989). Der Wassereindringprüfer nach Karsten - Anwendung und Interpretation von Messwerten. *Bautenschutz und Bausanierung, 12,* 110–115.

Van Beek, S., & Invernizzi Tettoni, L. (1999). *The arts of Thailand*, Periplus Editions (HK) Ltd., ISBN 962-593-262-3, 248pp.

Wendler, E., & Sattler, L. (1996). Bohrwiderstandsmessung als zerstörungsarmes Prüfverfahren. In F. H. Wittmann & A. Gerdes (Eds.), *Proceedings of the 4th International Colloquium Material Science and Restoration* (pp. 145–160). Freiburg: Aedificatio Publishers.

From Dry-Stone to Shell-Lime Bound: High Medieval Contrasts in Masonry Technique at Skellig Michael, High Island and North Rona

M. Thacker

Abstract Although most well-known for their remarkable dry-stone medieval buildings, the North Atlantic island sites of Skellig Michael, High Island and North Rona also contain evidence for the deposition of lime mortars. This paper re-considers the evidence for these materials in the light of recent on-site survey of the mortars on North Rona, Scotland, and subsequent microscopic analyses of samples from here and comparable sites in Ireland. Several themes are developed including: how taphonomy can problematicise interpretations of mortar manufacture and deposition; how recent dating evidence precludes a simple chronological evolution from dry-stone to lime-bonded masonry; and how microscopic analysis coupled with environmental survey can inform our understanding of material sources. Ultimately, it will be suggested that this evidence very clearly demonstrates the importance of lime mortar to communities across Europe in the High Medieval period.

Keywords Shell-lime · Landscape · High medieval · North Atlantic Church

1 Introduction

A number of island sites in North Atlantic Europe contain medieval ecclesiastical buildings which display striking contrasts in masonry technique associated with the manufacture and deposition of lime mortar. This evidence has often been regarded as chronologically contingent, although early evolutionary interpretational schemes which had suggested lime-bonded and arcuate churches had developed gradually and directly from their dry-stone corbel-vaulted predecessors (e.g. Leask 1955) have now been largely dismissed (Harbison 1970). Against a background in which most early medieval churches and chapels were built of organic materials such as timber

M. Thacker (✉)
University of Stirling, Stirling, Scotland, UK
e-mail: mark.thacker@stir.ac.uk

J. J. Hughes et al. (eds.), *Historic Mortars*,
https://doi.org/10.1007/978-3-319-91606-4_5

and/or turf, many scholars in Ireland now argue for a more binary model; in which dry-stone churches probably began to be constructed from the 8th-century but only attained a limited western distribution, whilst the first congregational churches of mortared masonry were constructed at 'very important' cathedral sites in the midlands and east of the country from the early 10th-century onwards (Manning 2000; White Marshall and Walsh 2005; Ó' Carragáin 2005, 32; 2010, 87).

On a national scale this dichotomy is broadly convincing, although from a North Atlantic perspective complexities remain. It is clear that by the 12th-century lime-bonded churches and chapels have a widespread distribution across much of both Scotland and Ireland, but other evidence indicates that those earlier dry-stone corbelled building techniques continued to develop (Rourke and White Marshall 2005, 112–121), and some chapel buildings (such as the chapels at Church Island and *Gallerus* considered below) may also have 11th or even 12th-century foundation dates (Harbison 1970; Hayden 2013). Even further, radiocarbon analysis of mortar materials removed from a range of ecclesiastical structures has suggested some smaller lime-bonded chapel buildings in western Ireland may have been constructed in the 8th and/or 9th centuries (Berger 1992, 1995; Harbison 1990, 149–152). These very early radiocarbon date ranges are not unproblematic (Manning 1997; Ó' Carragáin 2010, 66, 116) and until technical models can be improved should probably be considered as lower terminuses rather than accurate ascriptions (Thacker 2016, in prep. c), but the data clearly suggests there is a significant overlap in the Irish North Atlantic buildings' evidence and this prompts questions about the relationship between these apparently separate masonry traditions in the high medieval period when both building types were being constructed (cf. Rourke and White Marshall 2005, 121–122).

A few precious North Atlantic sites contain surviving examples of both types of masonry construction and in a Scottish context this includes the chapel of *Teampull Ronain* on the island of North Rona. I briefly visited this important site in 2012 as part of a wider Ph.D. research project, and a preliminary re-examination of the multiphase masonry fabric of this building was subsequently presented to the Historic Mortars Conference in Glasgow in 2013 (Thacker 2013). The lime mortar evidence displayed at *Teampull Ronain* clearly contrasts with the strictly dry-stone evidence reported from (almost) all other corbel-vaulted sites across the wider North Atlantic region introduced above, and the in situ evidence was often fragmentary and challenging to interpret. But close inspection suggested that at least one secondary phase of the chapel should be re-interpreted as lime-bonded, and some apparent layering and compositional contrasts in the in situ materials indicated multiple events of mortar deposition had taken place during the lifetime of this building (ibid.).

That preliminary discussion of *Teampull Ronain* will be reconsidered here and, drawing attention once more to some of the interpretative challenges presented by the evidence, I will suggest that mortar degradation may explain the earlier (monolithic) dry-stone characterisations of the structure. Microscopic analysis of loose mortar samples had previously suggested that at least some, if not all, of the mortars surviving on site were manufactured from calcined marine shells, I will

present additional evidence here to suggest that these mortars may have been manufactured on the island itself, and compare this with evidence for the probable use of shell-lime mortars reported from other high medieval island sites across the wider region.

The construction of dry-stone early to high medieval chapel buildings on treeless non-calcareous North Atlantic island sites such as North Rona and *Sceilig Mhichíl* may initially appear to be a simple environmental correlate, as timber and limestone building materials would be very difficult to source here. The mortar compositions presented at these insular sites, however, provides additional evidence for the range of mortar making strategies and techniques employed by various North Atlantic communities, and highlights how in this region it was possible to manufacture and/or use lime mortar in almost any physical environment. Indeed, some of the earliest evidence for lime mortar use across Scotland, Ireland and the rest of the north Atlantic appears to have been manufactured from marine shells, whilst dry-stone construction has also enabled a much greater number of early to high medieval chapel buildings to survive here, because the more commonly employed forms of organic (timber and turf) construction have left such little evidence elsewhere. The evidence at these sites, therefore, appears to present a particularly good (perhaps unique) illustration of contemporary contrasts in building techniques.

This interpretation draws attention to the processes by which these different building and mortar manufacturing techniques may have been disseminated and these issues will be examined more fully elsewhere (Thacker, in prep. a), but the preliminary investigation presented below will clearly illustrate that mortar analysis offers the potential to inform our archaeological interpretations, and at this early stage broader conclusions are probably more significant. Indeed, implicit within all of the different mortar manufacturing strategies discussed here is a very strong underlying motivation with much wider relevance. The evidence discussed here presents further very convincing evidence that lime mortar was fast becoming an almost essential agent of Christian power across north-west Europe during this period, and ultimately, I would suggest that the importance of this material to medieval society should be reflected in the significance we accord mortars and their constituent materials in archaeology more widely.

2 The Island and Chapel of North Rona in Context

The island of North Rona is located approximately 58 miles north-west of the coast of Scotland and 160 miles south of the Faroe Islands. Getting there in 2012 involved a journey time of approximately 3.5 h in a fast boat from the Isle of Lewis, and on arrival the island presented a bulwark of low but steep cliffs which, apart from small peninsulas to the north and south, form the island's fringe. It is important for our discussion to note that North Rona has no beach. Disembarking today, as in the past, involves jumping from a rising and falling small boat onto a

rock exposed by the retreating tide, before scrambling up the cliff to the flatter turf-covered plateau above.

Despite previously supporting a population for most of the previous 1000 years, however, North Rona has now been almost completely uninhabited for the last century and a half and, together with its apparently remote location, this is often cited as one of the main factors which have enabled the survival of a rare and fragile archaeological gem. Like the apparently similarly constructed 'Early Christian' dry-stone chapel buildings of south-west Ireland, to which this structure is often compared, the eastern cell of *Teampull Ronain* is a small rectangular, E-W oriented, corbel-vaulted building, with stone walls that 'converge as they rise' to support a roof of stone slabs at the apex and a small stone altar at its east end (RCAHMS 1928, 3–4; Nisbet and Gailey 1960). The internal wall faces of this chapel are composed of split gneiss slabs which are well-coursed and relatively tightly jointed, but no external masonry faces survive apart from a low straight wall in the north. Indeed, the cell is now only partially covered by eroding layers of turf, and large sections of internal masonry and core rubble are now visible from outside the building. Surrounding the chapel are the remains of an oval-shaped stone and turf enclosure wall, which defines a graveyard containing a number of small upright earth-fast cruciform crosses (ibid.).

These crosses have also been compared with apparently similar early medieval grave-markers at a number of monastic sites of south-west Ireland such as those on the well-known island of *Sceilig Mhichíl* (Fisher 2001), and a combination of this comparative (apparently) early medieval evidence and an historical account (reporting that Viking colonisation during the 9th-century had led to an exodus of religious Christian communities from the islands of the north North Atlantic), has led to an interpretation that a broad 7th to 9th century foundation date pertains for the whole North Rona complex (Nisbet and Gailey 1960). Remarkably then, this apparently holistic art-historical interpretation suggests that an extraordinarily coherent upstanding Early Medieval monumental landscape has survived on North Rona, and that the eastern cell of *Teampull Ronain* may be the oldest upstanding Christian building in Scotland.

This narrative, however, also receives some support by consideration of the upstanding structure as, unlike all other surviving examples of these corbel-roofed chapel buildings, *Teampull Ronain* is not unicameral but has another masonry cell bonded to the west of the structure described above. It may be that the rarity of this multi-cellular evidence has itself suggested to commentators that this western cell is not of the same phase as the corbelled eastern section, as interpretations of how these cells are joined have varied, but this multiphase interpretation has also been supported by highlighting the broadly contrasting masonry techniques on display. Unlike the eastern cell, the western cell of *Teampull Ronain* is enclosed by vertically-faced double-skinned stone walls displaying a spectrum of variously informal masonry styles, and no clear evidence for a roof structure appears to survive. A low lintelled doorway in the south wall provides the only entrance into the building, whilst a similarly low lintelled doorway in the west wall of the eastern cell (flanked by two side altars) connects the two parts of the church. All of these

Fig. 1 St. Ronain's from the north; the corbelled eastern cell is on the left. Scale 500 mm (*Photograph* M. Thacker)

architectural features strongly suggest that, like a number of other ruined bicameral buildings whose remains are widely distributed across nearby Caithness and the Northern and Western Isles of Scotland (Thacker 2011), *Teampull Ronain* was operating as a two-cell nave and chancel chapel in this period (Nisbet and Gailey 1960). Moreover, given that the majority of these structures were founded in the 12th-century (Fleming and Woolf 1992), it appears very likely that the western cell of *Teampull Ronain* was constructed within a high medieval Norse-Christian cultural milieu (Thacker 2015).

In summary, therefore, all previous interpretations have suggested that this Scottish building exhibits two classic North Atlantic medieval constructional forms which were translated in different periods from very different places. As currently interpreted, it would appear that an 8th-century Irish chapel site—including the sculpture, the enclosure, the chapel and its small high altar, survived on North Rona for four centuries before being converted to a Norse bicameral church (Fig. 1).

3 Extraordinary Material Evidence

With the exception of some minor details this remarkable narrative has remained unchallenged for well over a century (Muir 1861; RCAHMS 1928; Nisbet and Gailey 1960), although included within these previous descriptions are a number of apparently extraordinary pieces of physical evidence. This includes a mortar-archaeology which is not typical for either cell.

Within the corbel-vaulted eastern part of *Teampull Ronain*, for instance, large areas of lime mortar coat the wall faces in multiple layers to 10–15 mm thick (Fig. 2), beneath which the remains of clay mortar 'pointing' have also been observed (Nisbet and Gailey 1960). Whilst clay mortar retains a somewhat ambiguous chronological position in early to high medieval architectural typologies, and accepting the early medieval radiocarbon evidence from western Ireland,

Fig. 2 Corbelled eastern cell, facing west, displaying large patches of multi-layered lime coating. Scale 500 mm (*Photograph* M. Thacker)

according to generally accepted models lime mortar would be a very unusual material to find in an 8th-century Scottish North Atlantic constructional context otherwise dominated by structures built from timber, turf or dry stone. Indeed, lime mortar is widely considered not to have emerged within the archaeological record of western Scotland until the 12th-century (e.g. Fisher 2005, 85), and this threshold has even often been employed as a basis for dating lime-bonded buildings with otherwise chronologically-ambiguous architectural forms. Within all typological frameworks, therefore, this lime mortar evidence in the eastern cell must be interpreted as a secondary addition, and one perhaps related to the construction of the western cell.

Previous interpretations of the 12th century nave of *Teampull Ronain*, however, are also extraordinary, as although by this period almost all of the surviving bicameral chapels across the wider region are both lime-bonded and arcuate, the

most comprehensive recent survey of this building had also characterised the western cell as dry-stone and suggested that it too may have had a corbel-vaulted roof (Nisbet and Gailey 1960).

Doubtless some caution is required here. In the absence of independent scientific dating and in a region where simple rubble-stone medieval buildings with no contemporary documentary evidence are often very difficult to date, the bicameral (nave-and-chancel) plan-form provides a very useful and generally reliable (if broad) 12th-century architectural marker for church buildings across North Atlantic Europe. But an interpretative framework predicated on the presence or absence of lime mortar is much more problematic, and perhaps particularly so in the high medieval period when architectural forms can be more heterogeneous and mortared masonry techniques are being adopted by communities for the first time. Clearly buildings cannot be ascribed to the early medieval period simply on the basis of dry-stone constructional techniques when these are also apparent in later periods, and yet ascribing a building to the later high medieval period on the basis of the presence of lime mortar runs the risk of tautology—when that threshold is predicated on a lack of comparative early medieval evidence.

Examples of both of these interpretative schemes have been employed by scholars at various times, however, including in an important and influential paper suggesting that construction of the well-known single-celled corbel-vaulted chapel at *Gallerus* (in south-west Ireland) may be re-ascribed to the 12th-century partly on the basis of interstitial lime mortar evidence (Harbison 1970). Like *Teampull Ronain,* the *Gallerus* chapel had been previously ascribed to the 8th-century, but accepting Harbison's provocative argument requires that this Irish building should be re-interpreted as a late, mortared, example of the North Atlantic corbel-vaulting tradition, which may even have been constructed in the same period as the (apparently secondary) nave of *Teampull Ronain.* As described above, the multi-phase interpretations of this North Rona building may not have been completely typologically-driven, but it is now clear that the uniquely corbel-vaulted (rather than barrel-vaulted) structure of this bicameral church may not require such a chronologically-deep developmental history at all.

Given the entangled typological relationships between these high medieval building plan-forms, materials, techniques and chronologies, a number of questions regarding *Teampull Ronain* emerge from the above discussion: Should the corbelled structure at the east end of the church be characterised as dry-stone? Is this structure as early as previously suggested? What are the alternative historical contexts for each constructional phase? How convincing is the evidence for multi-periodicity across the site? Does the eastern chancel pre-date the western nave? Is the church contemporary with the enclosure wall? Is this corbelling technique a continuous Hebridean masonry tradition handed down since the Iron Age? Is this corbel-vaulting technique a continuous North Atlantic masonry tradition? Are these techniques a regional response to a lack of timber necessary to construct roof trusses? Is the western cell dry-stone? What evidence is there that this cell was corbel-vaulted? Were these masonry forms constructed in dry-stone as a response to the lack of calcareous geology or woodland to manufacture lime? From

what materials were the surviving North Rona lime mortars manufactured? Was the lime or its source materials transported to North Rona from elsewhere? When was the building coated with mortars of clay and lime? Were different mortar materials applied in different periods? Is there any lime in evidence in other buildings on the island? How does this mortar evidence compare to other North Atlantic sites? And finally, given the apparently remote location, long-lived dry-stone masonry traditions, challenging environment and restricted availability of materials—why was lime mortar used on North Rona at all?

4 Taphonomy Versus Deposition

The crucial piece of evidence upon which previous interpretations of *Teampull Ronain* have been predicated is the observation that the mortar evidence is limited to the wall faces. From this observation a number of interrelated interpretive leaps can be made (here as elsewhere) to suggest that these putative clay and lime-based mortar materials are overlying and therefore stratigraphically secondary. This secondary interpretation ultimately places these mortar materials in a chronologically-ambiguous position relative to the underlying stonework, and so the masonry of both cells of the chapel may be characterised as dry-stone. This mirrors the stratigraphic ambiguity evident in contrasting interpretations of the mortar evidence at the corbel-vaulted chapel of *Gallerus* in Ireland, which has been variously characterised as either secondary pointing and/or a structural medium, although unlike the Irish comparanda continued use of *Teampull Ronain* by North Rona communities into the later medieval period and beyond at least provides a number of convenient historical contexts for lime use at this site.

It was clear from my first rapid survey of the North Rona building in 2012, however, that the western cell of this structure has a much more complex masonry and mortar stratigraphy than had been previously recognised, and there is some fragmentary evidence that the fabric cannot be simply characterised as dry-stone. This was most clearly evident in the very thick west wall of the building, where localised collapse has enabled the masonry to be inspected in deep sections. Close examination here suggested that the core rubble of this wall is indeed almost completely unbound, but a number of face stones in the internal wall face (and some smaller packing stones immediately behind them) were clearly bedded in mortar to 200 mm deep. Moreover, even where masonry joints were very narrow the mortar associated with these contexts exhibited such a coarse texture that it seemed improbable that this material had been deposited in a secondary phase. In sum, therefore, both the context and character of this lime mortar evidence suggested that this mortar material was contemporary, at least with the construction of the face of the west wall.

Although no explanation for this apparent contrast between a mortar-bound face and dry-stone core was offered in the interim report presented to conference (Thacker 2013), it is probable that this heterogeneous masonry profile is the result

of taphonomy rather than deposition. A number of ruined buildings across the wider region have repeatedly presented evidence to suggest that single-phase mortars within composite masonry walls often degrade much faster in the core rubble than in the wall face, and this can lead to a surviving profile which looks more like a pointed or coated dry-stone structure than one which was previously fully lime-bonded (Thacker 2016; in prep. a, b). Interpreting such surviving evidence can be particularly challenging where core mortar degradation is very advanced, but partial dissolution lime mortar materials can also present evidence which looks very much like clay. It is not yet clear whether this process can account for the reported clay mortar evidence at *Teampull Ronain*, but in consideration of a west-facing masonry wall in an exposed position on an elevated site on a small island in the North Atlantic Ocean, extreme weathering and taphonomy is always likely to be a factor in our interpretation of surviving evidence. Indeed, although again requiring more work in terms of the phased development of the whole building, this interpretation of comparatively accelerated core mortar degradation in the west wall at *Teampull Ronain* may be supported by better mortar survival within the internal wall face.

Lime mortar is also evident within the masonry joints of the stonework of the (apparently earlier) corbelled eastern cell, although as this material only appears to survive to a general depth of 50–60 mm from the internal wall faces it was not possible to demonstrate during this site visit whether this structure might also have been constructed with this material. However, these chancel mortars are also leaching carbonate quite heavily in some contexts and, given that the tails of these internal face stones are also often exposed externally, it is clear that initial mortar deposition was more extensive here than current survival indicates. Another archaeological approach to this issue, therefore, will probably be required, and, as the surviving mortar associated with the west wall of the nave did appear more coarsely-textured and darker-coloured than those examined in the chancel, closer comparison of the mortars from the two cells may have some potential in this regard.

Together with the apparent layering of materials already described, this may suggest multiperiodicity, and it is certainly possible that a comparative multiphase mortar stratigraphy could inform our understanding of the relative chronologies of the materials and structures associated with each of these cells. Again, however, it is possible that the contrasts in material composition noted in situ could have resulted from differential weathering, and so, although there was clearly more complexity in the development of the surviving building than was currently understood, further materials analysis was considered desirable to inform preliminary interpretations and any further research design.

Ultimately, five small loose mortar samples from the upstanding ruined building, and one sample of possible temper sand from the island's northern peninsula, were collected for further lab-based examination.

5 In the Laboratory

In many respects lab-based analysis suggested that the loose mortar samples collected from the two cells of *Teampull Ronain* are made from similar materials: Both mortars appeared to be bound with lime manufactured from calcined marine shells and tempered with an aggregate which includes minerals derived from the underlying metamorphic and igneous geology of the island.

Cast in resin and thin sectioned, the natural 'sand' sample also contained a lithic and shell component. In thin section the lithic component was dominated by sub-rounded and sub angular grains between 25 μm and 2 mm diameter, displaying plagioclase, k—feldspar (microcline), hornblende, quartz, clinoproxene and some quartzofeldspathic rock fragments too small in thin section to denote a very specific rock type. In hand sample these graded up to 20 mm diameter and some micaceous minerals, which are probably biotite, were also noted. The shell clasts within this aggregate sample also generally display rounded angles and a range of grades, from 2 to 5 mm (this latter in hand sample) all appeared to display good internal microstructure. These are dominated by Gastropodae, displaying fusiform, turbinate and turriculate forms in the more longitudinal sections, with apertures and transverse sections elsewhere. Bivalve sections, however, were only very occasionally identified and only a single, rounded, internally prismatic or cellular coralline algae structure was observed.

In contrast to the clear microstructural evidence within the bioclasts of this sand sample, however, all examined mortar samples contained shell clasts which presented a spectrum of structural and textural alteration. These included: clasts which still retained some core relict shell microstructure within a well defined micritic carbonate rim; bioclasts without any relict microstructure, cracked grain boundaries and crazed rims; and more highly-altered, only vaguely shell-shaped concentrated areas of carbonate, with no well-defined grain boundary between the former shell and general mortar matrix. These altered bioclasts were interpreted as evidence of shell heating in order to manufacture a lime-based mortar binder, and no evidence of a geogenic carbonate (limestone) fraction was noted.

Although all of these samples were therefore interpreted as shell-lime mortars manufactured from similar source materials, two otherwise very different mortars are in evidence in the sample assemblage, and these may suggest different lime-burning and mortar-making processes pertained. Indeed, the loose mortar samples collected from the eastern cell contained an extremely high concentration of highly-altered shell fragments grading up to 6 mm long (Figs. 3 and 4), and these were tempered by a very fine (generally submillimetric) mixed shell/lithic aggregate containing angular to subrounded quartz, feldspars and biotite. It is important to recognise that the composition of this temper fraction appears to match that of the 'natural sand' sample also collected from North Rona, but these mortars did also contain a very high concentration of polycrystalline reaction products not noted in the sand sample, and the possible significance of these inclusions will require further discussion below.

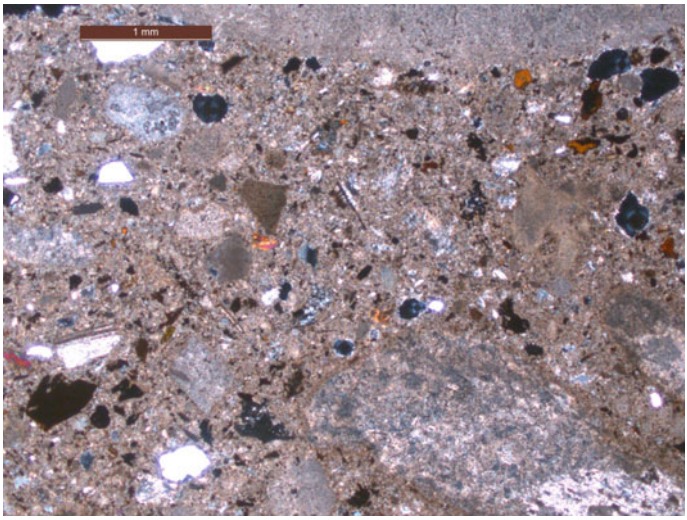

Fig. 3 Thin section of the mortar from the eastern cell displaying calcined shell/fine temper. XPL. scale bar 1 mm (*Photomicrograph* M. Thacker)

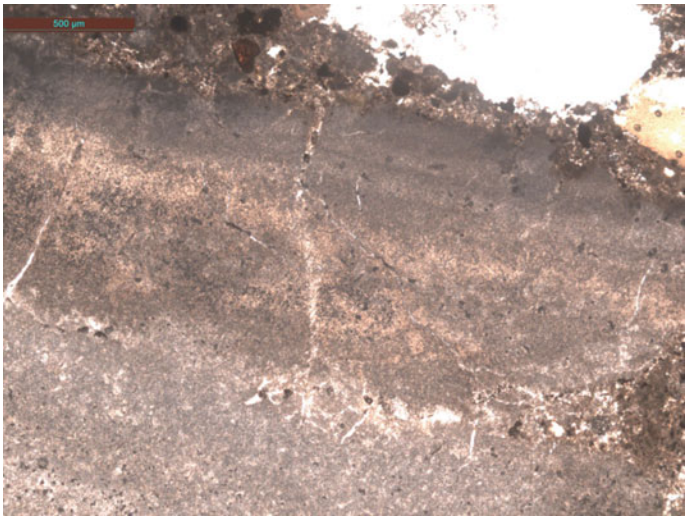

Fig. 4 Thin section of mortar from eastern cell displaying calcined and fractured shell with complete loss of internal microstructure. XPL. Scale bar 500 µm (*Photomicrograph* M. Thacker)

In contrast, only a very low concentration of fine (submillimetric) altered shell was noted within the mortar samples collected from the western nave. As already described during the on-site survey, this nave mortar appeared much more coarsely

textured on-site, and this is reflected in the temper profiles of the sectioned samples. These contained a much higher concentration of unaltered shells which occasionally graded up to 12 mm long and whilst the lithic fraction once more included quartz, feldspar, and microcline, at grades of up to 6 mm this is also much more coarse often appeared fractured or crushed. That some hornblende was also noted here provides another match with the hand sample of natural sand collected, although that these mineral clasts displayed contrasting textures and no polycrystalline glassy forms were noted in these sections, is notable.

In interim, therefore, the compositional differences in these thin-sectioned loose mortar samples collected from the nave and chancel of *Teampull Ronain* suggest that the textural contrasts noted on site are not simply the result of differential weathering, as these mortars contain contrasting grades of aggregate temper and different concentrations of altered shell. This thin section evidence suggests different firing and tempering techniques have pertained, whilst the in situ evidence suggests this compositional dichotomy may be associated with different constructional phases, rather than material heterogeneity. Indeed, including a fragmentary mortared context found in a later repair phase of the western cell, the archaeology of the wider chapel site indicates that at least three distinct lime-mortared phases survive here.

It is important to note that the microscopic evidence indicates the probable use of locally-sourced aggregate to temper the *Teampull Ronain* mortars, and it may now be possible to tentatively push the evidence further to suggest that the shell (and probably turf) materials used to make the lime were also harvested from North Rona itself. It is clear from petrographic analysis that the well-developed polycrystalline reaction products evident within the thin-sectioned mortar samples collected from the eastern cell of *Teampull Ronain* are highly-altered, previously molten, Iron- (magnetite and hematite) rich clasts of lithic origin, and this interpretation has now been supported by XRD analysis (Thacker 2016). A number of apparently similar ‘vitreous inclusions’ (isolated from various North Atlantic shell-lime mortars) have recently been subject to similar analyses, and this wider study suggested that these clasts may result from the incidental inclusion of a lithic fraction within the limekiln charge, perhaps during shell collection. Although there is no space here for a more comprehensive discussion, these clasts appear to have been altered in the hot and chemically very aggressive limekiln environment, and this suggested provenance for the reaction products may be supported by the range of amphibole textures also present. Compared to the unaltered amphibole evident in the natural sand collected from the island these appear to have dehydroxylated, so suggesting that an amphibole fraction was included in the kiln-charge. If this is accepted, it would follow that the lime was manufactured on the island of North Rona itself, and so we may presume that the kiln-charge also included locally-sourced (turf) fuel (Fig. 5).

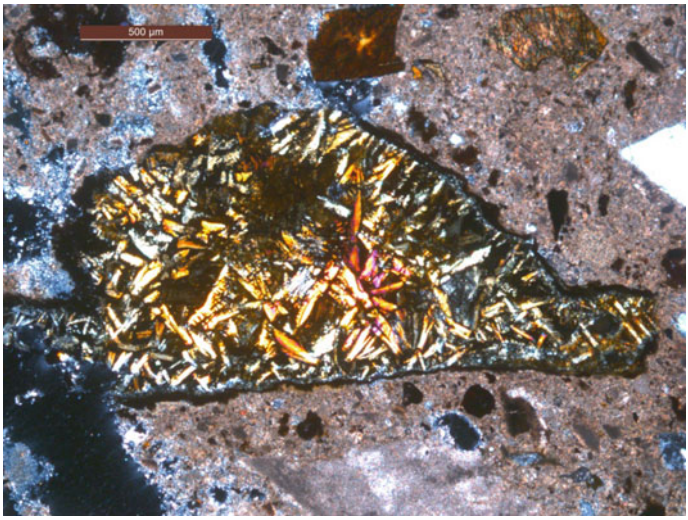

Fig. 5 Thin section of mortar from Teampull Ronain displaying Iron-rich 'vitreous; reaction product with well-deveploped crystal forms and some spinaflex textures. XPL. Scale bar 500 µm (*Photomicrograph* M. Thacker)

6 The Wider Perspective

In a wider Scottish North Atlantic landscape where the construction of buildings from dry-stone and earth materials is such an enduring feature of the regional archaeological record, the evidence suggesting that successive phases of *Teampull Ronain* are associated with lime mortar is notable. Indeed, that these materials appear to have been manufactured on this very small island, 58 miles from the Scottish mainland—with no limestone, no woodland, no peat, no coal, and no beach—appears to represent an extraordinary degree of technological resourcefulness and material investment. Moreover, although it is also clearly significant that the eastern cell of the chapel may be compared to apparently similar evidence in south-west Ireland, there are also some remarkable similarities in the mortar evidence between displayed by buildings within these two North Atlantic island regions, which will be considered further below.

At *Sceilig Mhichíl* there has been no reported evidence of single buildings with mixed or ambiguous dry-stone and lime-mortared contexts like those at at North Rona and *Gallerus*, but the island contains examples of both building types, with ruins of the rectangular lime-bonded church of St. Michael located on the same site as the more well-known corbel-vaulted and rounded dry-stone buildings of *Sceilig Mhór*. Like *Teampull Ronain*, St. Michael's exhibits multiple lime-mortared phases, but radiocarbon analysis of fuel-relicts from the primary phase mortar of this building have yielded calibrated dates which allow a lower terminus of the late 7th

to the late 9th-century (Berger 1995, 168), so presenting the possibility that these clearly contrasting dry-stone and lime-mortared buildings are near-contemporary.

More recently, a mortar sample from this early phase of St. Michael's has also been subject to microscopic analysis and, although comprehensive interpretation was somewhat limited by the degraded and voided sample condition, this material exhibited evidence considered likely to indicate a shell-lime provenance (Pavia 2010). Taphonomy, then, can also present interpretive issues at microscopic scales, but other apparent parallels between this shell-lime material and that at *Teampull Ronain* may be more limited. The laminated foliated microstructure of a bioclast noted within this mortar suggests *Ostrea* (oyster) shell may be a source material here and so (as *Sceilig Mhór* also doesn't have a beach) it is perhaps probable that component mortar materials for this building were transported to the island from mainland Kerry, rather than harvested locally.

Further north, a similarly beach-less topography also pertains on the small western Irish island site of *Ardoileán* (off County Galway), and some similar interpretative issues pertain. Indeed, again like *Teampull Ronain*, although a previous survey had suggested the ruined chapel surviving here was dry-stone and lime-coated (Herity 1990, 77, 96) the *Ardoileán* structure has also been more recently characterised as lime-bonded (White Marshall and Rourke 2000), perhaps suggesting a similar pattern of core mortar degradation has taken place. Moreover, this rectangular building also displays surviving evidence for multiple lime-mortared masonry phases which have been characterised as probable shell-limes (White Marshall and Rourke 2000, 74) although, as may be the case for the *Sceilig Mhichíl* building, it has been suggested that these shells must have been imported to *Ardoileán* for the manufacture of these mortar binders. Moreover, although fuel relicts from two samples of mortar form this (probably 11th-century) structure produced only very broad calibrated radiocarbon dates between the 3rd and 13th-centuries (Berger 1995, 166–167), this analysis does at least suggest that wood was used to fire the limekiln, and this fuel must also have been imported to the island (either as cargo or drift).

Given all of this imported evidence and the apparent lack of a limekiln at *Ardoileán*, it may not be possible to definitively demonstrate that the lime was burnt on the island, but it would surely have been mixed there. Indeed, and perhaps most remarkably, recent excavation has also highlighted evidence to suggest that in response to the lack of available sand the mortar temper was manufactured on the island itself—by mechanically grinding the local schistose bedrock in a medieval horizontal watermill excavated on the site (White Marshall and Rourke 2000, 74, 89).

The use of shell-lime mortars across the North Atlantic is not ubiquitous, but is widespread, and in addition to the Scottish and Irish sites discussed above shell-lime mortars have been reported from medieval sites in Isle of Man, the Faroes, Greenland and Denmark (Thacker 2016). The use of shell-lime is not restricted to regions without limestone or to very remote island sites, but like all material culture it is manufactured according to a confluence of different physical and cultural pressures. Whatever the provenance of the materials, however, it is clear that by the high medieval period the motivation to have lime mortar at

Teampull Ronain, *Sceilig Mhichíl and Ardoileán* was very strong, and in many respects this epitomizes similar evidence displayed across much of the wider North Atlantic during the High and Later Medieval periods. This is also clearly in evidence in Norway, where despite a strong tradition of timber church building in both earlier and later periods, there is sudden and widespread evidence for the construction of ecclesiastical buildings in stone and lime during the 12th-century.

7 Discussion

In the 2013 conference presentation I chose to highlight the chronologically broader medieval evidence which suggested that lime-mortared churches and chapels had in many ways taken over the role of free-standing crosses in defining the edge of the Christian world and that lime and off-shore islands presented similar cultural metaphors for liminality which had much wider relevance (Thacker 2013). Further consideration here may support this suggestion as, in contrast to the apparently fixed geographical remoteness and limited physical resources available at these island sites, it would appear that these ecclesiastical buildings present some of the earliest evidence for lime mortar known in the region. A convincing argument has been presented which equates the use of lime mortar at many of these early buildings with reform, romanitas and need to memorialise the grave sites of important local saints in new ways (Ó' Carragáin 2010), although the processes by which these different building techniques were adopted, translated and developed across the North Atlantic requires much more work.

Clearly, a number of cultural and physical factors combine to determine which building materials and techniques are used and survive in a given archaeological context, but the range of different methods by which lime mortar could be manufactured allows further comparisons to be made. Indeed, the material choices which have enabled constructional contrasts within the buildings of a number of settlements in Scotland and Ireland to be discerned, and the eventual spread of lime-bonded churches and chapels across the whole region draws attention to those areas where lime does not appear to have been employed. The complete lack of high medieval lime mortared masonry evidence in Iceland, for example, and the continuity of timber and turf building techniques can no longer be convincingly explained by the lack of limestone, and more complex cultural factors must also be at play.

Where lime mortar was adopted by North Atlantic communities, however, then it is probable that only one lime-mortared building was initially required by a community. Often this same building may be subject to repeated cycles of repair and adaption, and the evidence from North Rona illustrates that even in a very small chapel such as *Teampull Ronain* multiperiodicity and taphonomy can add great complexity to the surviving mortar evidence. At least one of the exceptional shell-lime mortars within this building does appear to be documented, however, as Iain MacKay reported that his family had "…put lime made from shells in among

the stones…" in the 19th-century (Muir 1861, 193). More detailed information on how this mortar was manufactured was (unfortunately) not forthcoming, but it is significant that although a number of domestic stone buildings survive on North Rona, none of these houses display evidence of lime mortar use (George Geddes, per. Com.). It does therefore appear that lime continued to have a special place within the religious life of North Rona islanders, long after the first mortared phase of the chapel had been constructed.

Acknowledgements Many thanks to: Jill Harden for enabling this survey and collecting the aggregate sample; to Jill and George Geddes (HES) for insightful discussions on site; to Geoffery Bromiley (University of Edinburgh) for supervision during the microscopic analysis and Mike Hall (University of Edinburgh) for thin section preparation; Tomás Ó' Carragáin (Cork University) and Grellan Rourke (OPW, Ireland) for discussion, and to Grellan for forwarding Pavia's analysis of the *Sceilig Mhichíl* materials.

References

Berger, R. (1992). 14C dating mortar in Ireland. *Radiocarbon, 34*(3), 880–889.

Berger, R. (1995). Radiocarbon dating of early medieval Irish monuments. *Proceedings of the Royal Irish Academy. Section C: Archaeology, Celtic Studies, History, Linguistics, Literature, 95*(4), 159–174.

Carragáin, T. (2010). *Churches in early medieval Ireland*. New Haven: Yale University Press.

Fisher, I. (2001). *Early medieval sculpture in the west highlands and Islands*. RCAHMS & The Society of Antiquaries of Scotland.

Fisher, I. (2005). The heirs of Somerled. In R. Oram & G. Stell (Eds.), *Lordship and architecture in medieval and renaissance Scotland* (pp. 85–96). Edinburgh: John Donald.

Fleming, A., & Woolf, A. (1992). Cille Donnain: A late Norse Church in South Uist. *PSAS, 122,* 329–350.

Harbison, P. (1970). How old is Gallarus Oratory? *Medieval Archaeology, 14,* 34–37.

Harbison, P. (1990). *Pilgrimmage in Ireland: The monuments and people*. London: Barrie & Jenkins.

Hayden, A. (2013). Early medieval shrines in north-west Inveragh: New perspectives from Church Island, near Valencia, Co., Kerry. *Proceedings of the Royal Irish Academy, 113C,* 67–138.

Herity, M. (1990). The Hermitage on Ardoilean, county Galway. *The Journal of the Royal Society of Antiquaries of Ireland, 120,* 65–101.

Leask, H. (1955). *Irish churches and monastic buildings* (Vol. I). Dundalk: Dundalgan press.

Manning, C. (1997). The date of the round tower at Clonmacnoise. *Archaeology Ireland, 11,* 12–13.

Manning, C. (2000). References to Church buildings in the Annals. In A. Smyth (Ed.), *Seanchas: Studies in early and medieval Irish archaeology* (pp. 37–52). History and Literature in Honour of FJ Byrne.

Muir, T. (1861). *Characteristics of old church architecture*. Edinburgh.

Nisbet, H., & Gailey, R. (1960). A survey of the antiquities of North Rona. *Archaeological Journal, 117,* 86–115.

Ó' Carragáin, T. (2005). Regional variation in Irish pre-Romanesque architecture. *The Antiquarries Journal, 85,* 23–56.

Pavia, S. (2010). *Analysis of mortar samples from Skellig St. Michael's Church, Co. Kerry*. (Unpublished document prepared for Grellan Rourke, Senior Conservation Architect National Monuments, Dun Scène).

RCAHMS. (1928). Ninth Report with inventory of Monuments and constructions in the Outer Hebrides, Skye and the Small Isles. Edinburgh: RCAHMS.

Rourke, G., & White Marshall, J. (2005). The drystone oratories of western Kerry. In *White Marshall and Walsh*, 103–124.

Thacker, M. (2011). *An archaeology of the lime and shell-lime mortars of the Western Isles'*. (Unpublished M.A. (Buildings Arch.) thesis, University of York).

Thacker, M. (2013). Making lime at the edge of the world. In *Proceedings of the 3rd Historic Mortars Conference*, Glasgow. Rilem: Glasgow.

Thacker, M. (2015). Cille Donnain revisited: negotiating with lime across Atlantic Scotland from the 12th century. *Journal of the North Atlantic Special Hebridean Edition*.

Thacker, M. (2016). *Constructing Lordship in North Atlantic Europe: The archaeology of masonry mortars in the medieval and later buildings of the Scottish North Atlantic*. (Unpublished Ph.D. (archaeology) thesis, University of Edinburgh).

Thacker, M. (in prep. a). The Norse Church in Northern Hebrides: A reassessment of the chapel of North Rona [working title].

Thacker, M. (in prep. b). The evidence for a number of previously undiscovered medieval chapel chancels [working title].

Thacker, M. (in prep. c.). An interdisciplinary approach to the radiocarbon dating of medieval masonry buildings: Evidence from the pilot phase of the Scottish Medieval Castles & Chapels C-14 Project [working title].

White Marshall, J., & Rourke, G. (2000). *High Island*. Dublin: Town house and Country house.

White Marshall, J., & Walsh, C. (2005). *Illaunloughan Island*. Wicklow: Wordwell.

Medieval Mortars and the Gothic Revival: The Cosmati Pavement at Westminster Abbey

Ruth Siddall

Abstract In the 1870s the architect Sir George Gilbert Scott was appointed Surveyor to the Fabric at Westminster Abbey and one of his major initiatives was to restore the Cosmati Pavement in the Sanctuary. Originally commissioned by Henry III in the late 14th Century, this luxury pavement employed the Cosmatesque technique with materials and possibly artisans imported from Rome. As such, this pavement is the only remaining example if this type north of the Alps, and is one of the very few examples which retains much of its original mortars. These original mortars were developed to cope with the damp conditions of the Thames riverbank and are hydraulic limes which use crushed terracotta as a pozzolana. During the restoration in the 1870s, Gilbert-Scott attempted to replicate the appearance of these materials whilst using contemporary Portland cement mixes with a series of special additives. This paper presents a textural and petrological study, using optical polarising light microscopy, and compares the compositions and manufacturing technologies of the original 14th Century mortars with those of the 19th Century restorations.

Keywords Cosmatesque · Cocciopesto · Westminster abbey · Portland cement

1 Introduction

Situated in front of the High Altar of Westminster Abbey, the Sanctuary Pavement is the centrepiece of both the current church and that of the Pavement's patron, Henry III. It is constructed in the Cosmatesque style, depicting nine roundels arranged in two superimposed quincunxes and surrounded by a further 20 roundels making up the border of the floor. These are interspersed with rectangular tomb covers at the north, south, east and west sides of the floor. However, the early date of construction of this floor, probably 1268–69, and subsequent survival with only

R. Siddall (✉)
UCL Earth Sciences, Gower Street, London WC1E 6BT, UK
e-mail: r.siddall@ucl.ac.uk

J. J. Hughes et al. (eds.), *Historic Mortars*,
https://doi.org/10.1007/978-3-319-91606-4_6

small patches of restoration, makes it an unique piece of architectural stonework. The Cosmatesque style is a form of *opus sectile* decorative stonework, where different shaped pieces of coloured stones are arranged, rather like a patchwork quilt within a framework, usually of marble, but in this case Purbeck Stone. The coloured stones are predominantly Roman *spolia*, typically green *lapis lacedaemonius* porphyry from Krokeai near Sparta and the purple porphyry of Mons Claudianus in the Egyptian Eastern Desert.

The floor was commissioned by Henry III as part of his reconstruction of Westminster Abbey arranged to coincide with the translation of the tomb of Edward the Confessor on 13th October 1269 and was probably finished at around this time or slightly later (Carpenter 2002; Binski 2002). The Confessor's shrine and the pavement surrounding this, as well as Henry III's tomb are also decorated in the Cosmatesque style and some aspects of this work necessarily post-date the floor (Binski 2002).

There are four main phases of construction or repair in the 13th, 17th, 18th and 19th Centuries, known respectively as the Primary, Secondary, Tertiary Mixes and Scott Repairs as defined by Foster (2002) and summarised by Durnan (2002). This paper will concentrate on the Primary Mix and the Scott Repair.

The Westminster Abbey Sanctuary pavement is arguably unique. It is the only surviving floor of its type north of the Alps, and evidence presented here suggests that it is potentially one of a kind; the large number of 12th and 13th Century Cosmati and Cosmatesque floors in Italy have been re-laid and few retain any evidence of their original mortars. Pajares-Ayuela (2001) has provided a comprehensive review of Cosmati and Cosmatesque work in terms of their precedents, designs, geometries and art historical significance. Foster (1991) similarly provides a comprehensive discussion of the Westminster Abbey pavement.

2 Methodology and Analytical Details

The floor was surveyed macroscopically, using as a base map the digitised plan of the Sanctuary Pavement produced by N. Durnan & The Downland Partnership (1997). Each section of inlaid Cosmatesque work with the same mortar characteristics was assigned a number and the materials, including the stones used, were described macroscopically. In this way, 145 separate areas were identified on the pavement. These are shown on the annotated copy of the map in Fig. 1. Macroscopic examination of the mortars allowed them to be grouped into main types based on their colour and visible inclusions. These corresponded well with the main identified phases of construction and restoration. Samples were collected from lose fragments when possible (Table 1). Otherwise they were removed using a hammer and chisel or a mechanical cutting instrument. The most useful method of analysing the mortar and aggregate composition is to use the standard method employed for the petrographic analysis of geological and ceramic materials, to make a thin section of the material, mounted on a glass microscope slide which may

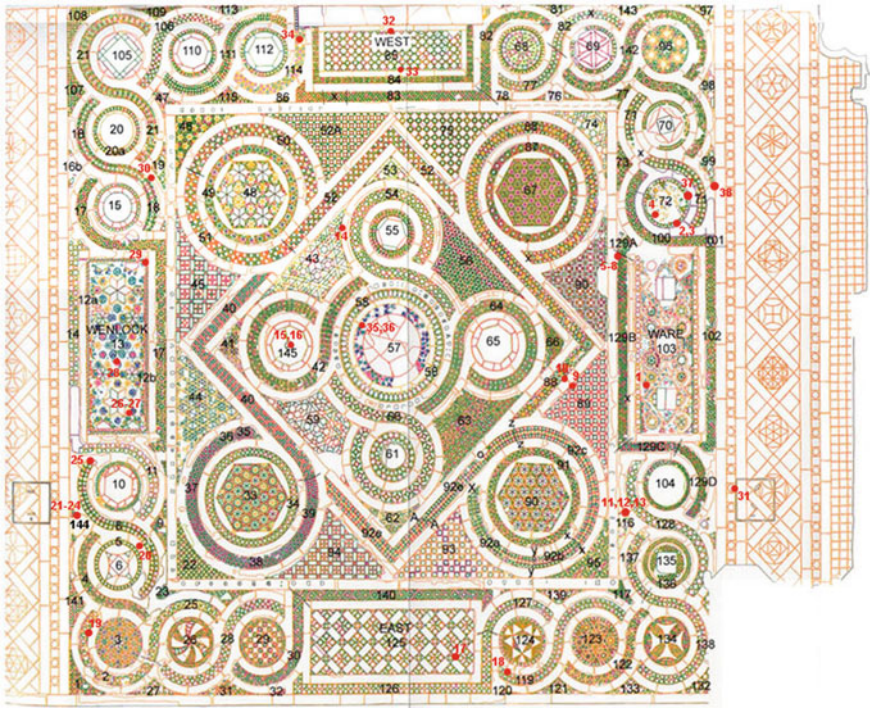

Fig. 1 Plan of the sanctuary pavement showing the numbering of the sectors (black) used in this report and the locations of mortar samples collected (red). Adapted from a survey made by N. Durnan & The Downland Partnership in 1997. The pavement is 7.58 m^2 (Color figure online)

Table 1 Sample locations and phases

Sample number	Location sector	Phase
1	103 Ware's Tomb	Primary Mix
3	72, North Border	Primary Mix
10	88, outer quincunx	Primary Mix
15	145, inner quincunx	Primary Mix
16	145, inner quincunx	Primary Mix
17	125, East Tomb	Scott's Repair
18	119, South Border	Scott's Repair
19	2, South Border	Primary Mix
25	8, South Border	Primary Mix
28	13, Wenlock's Tomb	Primary Mix
30	18, South Border	Scott's Repair
31	Pavement Border	Scott's Repair
33	85, West Tomb	Scott's Repair
34	57, Central Roundel	Primary Mix
35	57, Central Roundel	Primary Mix
38	72, North Border	Scott's Repair

then be analysed using polarised light microscopy (PLM; St. John et al. 1998). A sample needs to be larger than 10 mm^3 for effective use of this technique. Due to the very small fractions of mortar available for sampling in many cases, it was impossible to do this for all samples. From the remainder a sub-sample was taken which was pulverised to make a grain mount in MeltMount™ (RI = 1.662) for analysis using PLM. Samples were also prepared as stubs for analysis using scanning electron microscopy.

Optical analysis of the materials was carried out on a Leitz Orthoplan-Pol microscope with a maximum optimum magnification of 1000×. Photomicrographs were taken with a Nikon Coolpix digital camera. Observations were made in both plane-polarised light (PPL) and under crossed polars (XPL). The aggregate clasts, and to a certain extent, the fine grained cement paste, may be readily identified using techniques routinely used by geologists and described in texts including Deer et al. (1992), Tucker (1991) and Adams et al. (1991). In addition as man-made ceramic materials, terminology developed for the description of archaeological ceramics is also useful (Whitbread 1986, 1989 and Freestone 1995). Portland cements are entirely man-made materials and the phases present are not encountered occurring in nature.

A selection of samples were additionally analysed using scanning electron microscopy coupled with an Energy Dispersive System (SEM-EDS), carried out on a JEOL JSM-6480LV high-performance, variable pressure analytical SEM in UCL Earth Sciences. Scanning electron microscopy is a useful technique for examining the typically very finely crystalline cement pastes and when coupled with EDS analysis this technique can also provide a good determination of chemical composition. Stubs of paste were coated with carbon for EDS analysis and with gold for higher resolution SEM imaging. Samples analysed were small, with dimensions of 2–3 mm.

3 The Primary Mix Mortars

The Primary Mix mortars and stones were laid *c*. 1268 (Foster 2002). Over three quarters of the sectors analysed revealed evidence of either the original construction of the floor or very early repairs. These areas are distinctive in the use of *cocciopesto* mortars which are weakly hydraulic due to the use of crushed and ground ceramics as a pozzolanic additive.

The most striking aspect of this earliest phase of the mortars is that they were clearly intended to form an integral part of the design. The decorative stones are not closely fitted and each is surrounded by mortar, leaving several millimetres (between 2 and 10 mm) of mortar-filled spacing between each stone. Macroscopic examination of these mortars showed them to be distinctive, with cement pastes ranging in colour from deep red-orange to a pale ivory. The aggregate is formed from a pozzolanic additive of crushed and powdered ceramics plus a geological material with particles of variable composition (Fig. 2). The colour is due to

powdered ceramic sherds and colour intensity shows considerable variation across the floor. The surface has yellowed over time, and in places where the setting mortar is revealed (under the central roundel of sector 145 and 144) it is shown to be varying shades of pink. Aggregate is batched to the cement at ratios of ~2:1. In some cases, it would appear that an upper, ~2–3 mm thick layer of grout has come away, leaving a (usually) coarser and paler-coloured setting mortar below. By analogy with other sections of the floor, it would seem that there is an upper grout layer which is richer in powdered ceramic than the setting mortars and therefore more hydraulic. However, this 'layer' is not found universally across the Primary Mix areas of the floor.

When viewed under the microscope, the cement paste is optically very active under crossed -polars which indicates that it is well carbonated. However, the lime matrix is weakly hydraulic and this property is imparted by the presence of powdered terracotta sherds mixed in with the cement paste. Consequently there are patches visible where this reaction has been more extreme and these areas show lower birefringence. Individual phases within the cement matrix are beyond the resolution of the optical microscope. Also present are unreacted lime and rare particles of partially or unburned limestone. The latter are identified as particles of chalk based on their mineralogical textures and the presence of microfossils.

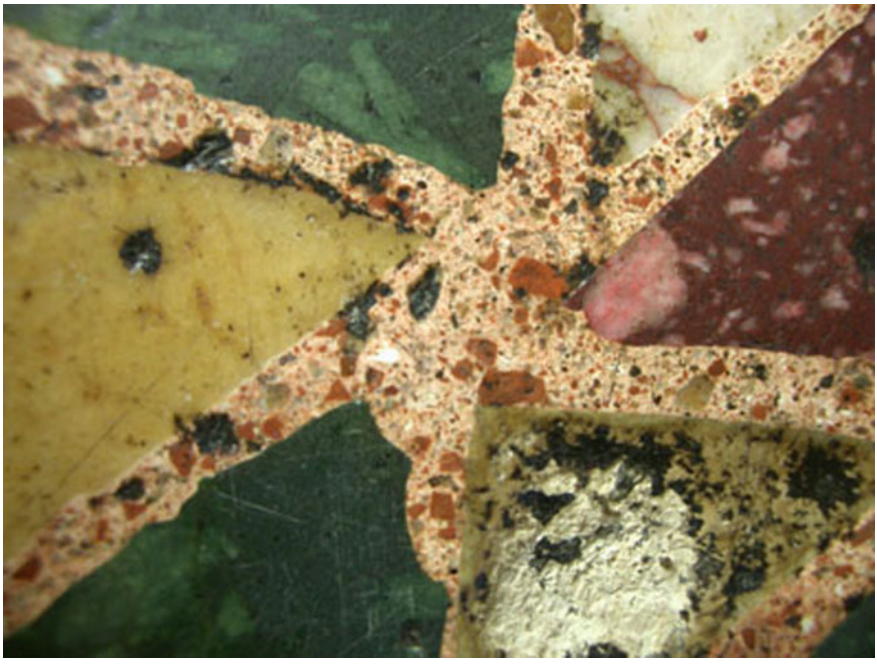

Fig. 2 Primary Mix mortars in sector 9, showing the typical pale pink cement paste with a poorly sorted aggregate of orange ceramics and lithic fragments. Field of view is approximately 10 cm wide

The aggregate is of two main fractions. Firstly, a sand of geological origin composed of well-rounded grains of single-crystal quartz, a few grains of poly-crystalline quartz, glauconite and flint. Grains of carbonate rocks (chalk) are also present. The sand is coarse, with particle size ranging from ~0.2 and 3 mm. By contrast, the second fraction of the aggregate, though of a similar size range, is composed of very angular fragments of ceramic tile or pot sherds. These particles predominantly have a red clay matrix, with low optical activity with inclusions of quartz and muscovite in varying proportions. A few ceramic particles have black, isotropic clay matrices which may indicate that they are derived from different wares or they may represent blackened cores of otherwise oxidised fabrics. A very fine grained fraction possibly existed, but this would have been consumed by hydraulic reactions. Three distinct ceramic fabrics were identified to be present a black-bodied quartz ware, a red-bodied quartz ware and a red-bodied quartz-muscovite ware.

SEM images showed the mortars to have a 1 μm particle size and grains had a subhedral to anhedral morphology with aggregates of platy and rhombic grains present. SEM-EDS analysis of sample 19 showed the chemical composition to be calcium carbonate and minor silica. Sample 35 also contained traces of alumina and sulphate.

4 George Gilbert Scott's Restoration: Main Floor

Sir George Gilbert Scott was responsible for the layout of the Sanctuary Pavement and the High Altar as we see them today. His restorations took place around 1867–89. Scott has taken considerable care to replicate the mortars used in the Primary Mix showing that he was quite capable of differentiating the various phases of restoration on the Pavement.

The roundels and tomb along the east border of the floor are replacements by Scott, who may have redesigned these sections completely (Foster 2002). The mortars employed on the Sanctuary Pavement employed by Scott are superficially very similar to those of the Primary Mix, though they lack the strong orange-pink colouration of some of these mortars. The cement paste matrix is cream to ivory in colour and is set flush with the top surface of the stones. It contains an aggregate, clearly visible to the naked eye, of lithic grains and red or orange fragments. These are well sorted, all particles are of a similar size, ~0.5 mm.

Samples 17, 18 and 30 were collected from the east border of the floor and were therefore securely dated to Scott's restoration. In addition, Samples 32 and 33 from the West Tomb were also identified, based on petrographic analysis described here to belong to Scott's phase of restoration. The small fraction of Scott's mortars meant that samples would necessarily be very small. In fact, none were large enough to make a useful thin section, and all were prepared as grain mounts. All samples showed very similar compositional variation.

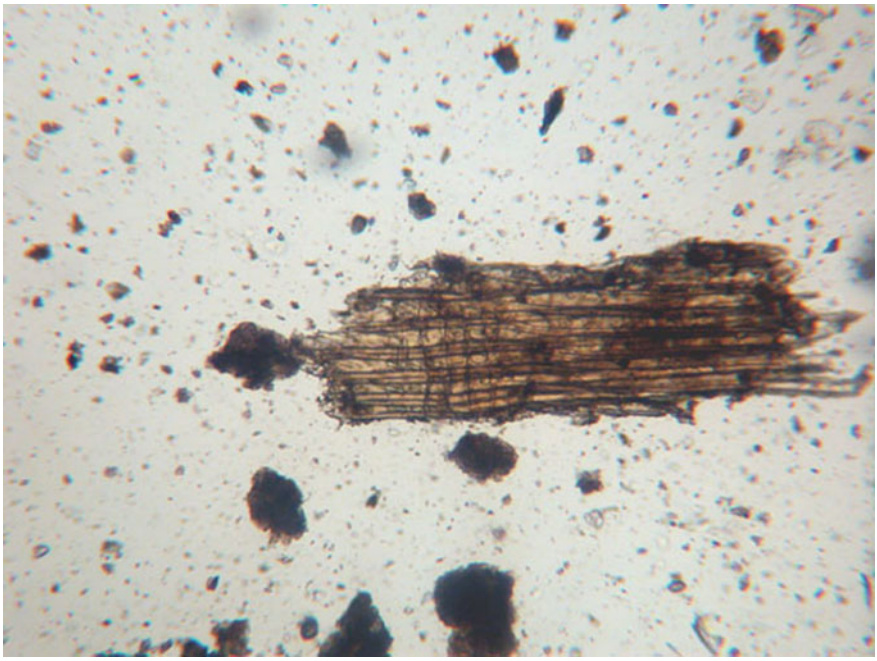

Fig. 3 Vegetable fibres in the grain mount of Sample 32. ×60, plane-polarised light. Field of view is 0.5 mm

The fine fraction (i.e. < 40 μm) observed on the grain mounts were calcium carbonate and a small amount of gypsum; the latter was present in distinctive lath-shaped crystals. Clumps of carbonate plaster, showing characteristic high birefringence were common. Grains of mineral aggregate are fine, sub-rounded, quartz and flint sand. Red-coloured ceramics are also present, but further identification of these is difficult using the grain mount technique. However, they were shown to be finely polycrystalline and interpreted to be made from iron-rich clays. Additionally present as an additive, and arguably diagnostic of these mortars, were particles of chopped plant bast fibres, which were yellowish in colour when observed under PPL. Under crossed polars, these fibres showed second order birefringence colours and inclined extinction (Fig. 3).

5 Scott's Mortars from the North and South Borders

The borders which flank the north and south edges of the pavement were designed by Sir George Gilbert Scott and laid by his contractors, Poole & Sons, in 1870 (Foster 1991, 2002; Jordan 1980). The borders are composed entirely of Purbeck Stone, grouted with cement. The design features roundels and diagonally-laid

sections which clearly echo the design of the floor. Mortars are used to set and point the Purbeck Stone slabs used in the borders. They are brownish-orange in colour and aggregate is not clearly visible to the naked eye.

Two samples were collected from the floor, one was of sufficient size to make a large thin section (Sample 38) but the second was small and a fraction of it was therefore pulverised to make a grain mount (Sample 31).

Sample 38 when viewed in PPL has an overall orange colour (Fig. 4). The cement paste is fine grained and mottled and this is particularly evident under crossed polars. In XPL it has high optical activity, and there is clearly a large amount of carbonate present. There is little evidence of unreacted Portland cement clinker kernels being present. Small patches which appear to be colourless, reveal meshes of needle-like crystals of ettringite at higher magnifications (×400). Areas of fine glass and/or tobermoreite gels are present. The orange colour is promoted by ferrite phases.

Aggregate is a fine quartz sand, and what appear to be crushed ceramics. However they have reacted well with the cement paste and now appear fuzzy and diffuse with blurred, low contrast boundaries between them and the cement paste. Also present are particles of slag containing a wide variety of phases and glasses. Larger particles show a decussate textured slag formed of elongate yellow crystals and interstitial brown crystals and glass. These are interpreted to be blast furnace

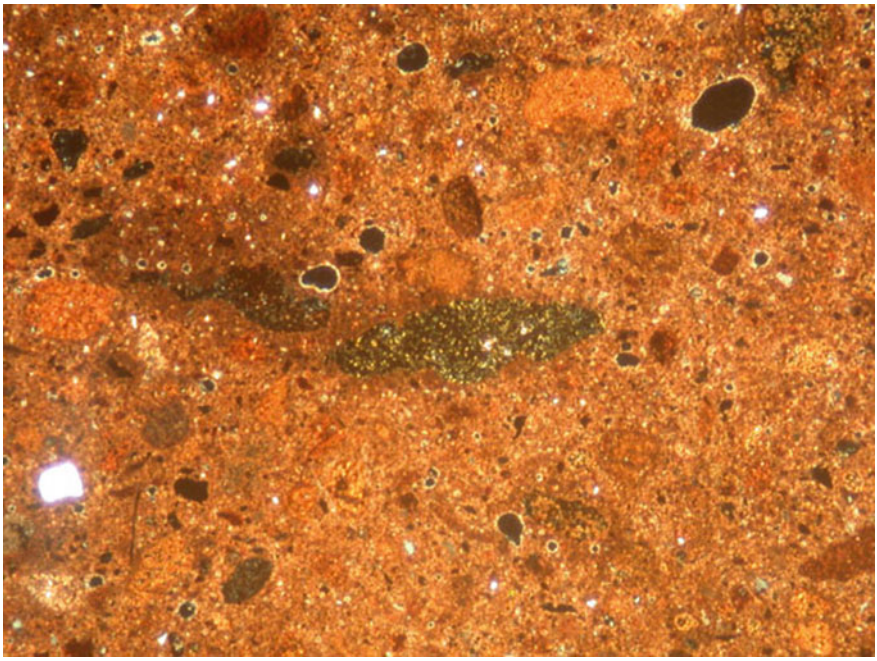

Fig. 4 Sample 38. Viewed under crossed polars, ×60, the field of view is 1.5 mm. Black patches are voids, the darker particle in the centre is blast furnace slag, with a large amount of glass present

slags containing melilite and associated phases. There is ~20% porosity in rounded to irregular voids. These are lined with a thin layer of portlandite and secondary calcium carbonate.

The grain mount of sample 31 showed a strong compositional similarity to the thin section of sample 38. The cement paste had a dark colouration in PPL and a range of birefringence colours in XPL. This is composed of glass and/or gel, carbonate, portlandite and possibly ettringite. Lath-shaped crystals showing first order grey birefringence are interpreted to be derived from slags used as an aggregate. Crumb-like aggregates of cement paste were identified and these were moderately well carbonated. Fragments of orange-coloured, particles were interpreted as reacted terracotta. Many particles were yellow in plane polarised light and some small aggregates of yellow and dark, red-brown grains were present. These are probably particles of metal-processing slag. A small amount of quartz is also present as aggregate.

6 Discussion

The Primary mix mortars were made using ancient hydraulic lime manufacturing techniques which were originally developed in the 2nd Century AD, for making hardwearing and waterproof floors. This involved mixing the slaked lime with crushed and powdered ceramic material. The Roman name for this material was *opus signinum*, but it was later called *cocciopesto* in Italy and this is an appropriate term to describe the mortars of the Sanctuary pavement. These materials were probably calcined using a flare kiln, although there is some evidence of underburning which enables the probable identification of the limestone charge as being the upper Cretaceous Chalk Formation. This may well support a continuation in thinking from the 1st Century AD to the 13th Century that the 'whitest' limestones made the best limes, as put forward by Vitruvius and Cato.

Particles of unreacted lime indicates an incomplete slaking process, whereby the lime was hydrated but contemporaneous with the addition of water, or soon after, it was mixed with the aggregate, before the lime had completely reacted to form portlandite. This shows that the 'hot-mix' technique, whereby the aggregate was added to the lime at the time of slaking and the mortar was used soon afterwards, rather than allowing a long time period for the lime to become completely slaked.

The chemical composition of the mortars, as assessed from EDS analysis of samples 19 and 35 showed them to be composed of calcium carbonate with minor amounts of silicate and sulphate present. This strongly suggests the presence of cement phase associated with hydraulic sets such as calcium silicates and/or calcium silicate hydrates and sulphates. However, actual phases may not be conclusively identified due to the low count totals obtained from the samples. They were probably formed from a mixture of lime and the ceramic pozzolana, with possibly a

small fraction of gypsum added. The ceramic sherds are terracottas (i.e. fired at temperatures < 1000 °C) and at least 3 different fabrics are identifiable amongst these, suggesting that a variety of waste ceramics were recycled as pozzolanic additives.

The geologically derived aggregates are Thames river gravels which were sourcing the Upper Cretaceous strata of the Thames Basin, the Upper Greensands (indicated by the presence of glauconite) and flints, derived from the Chalk. The relatively restricted grain size of the aggregate and the absence of a very fine fraction suggests that the materials was washed and sieved prior to incorporation with the cement paste.

The variation in colour within the mortars demonstrates that they were mixed in small batches as and when needed. The presence of larger quantities of powdered lime in the upper surface of the pointing mortars may well be as a result of the recently applied mortar being sprinkled with extra ground sherds to further enhance the hydraulic set of the uppermost layer. These regions possibly represent working shifts, whereby a section of foundation mortars was laid, the stones were arranged upon this, allowing for small changes and adjustments of the pattern, and then they were set in place by the pointing mortars. There is only one example of a section where areas of pattern were laid as prefabricated sections. It is possible that these areas represent early repairs to the floor.

Scott's mortars used on the Cosmatesque Pavement are traditional lime mortars, gauged with a small fraction of gypsum mortar. They contain an aggregate of quartz and flint sand and also contain chopped plant fibre. The mineral aggregate is well sorted indicating that it was graded. These materials are in contrast to the Primary Mix mortars which are very poorly sorted, showing aggregate particles of varying size. The presence of the plant fibre was also of note. This component was observed in all samples and was not found in Primary Mix samples, making it a diagnostic indicator of Scott's recipes. Consequently, evidence is presented here that the West Tomb was also re-laid by Scott, though largely using only original stones. It cannot be discounted that other small areas of Primary Mix stones and mortars were re-pointed by Scott, but no clear evidence for this was noted macroscopically.

Samples 31 and 38 belongs to Scott's restorations or later. It is feasible to relate it to Scott's construction of the border (1870) based on the similarity of the materials observed macroscopically here. The materials are more obviously hydraulic than the lime-ceramic mortars described previously. They bare some similarities to Portland cements, but with much more calcium carbonate present than would be expected in modern OPC. Scott (or in fact his contractors, Poole & Sons) have apparently added potsherds to try and match this material with the primary mix, however the sherds have reacted far more strongly and have almost been consumed by the reaction. They have promoted a strong orange colour to the materials. Quartz sand, and slag are also present. Blast furnace slag produces a strong pozzolanic reaction and was frequently used as an aggregate.

It is likely that Scott was experimenting here to produce a cement which resembled the Primary Mix mortars, but for a cheaper, harder wearing and damp resistant material to secure the Purbeck Stone of the borders. He possibly made

these with a mixture of lime with very finely ground ceramics and other pozzolanas. Portland Cement clinker was not obviously present in the samples; an hydraulic set may have been promoted by the mixture of finely ground pozzolanas with well slaked limes. The mixture was also probably gauged with gypsum (now reacted to form ettringite?) to retard setting.

The evidence presented by the floor, particularly after comparison with similar works in Rome show it to be a unique example of its kind, and of very great importance to the study of Northern European Medieval architectural decoration, appropriate use of materials and contacts with Rome. The floor is, as in the words of James Peller Malcolm, "*The most glorious work in England, venerable through age, costly in its materials and invaluable for its workmanship*" Malcolm (1802).

References

Adams, A. E., MacKenzie, W. S., & Guildford, C. (1991). *Atlas of sedimentary rocks under the microscope*. Longman Scientific & Technical. 104p.

Binski, P. (2002). The Cosmati and *romanitas* in England: An overview. In L. Grant & R. Mortimer (Eds.), Westminster Abbey: *The Cosmati Pavements., Courtauld Research Papers No. 3*., Ashgate., pp. 116–134.

Carpenter, D. (2002). Westminster Abbey and the Cosmati Pavements in Politics 1258–1269. In L. Grant & R. Mortimer (Eds.), *Westminster Abbey: The Cosmati Pavements., Courtauld Research Papers No. 3*. Ashgate. pp. 37–48.

Deer, W. A., Howie, R. A., & Zussman, J. (1992). *An introduction to the rock forming minerals* (2nd Ed.). Longman Scientific & Technical. 696p.

Durnan, N. (2002). The condition and conservation of the Cosmati pavements at Westminster Abbey. In L. Grant & R. Mortimer (Eds.), *Westminster Abbey: The Cosmati Pavements., Courtauld Research Papers No. 3*. Ashgate. pp. 92–99.

Foster, R. (1991). *Patterns of thought: The Hidden Meaning of the Great Pavement of Westminster Abbey*. London: Jonathan Cape. 184p.

Foster, R. (2002). The context and fabric of the Westminster Abbey Sanctuary pavement. In L. Grant & R. Mortimer (Eds.). *Westminster Abbey: The Cosmati Pavements., Courtauld Research Papers no. 3*. Ashgate Publishing Ltd. pp. 49–91.

Freestone, I. C. (1995). Ceramic petrography. *American Journal of Archaeology, 99,* 111–115.

Jordan, W. J. (1980). Sir George Gilbert Scott R. A., Surveyor to Westminster Abbey 1849–1878. *Architectural History, 23*, 60–85 (Appendices 188–190).

Malcolm, J. P. (1802). *Londinium redivivum; or, An Ancient History and Modern Description of London*. London.

Pajares-Ayuela, P. (2001). *Cosmatesque ornament: Flat polychrome geometric patterns in architecture*. (transl. M. Fleming Alvarez). W. W. Norton & Co., London. 320p.

St. John, D. A., Poole, A. W., & Sims, I. (1998). *Concrete petrography: A handbook of investigative techniques*. Arnold, London. 474p.

Tucker, M. E. (1991). Sedimentary petrology (2nd Ed.), Blackwell Scientific Publications. 260p.

Whitbread, I. K. (1986). The characterisation of argillaceous inclusions in ceramic thin sections. *Archaeometry, 28,* 79–88.

Whitbread, I. K. (1989). A proposal for the systematic description of thin sections towards the study of ancient ceramic technology. *Archaeometry, 31,* 127–138.

Terranova, a Popular Stone Imitation Cladding: Strategies and Techniques for Restoration

Yves Govaerts, Ann Verdonck, Wendy Meulebroeck and Michael de Bouw

Abstract At the beginning of the 20th century, the application of innovative finishes on façades became a popular phenomenon in Belgium. Decorative renders were frequently used to hide the aesthetically imperfect structure and to imitate valuable natural stone features. In order to create the appearance of French stone, ingredients such as lime, mica and crushed natural stone were added to white cement. Afterwards, the surface was scratched or scraped to shape a rough texture. As a result, a convincing 'simili-pierre' or 'stone imitation' masonry was obtained, after drawing simulated joints into the wet render layer. Today, these imitation finishes suffer in most cases from discoloration, cracks, peeling off and other damage which has completely changed the initial perception. Since knowledge is lacking concerning their composition, properties and application techniques, many questions remain unanswered within the conservation area. As a consequence, incorrect decisions may be made during restoration campaigns, which may lead to additional damages. A remarkable example of a simili-pierre render is the former commercial product *Terranova*, which is the focus of the research. By means of literature studies, the exploration of historical patents, laboratory analysis of representative samples and a comparative research between similar claddings, this paper proposes legitimate solutions to revitalize the Terranova finishes. It is found

Y. Govaerts (✉) · A. Verdonck
Department of Architectural Engineering, Vrije Universiteit Brussel, Brussels, Belgium
e-mail: Yves.Govaerts@vub.ac.be

A. Verdonck
e-mail: Ann.Verdonck@vub.ac.be

W. Meulebroeck
Department of Applied Physics and Photonics, Brussels Photonics Team (B-PHOT), Vrije Universiteit Brussel, Brussels, Belgium
e-mail: wmeulebr@b-phot.org

M. de Bouw
Department of Monuments and Landscape Conservation, Lab of Renovation, University of Antwerp, Belgian Building Research Institute, Antwerp, Belgium
e-mail: michael.de.bouw@bbri.be

J. J. Hughes et al. (eds.), *Historic Mortars*,
https://doi.org/10.1007/978-3-319-91606-4_7

that both original mortar formulas and historic application guidelines are key elements which form a fundamental contribution to restore stone imitating renderwork in a sustainable way, with respect for authenticity issues.

Keywords Terranova · Decorative render · Stone imitation · Restoration
Simili-pierre finishes

1 Introduction

One of the consequences of the Industrial Revolution in the 19th century was a tendency towards standardization of building materials. Instead of working with time consuming and expensive traditional techniques at the building site, prefabricated products such as cast iron elements and ready-mix plasters entered the trading markets. Particularly the introduction of Portland cement led to innovative compositions towards exterior decorative plasterwork. Besides the protection and conservation of the underlying structure, façade renderings had to fulfil an additional aesthetical function (Everaert sd.). For instance, to create the illusion of a perfect brickwork or stone appearance, many façades have been manipulated in the past, not only to camouflage damage or cover building traces, but chiefly to increase the status of a building with relatively cheap materials. Before the emergence of Portland cement, imitation brickwork for outdoor applications was mainly established by applying a lime mortar in which idealized brick contours were colour washed and simulated joints were oil painted (Verdonck et al. 2014). However, at the end of the 19th century, imitation mortars no longer needed paint layers; the colour and texture of the finishing mortar itself created an appearance of real natural stone after hardening.

Although the stone imitation industry is born in Germany (Danzl 2002), the material is generally accepted in Belgium from the beginning of the 20th century, where it is known as ‘simili-pierre’. As a consequence of its massive application, many of these façade finishes have survived and they still have an important share in the existing Belgian building stock. Being part of the streetscape, stone imitations are encountered in two different forms: as a render layer on masonry surfaces or as a precast decorative artificial stone which is integrated into the façade. In the Belgian context, the majority of the artificial blocks and decorative plasterwork was fabricated to approach as closely as possible the appearance of “French stone”, which is a collective term for light coloured rocks that were imported from France during the 19th century, such as *Euville* stone and *Savonnières* stone.

By using historic sources and characterization methods, this paper tries to formulate a repair render composition to restore the peculiar simili-pierre render *Terranova*. Although it is believed that most stone imitations were prepared on-site,

this type was a ready-mixed mortar (Kapferer 1911a). Since the ingredients were already mixed in correct proportions at the factory, a uniform result of high quality was acquired. As a consequence, the composition remains the same on different façades; only the texture can differ case by case, due to variations in the original finishing technique and erosion by the test of time. Therefore, the outcome of this research can be directly employed for specific conservation issues and the methodology may be useful for characterizing other historic mortars.

2 Terranova

A remarkable Terranova application can be found on the art deco façades of *De Roma*, a cinema complex from 1928 in Borgerhout, Antwerp, Belgium (Fig. 1-left). The composition of the façades is based on a rhythm of predominantly straight lines, balconies and bay windows. Uniform shades of the simili-pierre finish generate a striking architectural effect of light and shadows. The material itself performs an important decorative function. As shown in the microscopic image (Fig. 1-right), the mortar is applied in two layers: a rendering layer and top layer, each with a different composition.

From the late twenties on, the product Terranova regularly appeared in Belgian architectural journals, and technical handbooks, where it was promoted through

Fig. 1 Historic cinema "De Roma" (1928, north façade), Antwerp (Belgium): upper floors are finished with Terranova (Picture: Y. Govaerts) [left]; Terranova sample from the west façade of "De Roma" (Picture: L. Dekeyser) [middle]; Optical microscopic image of the layered structure of the historic sample: I. Top layer, II. Rendering layer (KIK-IRPA 2011) [right]

advertisements (Becker 1932) and case studies (La Cité, 1928) or presented as '*... a modern render with a characteristic vivid colour and sustainable properties ...*' (Oosterhof 1932).

Interesting examples of similar render finishes can be found in every urban area in Flanders, including the prominent residential boroughs of Brussels (Govaerts et al. 2016). The emerging popularity was principally a result of changing fashion within the domain of architecture. This new material perfectly fit into the vision of the rational architects, but it was also loved by ordinary people, who were now able to decorate their façades with an apparently good-looking and eminent material. However, imitation renders were hardly 'new' building materials. Carl August Kapferer already developed the Terranova render in 1893 near Freihung, Germany (Garda 2003). Given the success of this ready-mixed plaster, the firm *Terranova-Industrie C. A. Kapferer&Co* was able to expand and various subsidiary companies were found over Central Europe. No manufacturing unit could be traced in Belgium, because the product was imported and distributed by the company *Pommée & Köttgen,* which was located in the German-speaking region of Belgium. Although the product received less interest after the Second World War, its manufacturing continued, though with a slightly different composition formula to reflect other properties (Garda 2003).

3 In Search of the Terranova Composition

Today, professionals often encounter difficulties when dealing with stone imitating renders from the beginning of the 20th century, since there is a lack of restoration philosophy and knowledge with regard to their conservation. Although the Belgian cities are enriched with a considerable collection of historic claddings, an elaborate inventory does not exist. As a result, most claddings are not yet identified, including Terranova finishes. However, Terranova was a frequently used material, according to descriptions in old plasterer's manuals (Oosterhof 1932; Arendzen and Vriend 1936; Poptie 1948).

The present research is based on the Terranova finish of the old cinema building *De Roma* in Antwerp. Because of the uniform fabrication of this render product, the findings of this case study are considered to be representative for other cases making use of Terranova. Unfortunately, literature search on building specifications and old handbooks did not reveal any detailed descriptions on the composition of this particular finishing material. The authentic formula to produce Terranova is never mentioned, being a well-kept trade secret. However, an extensive patent search enabled the authors to trace the original ingredients.

The first patent of Terranova, requested by Kapferer in 1893, is not available in any European patent database. Presumably this document ended up in a private collection, just like a later patent from 1896, which is preserved in the archives of Weber & Broutin (Garda 2003). The oldest accessible patent signed by Kapferer dates from September 4, 1899. The focus lies on improvements in the manufacture

of cement (Kapferer and Schleuning 1899). As a reaction to the less attractive gray cement renders, which suffered from problems concerning their hardness, vapour transmission and stained aspect, an alternative for exterior plastering had to be found. The goal of the patent was to obtain a more attractive colour and to use this new cement both for decorative as well as structural purposes (for example as joint mortar for masonry). Clay (kaolin), feldspar (orthoclase), lime and pure quartz sand, the main components of the formula, were burned together to manufacture cement clinker. About 7 months later, a new patent appeared, focusing on the role of feldspar within the cement (Kapferer and Schleuning 1900). On the one hand, feldspar was necessary for the production of soluble silicic acid, which is needed for binding, and on the other hand it had to improve the flux or workability properties.

The year 1911 was a milestone in the development of Terranova. Instead of mixing the ingredients on site, Kapferer developed a ready-mix dry mortar, which only needed water to start the binding process. Through this industrialization of the production process, the quality and proportions of the plaster were easier to control. This implies that the finish of De Roma is not representative for buildings before 1911, since the early mixture was probably related to delicate fluctuations in its composition. At the time, it was also no longer recommended to paint the renderwork after application, because the mortar itself acquired aesthetic qualities.

> '… The new plastering mortars were employed where the plastering was not to be subsequently coated with paint. Very fine architectural effects were obtained by staining the mortar, by adding granular rocks and minerals to the slaked lime …' (translated by the authors, Kapferer 1911a)

In the same year another patent appeared, containing a *'Method of improving the permeability to air of dry plastering-mortar'* (Kapferer and Weber 1911b). This is considered as an important finding, since patents concerning this topic were requested in at least three countries within a few days. According to the patent, the composition comprised small powdery components, which resulted in a very compact, low vapour-permeable render. Adding oil or other fat additives would enhance the bonding capacity and at the same time a smaller amount of lime could be used in the mixture. This led to a mortar, which was considered less sensitive to rapid dehydration and therefore cracks would be reduced. The oil, however, increased the formation of micro-pores, which resulted in a volume expansion of about 10%. In addition, previous experiments indicated some problems to distribute the additives uniformly into the lime paste. The patent suggests adding a mixture of oil, acetone and starch additives. The main purpose of the starch was to increase the bonding process, without the need for more water. Immediately after the slaking process, the lime putty had to be sprinkled with the considered mixture. Because the lime paste would still possess internal heat, the acetone would evaporate quickly. As a result, the lime would be less sticky, making it easier to achieve a uniform distribution.

In 1926, one year before the construction of the case study, an 'improvement patent' refers to mortars for architectural purposes (Kapferer 1926). To create a sparkling, stone imitating effect, particles of mica, natural stone or stone-dust were

added to the mixture for the top layer. However, according to Kapferer, the aesthetic aspects tend to disappear. To avoid visual complications, the lime particles may not cover other elements such as mica minerals. By adding organic additives, which envelop the individual stone aggregates, the formation of a lime blanket is prevented. Consequently, mica fragments are situated in the surface layer, ensuring a sparkling effect. An example of such organic compound is mineral oil, but also glycerines can be added.

These patents from *Terranova-Industrie C. A. Kapferer&Co* give an overview of the chemical bonding processes, but unfortunately—apart from the cement formula—they do not mention any ratios or percentages of the applied ingredients. Only a scarce number of Belgian patents with formulas for stone imitating renders provide useful details. For example, in 1908 Jean Soille publishes a patent titled '*Composition pour pierre artificielle'* (Soille 1908). The product is named 'Pierreuse' and it reveals an approximate ratio for the addition of mica: 20–125 g of mica is used for 100 kg of crushed stone. Commonly used proportions for outdoor scrubbed mineral plasterwork are found in historic technical manuals, which are expressed in volume units[1] (Oosterhof 1932; Arendzen and Vriend 1936).

Chemical examination (SEM/EDX) of a sample from the west façade of the case study (Fig. 1-middle), performed by the Royal Institute for Cultural Heritage (KIK-IRPA 2011) reveals new information on the ingredients (Figs. 2 and 3). The binder (16.5% hydraulic) consists of calcium, silicon, and a small amount of magnesium, potassium and aluminium (feldspar). Presumably, the binder is a combination of white cement and lime, because non-hydrated hydraulic residues are observed; yet it is hard to identify them by optical microscopy. Note that the composition of historic 'white cement' is different from ordinary white coloured cement. 'White cement' was known as heavy white lime mixed with about 10% of bright coloured cement (Leduc 1902).

The aggregate is composed of 50% quartz sand and 50% limestone fragments, which are derived from coarse crushed Euville stone.[2] Because of the presence of limestone both in binder and aggregates, it is not possible to identify their ratio. The sand particles are characterized as angular, average coarse units and mica particles are recognized with a size of a few millimeters. In contrast to the patent specifications, no traces of oil addition are detected.

All patents from Kapferer generally correspond to the scientific findings. Consequently, if the instructions above are properly applied, it should be possible to reproduce a good approximation of the Terranova render. Nevertheless, grain sizes and colours may be different from the reference surface, because historically, there

[1]Recommended proportions for a scrubbed top render:
1 Portland cement: 2-3 sand,
1 slaked lime: 1,25 trass: 2,5-3 sand
1 Portland cement: 0,5-1 trass: 3 sand.

[2]Euville is a limestone, containing calcite cement and crinoid fragments. The particular stone was imported from the quarry of Euville-sur-Meuse (France) and commonly used in the Belgian building industry during the 19th century.

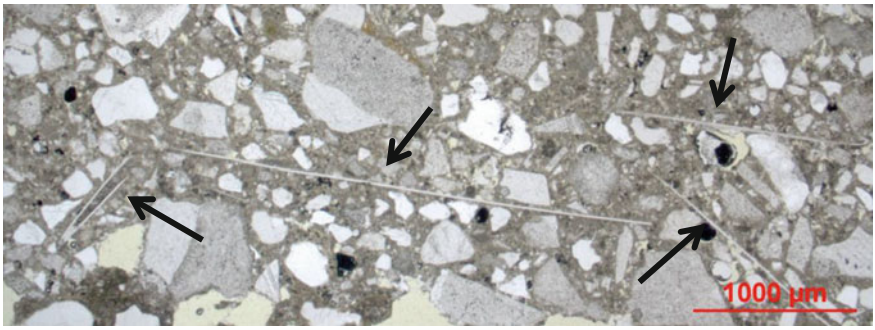

Fig. 2 Optical image of a thin sample section: the arrows indicate mica particles. (*Source* KIK-IRPA 2011)

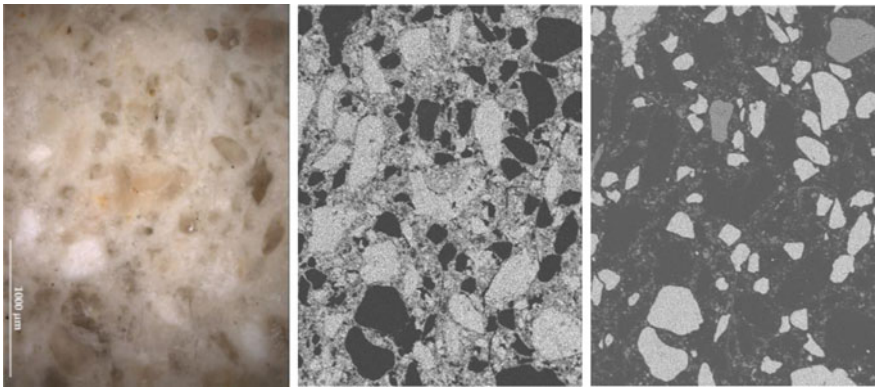

Fig. 3 Distribution of the elements in Terranova, measured with an electron microscope (SEM): sample [left], limestone fragments and the binder are highlighted as calcium [middle], quartz sand is visible through the mapping of silicon (white spots) [right]. (*Source* KIK-IRPA 2011)

were more versions of this render product (from fine to coarse). Therefore, it is always useful to perform preliminary test-strips on the façade before restoration, in order to verify the share of additives in the mixture.

4 Historic Guidelines for Application

Before spreading the rendering on the façade surface, the support has to be prepared by removing all impurities and flaking parts with a wire brush. In addition, the brick or concrete support gets a roughened texture to improve adhesion with render layers. As illustrated in Sect. 2, a stone imitation cladding is generally applied in 2 layers (in some cases even 3 layers). Building specifications and related documents

rarely focus on the rendering layer, yet this is an important element. This layer has to flatten the support and to give strength to extended ornamental elements. Therefore, its compatibility with the finishing Terranova layer is essential. One historic manual (Arendzen and Vriend 1936) provides a description of its composition, which has specifically to be used in case of Terranova: 14% cement, 14% shell lime and 72% sand, mixed with an appropriate volume of clean water. Shell lime is a weak hydraulic lime, which is no longer available in its original composition in Western Europe. According to the heritage agencies, an alternative for this ingredient is air lime. Besides these historic instructions, optical analysis reveals the presence of 4 units of binder material to 5 units of aggregate. However, it must kept in mind that the rendering layer formula varies depending on the case, because this mortar was prepared on site. In case of *De Roma*, the binder can be classified between strong hydraulic lime and early cement. The aggregate is identified as quartz sand with a smaller amount of feldspar, trass and stone fragments. This preparation layer is applied with a thickness of about 5–10 mm. To improve the adhesion with the top layer, grooves are drawn randomly into the wet base layer. This preparatory action is visually confirmed by many case studies. 'Het handboek voor den stucadoor' ('The plasterer's manual') describes the preparation of the top layer:

> '… It is recommended to mix the required amount of Terranova powder at the same time; this is for coarse granular material 1 bag for 3 m^2, and for fine-grained material 1 bag for 4 m^2. Terranova has to be mixed with clean water to become a solid mass. The craftsman should pay attention to the mixing process, in order to avoid lumps …' [Translated by the author from Dutch] (Oosterhof 1932)

This excerpt proves the existence of various Terranova products, varying from a coarse to a fine-grained texture. The mixing process was done mechanically, using a mortar mill with rotating blades (Fig. 4-left). By means of a trowel and wooden float the top layer was applied to the pre-wetted surface to a sufficient thickness of 5–8 mm. Such thickness is required because the finishing treatment involves material losses.

> '… The final stage is achieved by means of a sharp steel lath, making it possible to scratch the Terranova layer: it is clear that this action can only be carried out when the top layer is hardened and dry. By doing this, grains will sprout out the façade …'. [Translated by the author from Dutch] (Oosterhof 1932)

The scratching process can only be applied when the entire façade is rendered. As well as the standard Terranova type, a coarser grained version was popular: *Terranova grana*. However, the application technique of this type is slightly different: after roughening up the rendering layer, the top layer is pressed with a wooden float to compress the grains. By doing so, binder will come to the surface and has to be wiped off with a brush before the hardening process starts. In order to obtain a regular surface, it is necessary to repeat this treatment. After 3–4 days, the remaining binder sludge needs to be removed with dilute hydrochloric acid.

Fig. 4 Vertical mortar mixer [left] (Oosterhof 1932); simulated joint [middle] (Govaerts 2012); tool used for drawing joints into a recently rendered surface [right] (Geldof et al. 1969)

Previous methodologies are in accordance with similar patents for other types of stone imitation, such as the "Procédé de fabrication d'un produit imitant la pierre" (Leclercq 1921):

> '… Applications of the render on stone, brick, wood, metal and particularly on paper requires a division in layers, the render is applied by means of a knife; subsequently the surface is brushed to absorb remaining sludge. Afterwards the surface is divided according to the rules of architecture, sanded and washed after completion …'. [Translated by the author from French]

After a short period, simulated joints can be drawn into the plasterwork by means of a small wooden instrument (Fig. 4-middle/right).

5 Damage Typologies

In order to effectuate correct conservation strategies, an assessment of damage patterns is required. After all, it is important to have a proper idea of the origins of the problems, because improper treatment may lead to recurring damage. The following paragraphs describe the most important damage typologies that were observed within the case study (Fig. 5) and concentrate on the origins.

5.1 Soiling and Discoloration

In urban context, dark contrasts are principally generated by dirt concentrations from the air pollution, which have a major impact on the building's image. Especially when the render material contains limestone fragments—which is nearly always the case when dealing with stone imitation claddings—black crusts are formed. These crusts arise when limestone fragments interact with atmospheric SO_2, forming gypsum efflorescence. Higher concentrations of sulphate are linked to

Fig. 5 Damage assessment of the north façade (Govaerts 2012)

a greater amount of gypsum, leading to thicker crusts over time (Ozga et al. 2011). Subsequently, polluted air and rainwater containing dirt particles derived from oil or coil combustion, are absorbed by the render finish and triggers the black colour. On the other hand, rainwater can also possess a cleaning function. After all, a rain shower will rinse off dust and soot from these crusts. However, surfaces beneath cornices and windowsills are covered, and therefore unreachable for rain showers, resulting in major dirt spots (Vanhellemont et al. 2008).

5.2 Cracks

Crack formation can have different causes. Often it is not a consequence of the render itself, but caused by thermal expansion, settlement or corrosion of the support. On the other hand, the render composition may cause micro cracks during the drying process due to shrinkage, which may grow under the influence of water infiltration. Immediately after applying the mortar on a support, the binding process

starts and the strength is gradually achieved by hardening. A cement based plaster obtains its strength properties rather quickly, which implies the creation of a more brittle material in contrast to a pure lime mortar. The combination of shrinkage and a lack of elasticity lead inevitably to the appearance of small cracks. When the binder of a render consists of lime, the binding process will take longer, so the mixture has more time to correct the cracks. Since Terranova is a lime-cement mortar, hair cracks are limited because of the self-healing effect (BBRI 1998). Besides the nature of binder, also the proportions of the ingredients play a major role in shrinkage effects. A larger share of binder and a higher amount of water implies increased shrinkage. Hair cracks may seem harmless, but in case of water intrusion, there is a significant risk of frost damage in winter conditions.

5.3 Flaking and Peeling off

Due to a constant presence of moisture, ice formation will cause stresses between the render layers or at the edge between render and support. After a while, the adhesion between rendering and top layer will decrease and the mortar will peel off. Another possible cause is the presence of dissolved ions in rainwater or groundwater. After absorption of the substance by the façade and evaporation of the water, complex salts are formed. When the salts crystallize, they can also create mutual compressive stresses, resulting in salt contamination and peeling off phenomena (De Clercq 2012).

5.4 Vegetation

Vegetation, usually observed as algae, often occurs on windowsills causing green zones. Formation of algae is mainly caused by long-term high humidity levels. The architectural details and the orientation of the façade are decisive factors in their growth. Through lack of sunshine and high porosity of the finish, the cladding is not able to dry. This biological film may encourage an increase of water infiltration, making the material even more sensitive to frost damage. In addition, fluctuations in the moisture content encourage the film to swell and shrink, causing stresses in the render cladding.

6 Restoration Strategy

Before starting the conservation and rehabilitation campaign, a correct diagnosis is required. The damage assessment shows that it is essential to repair any affected support before applying a repair render. However, during restoration, attention

should be paid to the preservation of a maximum amount of authentic fabric (ICOMOS 1964). Visual inspection and systematically hammering the wall surface should help to distinguish damaged from intact surfaces. Reducing future decay can initially be accomplished by handling the current issues. Usually it is not feasible or appropriate to modify the detailing and geometry of the façade without compromising the historic integrity, but small invisible interventions may result in advantageous implications, such as providing all windowsills and protruding parts with a dripline in order to avoid moisture concentration beneath windows. Also stagnation of rainwater should be avoided and vegetation has to be treated at all times. Interventions to reduce the humidity in plasterwork are encouraged to minimize the risk of frost damage.

Performing test areas with cleaning techniques and a repair mortar is indispensable to establish correct cleaning, consolidation and restoration works. Contemporary cleaning techniques generally rely on hydro pneumatic blasting technology, but because of their potentially abrasive effects, it is useful to try more traditional dry (Wishab sponge) or wet cleaning methods (purifying chemical pastes) (Fig. 6).

Vegetation can be removed by brushing off the algae, but it is strongly recommended to apply a moss and algae killer to be sure that all organisms are eliminated. After the intact authentic material is cleaned, a repair mortar is needed to fill in cracks and lacunas. This repair mortar must be physically compatible with the existing materials and should visually match the sound parts, without causing damage. To strive for authenticity and similar properties as the original materials, a repair render should be composed on the basis of the historic patent study and laboratory research. A significant problem is the fact that some materials described in historic formula are no longer commercially available. For instance, according to an Italian manufacturing unit of Terranova, the ingredient Cromocemento (a high strength Portland cement), was used as binder for the top layer. Modern Portland cement can be used as a replacement, but this will not be representative due to the

Fig. 6 Two appropriate cleaning methods: Mora cleaning gel covered with Japanese paper [left] and scrubbing with a dry Wishab sponge [right] (*Source* Govaerts 2012)

large difference in hardness and alkali level. Since the binder is composed of both cement and lime, also the latter needs to be defined. The question is whether the measured hydraulicity level is caused by mixing hydraulic cement with non-hydraulic air lime, or by using a mixture of cement and hydraulic lime. This is not specified in the historic sources and not determinable by lab analysis. A good choice for hydraulic lime is the *Saint-Astier* natural hydraulic lime. This is an impure limestone with a relative high percentage of silica (13%), which approaches the results of the lab analysis (moderately hydraulic, NHL 3.5). Choosing natural hydraulic lime instead of non-hydraulic air lime has a considerable influence on the final render appearance; while air lime has got a very bright colour, NHL is characterized by a beige colour. Combining the binder with quartz sand, crushed Euville stone fragments and mica particles in correct proportions, should provide a good approximation of the original Terranova composition. In case of poor workability, the historic patents prescribe the addition of a small amount of linseed oil to the mixture. Adding organic additives, for example glycerines, would ensure the visibility of mica fragments in the top layer.

Before applying the repair mortar in accordance with the guidelines (Sect. 4), the damaged surface has to be prepared. Where the top layer has been peeled off, it is recommended to remove also other loose edges of the Terranova layer (Fig. 7a). To restore in an aesthetical way, a rectangular geometry is carved out along the simulated joints (Fig. 7b). The rendering layer is preserved and is successively dusted, wetted and roughened (Fig. 7c/d). When large cracks are noticed they need to be cleaned and they are usually injected with elastic sealant. The sealant is able to absorb small external and thermal forces, but if the crack is still active it is recommended to renew the rendering layer and add a reinforcement mesh. Finally, the new top layer can be applied, according to the historic formula (Fig. 8). In order to repair a large area or even the entire finishing, it is recommended to add profiles on the façade as a reference to obtain a uniform layer. The profiles are traditionally fixed by means of clamp hooks and clamp strips at a certain distance, which correspond with the desired layer thickness. However, in practice the profiles are fixed by throwing a piece of wet mortar against the wall to temporarily 'glue' the elements. During the restoration process it is advisable to use external scaffolding instead of ladders, to avoid scratches in the upper layer, due to shifting of the endpoints. In general, the finishing treatment has to be performed by one craftsman.

This is because every individual has got a very different feeling with the scratching technique, which creates lots of differences in texture. Moreover, it is essential to protect the new cladding with a canvas in case of heavy rain or exposure to sun, because they may provide a profusion or lack of binding liquid. To create simulated joints, straight lines have to be drawn in the top layer, when the fabric is still fresh. Subsequently, a cement based mortar is pressed in the joints right after hardening. In some case studies, it is observed that sometimes joints were painted, or that the grooves were left empty, creating shadow effects.

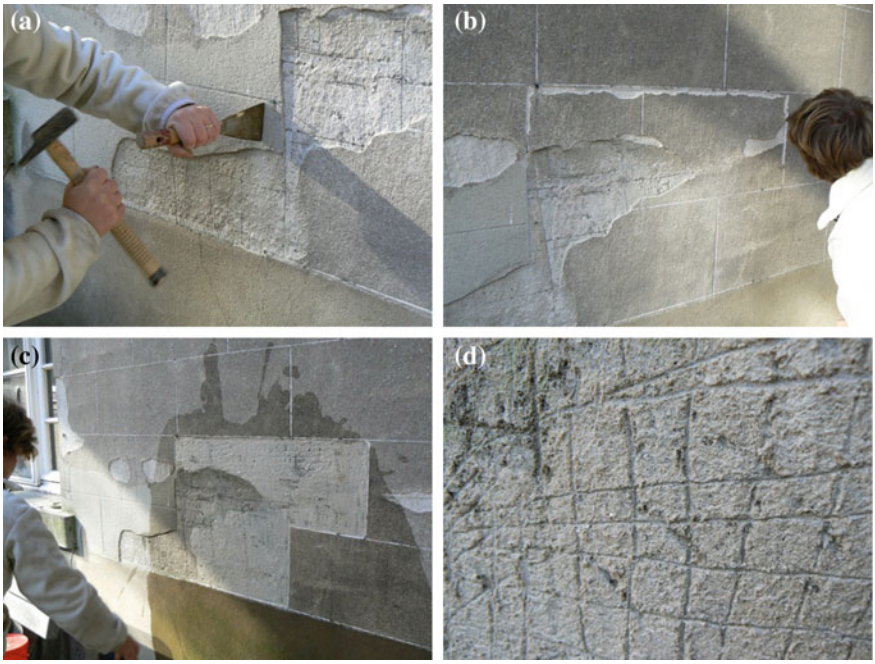

Fig. 7 **a–d** Preparations to repair a damaged stone imitation cladding. After the top layer is removed, the surface is moistened. Afterwards, a rough surface is created to improve adhesion (Govaerts 2012)

Fig. 8 Final stage to repair damaged exterior stone imitations. The stone imitation render is refabricated and spread onto the façade (Govaerts 2012)

7 Conclusions

Comparing the scientific analyses with relevant historic patents and technical literature resulted in a theoretical repair mortar formula for *Terranova*, a ready-mix stone imitating plaster used from the 1910s to the 1940s in Belgium. This research focuses on its application in Belgium and the search for a compatible repair render composition and appropriate finishing techniques, which are needed for conservation and restoration purposes. The current findings indicate that the considered Terranova cladding of the case study is in relatively good condition. A poor façade detailing and the long-term influence of weather conditions form the basis of the most commonly damage problems. With respect to the original historic fabric, the façade's integrity can be re-established by relying on a repair render which is similar to the authentic material. However, historic sources do not give detailed information with regard to the render ingredients, not mentioning any proportions concerning binder, aggregate and water content. Optical microscopy techniques and SEM/EDX analysis provide additional data, but considering this as the only source to formulate a repair mortar does not suffice. Both material characterization methods and historic literature are necessary to achieve a particular degree of authenticity. Yet, due to inaccurate mortar recipes as well as through ageing of the historic fabric, there is a chance that the repair render does not visually match with the intact material. Therefore, it is essential to perform further research towards historic stone imitation claddings, in which the outcome of mortar characterization is verified by a range of repair mixtures that are based on historic formulas. Finally, their appearance should be measured and linked to the mortar composition, and should be made accessible as a tool for conservation practitioners. This paper concentrates on the fundamentals for establishing a repair strategy during restoration of Terranova façades with respect for their heritage value.

References

Arendzen, G., & Vriend, J. J. (1936). *Constructie en uitvoering van Modern Stucadoorwerk*. Amsterdam: NV Uitgeversmaatschappij Kosmos.

Becker, A. (1932). Matériaux de Constructions et Entreprises Armand Becker. In *La technique des travaux*, number 9 (architectural periodical).

Belgian Building Research Institute. (1998). *Technische voorlichting 209: Buitenbepleisteringen*. Technical report, Brussels.

Danzl, T. (2002). Kunstputz (Edelputz)—Kunststein (Betonwerkstein)—Kunststeinputz (Steinputz). Die Bedeutung und Erhaltungsproblematik materialfarbiger Gestaltungen an Putzfassaden des 19. und 20. Jahrhunderts. In *Historische Architekturoberflächen Kalk—Putz—Farbe*, *Internationale Fachtagung des Deutschen Nationalkomitees von Icomos und des Bayerischen Landesamtes für Denkmalpflege* (pp. 146–159), München, 2002.

De Clercq, H. (20 March 2012). *Art and material technical science*. Presentation at the Free University of Brussels.

Garda, E. (2003). Terranova, history of a modern plaster: Smooth, hard, clean, perfect. In: S. Huerta & J. de Herrera (Eds.), *Proceedings of the First International Congress on Construction History* (pp. 970–977). Madrid: Instituto Juan de Herrera.

Geldof, P., Willemsen, A., & Schleicher, G. (1969). *Stukadoren*. Gravenhage: Technische Uitgeverij H. Stam's.

Govaerts, Y. (2012). *Materiaaltechnisch onderzoek van pierre-simili gevelafwerking: De Terranova bepleistering van De Roma (1928) te Borgerhout.* Dissertation, Free University of Brussels, Brussels, Belgium.

Govaerts, Y., Verdonck, A., Meulebroeck, W., & de Bouw, M. (2016). The many faces of early 20th century stone imitations in Belgium. In K. Van Balen, E. Verstrynge, I. Wouters, G. De Roeck, & D. Van Gemert (Eds.), *Proceedings of the 10th international conference on Structural Analysis of Historical Constructions (SAHC 2016)*, Leuven, 2016 (in press).

Icomos. (1964). The Venice charter—International charter for the conservation and restoration of monuments and sites. In *Second International Congress of Architects and Technicians of Historic Monuments*, Venice. Available via http://www.icomos.org/charters/venice_e.pdf. Accessed 6 July 2016.

Kapferer, C. A. (1911a). *Procédé d'amélioration de la perméabilité à l'air des mortiers d'enduit secs*. FR Patent 433321, 12 Aug 1911, retrieved from the online German patent database DEPATISnet, 3 pages. Original description: Les mortiers d'enduit modernes ont été employés tout d'abord dans les cas où l'enduit ne reçoit pas ultérieurement une couche de peinture ou un revêtement, et on obtenait des effets architectureaux, en colorant les mortiers, en ajoutant à la chaux éteinte de la roche granuleuse et des matières minérales.

Kapferer, C. A. (1926). *Procédé d'amélioration des mortiers d'enduit* (3 p). FR Patent 612932, 18 Mar 1926, retrieved from the online German patent database DEPATISnet, Paris.

Kapferer, C. A., & Schleuning. (1899). *Improvements in the manufacture of cement* (3 p). DE Patent 17853, 4 Sept 1899, requested by The Firm of Terranova Industrie, retrieved from the online German patent database DEPATISnet, Munich.

Kapferer, C. A., & Schleuning. (1900). *Verfahren zur Herstellung eines cementartigen Bindemittels* (1 p). AT Patent 5126, 12 April 1900, retrieved from the online German patent database DEPATISnet.

Kapferer, C. A., & Weber, J. (1911b). *Method of improving the permeability to air of dry plastering-mortar*. US Patent 1180775, 15 Aug 1911, retrieved from the online German patent database DEPATISnet, 2 pages. Based on Kapferer, C. A. (1910). *Verfahren zur Verbesserung der Luftdurchlässigkeit von Trockenputz Mortel*. DE Patent 74852, 30 Aug 1910, retrieved from the online German patent database DEPATISnet, 3 p.

KIK-IRPA, Royal Institute for Cultural heritage. (2011). Decoratieve bepleisteringen, materiaal-analysen, Staal M8, pierre-simili bepleistering in Borgerhout. Scientific report, Brussels.

L'architecture en Belgique—Les travaux de Jan B. Lauwers. (1928). In *La Cité*, number 7 (architectural periodical), pp. 85–95.

Leclercq, E. (1921). *Procédé de fabrication d'un produit imitant la pierre* (6 p). BE Patent 297606, 15 July 1921. Brussels: Belgian General State Archives, section contemporary archives.

Leduc, E. (1902). *Chaux et Ciments* (pp. 115–116). Paris: JB & Fils Baillière.

Oosterhof, A. P. (1932). *Handboek voor den stucadoor*. Amsterdam: Van Mantgem & De Does.

Ozga, I., Bonazza, A., Bernardi, E., et al. (2011). Diagnosis of surface damage induced by air pollution on 20th-century concrete buildings. *Atmospheric Environment, 45,* 4986–4995.

Poptie, A. (1948). *Handboek voor den stucadoor—Deel II*. Stam, Haarlem: De Technische Uitgeverij H.

Soille, J. B. (1908). *Composition pour pierre artificielle* (10 p). BE Patent 212606, 11 Dec 1908. Brussels: Belgian General State Archives, section contemporary archives.

Vanhellemont, Y., Van Peer, W., & Vernimme, N. (sd.) *Opleiding restauratievakman moderne bouwchemie, Module gevelreiniging*. Available via OE, WTCB & fvb-ffc constructive. http://www.vioe.be/images/uploads/projects/downloads/Module_gevelreiniging_WEB_1.pdf. Accessed 14 Jan 2013.

Verdonck, A., Deceuninck, M., & Govaerts, Y. (2014). The Gelmel castle in Hoogstraten (Belgium): towards visual perfection of the brickwork façades. In R. Meli, F. Peña, & M. Chávez (Eds.), *Proceedings of the 9th International Conference on Structural Analysis of Historical Constructions (SAHC 2014)*, Mexico City (MX), 2014.

Characterisation of Historic Mortars for Conservation Diagnosis

P. Hauková, D. Frankeová and Z. Slížková

Abstract Currently, several techniques are available for characterisation of mortar binders for research and conservation purposes but not all of them are suitable and affordable for routine diagnostic purposes. Cost efficiency is a very important factor for the scientific and conservation community and is always taken into account when designing a research conservation program. For the characterisation of historic mortars, generally the identification of the binder nature (air lime, hydraulic lime …) is of outmost importance as well as the mineralogy, granulometry, amount of the aggregate and porosity. The present paper presents a sequence of cost-efficient and technically effective procedure for mortar characterisation for conservation diagnosis aims.

Keywords Mortar analysis · Mortar characterisation · Binder · Aggregate Laboratory survey

1 Introduction

Characterisation of modern as well as historic building materials is a very important task in the field of conservation. The analysis of historical material is carried out for different purposes e.g. research, documentation, compatibility assessment before conservation intervention. Although physical and mechanical properties are essential for designing compatible repair mortar, the determination of chemical-mineralogical composition of historic mortar is most often required information by conservators in relation to the pre-conservation survey (mainly for

P. Hauková · D. Frankeová (✉) · Z. Slížková
Institute of Theoretical and Applied Mechanics AS CR, v. v. i., Prague, Czech Republic
e-mail: frankeova@itam.cas.cz

P. Hauková
e-mail: haukova@itam.cas.cz

Z. Slížková
e-mail: slizkova@itam.cas.cz

J. J. Hughes et al. (eds.), *Historic Mortars*,
https://doi.org/10.1007/978-3-319-91606-4_8

documentation purposes). Several recommendation documents and standards concerning this issue have been published but the selection characterisation analysis is determined by the laboratory equipment, technical effectiveness, amount of sample available and economic aspects.

Characterisation of composite building materials, particularly regarding the chemical and mineralogical composition, often requires a combination of several analytical methods. From our experience, the most accurate method to determine the binder nature of an historic mortar is the wet chemical analysis which comprises of dissolution of the binder in acid followed by aggregate separation (Alvarez et al. 1999; Middendorf et al. 2004; Van Balen et al. 1999). This method allows the determination of the main binders' components (e.g. soluble oxides of Ca, Mg, Fe, Al and Si) and amount of quantity silica which is an indicator of the hydraulicity degree of the binders. The main limitation of this method concerns materials containing acid-soluble aggregates. Other disadvantages of wet chemical analysis are the time taken and the fact that the accuracy of analysis is highly dependent on the analyst skills and experience. The present paper suggests a simplified analytical procedure for characterisation of historic mortars as a compromise between cost and information value. In this procedure binder identification is undertaken by a combination of thermogravimetry and x-ray fluorescence spectroscopy in place of the traditional wet chemical analysis.

2 Methodology of Mortars' Characterisation

Although several mortars properties can be identified in situ, laboratory analyses are indispensable for conservation diagnosis. Table 1 presents a list of basic laboratory methods used for characterisation of condition and composition of tested building material in the laboratories of Institute of Theoretical and Applied Mechanics of Czech Academy of Science in Prague.

According to Table 1 the total sample weight needed to perform all the analysis should at least 150–200 g. However, this amount depends on the sample homogeneity and on conservator´s requirements. For instance, when analysing a coarse mortar at least 100 g are needed for dry sieve analysis. When the amount of sample is limited, size and (or) number of testing specimens have to be reduced.

The overall analysis mentioned in Table 1 may take 3–5 days according to the number of specimens and selected methods.

For research aims there are other analytical methods for accurate mortar characterisation (e.g. ICP-OES, SEM-EDX, XRD, FTIR) but, generally, regarding the conservators goals these methods are too expensive and not all the information that provided is useful.

Table 1 Methods for mortar characterisation

Objective	Method	Mortar specimen size	Testing time (approx.)	Advantages	Disadvantages	Section
Mechanical and physical properties						
Flexural strength	Flexural strength at three-point bending	Non-standard min. 1 cm^3	2 days	Determination of modulus of elasticity	Time consuming specimen preparation before testing	3.1
Moisture content	Gravimetry Drying in oven at 60 °C	20 g	2 days	Specimen may be used in further analysis	Time consuming	3.2
Porosity	Mercury intrusion porosimetry	Min. 3 cm^3	1 h	Rapid and accurate testing procedure, determines pore size distribution	Expensive laboratory equipment is needed, specimen is destroyed	3.3
	Water absorption by immersion	Non-standard	2 days	Technically easy to perform using cost-efficient equipment	Time consuming	3.3
Water absorption coefficient	Water absorption by capillarity	Non-standard	1 day	Technically easy to perform	Time consuming specimen preparation before testing	3.4
Grain size distribution	Sieve analysis (dry)	Usually 50–100 g	1 h	Technically easy to perform	Separation of the aggregate	3.5
Mineralogical and chemical properties						
Mineralogy of mortars' constituents	Optical microscopy	Thin or polished section	1 h	Allows determination of grain size distribution	1 day for preparation of thin section	3.6
Type of binder	Thermo-gravimetry	30 mg sieved binder	3 h	Small consumption of sample	Expensive laboratory equipment is needed	3.7
	X-ray fluorescence	1 g sieved binder	1 h	Determine elemental composition	Equipment is needed, indicative measurement	3.7

(continued)

Table 1 (continued)

Objective	Method	Mortar specimen size	Testing time (approx.)	Advantages	Disadvantages	Section
Water soluble salt content	Analytical test strips	2 g	A few minutes	Cost-efficient and rapid	Wide intervals on the measurement scale	3.8
	Photometry	2 g	1 h	Acceptable accuracy	Expensive test kits	3.8
Mixing ratio B/A	Dissolution in hydrochloric acid	2 g	A few hours	Aggregate can be further used to determine grain size distribution	Can only be used when the mortar aggregate is insoluble in acid	3.9

3 Procedures and Evaluation

3.1 Mechanical Tests

The EN 1015-11: 1999 does not distinguish testing procedure for between historic and new construction mortar. For flexural strength determination it specifies specimens of 40 × 40 × 160 mm dimensions to be tested under three-point bending. Regarding historical mortars when only small sample is available, non-standard specimens may be used. In this procedure the small specimen is extended at both ends to the required testing length by a pair of prostheses. The mortar segment is positioned at the centre of the "prothesised" specimen and tested under three-point bending (Drdácký 2011).

3.2 Moisture Content

Moisture content is determined according to Czech technical standard (ČSN P 2000) by gravimetric method. The standard describes the principles for the design, research and monitoring of remediation systems in wet brick and stone masonry, which may be caused by several processes humidity increment. Mass content of moisture shown in Table 2 applies mainly to pooled masonry mortar samples that were collected from the masonry within 100–150 mm depth from the plaster surface.

3.3 Porosity

Mercury porosimetry: The procedure used for the measurement is determined by the equipment features. The software allows the presentation of the results in different forms, the most common used in literature is the distribution curve which is characteristic for the material and allows to easily differentiate between different binder types. RILEM 25 PEM (1980) procedure is used since there is not yet a Czech or European standard.

Table 2 Classification of masonry humidity according to ČSN P 730610:2000

Grade of moisture	Moisture content of the masonry (wt%)
Very low	>3
Low	3–5
Increased	5–7.5
High	7.5–10
Extremely high	>10

Water absorption by immersion: Open porosity and bulk density is performed according to EN 1936: 2006 (2006). The principle of the test is the hydrostatic weighing of samples after 24 h under vacuum (at 0.2 kPa pressure) and next 24 h immersed in water. According to the standard it is necessary to test at least 3 specimens with regular shape and size of approximately 50 × 50 × 50 mm which is not always possible concerning historical samples.

3.4 Water Absorption by Capillarity

The procedure is described in EN 1925: 1999 (1999) and EN 1015-18: 2002 (2002) standards. Samples are placed on tray with absorbent fabric or grid and water is poured to height about 3 mm, so water can rise only through base of sample. If the samples are not needed for further testing it is better to seal the lateral faces of the specimens with watertight coating. Based on weight change during time the water absorption by capillary coefficient is calculated. Three samples with block shape 50 × 50 × 50 mm are required, which can be hardly ever achieved with samples of historic mortars.

3.5 Grain Size Distribution

Dry sieve analysis: This method is described by EN 1015-1:1998 (1998). According to this standard the weight of sample should be at least 200 g, but it is difficult to get sufficient amount historical mortars sample, hence 50 g may be found enough to perform this test. Sieves are arranged according to increasing coarseness and the sample is sifted either manually or on sieve machine. The result of the analysis is weight of each faction in percentage. Faction size corresponds to the range between nearby sieves. The commonly used description of sieve is mesh size sieves expressed in millimetres, dimensions of mesh of test sieves according to the standard are: 8.00, 4.00, 2.00, 1.00, 0.500, 0.250, 0.125 and 0.063 mm.

The results are expressed graphically as grain size curve and can be presented in two ways: either cumulative (curve created by gradual addition of fractions) or as a histogram (bar graph). In both cases, the x axis is logarithmic or semi-logarithmic and the y axis is adapted to the percentage of factions or their sum. Presenting the results in a table makes the interpretation of results more difficult.

3.6 Mineralogy of Mortars' Constituents

Optical microscopy: Mineralogical composition and pore structure of mortars can be analysed by observing its thin section under microscope. A thin section of the

specimen with thickness of about 30 μm and approximate size 20 × 20 mm is made. It is also possible to determine the area or diameter of the selected particles even the aggregate/binder proportion in the area. There is no standard for this test hence RILEM 2001 recommendation (RILEM 2001) may be used.

3.7 Type of Binder

Thermogravimetry (TG): Thermogravimetry testing is carried out on the mortar fraction smaller than 63 μm (binder enriched fraction). Prior to sieving, the sample is carefully crushed without destroying the aggregate particles. The quality of the binder is derived from the measured TG curve according to the methodology for lime mortars published by Moropoulou et al. (2005). In principle, the total mass loss of the sample during heating is divided into three thermal intervals—from laboratory temperature up to 200 °C where release of physically bound water takes place; mass loss within the interval 200–600 °C represents amount of chemically bound water and above 600 °C the mass loss is attributed to the decomposition of carbonates. The rate of hydraulicity of the binder is expressed as CO_2/H_2O ratio (the amount of carbon dioxide released/amount of chemically bound water). This ratio inversely expresses the hydraulic character of the mortar and can be used for mortar´s classification into group of aerial lime, hydraulic lime or pozzolanic mortar.

Thermogravimetry is also a useful tool for detecting of organic matter or gypsum.

X-ray fluorescence spectroscopy (XRF): The binder of the mortar is separated from aggregate by the same procedure as for thermal analysis. To facilitate separation of binder from aggregate the bulk sample can be previously heated to 1000 °C in oven where decomposition of carbonated lime takes place. This process disintegrates hardened binder and helps to disrupt its bond to grains of aggregate. For analysis, about 0.5 g of sieved fraction (under 63 μm) is pressed into pellet with boric acid and analysed on EDXRF instrument. Chemical composition of the binder is then expressed in oxidic forms of determined elements. The nature of the binder can be subsequently expressed by calculated cementation index CI (Oates 1998). Furthermore, the hydraulicity of binder can be estimated by comparing the total CaO content from XRF analysis to CaO content bound in calcite (and portlandite if present) from thermogravimetry. The higher the difference between these values the higher is the share of CaO bound in hydraulic phases.

3.8 Water Soluble Salts Determination

The identification of soluble salts is described by the same standard for measuring moisture (ČSN P 2000). Levels of salinity shown in Table 3 represent the level of

Table 3 Classification of masonry salinity according to ČSN (2000)

Degree of salinity	Chlorides		Nitrates		Sulphates	
	mg/g	wt%	mg/g	wt%	mg/g	wt%
Low	<0.75	<0.75	<1.0	<0.1	<5.0	<0.5
Increased	0.75–2.0	0.075–0.20	1.0–2.5	0.1–0.25	5.0–20	0.5–2.0
High	2.0–5.0	0.20–0.5	2.5–5.0	0.25–0.50	20–50	2.0–5.0
Extremely high	>5.0	>0.50	>5.0	>0.50	>50	>5.0

aggression, especially for mortar and masonry mortar (ČSN P 2000). The amount of salt is presented in wt% of each salt. Samples are taken from a depth of 20 mm below the surface of the plaster. The degree of salinity is assessed for each type of salt separately.

3.9 Mix Ratio Binder/Aggregate

Dissolution in hydrochloric acid: The mass mixing ratio of the aggregate and binder is calculated by using the amount of insoluble residue in HCl and loss on ignition at 1000 °C (for example from TG). An important prerequisite for the calculation is that the aggregate must be totally insoluble in HCl and the loss on ignition belongs only to binder. To calculate the volume mixing ratio is necessary to know the bulk density of raw binder and aggregate.

For dissolution hydrochloric acid is used (diluted 1:5 by volume. To determine the proportion of insoluble fraction approximately 2 g of grounded sample is enough. If the aggregates are to be used for sieve analysis, it is necessary to have a greater amount of sample and only lightly crush and dissolve the whole sample. During the dissolution the carbonates and other components soluble in diluted HCl dissolve, and then the insoluble portion is separated by filtration and weighed.

This test is best interpreted when complemented with observation of thin section under the optical microscopy to determine the nature of the aggregate, e.g. crushed limestone can be also dissolved in HCl so it can distort binder analysis results (Frankeová et al. 2012).

4 Conclusions

The analytical procedure provides information about physical, chemical and mineralogical properties of historic mortars that can be performed in a cost efficient way. The aim of the procedure is to obtain the most important information regarding mortar characterisation within the aim of conservation diagnosis where the amount of sample, time or budget required for analyses are generally limited.

Most of the testing methods presented are carried out according to generally used standards, but with non-standard sizes of specimen. A different approach is undertaken for binder identification where wet chemical analysis is replaced by combination of thermogravimetry and XRF analysis.

All the mentioned properties have to be taken into account when designing a repair mortar compatible to historic building materials hence the obtained results may be used to design restoration mortars.

Acknowledgements The authors gratefully acknowledge the Ministry of Culture of the Czech Republic for support to project DF12P01OVV018—Conditions and requirements of compatible care of historic porous inorganic materials.

References

Alvarez, J. I., Martín, A., García Casado, P. J., et al. (1999). Methodology and validation of a HCl acid attack for the characterisation of ancient mortars. *Cement and Concrete Research, 29,* 1061–1065.

ČSN P 730610. (2000). *Waterproofing of buildings—The rehabilitation of damp masonry and additional protection of buildings against ground moisture and against atmospheric water*, Basic provision, Czech technical standard.

Drdácký, M. (2011). Non-standard testing of mechanical characteristics of historic mortars. *International Journal of Architectural Heritage: Conservation, Analysis, and Restoration, 5*(4–5), 383–394.

EN 1015-1:1998. (1998). *Methods of test for mortar for masonry—Part 1: determination of particle size distribution (by sieve analysis)*, European standard.

EN 1015-11:1999. (1999). *Methods of test for mortar for masonry—Part 11: Determination of flexural and compressive strength of hardened mortar*. European standard EN 1015-11:1999.

EN 1925:1999. (1999). *Natural stone test methods—Determination of water absorption coefficient by capillarity*. European standard.

EN 1015-18:2002. (2002). *Methods of test for mortar for masonry—Part 18: Determination of water absorption coefficient due to capillarity action of hardened mortar*. European standard.

EN 1936:2006. (2006). *Natural stone test methods—Determination of real density and apparent density, and of total and open porosity*. European standard.

Frankeová, D., Slížková, Z., & Drdácký, M. (2012). Characteristics of mortar from ancient bridges. In J. Válek, J. J. Hughes & C. Groot (Eds.), *Historic mortars: Characterisation, assessment and repair* (pp. 165–174). RILEM, ISBN 978-94-007-4634-3.

Middendorf, B., Hughes, J., Callebaut, K., Baronio, G., & Papayiani, I. (2004). Chemical characterisation of historic mortars. In C. Groot, G. Ashall & J. Hughes J. (Eds.), *Characterisation of old mortars with respect to their repair—Final Report of RILEM TC 167-COM* (pp. 39–56). RILEM Publications SARL, ISBN 978-2-912143-56-3.

Moroupoulou, A., Bakolas, A., & Anagnostopoulou, E. (2005). Composite materials in ancient structures. *Cement and Concrete Composites, 27,* 295–300.

Oates, J. A. H. (1998). *Lime and limestone* (p. 474). Weinheim: Wiley-VCH, ISBN 978-3-527-29527-2.

RILEM 25 PEM. (1980). Recommandations provisoires, Essais recommandés pour mesurer l'altération des pierres et évaluer l'efficacité des méthodes de traitement. *Matériaux et Constructions, 13*(75), 197–199.

RILEM. (2001). Recommendations of RILEM TC 167-COM: Characterisation of old mortars. *COM-C1 Assessment of mix proportions in historical mortars using quantitative optical microscopy*. ISSN 1359-5997.

Van Balen, K., Toumbakari, E. E., & Blanco-Varela, M. T. et al. (1999). *Environmental deterioration of ancient and modern hydraulic mortar*. Project ENV4-CT95-0096, EC Protection and Conservation of European Cultural Heritage.

Content and Topography of Salts in Historic Mortars

Ioanna Papayianni, Maria Stefanidou, Vasiliki Pachta and Stavroula Konopisi

Abstract Salt crystallization induces deterioration phenomena to masonry materials especially under favorable conditions which depend on a triple-fold system of factors: the salts' nature, the materials' type and structure and finally the environmental aspects. Among the oldest building materials, the lime-based mortars have been used for different construction purposes and exhibited admirable durability. The present paper presents the results of a statistical process of more than 1000 mortars from different monuments and historic periods in an effort to correlate salt formation with macroscopic and microscopic properties. Instrumental analysis of liquid ion chromatography has been applied for recording the type of soluble salts found into the mortar's structure; moreover, the location and the form of crystallization as well as the mechanical and physical properties of these mortars have been determined. The evaluation of the combined analysis shows that lime-based mortars sustained a significant load of salts without being destroyed.

Keywords Lime-based historic mortars · Soluble salts · Strength

I. Papayianni (✉) · M. Stefanidou · V. Pachta · S. Konopisi
Laboratory of Building Materials, Department of Civil Engineering, Aristotle University of Thessaloniki, 482, 54124 Thessaloniki, Greece
e-mail: papayian@civil.auth.gr

M. Stefanidou
e-mail: stefan@civil.auth.gr

V. Pachta
e-mail: vpachta@civil.auth.gr

S. Konopisi
e-mail: konopisi@civil.auth.gr

J. J. Hughes et al. (eds.), *Historic Mortars*,
https://doi.org/10.1007/978-3-319-91606-4_9

1 Introduction

The first indication of a salt rich environment affecting a masonry monument is often revealed by the accumulation of salts in mortars. The origin of salts may be variable, since they can originate from the materials themselves, the environment, or from human activities. In historic buildings, over centuries, often a high concentration of salts is accumulated (Papayianni 2006).

Under favorable conditions salts can penetrate into the materials' structure through different mechanisms such as capillary transport, diffusion or condensation (Binda and Baronio 1987) only if they are dissolved in water. Therefore, the influence of moisture transport through building materials is a key factor in salt-induced decay (Angeli et al. 2007; Groot et al. 2009). On the other hand, salts can be crystallized in a variety of forms and habits (Arnold and Zehnder 1988) The kinetic of salts and their damage degree has been closely related to the material's pore system (Fitzner et al. 1996). The main mechanism, which constitute salts as a disruptive agent is through crystallization and hydration pressures as well as thermal expansion. Salts concentrate in areas that retain moisture for longer and that means that the longer the saline solution remains within the pores the worse the damage may be (Charola 2008).

Stones, bricks and lime-based mortars are the fundamental building materials of historic structures and their behavior to salt enriched environment can present differences. When the conditions which adjust the solution supply and the evaporation rate are stable a steady system may develop (Rossi-Manaresi and Tucci 1991). High evaporation rate often means that salts crystallize on the material's surface. Soluble salts crystallization within the porous structure of a stone is considered to be one of the most important reasons for decay due to the mechanical volumetric expansion of salts which causes stresses and due to the chemical action as salts that may cause dissolution of mineral admixtures (Theoulakis and Moropoulou 1997; Mosquera et al. 2002). The main pathology form in stones due to salts is disruption and disintegration of the stone surface. Additionally the nature and structure of bricks have also proved to be vulnerable to salt action as they suffer from spalling and pulverization (Larsen and Nielsen 1990; Lubelli et al. 1994).

As the binding agents of the masonry elements in historic structures are usually lime-based mortars their role in salt movement phenomena is crucial. Lime-based mortars present a high evaporation rate and a low retentivity due to their porous structure (Stefanidou 2007; Stefanidou and Papayianni 2006). Porosity in these materials is a complex system of voids and cracks that are distributed randomly into the structure and present interconnectivity providing high open porosity values. Due to their high porosity, mortars are usually considered to be the veneers through which the solutions penetrate into the masonry. Therefore lime mortars can be considered as salt "carriers" not only in-between different masonry materials but also in different heights of the structure causing mainly aesthetical and often

Fig. 1 Salt crystallization into the pores of a structural mortar from Galerius Palace (4th century AD)

functional problems to the structures. According to theories, if the growing crystals exceed the pore size, significant pressures build up on the pore walls resulting in disruption of the structure (Scherer 2004). The low mechanical strength of lime-based mortars making them even more damage prone. Nevertheless, it seems exceptional rare salt crystals to fill the pores and cracks of the structure, since pre-existing cracks especially around the pores can lead the salt solutions away and give small possibility for their high concentration. The presence of fissures around large pores is often met in the structure of lime mortars and their origin is hard to define. Shrinkage phenomena and wet-drying cycles are few of the reasons that can generate cracks on the circumference of pores. Cracks and pores are not often filled with salts (Figs. 1 and 2). The mechanical behavior of the salt crystals is not predictable, as they may be broken or detached easily under favorable conditions.

In the present study more than 1000 mortars were analysed in terms of determination of salt content in Cl^-, SO_4^{2-}, and NO_3^-, of physico-mechanical and microstructure properties in an effort to correlate the salt content with the role and structure of the mortars.

2 Materials and Methods

982 structural mortars and 265 renders from monuments covering a wide historic period (from Hellenistic, to modern—19th century) have been analysed in order to record their microstructure, physical and mechanical properties as well as the determination of water soluble salts Cl^-, SO_4^{2-}, and NO_3^-, made with HPLC ion chromatography. All results have been recorded to a flexible data system from which interesting conclusions could be extracted. The research refers to lime-based mortars (either pure air lime or more often combination of lime with a hydraulic binder). The binder in early periods (Hellenistic was clay of low hydraulicity or

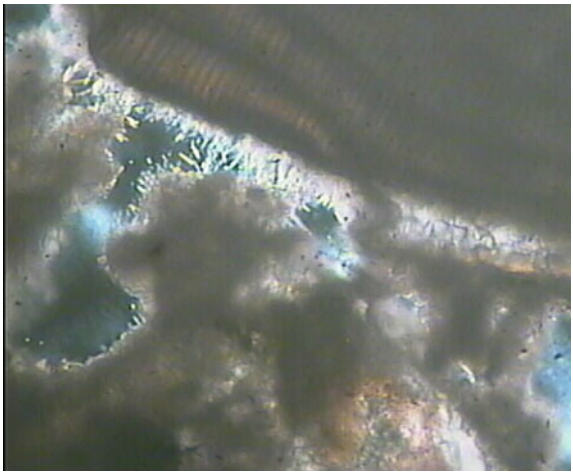

Fig. 2 Salts covering a part of a pore by optical microscope in a structural mortar of the medieval monuments of Rhodes

combination of lime and clay while later (during Roman and Byzantine period) natural pozzolans and brick dust were combined with lime, for enhancing the hydraulic role of the binder.

Based on the determination of the water soluble salt content of the above mentioned old mortars, the highest values found for each type of anions are given in Table 1.

The results regarding the quantitative assessment of salt presence in old mortars, regardless the historic period, in which they belong, are shown in Table 2. The content of each type of salt found in mortars was categorized in three groups: (a) lower than 0.1% w/w, (b) between 0.1 and 1% w/w and (c) higher than 1% w/w. The frequency of the values corresponding to these categories for each type of mortar (structural or render) is shown in the second and third columns of Table 2.

Regarding the numbers, it is obvious that most of the samples contain a small amount (<0.1) of salts. The maximum rates of the soluble salts in the tested samples ($\geq$ 1%w.w.), are met with high frequency in renders. For sulfates, the corresponding percentage of renders (17.0%) is even higher (almost triple) compared to structural mortars (6.0%). In nitrates the corresponding percentage for renders and structural mortars is almost the same (5.5% per structural and 5.7% per renders). Considering the role of renders which were applied as the "skin" of the structure in order to protect it from environmental exposure effects it seems that renders live up to their role and carry a large amount of salts. This observation indicates that the main mechanism that has an important role to salt enrichment of the materials is condensation or diffusion for solutions deriving from the atmosphere.

Table 1 The upper values of water soluble salt contents in historic mortars

	Salt content (%w/w)		
	Cl^-	SO_4^{2-}	NO_3^-
Structural	2.9	4.2	5.3
Render	2.5	3.0	5.0

Table 2 Frequency of salt appearance in mortars and renders in a statistical sample of more than 1000 mortars

Salt type	Percentage of samples (%)		Salt content rate limits (%w/w)
	Structural	Renders	
Cl^-	4.8	9.7	≥ 1
	32.4	28.9	0.1–1
	62.8	61.4	≤ 0.1
SO_4^{2-}	6.0	17.0	≥ 1
	48.3	43.8	0.1–1
	45.7	39.2	≤ 0.1
NO_3^-	5.5	5.7	≥ 1
	32.4	27.3	0.1–1
	62.1	67.0	≤ 0.1

In Table 3 the results from the indicative analysis of 12 historic mortars with high salt content are presented, from various monuments of Greece and of different regions and historic periods. From the correlation of salt content and the binding system of old mortars tested, it is concluded that in all cases the mortars were lime-based, either manufactured by pure lime or by a combination of lime, pozzolana and/or brick dust. As it is testified by the results presenting in Table 2, the salt contents are not affected by a specific binding system. It is not clear how the salt content affects the open porosity values of mortars as well as other technical characteristics of the mortars.

Despite the salt content there is a large variation in the compressive strength and porosity values, since they are affected by many other parameters. Therefore, salt accumulation may certainly have an impact on the physico-mechanical properties of mortars, but they cannot be directly correlated. In order to have an impression on the impact of salt content on mechanical and physical properties of old mortars, a very systematic sampling from sound and deteriorated areas, as well as a holistic type analysis (Papayianni 2006) should be made.

Trying to pattern the position of the salt in the mortars, microscopic examination revealed their appearance in open spaces(pores cracks around large aggregates) which are in abundance in the lime-based mortars. Figures 3 and 4 are representative of the situation. Salts rarely fill the space into which they form and their structure seems rather fragile.

3 Conclusions

Salt accumulation phenomena appear to be unavoidable during the service life of historic mortars. Considering the types of salts anticipated in different types of mortars (structural, renders), it could be said that regardless the composition of

Table 3 Analysis results of various historical mortars with high salt content

Monument	Region	Type	Salt content (%w.w.)			Binding system L = lime P = pozzolana B = brick dust C = clay	Open porosity (%)	Comp. strength (MPa)
			Cl^-	SO_4^{2-}	NO_3^-			
Fortress of HagiosNikolaos (Medieval, Rhodes)	Sea side	Structural	1.83	0.58	0.04	L+P	18.34	3.80
Byzantine wall of Chania (Crete)	Sea side		2.72	2.94	1.60	L+P	30.60	1.64
Galerius Palace (Roman)	Urban		0.16	1.45	1.21	L+P	26.70	1.32
Panagia Acheiropoiitos (Byzantine)	Urban		0.05	1.14	0.16	L+P+C	17.80	2.82
Byzantine Castle of Servia	Rural		0.84	2.18	0.70	L	20.40	1.09
Byzantine castle Fanariou of Karditsa	Rural		1.46	2.61	2.61	L+P+C	25.46	0.65
Fortress of Saint Nikolaos (Medieval, Rhodes)	Sea side	Render	0.83	1.99	0.12	L+P	33.90	–
I.M. Pantokratoros (Mount Athos)	Sea side		1.58	0.53	0.09	L	10.40	0.76
Galerius Palace (Roman)	Urban		0.05	1.25	0.13	L+P+B	24.30	2.45
Roman Forum	Urban		1.00	1.32	3.00	L+P+B	13.50	–
Byzantine Castle of Servia	Rural		1.80	1.20	1.11	L+P	8.80	0.90
I.M. Chilandrariou (Mount Athos)	Rural		1.22	1.11	0.52	L	20.40	1.30

Fig. 3 Stereoscopic observation of salt crystallization into mortars

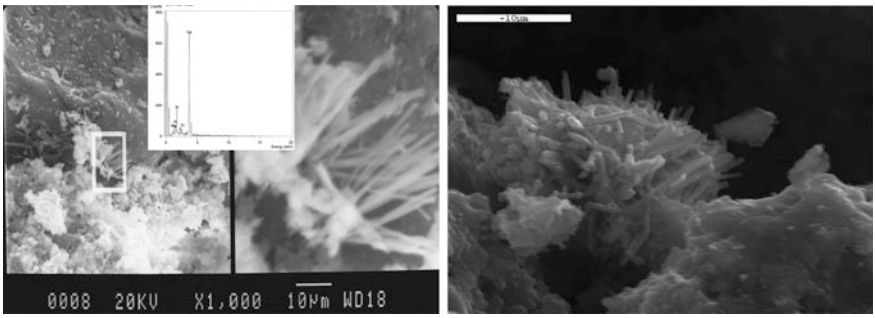

Fig. 4 SEM analysis of chlorite salts in the mortar structure

mortars, the more prone materials for salt accumulation (mainly chlorides and sulfates) are, as logically expected, renders. Salt penetration in renders is mainly attributed to the arid deposition of salts by salt spray (seaside regions) or by air pollution (urban centers). The presence of chlorides is mainly attributed to the proximity of the sea, while sulfates can be due to a synergy of factors such as raw materials with high sulfate content (gypsum, brick dust, cement), air pollution, or even to the foundation ground. Finally, nitrates mainly come from oxidation of NO_x in air-polluted environments, due to the vegetation growth (plants or inferior biological organisms), to high content of nitrates in the ground and to human activities. Considering statistically more than 1000 old mortars it seems that the salt content can not be directly related to physico-mechanical properties that these mortar present as a series of other parameters (technological aspects, microenvironment, structural phases) can influence mortar's properties.

The basic conclusion from the present study is that historic mortars can attain high quantities of soluble salt without diminishing their physico-mechanical properties. The pore system of lime-based mortars probably facilitates the action of

soluble salts during their perpetual cycles of hydration and crystallization. Pores and cracks are the favourable places for salt crystals to grow and usually these places are spacious enough and interconnecting so the concentration of salts rarely exceeds a critical point that can damage the structure. Historic mortars can therefore work as conveyors of salts when their 'breathing' capability is retained.

References

Angeli, M., Bigas, J-P., Benavente, D., Merendez, B., Hebert, R., David, C. (2007). Salt crystallization in pores: quantification and estimation of damage (S. Siegesmund & M. Steiger, Eds., Springer Science). *International Journal of Geosciences Environmental Geology Salt decay, 52*(2), 205–213.

Arnold, A., & Zehnder, K. (1988). Decay of stony materials by salts in humid atmospheres. In *Proceedings of the 6th International Congress on the Deterioration and Conservation of Stone* (pp. 138–148), Torun.

Binda, L., & Baronio, G. (1987). Mechanisms of masonry decay due to salt crystallization. *Durability of Building Materials, 4,* 227–240.

Charola, A. E. (2008). Salts in the deterioration of porous materials: An overview. *Journal of the American Institute for Conservation, 39*(3), 327–343.

Fitzner, B., Heinrichs, K., & Volker, M. (1996). Model for salt weathering at Maltese globigerina limestones. In F. Zecca (Ed.) *European Commission Research Workshop Proceedings Origin, Mechanisms and effects on salts on degradation of monuments in marine and continental environments* (pp. 25–27), Bari, Italy.

Groot, C., van Hees, R., & Wijffels, T. (2009). Selection of plasters and renders for salt laden masonry substrates. *Construction and Building Materials, 23,* 1743–1750.

Larsen, E. S., & Nielsen, C. B. (1990). Decay of bricks due to salts. *Materials and Structures, 23,* 16–25.

Lubelli, B., Van Hees, R. P. J., & Groot, C. J. W. P. (1994). The role of the sea salts in the occurrence of different damage mechanisms and decay patterns on brick masonry. *Construction and Building Materials, 18,* 119–124.

Mosquera, M. J., Benitez, D., & Perry, S. H. (2002). Pore structure in mortars applied on restoration, Effect on properties relevant to decay of granite buildings. *Cement and Concrete Research, 32,* 1883–1888.

Papayianni, I. (2006). The longevity of old mortars. *Applied Physics A: Materials Science and Processing, 83,* 685–688.

Rossi-Manaresi, R., & Tucci, A. (1991). Pore structure and the disruptive or cementing effect of salt crystallization in various types of stone. *Studies in Conservation, 36,* 56–58.

Scherer, G. W. (2004). Stress from crystallization of salt. *Cement and Concrete Research, 34*(9), 1613–1624.

Stefanidou, M. (2007). A contribution to salt crystallization into the structure of traditional repair mortars through capillarity. In *11th Euro seminar on Microscopy Applied to Building Materials*, 5–9 June, Porto, Portugal.

Stefanidou, M., & Papayianni, I. (2009). Salt accumulation in historic and repair mortars. In R. Fort, M. Alvarez de Buergo, Gomez-Heras, & Vazquez-Calco (Eds.), *Heritage, Weathering and Conservation* (pp. 269–272). Abingdon: Taylor & Francis.

Theoulakis, P., & Moropoulou, A. (1997). Microstructural and mechanical parameters determining the susceptibility of porous building stones to salt decay. *Construction and Building Materials, 11*(1), 65–71, Elsevier Science Ltd.

Part II
New Materials' Development for Conservation

Portland Cement-Lime Mortars for Conservation

S. Pavia and O. Brennan

Abstract It is currently widely accepted that lime, rather than Portland cement (PC), should be used for the repair of historic fabrics as most historic mortars were lime based and properties of PC mortar such as strength, stiffness and permeability can be incompatible with historic stone and brick, with consequent damage to fabrics. As a result, PC mortars are no longer used in conservation. However, lime addition significantly alters the properties of PC mortars. This paper investigates the variation of PC mortar properties with increasing hydrated lime addition (CL90s), and compares the results with typical values of natural hydraulic lime (NHL) mortars often used in conservation. The results evidence that PC/lime mortars display good workability with a high water retention, low air content and a reliable bond. Their properties are comparable to those of NHL mortars therefore, they are probably compatible with certain historic fabrics. The air content of the PC/lime mortars is low, similar to the typical air content of NHL mortars. Their water retention is high, significantly superior to those of equivalent PC mortars and comparable to typical NHL mortar values. The compressive and flexural strength and elastic modulus of the lower-lime-content mortars (1/0.25/6 and 1/1/6-PC/lime/sand) are superior to the values typically reached by NHL mortars however, their bond strength is similar. The strength, elastic modulus and bond of the PC/lime mortar with higher lime content (1/2/6) are comparable to the values typically reached by NHL2 mortars. Low lime contents produced stronger, stiffer mortars with greater bond, increased flexibility and water retention and lower air content than PC alone.

Keywords PC/lime mortars · Bond-strength · Air-content · Water-retention Strength/stiffness

S. Pavia (✉) · O. Brennan
Department of Civil Engineering, Trinity College Dublin, Dublin, Ireland
e-mail: pavias@tcd.ie

O. Brennan
e-mail: obrennan@tcd.ie

J. J. Hughes et al. (eds.), *Historic Mortars*,
https://doi.org/10.1007/978-3-319-91606-4_10

1 Introduction: Functionality of Hydrated Lime in PC Mortars

It is well known in construction that lime addition to PC improves workability facilitating mixing and application simultaneously delaying set and lowering strength of PC mortar. As a result, hydrated lime has been added to PC for decades. Lime addition results in longer lives: the mortar remains workable for longer due to a lower hydration so that it can be reworked without loss of quality. In general, lime mortars are slower to set and have lower strength and a greater water retention, porosity, permeability and deformability/flexibility than PC mortars therefore, by adding lime to PC, one would expect these properties to rise or drop accordingly. For example, it is generally accepted that lime in PC mixes lowers strength, avoiding problems associated to excessively strong mortar such as the concentration of stresses in masonry units leading to cracking. Lime also confers plasticity lowering stiffness, so that PC mortars become more deformable and thus tolerate masonry movement by deforming on stress application. The ability of PC/lime mortars to accommodate movement has been known for decades, Tate (2005) citing Boynton (1980), refers to a specification for mortars of tall chimneys subject to wind movement at 1/2/5 (PC/lime/sand).

PC/lime mortars are advised for most structural functions and degrees of exposure including external, internal and parapet walls; copings; earth-retaining and free-standing walls (EN 998-2; BRE 362; BS 5628). BS 5628-1 allows the use of lime in all mortar designations—even class i which is the strongest. Only in special cases (when exceptionally high loads are involved) the use of lime is not advised. For example, to use the full capacity of a high strength brick (>70 N/mm^2) a 3:1 (aggregate: PC) is needed.

2 Mortar Properties that Determine Quality, Durability and Performance

Mortars used for repair are often applied to high-suction substrates such as weathered stone, clay-brick or lime mortars therefore, repair mortars would benefit from a high water retention to hold moisture for proper curing and bonding, and to avoid shrinkage cracking due to sudden water loss. It is accepted that repair mortars should be deformable and display low to medium strengths to allow masonry movement and avoid stress concentration leading to cracking of masonry units. This paper measures the effect of lime addition on water retention, air content, compressive, flexural and bond strength and elastic modulus of PC mortar. These properties are interrelated and they are vital, as they rule the quality of mortar in masonry.

Water retention is essential so that the paste remains workable and retains water for proper curing and bonding. A mortar with high water retention maintains flow (workability) enhancing contact with masonry units. An increase in water retention results in increased bond strength (Borchelt and Tann 1996; BIA 2003; Pavía and Hanley 2010). Water retention is a function of the amount of free lime, thus lime mortars have superior water retention: values from 94.2 to 99.5% have been consistently measured vs. those of 60–80% of PC equivalents (Brennan 2009; Pavía and Hanley 2010; O'Looney 2010).

High air contents undermine bond and compressive strength (Wright et al. 1993; Fried and Law 1995). As a result, ASTM standards restrict air content to a maximum of 12–14%. Fried and Law (1995) state that bond strength (couplet method) decreased from 0.3 to 0.1 N/mm^2 as the entrained air rose from 2 to 18%.

Bond strength between the mortar and the masonry unit is a most significant property because it ensures the structural integrity of masonry (adequate resistance to compressive and tensile loading) and seals against weathering agents. The strength of the bond is largely determined by air content, water retention and the moisture transfer between the mortar and the unit. High water retention enhances workability which improves contact between mortar and substrate increasing bond: Hanley and Pavía (2008) showed that the bond strength of hydraulic lime mortar masonry increases proportionally to the mortar's water retention. The initial rate of absorption and moisture content of the units also determine bond: wetting of brick prior to construction reduces initial absorption and hence the mortar retains water for complete curing. (Sinha 1967) found that optimum bond strength was developed when the bricks had been wetted to 80% of their saturation point. The evolution of bond strength on lime addition is not clear. Some authors state that lime addition reduces bond strength while others state that low lime addition enhances bond. Bond strength is due to the mechanical interlock of cement hydrates into the brick pores (Lawrence and Cao 1987; Groot 1993; Wright et al. 1993). Groot (1993) states that PC mortars show greater bond strength than PC/lime mortars due to the higher quantity of hydrates. Melander and Conway (1993) agree, stating that lime addition (0–4 parts by volume) to PC mortars reduces compressive and bond strength; and that a 1/2 (PC/lime) ratio is the maximum advisable lime content. However, other authors have found that, in spite of their reduced mechanical strength, PC/lime mortars develop greater bond strength than PC mortar (Venumadhava Rao et al. 1996; Sugo et al. 2001). According to Sugo, a 1/1/6 (PC/lime/sand) mortar reaches a greater bond than a 1/6 (PC/sand) mortar because it experiences less reduction in the volume of the paste due to its higher water retention and, as a result, there is a greater provision of hydrates over the mortar-unit interface which increases bond. Surface roughness and the presence of frogs enhance bond (Lawrence and Cao 1987; Sarangapani et al. 2005).

Flexural (tensile) strength is a function of the compressive strength and determines the mortar's resistance to tensile stresses resulting from loading, frost action and/or expansion caused by salt or swelling clays. Compressive strength informs on

mechanical resistance and relates to durability (stronger materials usually have longer lives). It is often used as a principle criterion for material specification and quality control, e.g. the classifications and designations of limes, cements and mortars are based on compressive strength. Flexural and compressive strength are expected to be superior in mortars with higher cement contents due to their greater hydrate content. Elastic modulus relates to mortar stiffness and the ability to deform or strain on stress application. This is often more important than the ultimate strength (at peak load) as it is desirable for mortars to exhibit an ability to deform under stress without cracking. Historic masonry often experiences deflection over time therefore a low elastic modulus is of interest to those specifying mortars for repairs.

3 Materials and Methods

CEM I and hydrated lime (CL90s), complying with EN 197-1 and EN 459-1 respectively, were mixed with 5 mm Wexford sand. Frogged, machined-pressed, fired-clay brick of dimensions 210 × 105 × 65 mm were used in the bond strength test (frog dimensions 160 × 60 mm with triangular prism depth 40 mm). The aggregate's particle size distribution was determined by sieve analysis EN 812.103-1 and compared to the CEN reference sand (Fig. 1). The results indicate that the sand has a suitable grading.

3.1 Mixing, Compaction and Curing

Four mortars with PC/lime/sand ratios (by volume): 1/0/6, 1/0.25/6, 1/1/6, 1/2/6 were mixed in accordance with EN 196-1 (2005). The water content (Table 1) was consistent and determined with the initial flow test (EN 459-2 2010). 160 × 40 × 40 mm prisms were cast for flexural and compressive strength testing in accordance with EN 196-1 (2005). Compaction was undertaken on the jolting table. The mortars were cured in a chamber at 90% relative humidity and 20 +/− 1 °C for 28 days.

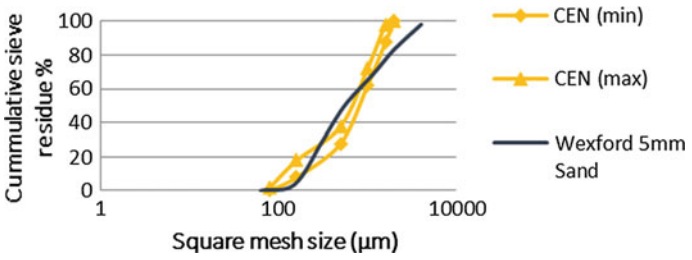

Fig. 1 Grading of the aggregate compared to the CEN reference sand

Table 1 Water demand and water retention of PC mortars with increasing lime content

Mortar (PC/lime/sand)	Lime/PC	Initial flow (mm)	Water retention (%)	% Water to flow 185 ± 3 mm
1.0/0.0/6.0	0	185 ± 3 mm	64.53	12.80
1.0/0.25/6.0	0.25		77.19	12.40
1.0/1.0/6.0	1		85.62	15.25
1.0/2.0/6.0	2		91.40	22.51

3.2 Initial Flow

The flow test was carried out as specified in EN 459-2 (2010). The mould is placed in the centre of the table and filled to ensure compaction. The flow table was raised 10 mm and jolted 15 times and the diameter of the resulting pat measured.

3.3 Water Retention

Assemblies were built with filter paper, plastic plate, nonwoven tissue, ring and mortar as specified in EN 459-2 (2010) and weighed. The water content of the mortar (W_2) and the mass of water absorbed by the filter plate (W_3) were calculated and the water retention (*WRV%)* determined from the equation below as the arithmetic mean of two test results.

$$WRV = 100 - 100(W_3/W_2) \quad (1)$$

3.4 Air Content

The air content was measured with the pressure method as set out in EN 1015-7 (1999). A metal bowl was filled with fresh mortar and tampered to ensure compaction. The cover was sealed and the air replaced by water. The pressure is released and the air content given on the dial as a percentage. The air content is the average of two test results.

3.5 Flexural and Compressive Strength EN 196-1 (2005)

The 28-day flexural strength was determined using the three point loading test. The prism is positioned on two contact points 10 cm apart, opposite to the side being loaded. A load is applied (50 ± 10 N/s) at mid-point until failure occurs.

To calculate the flexural strength R_f the following equation is used. The values reported are the mean of three test results:

$$R_f = \frac{1.5 \times F_f \times l}{b^3} \left(\text{N/mm}^2\right) \tag{2}$$

where b is the side of the square section of the prism (mm); F_f is the load applied at fracture (N); and l is the distance between the supports (mm).

The 28-day compressive strength (R_c) was measured by recording the peak stress at failure on uniaxial load application. The values reported are the arithmetic mean of six tests. The compressive strength was calculated with the following equation:

$$R_c = \frac{F_c}{6400} \left(\text{N/mm}^2\right) \tag{3}$$

where, F_c is the maximum load at fracture (N); 1600 is the area of the auxiliary plates.

3.6 Elastic Modulus

The elastic modulus in compression and flexion (E) was calculated to determine the stiffness of the material and the amount of deformation on stress application. During compression and flexion, the distance travelled by the loading point (or plate) from the position at which it started, is recorded along with the load applied at that time. Therefore, force vs strain over time were recorded. E was calculated as the slope of the linear part of the stress/strain curve by dividing the stress by the strain according to the equation below.

$$\text{E} = \text{F/a}\Delta\text{L/hE} = \text{F/a}\Delta\text{L/h} \left(\text{N/mm}^2\right) \tag{4}$$

F = force (N); a = area on which load is applied (m^2); ΔL = change in height; h = original height of sample (m).

3.7 Determination of the Flexural Bond Strength with the Bond Wrench Test

The bond wrench test determines bond strength by subjecting a masonry prism to an eccentric load which 'wrenches' the top brick from the rest of the assembly, allowing to test several mortar joints in a single prism. Loads, applied through a cantilevered arm, induce tension over half the mortar joint and compression over

the other half. This test was carried out according to EN 1052-5 (2005) at 28 days. Two prisms of 6 bricks each were assembled with each of the four mortar types, thus 40 bond strength measurements were carried out (10 for each mortar type). A mortar joint template ensured consistent joint thickness of 12 mm before tamping. The lower and upper clamping brackets were tightened to the second and top brick respectively and the load applied incrementally by adding weights to the extension arm. Following failure, the brackets were removed and the prism risen in order to test the next joint. The flexural bond strength was calculated using the equation below:

$$F_n = \frac{(PL + P_1L_1)}{S} - \frac{(P + P_1)}{A} \quad (5)$$

where:

F_n = net area flexural tensile strength (N/mm^2); P = maximum machine applied load (N); P_1 = weight of loading arm and brick unit (N); L = distance from center of prism to loading point (mm); L_1 = distance from center of prism to centroid of loading arm (mm); S = section modulus of net bedded area (mm^3); A = net bedded area (mm^2).

The brick's initial rate of absorption, compressive strength, net bedded area, volume, moment of inertia, dry mass and section modulus were calculated (EN 772-1 and 16 2000); and the mean value of six specimens and the coefficient of variance calculated.

4 Results and Discussion

4.1 Water Demand by Initial Flow and Water Retention

Even though water demand and water retention should escalate with increasing lime addition as a result of rising binder content, the results evidence the higher water demand of lime when compared to hydraulic binders. The water required to attain the specified initial flow (185 ± 3 mm) increases with increasing lime content (Table 2) agreeing with the known fact that hydrated lime has a greater water demand than hydraulic binders. The results also evidence that increasing lime/cement ratio enhances water retention (Fig. 2; Table 1), agreeing with previous authors (Lawrence and Cao 1987; Adams and Hobbs 1994; Borchelt and Tann 1996; Schuller et al.1999; Sebaibi et al. 2003). Brocken et al. (2000) report that PC/lime mortars retained three times as much water at the joints than air-entrained PC mortars (measured over the initial 140 min).

Table 2 Compressive strength (Rc), flexural strength (Rf) and modulus of elasticity in compression and flexion (Ec and Ef respectively)

Mix	Rc (N/mm^2)	Rc COV %	Ec (N/mm^2)	Ec COV %	Rf (N/mm^2)	Rf COV %	Ef (N/mm^2)	Ef COV %
1/0/6	9.82	11.5	2924.6	15.8	3.49	10.0	5155.4	24.9
1/0.25/6	12.67	11.2	3602.6	31.9	4.39	2.1	8167.7	21.8
1/1/6	5.98	5.6	1744.3	15.8	2.14	5.6	4049.6	13.9
1/2/6	2.65	17.4	1235.3	57.6	0.88	14.3	2121.4	45.2

COV—coefficient of variation

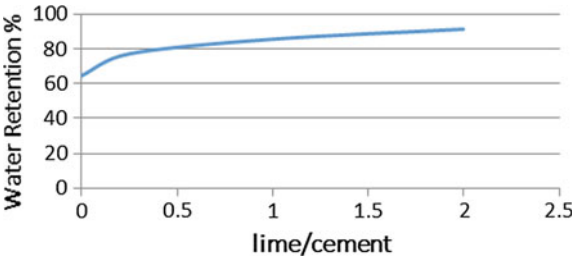

Fig. 2 Water retention versus lime content

4.2 Air Content

Air content is highest in the PC mortar with no lime (1/0/6) (Fig. 3). Lime addition up to a 1/1 ratio (PC/lime) reduced air content. Increasing lime/cement ratio thereafter increased the air content however, not to the level of the PC (1/0/6) mortar. This agrees with previous authors that noted a reduction in air content following lime addition (Schuller et al. 1999; Sugo et al. 2001). All air contents fall under the aforementioned 12–14% threshold which is assumed to undermine bond strength.

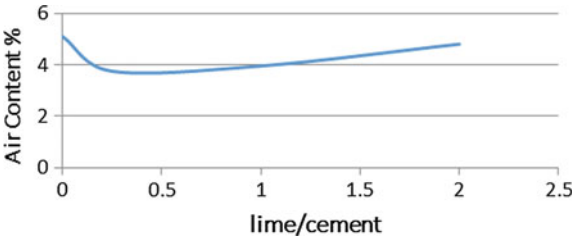

Fig. 3 Air content versus lime content

4.3 Flexural, Compressive Strength and Elastic Modulus

Except for the elastic modulus of the high lime content mix (1/2/6), the COV values suggest consistent results (Table 2). The results evidence that the effect of lime addition on the strength of cement mortar is heavily dependent on the quantity added. In both flexion and compression, the low lime content mix (1/0.25/6) is the strongest and the mortar with the highest lime content (1/2/6) the weakest. The 1/1/6 mortar is 39% weaker than the 1/0/6 mix. The flexural and compressive strength results are consistent, ranking the mortars, in decreasing strength as follows: 1/0.25/6, 1/0/6, 1/1/6, 1/2/6.

The modulus of elasticity shows the same trend as the strength (Table 2; Fig. 4): the low lime content mix 1/0.25/6 is the stiffest. The high modulus of elasticity of the 1/0/6 mix was expected given the rapid appearance, strength and stiffness of cement hydrates. As lime addition increases, the mortars deflect to a greater extent under less loading. However, interestingly, even though the low lime content mortar 1/0.25/6 is the stiffest, it shows a significant plastic deformation therefore, not only it can resist higher loads but can also deform on stress application to a significant extent (Fig. 4).

As expected, the mortars are stronger in compression than in tension, however, as it can be seen from Table 3, the percentage change in strength and stiffness of the PC mortar resulting from lime addition is similar in both compression and flexion. The mortars are stronger in compression (the compressive strength is higher than the flexural strength) but stiffer in tension (elastic moduli are superior in flexion than in compression). This means that the mortars resist higher loads before failure in compression however, it takes longer for them to deflect under a given load in tension.

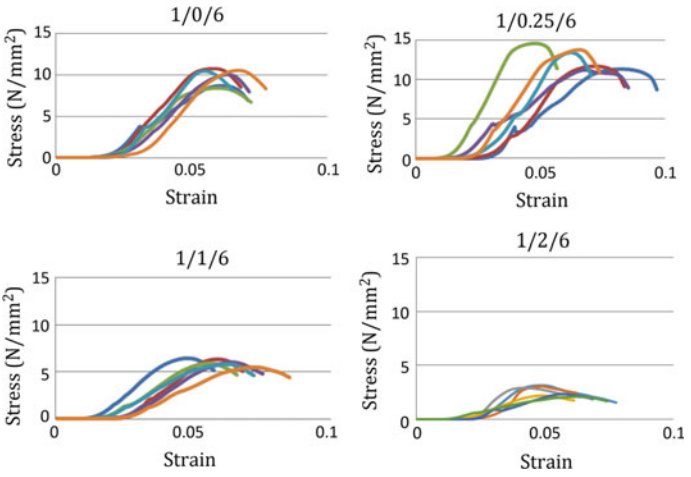

Fig. 4 Deformation of PC/lime mortars under compression showing greater deflections with increasing lime addition and lower stiffness for the higher lime contents. The low lime mortar 1/0.25/6 is the stiffest however showing significant deformation

Table 3 Percentage change in strength and stiffness of the PC mortar resulting from lime addition in both compression and flexion

Mortar PC/lime/sand	Rc/Rc 1/0/6 (%)	Ec/Ec 1/0/6 (%)	Rf/Rf 1/0/6 (%)	Ef/Ef 1/0/6 (%)
1.0/0.25/6.0	129	123	125	158
1.0/1.0/6.0	61	60	61	77
1.0/2.0/6.0	27	42	25	41

Rc compressive strength, *Rf* flexural strength. *Ec* and *Ef* modulus of elasticity in compression and flexion (respectively)

Despite a high sand content which lowers strength, the 1/0.25/6 mortar is slightly stronger than its BS 5628 equivalent (M12-class I; 1/0-0.25/3 at 12 N/mm^2). The 1/1/6 mix meets the strength requirements of BS M6 (class ii; 1/0.5/4-4.5 at 6 N/mm^2) and ASTM mortar N (1/0.5-1.25/4-6.75 at 5 N/mm^2) while the 1/2/6 mix is slightly stronger than the BS and ASTM equivalents M2 (1/2/8-9 at 2 N/mm^2) and O (1/1.25-2.5/5-10 at 2.4 N/mm^2) respectively.

4.4 Bond Strength

The brick's initial rate of absorption-IRA-was calculated at 1.05 kg/m^2/min (arithmetic mean of 6 tests at 15.9%COV) falling within the lower range. Of all mortars, the 1/1/6 provided the best balance of workability and adhesion to masonry while 1/2/6 was overly sticky causing problems in trowel and joints. The results (Table 4) suggest that low lime addition improves bond strength of PC mortar: the 1/0.25/6 mortar bond is 16% greater than the 1/0/6 bond and approximately 30 and 70% larger than the 1/1/6 and 1/2/6 bonds respectively. This agrees with previous authors reporting that lime addition enhances bond strength of PC mortars (Venumadhava Rao et al. 1996; Sugo et al. 2001; Sarangapani et al. 2005).

With the exception of the high lime content mortar (1/2/6), the most common failure mode was at the interface between the mortar and the upper unit (failure mode A1 Fig. 5), suggesting a good bond with the frog. In contrast, 80% of the high lime content mortar (1/2/6) failed at the interface mortar-frog (mode A6). This, together with the lower bond strength measured, suggest that this mortar did not flow into the brick pores and frog sufficiently. Its highly adhesive nature may have resulted in poor placing (also evidenced by the inconsistent results the high COVs at 45% indicate).

Table 4 Flexural bond strength (arithmetic mean of 9–10 tests)

Mortar	Bond strength (N/mm^2)	Failure mode
1/0/6	0.52	100% A1
1/0.25/6	0.62	60% A1; 40%A6
1/1/6	0.42	70% A1; 30%A6
1/2/6	0.17	20%A1; 80%A6

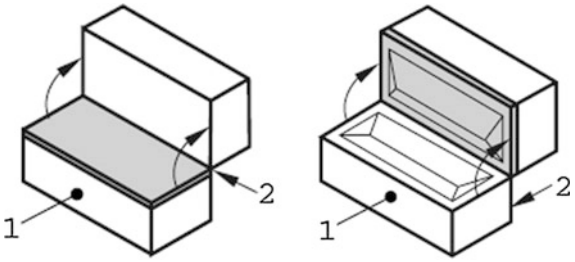

Fig. 5 Flexural bond strength failure modes: left A1, right A6. EN 1052-5 (2005)

4.5 Comparison of Properties PC/Lime Mortars with Those of Hydraulic Lime Mortars

The water retention of the PC/lime mortars is high (77–91%). The values are significantly superior to those of equivalent PC mortars (65–80%) and comparable to the typical NHL mortar values which range from 81 to 99% (Table 5). The air content of the PC/lime mortars is low (3.7–4.8%), comparable to values reported by previous authors (Schuller et al. 1999; Sugo et al. 2001; Brennan 2011; Draper 2010) and similar to the typical air content of fresh NHL mortars (2–5%-Table 5). The values are well under the 12% limit which is considered to adversely impact bond. The compressive and flexural strengths and elastic modulus of the lower-lime-content PC/lime mortars investigated (1/0.25/6 and 1/1/6) are consistent with previous authors (O'Looney 2010; Brennan 2011; Draper 2010; Sarangapani et al. 2005; Costigan 2013) and superior to values reached by NHL mortars (Table 5). The bond strength of PC/lime and NHL mortars is similar: to NHL mortars ranging from 0.20 to 0.60 N/mm^2 which have been consistently reported by previous authors for $1:3\text{-}2^{1/2}$ (NHL:sand) mortars and brick with similar absorption (Table 5). These compare well with the 0.13–0.62 values recorded for PC/lime mortars (Groot 1993; Melander and Conway 1993; Sugo et al. 2001; Lawrence and Cao 1987; Venumadhava Rao et al. 1996; Costigan 2013; Sarangapani et al. 2005). The strength, elastic modulus and bond of the PC/lime mortar with a higher lime content (1/2/6) is comparable to the values reached by NHL2 mortars.

5 Conclusion

PC/lime mortars are versatile materials whose properties span over a wide range of values that can be adjusted to suit different applications. They display good workability and high water retention, low air content and reliable bond. Their properties compare well to NHL mortars therefore they are probably not incompatible with certain historic fabrics. However, there are advantages relating to the

Table 5 Properties of NHL mortars used in conservation. All cured according to EN 499-2 and tested at 28 days except for the air content tested fresh

Mortar	W retention (%)	Air content (wet) (%)	Rc (N/mm^2)	Rf (N/mm^2)	Ec (N/mm^2)	Bond[a] (N/mm^2)
(1) NHL2 NHL3.5 NHL5 2.5:1	96–99 93–94 94–95	_	1–2 2.6–3 3–4	0.5–0.6 0.7–1 1	_	0.27–0.42 0.20–0.60 0.32–0.50
(2) NHL2 NHL 5	87–89 81–86	2–3 3–4.5	1–2 4–5	0.33 0.25	_	0.27–0.40 0.20–0.35
(3) NHL2 NHL3.5	86 83	2.8 2.8	4 3.8	1.4 1	_	_
(4) NHL2 NHL3.5 NHL5	_	_	1.7 3.2 9.2	0.3 0.7 2.1	_	_
(5) NHL2 NHL5	87 83	3.3 3.6	3 6	0.8 1.4	_	_
(6) NHL3.5 NHL5	86 84	3.5 3.5	3.8 4.4	0.4 1.5	1570 2630	_
(7) NHL2 NHL3.5 2.25:1 @90d	_	_	0.9 1.3	_	_	0.22–0.39 0.40–0.80
(8) NHL2 NHL3.5 NHL5	95–96 93–94 90–92	_	2 3.8–4 3.8–4.4	0.3 0.6–0.8 1.3	1160–1300 1840–2770 2770–3070	0.12 0.18–0.25 0.21–0.28

(1) Hanley (2006); (2) Carvill (2008); (3) Schiffner et al. (2008); (4) Cosgrove (2007); (5) O'Donohue (2008); (6) Duignan (2009); (7) Walker (2010); (8) Costigan (2013). All 3:1 mixes except when specified

[a]All wrench test method: brick IRA = 1–3 $kg/m^2/min$

use of NHL mortars including their low E-modulus combined with their low thermal expansion coefficient which impose low stresses in masonry under changing environmental conditions (a property especially favorable for repointing mortars). In addition, the greater porosity and water vapour transfer of NHLs preserves the masonry units; and the slow strength development and low E-modulus of NHL mortars allows to accommodate masonry movement without cracking.

The air content of PC/lime mortars is low, similar to the typical air content of NHL mortars. Their water retention is high (77–91%), significantly superior to those of equivalent PC mortars (65–80%) and comparable to typical NHL mortar values (81–99%). The compressive and flexural strength and elastic modulus of the lower-lime-content mortars (1/0.25/6 and 1/1/6) are superior to the values reached by NHL mortars however their bond strength is similar. The strength, elastic modulus and bond of the PC/lime mortar with higher lime content (1/2/6) are comparable to the values typically reached by NHL2 mortars. Low lime addition (1/0.25-PC/lime) increases the compressive and flexural strength, stiffness, water retention and bond strength of PC mortar simultaneously lowering air content and increasing flexibility. The increase of strength and stiffness triggered by low lime addition can be due to the high water retention of lime enhancing the hydration of PC.

References

Adams, M. A., & Hobbs, D. W. (1994). Bond strength of brickwork from crossed couplet and wallette tests: Some comparative results. *Masonry International, 8*(1), 16–20.

ASTM C270. (2002). *Standard specification for mortar for unit masonry*. Philadelphia: ASTM International West Conshohocken.

BIA. (2003). *Mortars for brick masonry. Technical notes on brick construction*. Reston, VA: The Brick Industry Association.

Borchelt, J. G., & Tann, J. A. (1996). Bond strength and water penetration of low IRA brick and mortar. In *Proceedings of the 7th North American Masonry Conference*, Masonry Society, Boulder Co.

Boynton, R. (1980). *Chemistry and technology of lime and limestone*. New York: Wiley.

BRE. (2001). *Building research establishment, digest 362*. London: Spon Press.

Brennan, A. (2011). *Influence of air content on the freezing strength of masonry mortar* (Research thesis, unpublished, Dept of Civil Engineering, Trinity College Dublin).

Brennan, O. (2009). *Effect of lime addition in the physical properties of PC mortars* (Research thesis, unpublished, Dept of Civil Engineering, Trinity College Dublin).

Brocken, H. J. P., Van der Pers, N. M., & Larbi, J. A. (2000). Composition of lime-cement and air-entrained cement mortar as a function of distance to the brick-mortar interface: Consequences for masonry. *Materials and Structures, 33,* 634–646.

BS 5628-1. (2005). *Code of practice for the use of masonry: Structural use of unreinforced masonry*.

Carvill, E. (2008). *Assessment of the tensile strength of masonry—Improving bond strength* (Research thesis, unpublished, Dept of Civil Engineering, Trinity College Dublin).

Cosgrove, K. (2007) *A comparative study of the mechanical and fluid transfer properties of lime and PC mortars* (Research thesis, unpublished, Dept of Civil Engineering, Trinity College Dublin).

Costigan, A. (2013) *An experimental study of the physical properties of lime mortar and their effect on lime-mortar masonry* (PhD thesis, unpublished, Dept of Civil Engineering, Trinity College Dublin).

Draper, J. (2010) *Use of plasticisers as lime replacement in masonry mortars* (Research thesis, unpublished, Dept of Civil Engineering, Trinity College Dublin).

Duignan, P. (2009). *An assessment of the elasticity of hydraulic lime mortars* (Research thesis, unpublished, Dept of Civil Engineering, Trinity College Dublin).

EN 196-1. (2005). *Methods of testing cement Part 1: Determination of strength*. Brussels: European Committee for Standardization.

EN 197-1. (2011). *Cement: Composition, specifications and conformity criteria for common cements*. Brussels: European Committee for Standardization.

EN 459-1. (2010). *Building lime, Part 1: Definitions, specifications and conformity criteria*. Brussels: European Committee for Standardization.

EN 459-2. (2010). *Building lime, Part 2: Test methods*. Brussels: European Committee for Standardization.

EN 772-16. (2000). *Methods of test for masonry units, Part 16: Determination of dimensions*. Brussels: European Committee for Standardization.

EN 998-2. (2003). *Specification of mortar for masonry. Masonry mortar*. Brussels: European Committee for Standardization.

EN 1015-7. (1999). *Methods of test for masonry, Part 7: Determination of air content of fresh mortar*. Brussels: European Committee for Standardization.

EN 1052-5. (2005). *Determination of bond strength by the bond wrench method*. Brussels: European Committee for Standardization.

EN 812.103-1. (2005). *Testing aggregates, Part 1: Method for determination of particle size distribution. Sieve tests*. Brussels: European Committee for Standardization.

Fried and Law. (1995). Factors influencing masonry flexural strength. *Proceedings of the Fourth International Masonry Conference*.

Groot, C. (1993). *Effects of water on mortar-brick bond* (Ph.D. thesis, University of Delft, Delft, The Netherlands).

Hanley, R. C. (2006). *The relationship between workability and bond strength of lime mortars* (Ph. D. thesis, unpublished, Dept of Civil Engineering, Trinity College Dublin).

Hanley, R., & Pavía, S. (2008). A study of the workability of natural hydraulic lime mortars and its influence on strength. *Materials and Structures, 41*(2), 373–381.

Lawrence, S. J., & Cao, H. T. (1987). An experimental study of the interface between brick and mortar. In *Proceedings of the 4th North American Masonry Conference*, Masonry Society, Boulder, Colo. (pp. 1–14).

Melander, J. M., & Conway, J. T. (1993) Compressive strengths and bond strength of Portland cement-lime mortars. In J. M. Melander & L. R. Lauersdorf (Eds.), *Masonry: Design and construction, problems and repair*. ASTM 1180. American Society for Testing and Materials, Philadelphia.

O'Donohue, N. (2008). *Influence of preparation and curing on physical properties of lime mortar* (Research thesis, unpublished, Dept of Civil Engineering, Trinity College Dublin).

O'Looney, D. (2010). *Hydrated lime versus chemical admixtures in Portland cement composites* (Research thesis, unpublished, Dept of Civil Engineering, Trinity College Dublin).

Pavía, S., & Hanley, R. (2010). Flexural bond strength of natural hydraulic lime mortar and clay brick. *Materials and Structures, 43*(7), 913–922.

Sarangapani, G., Venkatarama Reddy, B. V., & Jagadish, K. S. (2005). Brick mortar bond and masonry compressive strength. *Journal of Materials in Civil Engineering ASCE, 17*(2), 229–237.

Schiffner, H. et al. (2008). European Round Robin test—test procedures for physical parameters CEN TC 51/WG 11/TG1, IKM Cologne (Unpublished report).

Schuller, M., Van Der Hoeven R., & Thomson, M. (1999). Comparative investigation of plastic properties and water permeance of cement-lime mortars and cement-lime replacement mortars. Water Problems in Building Exterior Walls: Evaluation, Prevention, and Repair.

Sebaibi, Y., Dheilly, R. M., & Queneudec, M. (2003). Study of the water retention capacity of a lime-sand mortar: Influence of the physicochemical characteristics of the lime. *Cement and Concrete Research, 33*(5), 689–696.

Sinha, B. P. (1967). *Model studies relating to load bearing brickwork* (Ph.D. thesis, University of Edinburgh, UK).

Sugo, H. O., Page, A. W., & Lawrence, S. J. (2001). The development of mortar bond. In *Proceedings of the 9th Canadian Masonry Symposium*. University of New Prunswick, Canada.

Tate, M. (2005). The most important property of cement lime mortar in masonry construction is. *International Building Lime Symposium*, Orlando, Florida.

Venumadhava Rao, K., Venkatarama Reddy, B. V., & Jagadish, K. S. (1996). Flexural bond strength of masonry using various blocks and mortars. *Materials and Structures (RILEM), 29* (186), 119–124.

Walker, P. (2010). Properties of lime-mortared masonry. *Journal of the Building Limes Forum, 17,* 50–53.

Wright, B. T., Wilkins, R. D., & George, W. J. (1993). Variables affecting the strength of masonry mortars. In J. M. Melander & L. R. Lauersdorf (Eds.), *Masonry: Design and Construction, Problems and Repair.* ASTM 1180, American Society for Testing and Materials, Philadelphia.

Choosing Mortar Compositions for Repointing of Historic Masonry Under Severe Environmental Conditions

Caspar J. W. P. Groot and Jos T. M. Gunneweg

Abstract The quality of repointing work in historic masonry is to an important degree determined by the composition of the repair mortar. Apart from this, good workmanship is a basic requirement for durable repointing. Over the past decades awareness has grown that the mortar composition of repointing should always be considered and applied taking into account the hygric and mechanical properties of the existing adjacent materials. Often this is easy enough to realize. However, choosing the composition of a repointing mortar there are situations where various damage risks seem to point at opposing materials properties. In the paper this problem is approximated analysing a number of damage cases with the aim to define more precisely which requirements and to what extent should be maintained. Subsequently, from lab studies and experiences with the application of natural hydraulic lime (NHL) in specific repointing projects a set of requirements is proposed. The context of this repointing study is repair of low-strength historic fired clay brick masonry in the coastal area of the Netherlands; environmental conditions: sea salt laden, heavy rain load and freeze-thaw cycling.

Keywords Repointing · Damage · Requirements · Restoration

1 Introduction

Historic masonry in the Netherlands (before 1850) is mostly composed of relatively low-strength bricks held together with a relatively low-strength mortar (often pure lime mortars). In most cases the mechanical strength of the masonry, although low,

C. J. W. P. Groot (✉) · J. T. M. Gunneweg
Faculty of Civil Engineering and Geo Sciences,
TU-Delft, Stevinweg 1, 2628CN Delft, The Netherlands
e-mail: c.j.w.p.groot@tudelft.nl

J. T. M. Gunneweg
e-mail: j.t.m.gunneweg@tudelft.nl

J. J. Hughes et al. (eds.), *Historic Mortars*,
https://doi.org/10.1007/978-3-319-91606-4_11

is sufficient to show a satisfactory durability. Low mechanical strength mostly goes together with a high-porosity: 25–40 vol.%.

In the past repointing of historic masonry was often done using shell lime. The shell lime was obtained by burning shells from the sea. This lime was supposed to be weakly hydraulic however more importantly, these mortars (the lime being relatively coarse) showed excellent drying behaviour. For a good quality the preparation of the shell lime mortar was rather time-consuming. With time the use of shell lime mortars for repointing stopped as the production of shell lime came to an end in the Netherlands. The durability of shell repointing often turned out to be excellent.

In the repointing practice of historic masonry, with the disappearance of shell lime, cement as the basic binder was introduced. Speed of production (early strength) and the idea that the use of an, in itself, durable material were important incentives for the application of cement-based repointing mortars in historic masonry. Subsequently, there was amazement at the occurrence of damage as a result of this type of repointing. Mostly the problems are caused by incompatibility between the repair material and the adjacent historic materials. Since the joint material in itself generally remains undamaged, the repointers doing the job are reluctant to adapt their composition, as a change in general will diminish the durability of their joint (it's about who is responsible for an eventual damage).

From a restoration point of view, however, the repair mortar should not have a negative effect on the durability of the existing masonry and other components in the masonry. With this constraint in mind, the service life of the repair mortar should be as long as possible (be durable).

Service life not only depends on the mortar components but also on how it is installed (workmanship) and cured, on the compatibility between the masonry unit and the mortar, and on the severity of the environmental exposure, which in turn depends on weather, design, construction practice, operation, and maintenance.

2 Requirements Related to Damage Risks

Main causes of damage in or as a result of repointing are: (i) freeze-thaw cycling (ii) salts and (iii) thermal/moisture expansion/shrinkage or a combination of these three. These types of damage may be the result of inappropriate materials behaviour and/or unskillfull execution.

2.1 Freeze-Thaw Damage

Freeze-thaw damage may occur *in* a repointing (see Fig. 1) if the binder is an air lime and not sufficiently carbonated at the onset of winter. Under average weather conditions, after 4 weeks, carbonation should have occurred to a depth of at least

5 mm (Tim and Jeff 1997); carbonation depths of 8 mm after 2 months are reported by (Waldum Alf 2009). This means that the application of air lime has to take place in the right season and at least 2–3 months before the frost season. This seasonality also plays a role with regard to the application of Natural Hydraulic Lime (application at least 1 month before the frost season).

For many appliers the use of pure air-lime mortars without the addition of hydraulic components is often considered too risky, especially if the masonry is very exposed. The reason being that non-carbonated lime has a high solubility and is easily leached out by rain. Given the relatively long period of sensitivity to weather conditions pure air lime repointing is in fact not a very favourable option.

Freeze-thaw damage may also occur indirectly: applying a very dense (e.g. cement-based or repointing mortars containing water repellents) repointing on a historic air-lime bedding mortar may have serious consequences for the drying conditions in the masonry. With an open porous structure in the repointing, moisture may easily move from the bedding mortar to the repointing; with a dense structure in the repointing the moisture will necessarily pass through the adjacent brick; this is a slower process, causing longer periods of high moisture content in the bedding mortar; as a result of this the bedding mortar may become frost prone. Cases are known of centuries-old sound bedding mortars showing this type of frost damage caused by the application of the wrong restoration practice (a typical example of an incompatible use of a repair material).

2.1.1 Requirements—Materials Properties

When considering freeze-thaw the most important material characteristics are:

- strength development
- frost resistance
- drying behaviour (moisture transport, porosity)

Fig. 1 Horizontal layering (see arrows) in an uncarbonated air lime repointing as a result of freeze-thaw cycling

2.1.2 Requirements—Execution Techniques

Related damages in addition to the execution technique may play a role in the further occurrence of freeze thaw damage. For instance: a hollow between repointing and bedding, as a result of insufficient filling of the joint may result in push out by frost (where a period of heavy rain is directly followed by a frost period); other causes of damage may be insufficient depth of the repointing, a V-form instead of a rectangular form of the joint etc.

2.2 Salt Damage

Salts may have a harmful influence on the durability of the mortar as well as the brick. The influence of sea salt (containing a high content of NaCl) can be observed in many buildings, especially on the North sea coast of the Netherlands. In Fig. 2 two examples are presented of damage caused by NaCl.

Figure 2 (left), shows damage to a pure air-lime repointing mortar. In this case the highly soluble chemical compound calcium chloride ($CaCl_2$) is formed with calcium from the mortar binder and chloride from the seasalt. Rain, subsequently, causes the leaching out of the mortar. The binder choice is obviously an important parameter in limiting salt damage.

In practice the start situation of the substrate on which the repointing is applied is important: high contents of salt may limit the use of lime-based mortars such that only cement seems to be appropriate. For other reasons this maybe very inappropriate (too dense, too strong). Desalination of the masonry may then be a solution.

Also crystallization-dissolution cycling, especially around 75% Relative Humidity, resulting in swelling-shrinkage cycling, may cause considerable damage (Lubelli 2006).

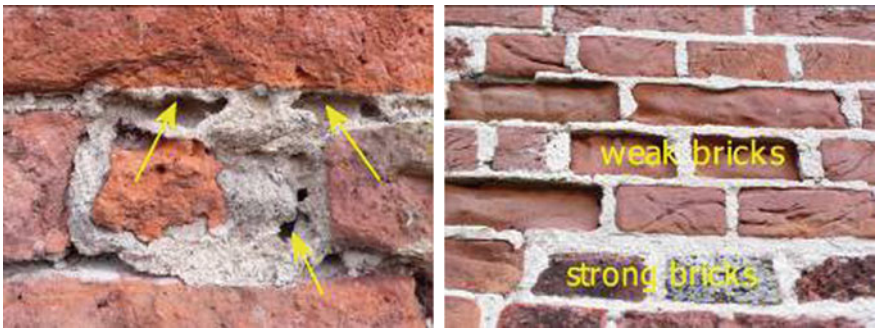

Fig. 2 Cases of NaCl damage. Left: voids in the repointing stemming from leaching of calcium chloride from the air lime repointing. Right: weathering of underfired brick through NaCl crystallization-dissolution cycling

Figure 2 (right), presents damage to fired clay bricks by NaCl. In this case the underfired bricks are apparently not strong enough to resist the crystallization-dissolution cycling caused by NaCl. The stronger bricks don't show damage (compressive strength values of 10–15 MPa are suggested by practice as strong enough to withstand salt damage through crystallization-dissolution cycling).

2.2.1 Requirements—Materials Properties

When regarding salt damage the most important materials characteristics are:

- the choice of the binder
- chemical composition such that no soluble compounds are formed
- resistance against salt crystallisation requires a certain degree of mechanical strength

2.3 Deformation Damage

In practice there is often more of an awareness regarding the risks of damage as a result of thermal and moisture deformation on a macro scale (building element), than there is for that on a meso scale (joint).

Differences in macro deformation behaviour of modern (left) and traditional masonry (right) is shown in Fig. 3. The fear of cracks, apparently a risk in modern cement masonry, is solved by extensively applying dilations. The long wall constructed with a traditional natural hydraulic lime mortar, NHL3.5 type St. Astier, (right) does not need any dilation.

Fig. 3 Left, the yellow lines indicate the dilations applied in a modern masonry. Right, a wall without dilation in traditional masonry (Color figure online)

Fig. 4 Detachment of repointing caused, in particular, by thermal deformation enhanced by a wrong cross-sectional form (V-shape instead of rectangular) of the repointing

At meso scale thermal resp. moisture deformation may as well be a serious cause of damage (see Fig. 4). Not only do material properties such as the (linear) thermal respective moisture expansion coefficient play a role in the detachment process, but so does the execution technique in for example the pointing.

2.3.1 Requirements—Materials Properties

- (linear) thermal respective moisture deformation coefficients
- stiffness (E-modulus).

2.3.2 Requirements—Execution Technique

- rectangular cross section of the repointing (no V-cross section form!!)

2.4 Overview—Requirements

In order to facilitate the analysis of the (in)consistency of the materials and execution requirements of the different damage risks, they have been collated in Table 1.

It is quite clear from the table that there is a friction between the required mechanical characteristics relating to frost and deformation risks, when compared to those relating to the salt damage risk.

Table 1 Relative requirements related to major damage risks of repointing in weak historic masonry

	Frost damage	Salt damage	Deformation damage
properties			
strength development	winter proof [1]		[4]
drying (porosity)	quick		
strength (compressive)		≥ medium	low
stiffness (E-mod)		≥ medium	low
expansion coefficient			low
frost resistance	+		
salt resistance		+	
execution [2]			
prep,prewett,curing etc	+	+	+
form joint	+		+
depth joint	+		+
filling joint	+		

1) strong enough to pass the first winter without frost damage
2) specialised execution required
3) + high importance
4) empty box: low importance or not specified

The easiest solution seems to be to opt for the stronger and less deformable mortar as required for a better salt damage resistance. This may provide an increase of durability in the repointing mortar; however, such a mortar will also be typically less porous, leading to slower drying of the bedding mortar, and also a higher thermal expansion combined with a higher stiffness, increasing the risk of deformation damage.

In fact a compromise should be reached between the durability requirements of the repair mortar and the compatibility requirements of the adjacent masonry (drying affecting frost resistance) and stresses (resulting from deformation behaviour).

3 Tests in Practice and in the Laboratory

In practice as well as in the laboratory a series of site-mixed and prefabricated repointing mortar compositions were tested. The starting point were recent experiences with repointing mortars used in historic towers and windmills located on the

West coast of the Netherlands. These buildings are composed of relatively weak masonry which is exposed to sea salts, heavy rain and frost. In such cases the choice of the binder is essential, as this determines whether the mortar will be salt resistant, have adequate strength (not too high and not too low, in comparison to the existing masonry materials), is frost resistant, and shows low thermal deformation.

With regard to the needed salt resistance recent experiences in restoration projects with natural hydraulic lime (NHL 3,5) showed such good sea salt resistance, that this binder was chosen as a basis for the site-mixed repointing mortars.

In the laboratory, properties like compressive strength, dynamic E-modulus, free water absorption, drying characteristics, thermal expansion and frost resistance were determined. In this paper the attention is focused on freeze-thaw testing and deformation testing, being of major importance with regard to durability.

3.1 Mortar Compositions

Materials used in the site mixed mortars:

- Natural Hydraulic Lime (NHL 2 and NHL 3,5 from St Astier, France).
- BFC: blast furnace cement (HC CEM III/B).
- Pozzolan: Trass (Rheinische Trass).
- Air limes: 'Lime (Harl)' (CL70).
- Sand 1: standard repointing (rounded river) sand with Fineness Modulus of 1.8.

The composition of the prefabricated repointing mortars is unknown; from the hardening process it can be concluded that they are Portland cement-based mortars (Table 2).

Table 2 Repointing mortars used in the laboratory tests and their constituents by volume proportions

Site-mixed mortars									Prefab mortars	
VB02	NHL3,5	BFC	Sand 1	VB06	NHL2	add	BFC	Sand 1	VP01	A
	6	1	17		3		1	10		
VB03	NHL2	BFC	Sand 1	VB07	Lime	trass	BFC	Sand 1	VP04	B
	3	1	10		1.3	0.4	0.25	3.2		
VB04	NHL3,5		Sand 1						VP05	C
	1		2,5							
VB05	Lime	BFC	Sand 1						VP06	D
	5	1.5	16							

3.2 Freeze-Thaw Testing

The freeze-thaw tests were based on the test set-up used in the EU-Pointing project (Wijffels et al. 2001). In this test the freeze-thaw cycle is applied from one side of the test specimen, and fresh water is used in the test. Precise details on the freeze-thaw cycle tests are given in (Groot and Gunneweg 2012) (Fig. 5).

The test specimens were evaluated regarding:

- damage of the repointing itself
- deterioration of the bond between mortar and brick
- damage of the bedding mortar behind the repointing
- push out (sound test)

The results are presented within Table 3. None of the repointings of the test specimens were pushed out. Push out may occur in case the depth of the repointing is small (see tests Wijffels et al. 2001); in this testing series the depth of the repointing was greater than two times the width of the joint.

Frost damage behind the repointing (in the bedding mortar) occurred within three of the test specimens of the cement-based prefab mortars and within only one test specimen of the lime-based site mixed mortars: a clear indication that the drying conditions of the site mixed specimens are more favourable than the prefab mortars.

3.3 Thermal Deformation

In the following the effects of stress development in repointing mortars are given in a simplified model considering only a linear deformation and also neglecting the surrounding materials and other boundary conditions.

Fig. 5 The test specimens in the freeze-thaw container

Table 3 Results Freeze-Thaw testing

Site-mixed mortars					Results
VB02	NHL3,5		BFC	Sand	interface-damage bedding mortar
	6		1	17	
VB03	NHL2		BFC	Sand	OK
	3		1	10	
VB04	NHL3,5			Sand	interface-damage bedding mortar
	1			2,5	
VB05	Lime		BFC	Sand	frost damage behind repointing
	5		1,5	16	
VB06	NHL2	additive	BFC	Sand	OK
	3		1	10	
VB07	Lime	trass	BFC	Sand	OK
	1,3	0,4	0,25	3,2	
Prefab mortars					
VP01	A				frost damage behind repointing
VP04	B				frost damage behind repointing
VP05	C				OK
VP06	D				frost damage behind repointing

Thermal deformation may result into stresses in the masonry (Hayen and van Balen 2001; Vermeltfoort et al. 1999). The thermal stress (σ), developing under restrained conditions is given by the following equation,

$$\sigma = \alpha.E.\Delta\emptyset \text{ [MPa]} \quad (1)$$

where:

α: linear thermal deformation coefficient [1/K × 10^{-6}]

E: dynamic E-modulus [MPa × 10^{3}]

Δ(T): temperature change [K]

α.E is the materials-dependent stress coefficient, specific for every different type of repointing mortar (see Fig. 6).

The significant influence of the choice of material on the possible stress development in masonry can be shown, by comparing the thermal stresses developed by the cement-based repointing VP01 and the lime-based repointing VB06

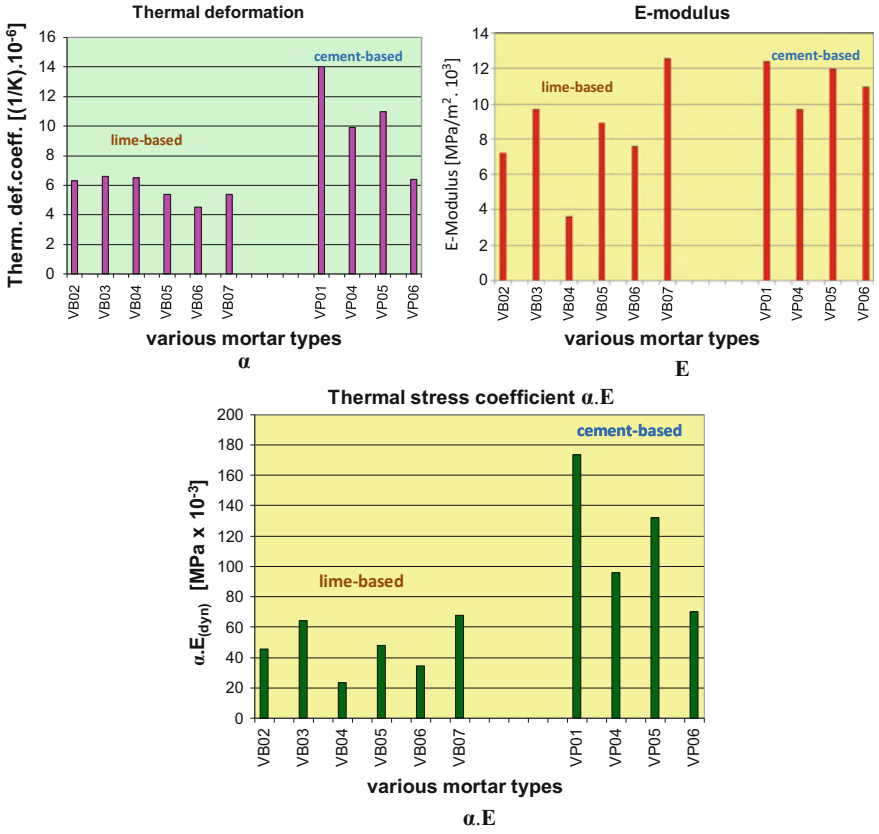

Fig. 6 Materials-dependent stress coefficients **α.E**

(see as well Fig. 6). Note: for the determination of the dynamic E and the thermal deformation coefficient α, see Groot and Gunneweg (2012).

Stress development under restrained conditions, with a temperature increase of 50 K (south or west facade) is as follows:

VP01:

Stress coefficient (see Fig. 6): $\alpha.E = 170 \times 10^{-3}$ MPa/K.
Restrained stress with a temp increase of 50 K: $\sigma = \alpha.E.\ \Delta\emptyset = 170 \times 10^{-3} \times 50 = 8.5$ MPa.

VB06

Stress coefficient (see Fig. 6): $\alpha.E = 34 \times 10^{-3}$ MPa/K
Restrained stress with a temp increase of 50 K: $\sigma = \alpha.E.\ \Delta\emptyset = 34 \times 10^{-3} \times 50 = 1.7$ MPa

3.4 Guideline Requirements

A series of guidelines with the necessary requirements for a suitable repointing mortar could be developed from the results of the laboratory testing combined with the practical experience obtained in a series of repointing projects.

The guidelines for requirements applicable to the repointing of low-strength historic fired clay brick masonry in the coastal area of the Netherlands where conditions encountered are sea salt, heavy rain load and freeze-thaw cycling, are as follows:

- Workability, evaluated as good by an experienced mason/pointer
- Choose preferably NHL-based binder (or at least lime-based)
- Depth of the joint ≥ 2 times joint width
- Compressive strength 3–7 [MPa]
- Dynamic E-modulus (6–10) $\times$ 10^3 [MPa]
- Linear Expansion Coefficient (4–7) $\times$ 10^{-6} [1/K]
- Water Absorption Coefficient (WAC) 0.3–0.9 [kg/(m^2. $min^{0.5}$)]
- Freeze-thaw test: no damage to the joint, no debonding within the joint, no frost damage to the bedding mortar *behind* the repointing (acc. to EU-Pointing Project, see also Wijffels et al. 2001, Groot and Gunneweg 2012).

Acknowledgements The financial support by the Province of Zuid Holland (The Netherlands) for the execution of this project is gratefully acknowledged.

References

Groot, C., & Gunneweg, J. (2012). *Repointing of historic masonry (in Dutch)*, TU Delft, Institutional Repository http://repository.tudelft.nl/.

Hayen R., & Van Balen K. (2001). *Thermal expansion of historic masonry, looking for physical compatibility*. Paper 5.10. Maintenance of pointing in historic buildings; Decay and replacement; EC Environment Programme ENV4-CT98-706.

Lubelli, B. A. (2006). Sodium chloride damage to porous building materials (Ph.D. dissertation, TU-Delft, ISBN 90-9020343-5).

Tim, R., Jeff, O. (1997). Success with lime renders, SPAB http://www.ihbc.org.uk/context_archive/59/limerender_dir/limerender_s.htm.

Vermeltfoort, A. T, Groot, C. J. W. P., & Wijen, E. (1999). *Thermal strains in repointed masonry: Preliminary investigations using ESPI*. RILEM pro 12, paper 21.

Waldum Alf M. (2009). Historic Materials and their Diagnostic State of the Art for Masonry Monuments in Norway. www.arcchip.cz/09.

Wijffels T., Van Hees R., & Van de Klugt L. (2001). *Pointing Report* ENV4-CT98-706 paper 5.2. TU Delft, Institutional Repository.

High-Performance Repair Mortars for Application in Severe Weathering Environments: Frost Resistance Assessment

Dana Křivánková, Cristiana Lara Nunes, Zuzana Slížková, Dita Frankeová and Krzysztof Niedoba

Abstract Frost is one of the main degradation processes affecting historic buildings in cold environments. Lime mortar is particularly sensitive to degradation by freeze-thaw cycles due to its high porosity and low mechanical resistance. The aim of the present research is to assess the frost resistance of seven lime-based mortars to be used in repairs. Mortars with different binder composition and a traditional hydrophobic additive were tested. Specimens with three months of age were subjected to freeze-thaw cycles and the ageing action was evaluated by means of mechanical and physical measurements. Improved durability of lime-based mortars with hydraulic binders and linseed oil additive has been confirmed and the different mortar formulas may be promising for repairs according to specific environmental conditions.

Keywords Mortar · Frost · Durability · Hydrophobic

1 Introduction

During the 20th century, the building technology changed drastically and newly developed materials began to be also used for historic building repairs as the use of traditional techniques and materials fell into oblivion.

D. Křivánková (✉) · C. L. Nunes · Z. Slížková · D. Frankeová · K. Niedoba
Institute of Theoretical and Applied Mechanics,
Czech Academy of Sciences, Prague, Czech Republic
e-mail: krivankova@itam.cas.cz

C. L. Nunes
e-mail: nunes@itam.cas.cz

Z. Slížková
e-mail: slizkova@itam.cas.cz

D. Frankeová
e-mail: frankeova@itam.cas.cz

K. Niedoba
e-mail: niedoba@itam.cas.cz

J. J. Hughes et al. (eds.), *Historic Mortars*,
https://doi.org/10.1007/978-3-319-91606-4_12

Currently, air lime mortars with compositions similar to ancient mortars and thus more suitable to ensure the aesthetical and functional compatibility with pre-existing materials, are very porous and their mechanical strength and durability are low when exposed to water and frost even if this occurs only occasionally (Veiga 2003).

One way to improve the strength and durability of air lime mortars is to partially replace lime by other materials such as pozzolans. Metakaolin is a promising pozzolanic material and it has also been used ancient times. An adequate combination of air lime and metakaolin can reach higher mechanical strength than pure air lime mortar while not being strong enough to generate stress in the original system to be repaired (Fortes-Revilla et al. 2006; Slížková 2009; Válek et al. 2007). The water transport by capillarity is reduced, the water vapour transport is slightly increased and the thermal properties are comparable (Vejmelková et al. 2011).

Naturally hydraulic limes (NHLs) were traditionally used as binders for preparing mortars in the Czech Republic (Válek et al. 2007) and are nowadays often used in commercial mixes because of their rapid setting and hardening, and good mechanical performance thanks to their hydraulic reactivity (Gulotta et al. 2013). Currently, NHLs are not produced in the Czech Republic, so there is not much experience in their use. Hence, the NHL binders used in this study were imported from Germany.

Mechanical resistance of pure lime plaster was also often improved by adding "a small amount of cement." Although increased resistance of hardened lime mortar may be achieved a ratio of lime: cement = 2:1 to 1:1 is considered too hard and brittle and therefore cannot be used for repairs of most historic buildings (Rovnaníková 2001).

When building materials are affected by severe weathering by water the application of lime or weak lime-based repair mortar is not suitable, particularly when the materials are susceptible to frost (WTA 2-7-01/D 2007).

The present study presents the first results of an on-going Czech national project focused on the development of compatible and durable repair mortars for application in severe weathering environment. The paper focuses on the resistance to frost damage of six mortar formulas and compares their performance. The six mortars comprise different binder mixtures and also a traditional hydrophobic additive.

The main reason for using oil as an additive for mortars lies in its hydrophobic properties. Hence, it may be a very efficient additive to improve durability by restraining water penetration. Linseed oil was one of the main lipidic additives used for mortar formulas in ancient times according to ancient treatises, e.g. Vitruvius, Pliny, Palladio. However, there is lack of information about the formula composition and preparation technique. Owing to the proven positive influence of linseed oil on the durability of mortars (Čechová et al. 2010) the present study encompasses the use of this traditional hydrophobic additive. Mortar specimens of lime and lime-metakaolin were enriched with 1.5%-w linseed oil (to the weight of binder) and subjected to freeze-thaw cycles.

2 The Experiment

2.1 Materials

Mortar mixtures were prepared in laboratory conditions with binder:aggregate proportion of 1:3 (by weight) using siliceous sand as aggregate (granulometry: 27% of 0.1–0.5 mm, 26.2% of 0.5–1.0 mm, 17.6% of 1.0–2.0 mm and 29.2% of 1.6–4.0 mm). Designations and mix proportions of the mortars are presented in Table 1.

The commercial hydrated air lime powder (class CL 90) was supplied by Vápenka Čertovy Schody a.s. Čerták® and the aggregate by Provodínské písky a.s. The metakaolin corresponds to burnt Czech clay shale Mefisto L05 and was supplied by České Lupkové Závody a.s. The moderate hydraulic lime NHL3.5 Calcidur® and the strong hydraulic lime NHL5 Hydradur® were both supplied by Zement- und Kalkwerke Otterbein and the Portland cement HET (CEM I 52.5 R) by Aalborg Portland A/S, Denmark. The raw linseed oil was supplied by GRAC s.r.o.

2.2 Specimen Preparation

Binder and aggregate were mechanically mixed for 6 min. using an automatic mortar mixer MATEST-E093 at low speed. Regarding mortars with linseed oil addition, binder and aggregate were mixed for 3 min. and a bit of dry mixture (approximately 50 g) was blended with oil in a plastic cup and mixed manually for 3 min. The oiled mixture was then added to the dry mixture and blended for plus 3 min. in the automatic mixer. Water was then added and the mixtures were blended for 3 min. in the automatic mixer. The amount of kneading water was ascertained in order to achieve comparable consistencies using the flow table test (170 ± 5 mm). Mortars were mechanically compacted in prismatic 40 × 40 × 160 mm steel casts. The specimens were kept for one day inside the casts and then de-moulded. During

Table 1 Mortar designation and composition (by weight)

Mortar code	Composition
L	Lime: sand (1:3-w)
LO	Lime: sand (1:3-w) + 1.5% linseed oil
LM	Lime: Metakaolin: sand (0.75:0.25:3-w)
LMO	Lime: Metakaolin: sand (0.75:0.25:3-w) + 1.5% linseed oil
NHL3.5	Natural hydraulic lime: sand (1:3-w)
NHL5	Natural hydraulic lime: sand (1:3-w)
CL1	Lime: Portland cement: sand (0.9:1:15-w)
CL2	Lime: Portland cement: sand (0.5:1:10-w)

Table 2 Fresh mortar properties

Mortar	Water/binder ratio	Consistency (cm)	Air content (%)
L	1.04	16.8 ± 0.1	2.6 ± 0.1
LO	1.08	16.6 ± 0.1	5.4 ± 0.2
LM	0.96	17.1 ± 0.3	2.2 ± 0.1
LMO	1.02	16.5 ± 0.1	4.0 ± 0.1
NHL3.5	0.66	16.6 ± 0.1	3.4 ± 0.18
NHL5	0.70	17.0 ± 0.3	3.1 ± 0.07
CL1	1.04	16.7 ± 0.2	6.0 ± 0.21
CL2	0.83	16.5 ± 0.3	4.8 ± 0.2

The values correspond to the average of 3 measurements ± standard deviation and were determined through the preparation of 2 kg of dry mixture

the first day inside the casts and for six days further, the samples were stored at 90 ± 5% relative humidity (RH). The mortar prisms were further stored for 90 days under controlled conditions at a temperature of 20 ± 5 °C and 60 ± 10% on grid-lined shelves to ensure the contact of all the sides with air and homogeneous progress of the carbonation reaction. The level of RH used for curing the specimens is considered too low for the mortars with hydraulic or pozzolanic components to develop satisfactory strength. However, the average RH of the ambient air in Prague during the construction activity period (April–September) is 60% (Czech Hydrometeorologic Institute Average 2011). Therefore, this level of RH was chosen as the most representative of the on-site conditions to compare the performance of all mortar types at a young age (90 days). Table 2 summarizes the results of water/binder ratio, consistency and air content obtained for the fresh mortars.

The water-binder ratio of the different mortar mixes is only slightly higher for the mortars enriched with oil but the air content is significantly higher. A high amount of kneading water is not desirable because it may slow down the carbonation process (Izaguirre et al. 2010). However, thermogravimetric results previously studied (Nunes et al. 2012) do not show significant differences in the carbonation process between reference mortar and mortar with oil.

The air content increased within a similar range of values as for sodium oleate (Izaguirre et al. 2010) added in 0.3 and 2.4% to lime mortar (1:1-v). Water/binder ratio was slightly higher for the 2.4% mixture (increment of 0.09%).

The air content of the hydraulic lime mortars is slightly higher than for pure lime mortars but cement mortars show considerably higher values, particularly CL1 which can probably be assigned to the different binder:sand ratio.

2.3 Hardened Mortar Testing Methods

2.3.1 Mechanical Strength

Flexural and compressive strength were determined, based on the standard (EN 1015-11 1999) with three specimens 40 × 40 × 160 mm of each mortar category using a universal traction machine. The broken specimens were used for the further characterization methods.

2.3.2 Porosity and Porosimetry

The open porosity test was performed according to the standard (EN 1936 2007) by total saturation with water under vacuum and hydrostatic weighing. The specimen halves remaining after the mechanical strength tests were used for this experiment. Water absorption by total immersion at atmospheric pressure was determined according to the procedure described in (ICCROM 1999) and the weight of the wet specimens was registered after 24 h of immersion. Pore size distribution was performed with a mercury porosimeter Quantachrome Poremaster® PM-60-13 with a specimen from each mortar. The mercury parameters were set to values of 480 erg/cm^2 for the surface tension of mercury and 140° for the contact angle.

2.3.3 Water Vapour Diffusion

Water vapour diffusion coefficient test was carried out based on the dry cup method described by RILEM II (1980). Containers with a layer of approximately 1 cm of anhydrous calcium chloride were closed by a sample of 10 mm in thickness. The containers were placed at a controlled temperature of 25 ± 3 °C and in an environment of 30 ± 5% relative humidity, maintained by a solution of calcium chloride. The containers were weighed at 24 h time intervals and the water vapour diffusion rate was determined by the change in mass. This test was run for 10 days when the required stability in the sample weight was obtained. Vapour diffusion values are expressed in m^2 s^{-1}.

2.3.4 Water Absorption by Capillarity

Water absorption by capillarity was performed based on the testing procedures of the standards (EN 1925 1999; EN 1015-18 2002). The specimen halves remaining after the mechanical strength tests were used for this experiment. Lateral surfaces of

specimens were sealed. Half of each sample 40 × 40 × 160 mm was immersed in 1 mm of water (over glass rods) inside a covered box to maintain constant hydrothermal conditions and to limit the water evaporation from the samples. The weight of the absorbed water per unit of the exposed surface immersed as a function of the square root of time (in hours), was registered. The tests were carried out until the absorption reached an asymptotic value. The capillary water absorption coefficient was determined by the angular coefficient of the curve.

2.4 *Frost Ageing Test*

Frost cycles were performed with samples of 90 days of age according to the Czech standard (ČSN 72 2452 1968). Three sets of specimens of standard dimensions 40 × 40 × 160 mm of each mortar category were tested. One group of specimens (Reference-Not Aged) remained stored in air at constant temperature and humidity during the entire ageing period (approximately one month at 24 ± 2 °C and 60 ± 8% RH). The second set of reference specimens was dried to constant mass at 60 °C and then immersed in water (Water-Aged) and kept at room temperature (Water-Aged). Samples to be subjected to the frost test (Frost-Aged) were initially dried to constant mass at 60 °C and then immersed in water at ambient temperature (20 ± 5 °C) for 24 h and then exposed to −20 °C (±5 °C) in a freezer during 4 h (Fig. 1). Specimens were then thawed in water at ambient temperature (20 ± 5 °C) for at least 2 h before performing another cycle.

Freezing cycles were interrupted when specimens showed moderate to severe degradation and the mass loss was determined after drying the specimens at 60 °C until achieving constant mass. Flexural strength test was then performed according to the procedure previously described. Half of each specimen 40 × 40 × 160 mm remaining from the mechanical test were also used for water absorption by capillarity determination after being dried to constant mass at 60 °C. Mortars enriched with linseed oil were tested with lateral surfaces unsealed.

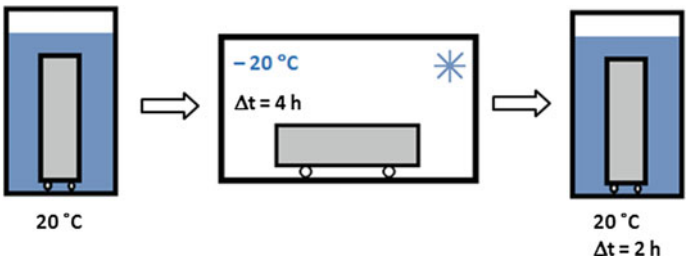

Fig. 1 Scheme of the frost ageing test representing the steps for performing one cycle

3 Results and Discussion

3.1 Hardened Mortar Characterization

Results of pore space properties of each mortar are given in Table 3. Pore size distribution curves are plotted in Fig. 2 and represent the calculated pore size diameter of each mixture for the stated measurement conditions.

The porosity of lime and lime-metakaolin mortars with and without oil may be considered relatively similar when compared to the hydraulic lime and cement mortars. However, the water absorption values obtained at atmospheric pressure show considerably lower values for LO and LMO mortars, which are assigned to the water-repellent properties granted by the oil and are not detected when pressure is used to fill the specimen pores.

The pore size distribution curve of lime mortar L is characterized by the presence of two peaks (Fig. 2): the 0.1–1 μm range is assigned to the binder and the 10–100 μm range is assigned to shrinkage cracks. LM pore size distribution curve shows the presence of pores smaller than 100 nm that are probably to be assigned to the formation of CSH gels. The most significant difference between LM mortar and the reference L can be observed within the interval 0.01–0.1 μm. Vejmelková et al. (2012) assigns the significantly higher amount of 0.01–0.1 μm pores in LM mortar to the formation of CSH gels resulting from the pozzolanic reaction of metakaolin with calcium cations. It is worth mentioning that LM mortar did not develop shrinkage cracks like L mortar which is probably related to the improvement of the mechanical properties granted by the rapid pozzolanic reaction (Gameiro et al. 2012).

Table 3 Values of open porosity, water absorption at atmospheric pressure, water vapour diffusion and water absorption by capillarity

Mortar	Open porosity (%)		Water absorption at P_{atm} 24 h (%-w)	Water vapour diffusion coefficient ($m^2\ s^{-1}$)	Water absorption by capillarity coefficient (kg $m^{-2}\ h^{-1/2}$)
	Mercury accessible	Water accessible			
L	31.75	32.01 ± 0.19	15.62 ± 0.49	(2.09 ± 0.06) × 10^{-6}	28.5 ± 0.42
LO	35.72	34.44 ± 0.58	2.35 ± 0.58	(2.28 ± 0.03) × 10^{-6}	3.95 ± 1.66
LM	33.15	34.35 ± 0.13	21.62 ± 0.85	(1.34 ± 0.09) × 10^{-6}	13.4 ± 0.30
LMO	34.88	32.41 ± 0.50	5.98 ± 2.63	(1.03 ± 0.04) × 10^{-6}	1.98 ± 0.04
NHL3.5	24.58	27.43 ± 0.17	12.96 ± 0.14	(1.21 ± 0.06) × 10^{-6}	16.26 ± 0.04
NHL5	23.34	28.13 ± 0.31	13.31 ± 0.13	(1.30 ± 0.10) × 10^{-6}	19.08 ± 0.88
CL1	20.79	24.85 ± 0.23	10.09 ± 0.21	(1.14 ± 0.05) × 10^{-6}	9.64 ± 1.22
CL2	20.63	22.40 ± 1.62	8.44 ± 0.06	(1.22 ± 0.10) × 10^{-6}	3.99 ± 0.11

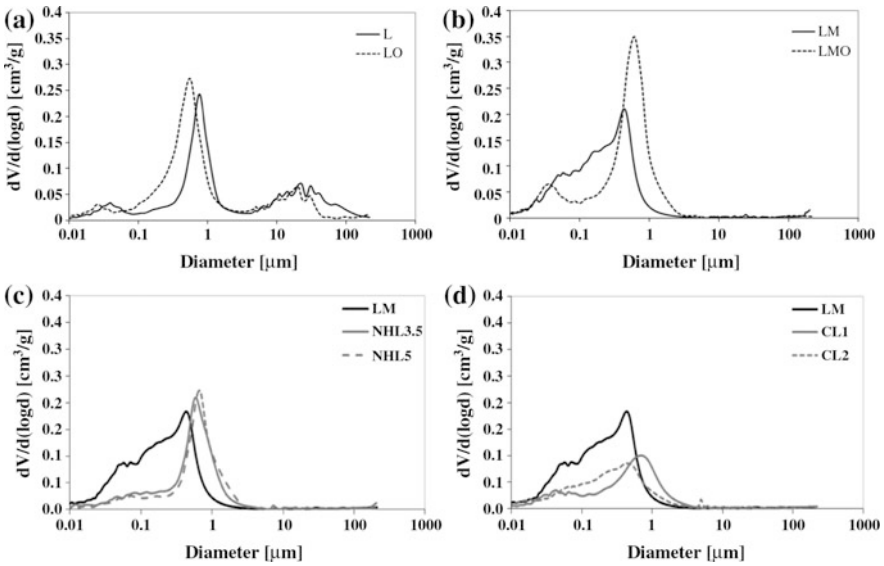

Fig. 2 Mercury intrusion curves of each mortar: **a** lime and lime with oil mortars; **b** lime-metakaolin and lime-metakaolin with oil mortars; **c** lime-metakaolin with NHL3.5 and NHL5; **d** lime-metakaolin with cement-lime mortars CL1 and CL2

Hydraulic mortars are characterized by lower porosity (approximately 4–5%). Similarly to LM mortar shrinkage is also reduced which can be also assigned to the fact that some water is consumed during hydration instead of evaporating. This phenomenon plays an important role in the performance and durability of the hydraulic mortars after curing. Pore size distribution of hydraulic lime is comparable to pure lime (approximately 1 μm). The addition of hydraulic components and cement binder to lime mortar visibly shifts the pores to a lower range (smaller than 100 nm) which is characteristic of mortars containing cement (Mosquera et al. 2006).

The addition of linseed oil to lime mortar slightly increased water vapour permeability but had the opposite effect when added to the lime-metakaolin mortar. Lime-metakaolin and hydraulic lime and cement mortars show relatively similar values and it is worth noticing that LM and NHL5 have almost equal coefficients.

Water absorption by capillarity was drastically reduced by the addition of oil although porosity values are similar between reference and mortars enriched with oil. Similarly to the water absorption under atmospheric pressure, water absorption by capillarity clearly illustrates the water-repellent effect granted by the oil. CL2 also induced comparable water absorption to LO mortar, but the capillarity values may be related to the binder pore size and to the dense structure achieved with the high amount of cement added to this mortar.

3.2 Resistance to Frost Ageing

Figure 3 shows the aspect of mortars after ageing. Lime mortar specimens crumbled after one freezing cycle. According to results obtained with the Phenolphthalein test, the lime mortars were not fully carbonated at the age of 90 days. Lime with linseed oil mortar was subjected to 10 cycles after which the samples showed moderate to severe degradation by binder powdering and, consequently, sand disintegration. Hence, after 10 cycles it was decided to finish the ageing cycling. Hydraulic lime mortars showed several longitudinal cracks already after the 3rd cycle although the specimens maintained their cohesion. Degradation was faster for NHL5 mortar. After the 3rd cycle, LM mortar also showed significant degradation signs as a dense network of fine surface cracks on the specimen's surface. Immediately after the freezing step very fine ice crystals were observed growing from these cracks. After completion of the test and final drying, the specimens emitted a hollow sound when tapped. Cement-lime mortars CL1 and CL2 exhibited fine fissures in several areas after the 8th and 15th cycle, respectively.

Through visual inspection, it can be inferred that metakaolin mortars develop surface fissuration whilst hydraulic lime mortars develop deep fissures. The higher mechanical strength values of cement-lime mortars may explain why the cracks formed during ageing are finer than those observed on hydraulic lime mortars.

Table 4 presents the results of mortar's characterization after ageing. The mass variation was measured after completion of the ageing test and is given in Table 4 in weight percentage. The highest mass variation was registered on specimens containing air lime binder. The high standard deviation values of LO mortar are probably assigned to mass loss by granular disintegration during specimen handling.

CL1 mortar showed higher mass loss than CL2, which can probably be assigned to its higher content of hydrated lime.

Specimens with metakaolin and hydraulic and cement binders exhibited strength increment after being stored in water (Water-Aged) which is probably to be assigned to the improvement of the hydraulic reactions in a wet environment. Reference specimens NHL3.5 and NHL5 showed very low strength values which fall within the range of L mortar. These results are probably related to the insufficient amount of kneading water. According to Hanley and Pavia (2008), the optimal initial consistency for NHL2 lime is 165 mm, while for mortars with NHL3.5 and NHL5 lime the value should be close to 185 mm which may explain why the mechanical strength of the tested specimens is lower than expected. CL1 and CL2 presented the highest flexural strength values although Frost-Aged specimens showed only slight fissuration after 10 or 20 cycles and the decrease in flexural strength corresponded to 40 or 70% in comparison to Water-Aged samples.

The frost resistance coefficient (K) was calculated for each mortar according to the respective number of freeze-thaw cycles. Coefficient K was expressed as a ratio of the average values of flexural strength of frost-aged and water-aged and of

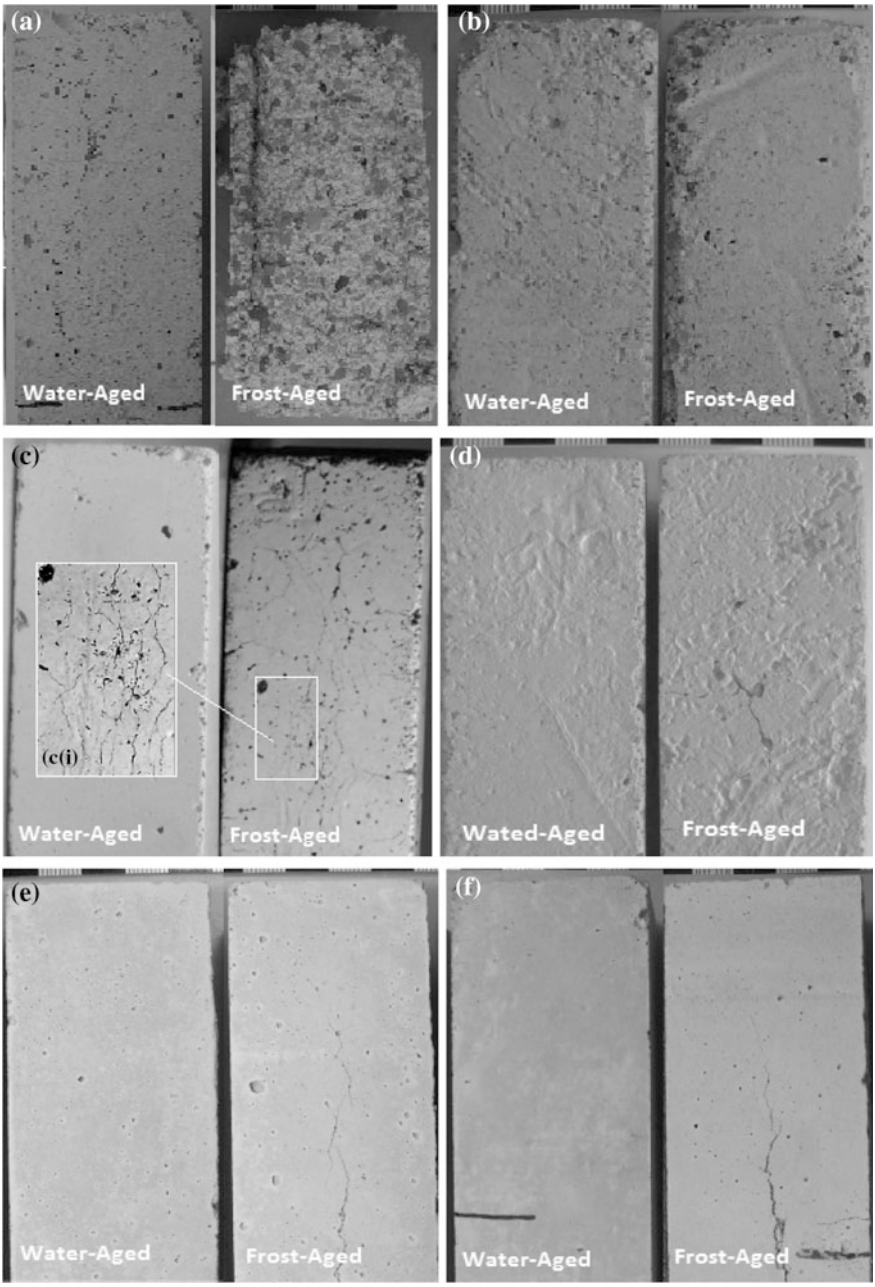

Fig. 3 Aspect of specimens after the frost ageing test: **a** L after 1 cycle; **b** LO after 10 cycles; **c** LM after 10 cycles; **c.i** detail of LM; **d** LMO after 20 cycles; **e** NHL3.5 after 10 cycles; **f** NHL5 after 10 cycles; **g** CL1 after 10 cycles; **h** CL2 after 20 cycles; **h.i** detail of CL2 (scale above the specimens shows 1 mm intervals)

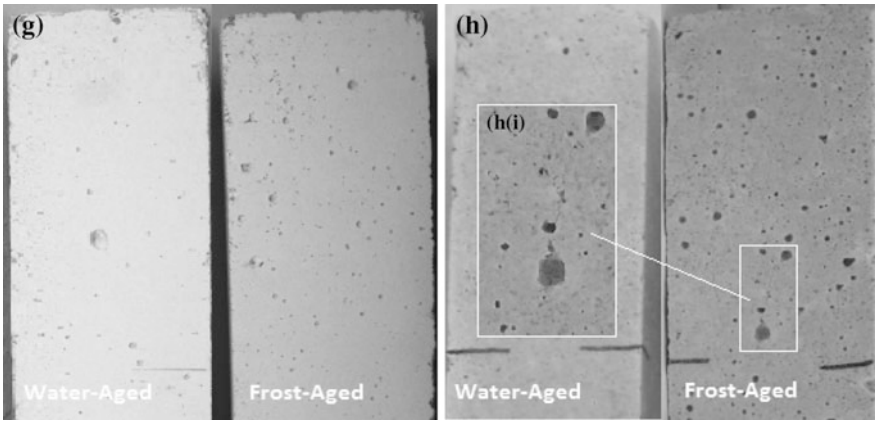

Fig. 3 (continued)

reference-not aged specimens. According to the Czech standard (ČSN 72 2452 1968) the mortar may be classified as frost-resistant when the loss of flexural strength after ageing is not higher than 25%. Frost resistance coefficient calculated as the ratio between Frost-Aged and Not-Aged indicates only NHL3.5 and CL1 mortars 10 cycles aged and LMO 20 cycles aged as frost-resistant. Regarding frost resistance coefficient determined as the ratio between Frost-Aged and Water-Aged, only LO aged 10 cycles and LMO may be classified as frost-resistant.

The rate of water absorption by capillarity is highest for pure lime mortar (L). Capillarity coefficient increased for all Frost-Aged specimens whilst Water-Aged specimens where the hardening process encompasses hydraulic reactions had their water absorption rate reduced. This phenomenon is also expressed on the flexural strength results and is probably assigned to the improvement of the hydraulic reactions in a wet environment.

4 Conclusions

The frost resistance procedure tested within the present research proved to be too severe for air lime mortar. According to the frost resistance coefficient results, only NHL3.5 and CL1 mortars subjected to 10 cycles and mortars with the addition of linseed oil LO and LMO aged 10 and 20 cycles respectively may be classified as frost resistant. However, taking into account that NHL3.5 showed severe fissuration after ageing the frost resistance coefficient should not be taken as an individual classifying parameter. The higher resistance to freeze-thaw cycles of mortars enriched with linseed oil is apparently assigned to the hydrophobic action granted by the oil whilst physical characteristics such as pore space properties and

Table 4 Mass variation, flexural strength, frost resistance coefficient and water absorption by capillarity of mortar specimens subjected to freeze/thaw ageing cycles (average values of 3 samples ± standard deviation)

Mortar (Nr. of cycles)		Mass variation (%-w)	Flexural strength (MPa)	*K* as the ratio of flexural strength		Water absorption by capillarity (kg m^{-2} $h^{-1/2}$)
				Frost-aged: water-aged	Frost-aged: not-aged	
L	Frost- aged	*	–	–	–	–
	Water-aged	–	–			–
	Not aged	–	0.5 (±0.01)			27.70 (±0.34)
LO (10 cy)	Frost- aged	−1.94 (±0.50)	0.30 (±0.03)	0.94	0.22	4.63 (±0.69)
	Water-aged	−1.99 (±0.37)	0.32 (±0.04)			3.49 (±0.19)
	Not aged	–	1.34 (±0.07)			0.86 (±0.11)
LM (10 cy)	Frost- aged	−0.15 (±0.01)	0.27 (±0.02)	0.13	0.16	16.71 (±1.32)
	Water-aged	−0.06 (±0.00)	2.11 (±0.30)			12.82 (±0.26)
	Not aged	–	1.65 (±0.20)			13.38 (±0.29)
LMO (20 cy)	Frost- aged	−0.35 (± 0.03)	0.95 (±0.26)	0.88	0.75	1.11 (±0.61)
	Water-aged	−0.11 (±0.01)	1.80 (±0.44)			1.15 (±0.21)
	Not aged	–	1.26 ± 0.26			3.36 (±0.08)
NHL3.5 (10 cy)	Frost- aged	−0.04 (±0.03)	0.57 (±0.12)	0.33	0.97	19.33 (±1.02)
	Water-aged	−0.00 (±0.00)	1.71 (±0.23)			13.57 (±0.31)
	Not aged	–	0.55 (±0.15)			16.26 (±0.04)
NHL5 (10 cy)	Frost- aged	−0.04 (±0.01)	0.28 (±0.04)	0.24	0.47	25.46 (±3.21)
	Water-aged	−0.01 (±0.00)	1.19 (±0.21)			17.24 (±0.75)
	Not aged	–	0.60 (±0.03)			19.08 (±0.88)
CL1 (10 cy)	Frost- aged	−0.10 (±0.02)	1.46 (±0.18)	0.28	0.87	9.13 (±0.26)
	Water-aged	−0.03 (±0.00)	3.34 (±0.34)			6.82 (±0.40)
	Not aged	–	1.47 (±0.45)			9.64 (±1.22)

(continued)

Table 4 (continued)

Mortar (Nr. of cycles)		Mass variation (%-w)	Flexural strength (MPa)	*K* as the ratio of flexural strength		Water absorption by capillarity (kg m^{-2} $h^{-1/2}$)
				Frost-aged: water-aged	Frost-aged: not-aged	
CL2 (20 cy)	Frost- aged	−0.03 (±0.02)	1.60 (±0.65)	0.44	0.38	5.29 (±0.44)
	Water-aged	−0.01 (±0.00)	5.72 (±0.65)			2.39 (±0.08)
	Not aged	–	4.25 (±0.17)			3.99 (±0.11)

Note *Lime specimens were destroyed after the first ageing cycle

mechanical strength may be pointed out as the most important features determining frost resistance of lime-metakaolin, hydraulic lime and cement mortars.

Mortars with hydraulic binders did not reach the expected mechanical strength values which may probably be assigned to the low amount of kneading water and low level of relative humidity during curing. However, these mortars 10–20 freeze-thaw cycles.

Improved durability of all mortar formulas studied was proven but further research will be focused on in situ tests in order to confirm mortar resistance under natural conditions and to ascertain in which situations, according to building characteristics and environmental conditions, its application is suitable.

Acknowledgments This study was supported by the Czech national project of the Ministry of Culture of the Czech Republic NAKI DF11P01OVV008 entitled "High Valuable and Compatible Lime Mortars for Application in the Restoration, Repair and Preventive Maintenance of the Architectural Heritage".

References

Čechová, E., Papayianni, I., & Stefanidou, M. (2010). Properties of lime-based restoration mortars modified by the addition of linseed oil. In J. Válek., C. Groot & J. J. Hughes. (Eds.), *Proceedings of the 2nd Conference on Historic Mortars and RILEM TC 203-RHM final Workshop* (pp. 937–945). Prague: Institute of Theoretical and Applied Mechanics.

ČSN 72 2452. (1968). Testing of frost resistance of mortar.

Czech Hydrometeorologic Institute Average relative humidity data in Prague during the period from April to September 2011 reported on the website of the Czech Hydrometeorologic Institute (retrieved on November 2017): http://portal.chmi.cz/historicka-data/pocasi/mesicni-data.

EN 1015-11. (1999). Methods of test for mortar for masonry: Determination of flexural and compressive strength of hardened mortar.

EN 1925. (1999). Natural stone test methods. Determination of water absorption coefficient by capillarity.

EN 1015-18. (2002). Methods of test for mortar for masonry. Determination of water absorption coefficient due to capillary action of hardened mortar.

EN 1936. (2007). Natural stone test methods. Determination of real density and apparent density, and of total and open porosity.

Fortes-Revilla, C., Martínez-Ramírez, S., & Teresa Blanco-Varela. (2006). Modelling of slaked lime-metakaolin mortar engineering characteristics in terms of process variables. *Cement and Concrete Composites, 28*, 458–467.

Gameiro, A., Santos Silva, A., Veiga, R., & Velosa, A. (2012). Hydration products of lime–metakaolin pastes at ambient temperature with ageing. *Thermochimica Acta, 535,* 36–41.

Gulotta, D., Goidanich, S., Tedeschi, C., Nijland, T. G., & Toniolo, L. (2013). Commercial NHL-containing mortars for the preservation of historical architecture. Part 1: Compositional and mechanical characterisation. *Construction and Building Materials, 38,* 31–42.

Hanley, R., & Pavia, S. (2008). A study of the workability of natural hydraulic lime mortars and its influence on strength. *Materials and Structures, 41,* 373–381.

ICCROM. (1999). Water absorption by total immersion, conservation of architectural heritage, historic structures and materials, laboratory handbook. Rome, ATEL Sp.A, 12–14.

Izaguirre, A., Lanas, J., & Álvarez, J. I. (2010). Ageing of lime mortars with admixtures: Durability and strength assessment. *Cement and Concrete Research, 40,* 1081–1095.

Mosquera, M. J., Silva, T. B., Prieto, B., & Ruiz-Herrera, E. (2006). Addition of cement to lime-based mortars: Effect on pore structure and vapor transport. *Cement and Concrete Research, 36,* 1635–1642.

Nunes, C., Slížková, Z., Křivánková, D., & Frankeová, D. (2012). Effect of linseed oil on the mechanical properties of lime mortars. In *Proceedings of the engineering mechanics conference* (pp. 955–967). Prague: Institute of Theoretical and Applied Mechanics.

RILEM II. 1 Air permeability. RILEM 25-PEM. (1980). Recommandations provisoires. Essais recommandés pour mesurer l'altération des pierres et évaluer l'efficacité des méthodes de traitement, Matériaux et Construction. 13, Nr. 75, 197–199.

Rovnaníková, P. (2001). Vápenné omítky a pucolánovými přísadami. Proc. Sanace a rekonstrukce staveb 2001, 118–123.

Slížková, Z. (2009). Charakteristiky malt modifikovaných metakaolinem aplikovaných na historických objektech. Proc. Seminář Metakaolin 2009, Brno, Fakulta stavební VUT v Brně, 146–155.

Válek, J., Slížková, Z., & Zeman, A. (2007). Mechanické a fyzikální zkoušky vápenných malt přídavkem metakaolinu a jejich vhodnost pro opravy památkově chráněných objektů, Proc. Seminář Metakaolin 2007, Brno, Fakulta stavební VUT v Brně, 121–129.

Veiga, R. (2003). *As Argamassas na Conservação, Actas das Primeiras Jornadas de Engenharia Civil da Universidade de Aveiro, COM 103* (pp. 1–2). Lisbon: LNEC.

Vejmelková, E., Keppert, M., Rovnaníkova, P., Keršner, Z., & Černý, R. (2011). Properties of lime composites containing a new type of pozzolana for the improvement of strength and durability. *Composites: Part B: Engineering, 43,* 3534–3540.

Vejmelková, E., Keppert, M., Keršner, Z., Rovnaníková, P., & Černý, R. (2012). Mechanical, fracture-mechanical, hydric, thermal, and durability properties of lime–metakaolin plaster for renovation of historic buildings. *Construction and Building Materials, 31,* 22–28.

WTA 2-7-01/ D. (2007). Lime-based plaster for architectural heritage. ISBN: 978-80-02-01986-2.

Compatibility Assessment for Repair Mortars: An Optimized Cement-Based Mix for Tuffeau de Lincent

A. Isebaert, L. Van Parys, V. Cnudde, T. De Kock and J. M. Baele

Abstract Mortars developed for the reconstitution and 'plastic repair' of natural stones have become increasingly popular. They are an alternative for the replacement of deteriorated stones, since they are capable of preserving the (memory of) diversity in building materials. This article addresses some key elements for the compatibility between repair mortars and stones. This research accordingly studies the compatibility of a repointing mortar designed for the Tuffeau de Lincent (Belgium), a friable stone in need for restoration and replacement, which was developed using an auto-formulation tool, based on strength and colour compatibility. The selected repointing mortar was further tested in order to assess its use as plastic repair mortar for the Tuffeau de Lincent stone. The developed mortar was considered compatible in colour with the stone and had a strength of 14 MPa, which falls within the strength range of the stone (8–18 MPa). However, porosity and pore size distribution measurements indicated that the stone and the mortar were different. This study compares the first product of the prototype formulation tool and lays the foundations for a more expanded and larger auto-formulation tool for the repair of natural stone.

A. Isebaert (✉) · L. Van Parys
Civil Engineering Department, Faculty of Engineering,
University of Mons, Mons, Belgium
e-mail: aurelie.isebaert@gmail.com

L. Van Parys
e-mail: laurent.vanparys@umons.ac.be

V. Cnudde · T. De Kock
Geology Department—PProGRess-UGCT, Faculty of Sciences,
Ghent University, Ghent, Belgium
e-mail: veerle.cnudde@ugent.be

T. De Kock
e-mail: tim.dekock@ugent.be

J. M. Baele
Applied Geology Department, Faculty of Engineering,
University of Mons, Mons, Belgium
e-mail: jean-marc.baele@umons.ac.be

J. J. Hughes et al. (eds.), *Historic Mortars*,
https://doi.org/10.1007/978-3-319-91606-4_13

Keywords Repair mortar · Compatibility · Colour · Strength · Pore connectivity

1 Introduction

Building stones weather due to a combination of processes (Přikryl and Smith 2007; Kourkoulis et al. 2006; Amoroso and Fassina 1983). Since many of these processes interact with one another, the alteration pattern can be very complex and can evolve through time (De Kock et al. 2012; Papida et al. 2000). Stone degradation can have an extrinsic or intrinsic origin. Extrinsic degradation causes derive from the environment of the stone, such as the climate, the location of the stone blocks in the building, or water penetrating the stone (André et al. 2012). In addition to these natural causes, atmospheric pollution and other anthropogenic factors also play a role in the degradation of stones.

However, the stone's intrinsic characteristics also influence its alteration (Warscheid and Braams 2000; Amoroso and Fassina 1983). To start with, stones will always be in a certain physico-chemical disequilibrium once they leave their original environment in the earth's crust (Amoroso and Fassina 1983). Secondly, stones are also spatially variable and heterogeneous, and thus will alter heterogeneously as well (Graue et al. 2012). Furthermore, the orientation of the rock fabric and the surface roughness also play a role in the deterioration of the stone.

To restore weathered and deteriorated building stone, several interventions are possible. When filling in missing parts of stone, surface repair mortars can be used. Surface repair mortars allow the preservation of as much of the original stone as possible. This is an important advantage in the conservation of built heritage, because it allows the preservation of the stone's integrity and the construction's authenticity. Otherwise, the stone will be replaced by an alternative stone if the original stone is no longer available. Another advantage of surface repair mortar is that it can be adapted to the condition of the weathered stone present in the building, for example, the colour of the mortar can be adapted to the weathered stone's colour.

2 State of the Art of Plastic Repair of Stone

The greatest difficulty in designing a repair mortar is that this mortar should imitate and behave like a material that is in se heterogeneous and spatially variable. Moreover, the properties of this heterogeneous material differ from stone type to stone type, and from building to building, depending on variable extrinsic factors. When looking at the principles of the Venice Charter and the Nara Document of the International Council of Monuments and Sites (ICOMOS 1964, 1994), a repair mortar should be durable and adherent enough to last a long time alongside the original stone. The repair mortar, as any other restoration material, should not

accelerate the decay in any way nor introduce harmful materials into the stone. Therefore, a repair mortar should not only be ideal in its initial state, but also during its weathering: it should be durable enough, whilst self-sacrificing in the long run.

In the literature, the following properties are most commonly considered to be important when developing a stone repair mortar: colour, strength, porosity and permeability.

1. *Appearance*

Colour and surface roughness are considered important indicators for the compatibility of a repair mortar, because they affect the visual aspect. Since they are visible properties, they can and will be judged by professionals, visitors etc. Designing a mortar with the right colour and nuances is a significant problem, even more so when taking into account the possible chromatic alterations in the stone and in the mortar in the long run.

2. *Chemical aspects*

Several mortar types can induce or attract minerals and liquids that influence the deterioration of the stone. For instance, they can contain salts (e.g. sulphates), which crystallize, leading to efflorescence or subflorescence (Hayen 2010; O'Brien et al. 1995). The presence of organic polymers can also be a source for a more rapid deterioration of the stone: they speed up the biological colonisation of the stone, since biological organisms feed on these polymers (Warscheid and Braams 2000).

3. *Physical and mechanical aspects*

Next to the chemical composition, the physical and mechanical aspects determine the 'intrinsic' durability of the mortar, as well as its influence on the durability of the original stone. This has three aspects:

(a) *Water transfer properties*: Water plays an important role in the deterioration process as it can make the material crack due to crystallization of ice (freezing) or by transporting salts that crystallise through evaporation of water. It catalyses the growth of biological organisms, and it erodes and dissolves material. Consequently, the water transfer properties of a mortar are important. Preferably, the water transfer capacity of the mortar should be equal or higher than the stone in order to avoid deterioration of the stone due to water trapping. Therefore, not only chemical, but also physical compatibility has to be investigated (Dewanckele et al. 2012; André et al. 2012; Beck et al. 2003). André et al. (2012) reported a case study where the original stone surface receded 100 times faster in the restored zones, repaired with cement mortar compared to other zones with a different replacement stone. The repairs with cement mortar led to water retention in the original stone, leading to granular disintegration and alveolisation.
(b) *Modulus of elasticity*: An indication of the mechanical response to stress in various modes (e.g. compression, flexural) can be derived from the modulus of elasticity. This property is significant when the repair mortar is used for filling in large or structural parts of stones and its importance depends on the shape of the

repair and the way it fits into the whole (Hayen 2010). In all these cases, the rigidity of the material plays an important role. Deterioration such as loss or cracks can occur to both the repair mortar and to the stone if this mortar property is not adapted to the stone.
(c) *Thermal response*: High temperature differences on walls exposed to the sun cause the minerals in stones to expand and contract. Consequent expansion/contraction cycles will cause internal stress. The difference in expansion between a stone and its repair mortar can lead to detachment, deformation or cracking of either the mortar or the stone (Hayen 2010).

Other compatibility aspects include the mineralogical composition and the weathering behaviour of both the mortar and the stone. Conclusively, when designing a repair mortar, the properties must be compatible so that the stone is not damaged and will only benefit from the use of the repair mortar.

Currently, there are three possible approaches to design repair mortars for natural stone. The first utilises commercial mixtures, looking for an acceptable repair mortar that meets the required standards (Torney et al. 2012; Steenmeijer 2010; Bromblet 2005; Marie-Victoire 1999). Sometimes, the mixture is adjusted: the binder-aggregate ratio (B/A ratio) is altered, or additives are mixed into the product (Szemerey-Kiss and Török 2011; Blauer 2010). The second approach, involves the design of a repair mortar for rarely used building stones that do not have commercial mixes available. The goal of this second bottom-up approach is to build up a mortar from scratch, in order to obtain a composition that lies as close as possible to that of the stone (Stefanis and Theoulakis 2010; Beck et al. 2008; Bromblet 2000). These two approaches create highly specialised end products, and need a large amount of time and money. A third, more recent approach is to create a system that can be applied for more than one stone and his suitable repair mortar. It starts from the raw mortar components such as sand and binder and attempts to find links and relations between the mortar components' properties and the mortar properties. Ramge and Kühne (2012) for example, created a modular system, and applied it for a specific stone, using a limited number of sands and binders.

3 Case-Study: A Repair Mortar for the Tuffeau de Lincent

3.1 Repair Mortar Design: Auto-Formulation Tool

The researchers aimed to find another means to develop a repointing mortar, by using a prototype of an auto-formulation tool developed at the University of Mons (Van Parys et al. 2013; Léoskool et al. 2012a). The tool manages simultaneously two objectives, strength and colour. The operator introduced the strength and colour the mortar ideally should have, and the tool, using a database from aggregates and binders, generated accordingly several possible matching repair recipes. The tool

was able to do this using an optimisation (genetic) algorithm, the Elitist Non-Dominated Sorting Genetic Algorithm (NSGA-II). The NSGA II has frequently been used for multi-objective engineering problems: it creates first a 'population' of various mortar recipes at random, and verifies every one of the mortar recipes with the desired properties using (empirical) estimation methods. By selecting every time the best individuals from the population, it is able to create new and better individuals. In order to know which elements of a mortar recipe influence which property, the algorithm had to be 'nourished' with estimation functions for both colour and resistance (Van Parys et al. 2013; Léoskool et al. 2012a). Simple and frequently used mortar components were introduced in the tool's database, such as sand and cement. Other binders than cement were considered, but cement was the only binder type for which mortar formulation laws were already known and developed. The introduction of more complex materials such as air entrainers or pigments was avoided, in order to keep the recipe easily adjustable and comprehensible.

This tool was first tested for the repointing mortar development for the St Christopher's Church at Racour, Belgium. The church comprises two parts: (1) the tower and (2) the nave and choir. The 14th-century tower is constructed with Gobertange limestone (Belgium), and Tienen quartzite (Belgium). The nave and choir from the 15th century were built with Tuffeau de Lincent (Belgium). In 2011, a project to restore the Tuffeau de Lincent ashlars began. The stone had to be replaced and joints repointed (Dagrain 2011) (Fig. 1a, b). In the following sections the compatibility of this mortar is investigated to verify if the tool would also be adequate for the development of plastic repair mortar for the stone itself.

In order to know which colour and strength the mortar ideally should have, these properties first had to be determined on the stone. Colour measurements were

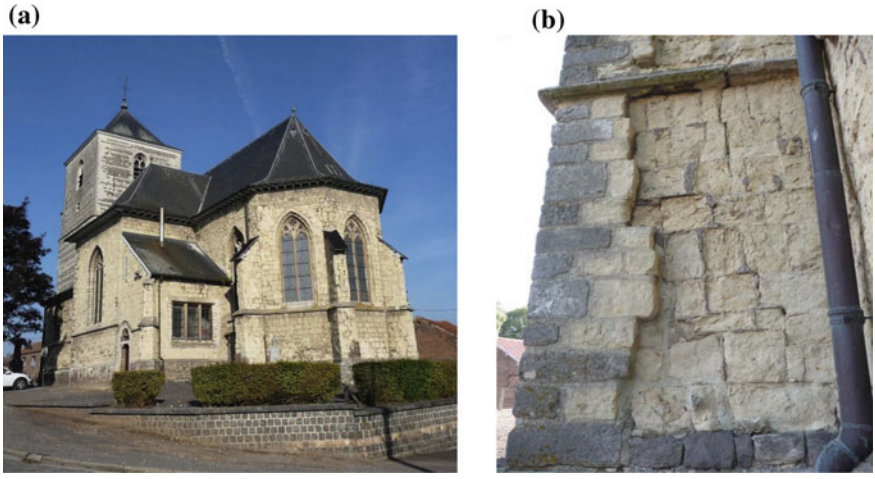

Fig. 1 **a** St Christopher's Church. View of nave and choir built with tuffeau. **b** Weathered Tuffeau de Lincent at the St Christopher's Church in Racour

performed on Tuffeau de Lincent with a luxmeter-chromameter (Konica Minolta C200) in a dark room, with a TL Philips TLD (605 K) as incident light source, a method according to Léoskool et al. (2012a). The CIE Y*x*y*-values were introduced in the formulation tool. Resistance values obtained through a translational cutting test developed at the University of Mons (Belgium) were introduced as well. In this test, a rectangular PDC cutter of a fixed width makes a deep groove of a certain depth, by removing consecutively thin material layers from the surface. The resistance the cutter encounters in making this groove denotes the intrinsic specific energy of each material, which is independent of any side effects such as the bit wearing off, and it represents the resistance of the stone on a local scale (Léoskool et al. 2012b; Van Parys and Dagrain 2006; Dagrain 2001). In addition, the mortar and stone were also tested on their compressive strength according to EN 1015-11. For this purpose, the stone was cut into cubes of 40 mm^3.

The second step was to nourish the database of the tool with sands and binders. The database of the tool was comprised of white cement II 42.5 N, yellow sand (D_{50} = 0.25 mm), Rhine sand (D_{50} = 0.3 mm) and green sand (D_{50} = 0.2 mm). White cement was chosen here because colour variations between several batches can be considered negligible due to the white cement's quality controls.

3.2 *Description of the Stone*

Tuffeau de Lincent is a soft calcarenite with an opal cement and dispersed microcrystalline calcite (micrite) (Fig. 2a–c). It dates from a marine period in the late Paleocene (Cenozoic) and was quarried in the Gete basin, in a region between Brussels and Liege in Belgium. Tuffeau de Lincent has a homogeneous light greyish yellow colour. There are zones richer in opal cement, and others richer in micrite. Sparite, associated with fossils, was also detected, although not abundant. Diverse fossil bioclasts such as bivalves, foraminifera and sponge spicules are found. The spicules are sometimes casts, creating large voids. In other cases, the opal skeleton is still (partially) present. Glauconite is present in both fresh and weathered state, as grains, and within fossils. Angular quartz grains are detected. Iron oxides from secondary origin were found in the voids of a sponge. Pyrite and rare feldspar minerals were also detected. Cathodoluminescence images also highlighted the presence of aragonite, with its typical green luminescence. This description largely agrees with the stone's mineralogical description in literature (Dusar et al. 2009; Macar et al. 1947).

Tuffeau de Lincent was used locally, in buildings dating from the Romanesque and Gothic period. Afterwards, it was preferentially used for the construction of ordinary vernacular buildings. The stone is not susceptible to sulphur dioxide attack; therefore gypsum crusts are rare (De Geyter 1991). The stone is, however, highly susceptible to freeze-thaw cycles, leading to delamination and disintegration of the stone. Therefore, replacement is, most of the time, the only repair option.

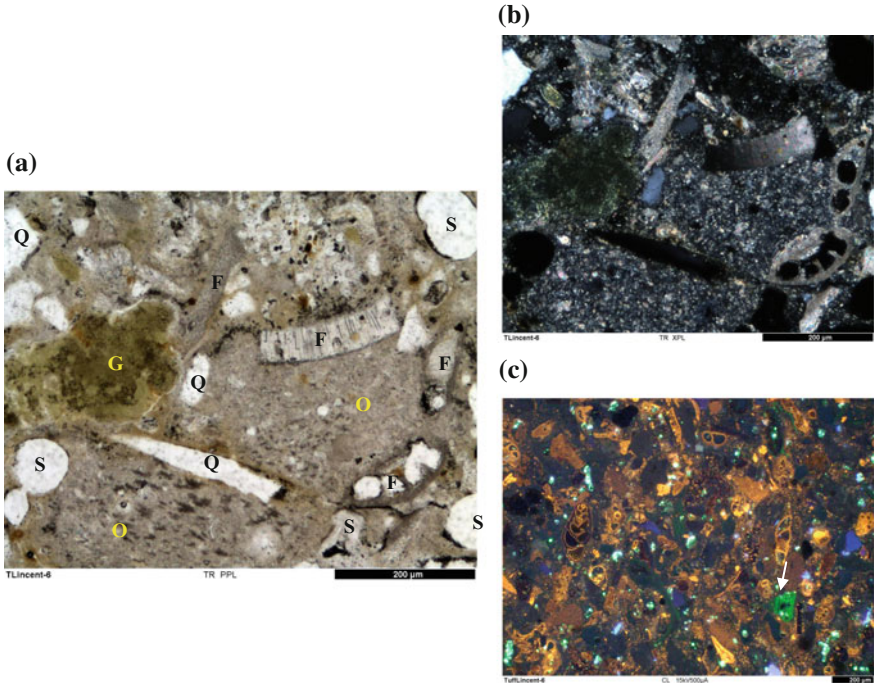

Fig. 2 **a**–**c** Microscopic images of Tuffeau de Lincent at the St Christopher's Church in Racour. **a** Image in plane polarised light. F: fossils (bioclasts); Q: quartz; S: sponge spicule; G: glauconite; O: opal (with scatterred micrite) groundmass. **b** Corresponding image in crossed polarised light. **c** Image in cathodoluminescence. Calcite is brown to yellow, feldspar is bright blue, quartz is dark blue, and aragonite is green (arrow). Other components are weakly or non-luminescing and appear dark. Very bright greenish spots are artifacts. The black scale in the right bottom corner is 200 µm (color figure online)

3.3 Possible Replacement Stones

Previously, Tuffeau de Lincent was replaced by freshly quarried tuffeau, or stones from a demolished building were re-used. However, this was not always possible and it certainly became very difficult when the last quarry closed in the second half of the 20th century (De Geyter 1991). Nowadays, the old quarries cannot be reopened again, nor deliver stone blocks of good quality. Replacements were and are still made with the French Savonnières limestone and the local Maastrichter limestone (Dagrain 2011; Dusar et al. 2009). However, they are just a second best alternative for Tuffeau de Lincent, in terms of compatibility. Maastrichter stone has a much lower strength than Tuffeau de Lincent, while Savonnières stone has a lower porosity and a very high dynamic elastic modulus in comparison with Tuffeau de Lincent (Fig. 3). Dagrain (2011) explored the possibilities for other replacement stones (Table 1). The Richemont limestone from the Upper Cretaceous of Poitou-Charentes (France) accorded best with Tuffeau de Lincent, in terms of

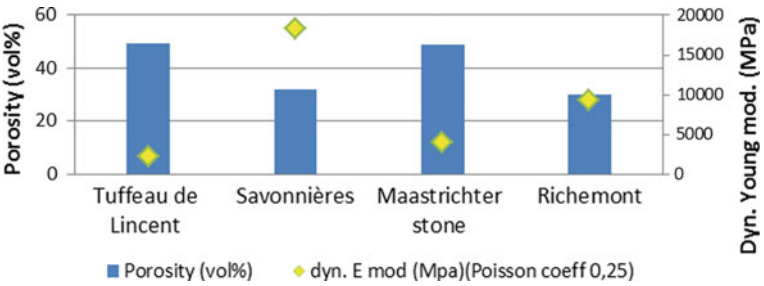

Fig. 3 Porosity and elastic dynamic modulus values for Tuffeau de Lincent and replacement stones after Dagrain (2011)

Table 1 Properties of the Tuffeau de Lincent stone and possible replacement stones

Stone	Density (kg/m^3)	Total porosity (%)	Local strength (MPa)	Compressive strength (MPa)*	Young's modulus (MPa) (Poisson c. 0.25)	Sound Propagation velocity (m/s) *
Tuffeau de Lincent	1180	55	15.1	6	2233	1481–1792
Savonnières	1850	32.1	18.3	14.4	18,328	3389
Maastrichter stone	1313	52.4	2.2	2.1–4.6	3952	1277–1868
Richemont	1897	30.1	13.2	24	9227	2416

Values were taken from Dagrain (2011), apart from properties with (*), where values are also from Dusar et al. (2009), Platroz (2006) and Cnudde (2005)

resistance, dynamic modulus of elasticity, and availability. Therefore, this stone was chosen as replacement stone for the St Christopher's Church in Racour.

The next step was the development of a suitable repair mortar for the repointing of the stone ashlars.

Mortar samples were made based on the recipe provided by the auto-formulation tool. The tool suggested using a mortar made with 44.2 wt% of white cement, 21.06 wt% of yellow sand, 5.75 wt% of green sand, and 29 wt% of water. This large amount of water had to compensate for the white cement's normal resistance, in order to give a final mortar strength in the range of the stone. After 28 days of curing, the samples were tested for their colour and resistance and compared with the values from the stone samples. The stone had following colour values (Y,x,y): 0.58; 0.3378; 0.3625 and the mortar samples had following colour values: 0.65; 0.3353; 0.3558. This colour difference is not distinguishable to the human eye according to Trouvé (1991); in L*a*b*, this would give a colour difference (ΔE*) of 3.12 (Fig. 4).

Fig. 4 Comparison between the original Tuffeau de Lincent in the middle and the mortar from the auto-formulation tool on the right

The stone displayed a large variation in local strength (±8.5–18.8 MPa). The mortar showed a homogeneous local strength pattern that is compatible with the stone values (±14 MPa). The difference of the average local strength in the mortar was about 3%. Compressive strength tests performed according to EN 1015-11 indicated a compressive strength of the stone of 12.45 (±0.82) MPa, while the mortar had a compressive strength at 28 days of curing of 8.98 (±0.47) MPa.

In addition, the mortar was investigated by optical microscopy (Fig. 5). The mortar was not designed for mineralogical compatibility with the stone, and it is therefore no surprise to see a very different mineralogical composition between stone and mortar. The images also show a different fluid flow might be expected between the two, since their pore network is very different. Next to the hydrate gel matrix, the mortar consisted of many angular quartz grains and some rare glauconite grains, and rare fossils. The latter two originate both from the sands used. On some of the quartz grains, iron oxide coating was present, and was therefore thought to be from the yellow sand used in the mix. The matrix is heterogeneous in colour since some zones are more carbonated than others.

In order to know more about the general chemical similarity between mortar and stone, an Electron Probe Micro-Analyser (EPMA, model SX50) was used for mapping Si, Al and Ca by Wavelength Dispersive Spectroscopy. The thin sections were coated with a thin carbon layer. The mapped area was about 1 mm^2, the beam size was 2 μm, the beam conditions were 15 kV acceleration voltage and 20 nA

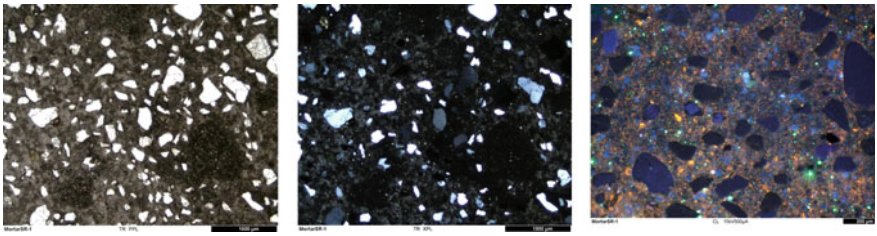

Fig. 5 Optical microscope images of the mortar prism in plane polarised light (left), crossed polarised light (middle) and cathodoluminescent (right). The scale in the right bottom is 1000 µm for the left and middle images and 200 µm for the right image. Angular and rounded quartz grains can be detected in the partially calcitized mortar matrix

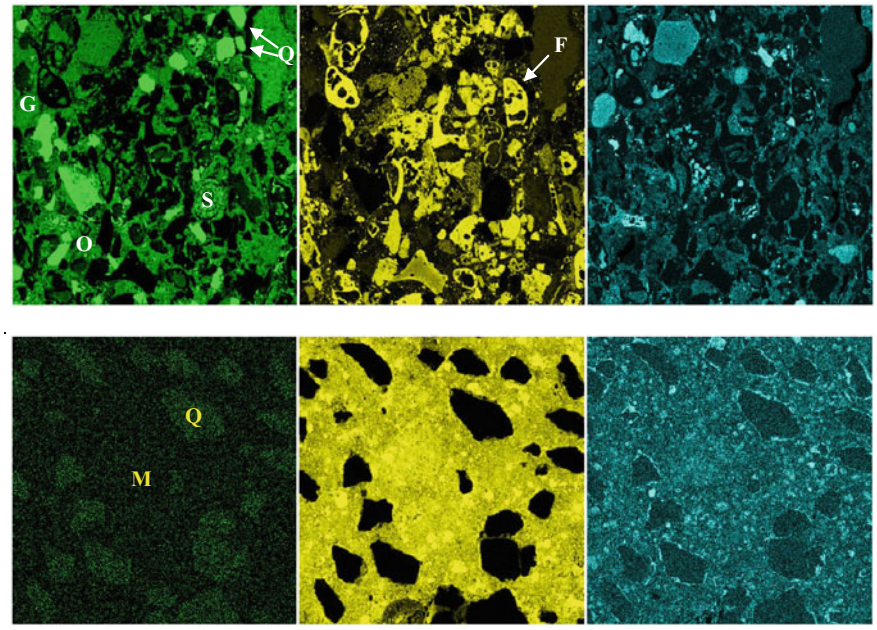

Fig. 6 Electron microprobe (EPMA) maps of the Tuffeau de Lincent stone (upper) and the mortar (lower) showing the distribution of Si (green), Ca (yellow) and Al (blue). F: fossils (bioclasts); Q: quartz; S: sponge spicule; G: glauconite; O: opal groundmass; M: matrix. The size of the maps is approximately 1 mm^2. The less contrasted lower Si and Al images result from a shorter integration time (e.g. the quartz grains in the lower Si image should appear as bright as in the upper image) (color figure online)

beam current (Fig. 6a, b). The stone's opal cement (groundmass) is clearly visible in EPMA maps, lighting up clearly for Si and also a little for Al, and here and there, some Ca is also detected. The mortar's matrix consists of two distinct Ca concentrations. Smaller grains that are bright in the Ca map likely correspond to portlandite

and/or calcite (calcite as small grains is detected under cathodoluminescence: cf. Fig. 5). The remainder of the matrix could correspond to carbonated ettringite and C–S–H in the brighter (Ca-rich) and darker (Ca-poor) areas, respectively. The Al map shows the presence of possible C–A–H grains and coatings in the matrix.

For the actual repointing of the stone ashlar, the mortar used was based on the mortar recipe proposed by the auto formulation tool, but it was slightly adjusted: the white cement was replaced by natural hydraulic lime (NHL 3,5). The original recipe proposed by the tool also comprised a large amount of water, in order to compensate for the high resistance of the cement. Since NHL 3,5 has a lower resistance than white cement, the amount of water was decreased, and a workable mortar could be made for the repointing of the Tuffeau de Lincent ashlars.

3.4 A Possible Repair Mortar for the Stone?

This study examined whether this repair mortar could also be used as a plastic repair mortar for Tuffeau de Lincent. Next to the colour and mechanical properties, the water (vapour) transfer of the mortar and the stone is also a key factor in the compatibility. Therefore, several complementary tests which all indicate in lesser or greater extent this key factor, were performed on Tuffeau de Lincent and the mortar.

Porosity, volume and density were measured with two pycnometers, the Helium pycnometer Accupyc II 1340 and the envelope pycnometer Geopyc 1360 (Micromeritics). The repair mortar had a porosity of about 34.2%, and a density of 1550 kg/m^3. It contains fewer pores and is therefore denser as well.

Additionally, a steady state nitrogen gas permeameter GPL30 (Vinci Technologies) was used to determine the permeability. Through Darcy's Law, the permeability of the nitrogen gas through the Tuffeau de Lincent could be set on 16.85 mD. The repair mortar's permeability on the other hand, was below the detection limit of 1 mD. Since porosity tests with Helium gas pycnometers indicated a porosity of about 30%, it is suspected that the nitrogen gas is too dense to be able to penetrate the smallest pores of the mortar that connect the larger pores.

X-ray micro-computed tomography (micro-CT) (Cnudde and Boone 2013) has already proven its use in the research of stone and their weathering patterns (De Kock et al. 2017; Dewanckele et al. 2012; Cnudde et al. 2011). Samples (height 4 mm) of Tuffeau de Lincent stone and of the mortar were scanned with a micro-CT scanner at the Centre for X-ray Tomography, of Ghent University (Masschaele et al. 2007). The obtained images had a voxel resolution just below 5 μm and were analyzed with the in-house developed software Morpho+ (Brabant et al. 2011).

As could be expected, the pore size distribution of the natural stone is different than that of the repair mortar. The numbers of pores detected in both materials differ largely. Figure 7 visualizes in 3D the results of the micro-CT scans. The tuffeau contains more than ten times the number of pores of the mortar (17494 vs. 1267 counts) in the size range above the resolution. Tuffeau de Lincent has a very variable pore size distribution, with many small sphere-like pores and a number of

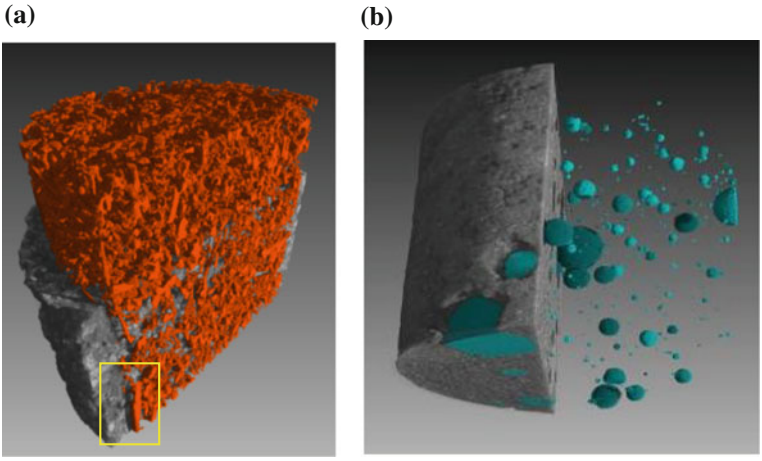

Fig. 7 3D-renderings of the 4 mm-sized stone and mortar samples. **a** The stone (grey) with pores connected to the exterior marked in orange. Note the flat-shaped pores from dissolved spiculae (yellow frame). **b** the pores (blue) in the mortar sample (grey). Note the sphericity of the pores and their closed character (color figure online)

very large flat-shaped pores. 80% of the pores have a maximum opening (m.o.) between 10.16 and 30 µm, i.e. the maximum circle diameter that fits into these pores. Looking at the equivalent diameter (e.d.), which is a way of expressing the volume of the pore, pores between 10.16 and 295 µm were detected. Combining both elements indicates that the larger pores are flat-shaped, and are most likely the dissolved spiculae in the stone. There are also numerous small, sphere-like pores, which do not seem to be connected with the exterior.

On the other hand, the pores of the mortar are much larger than those of the stone, going up to 670 µm e.d. in comparison to the 295 µm e.d. from Tuffeau de Lincent. Most of the pores of the mortar have an equivalent diameter between 0 and 100 µm.

Conclusively, the mortar has fewer pores, which are reasonably sphere-like. There are also some very large pores that take up a lot of volume. The mortar has a much less varied pore structure than the stone.

Mercury porosimetry was performed with an Autopore III 9410 (Micromeritics) to evaluate the pores in the range of 0.02 to approximately 100 µm, pores that are undistinguishable with micro-CT. The mortar has many pores in the region of 0.10–0.55 µm, while the stone has a well-dispersed curve starting from 0.06 µm (Fig. 8). The well-dispersed curve might be interpreted as a good pore connectivity, certainly in the range 5–80 µm, where pores in this range make out more than 10 vol.% of the absolute porosity. This pore range is not present in the mortar. The mortar clearly contains pores larger than 80 µm, but the pores are clearly connected by the pores smaller than 5 µm. Some ink-bottle effects might be expected here, but this could not be validated since there was no extrusion curve available. According to

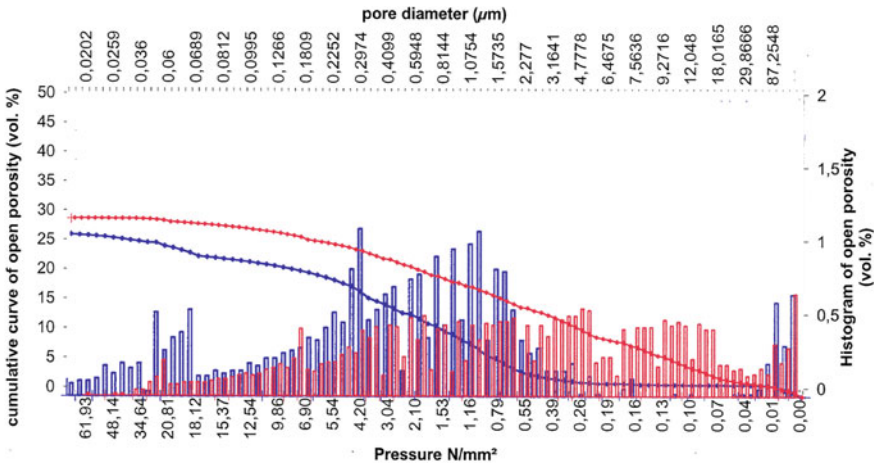

Fig. 8 Pore diameter histogram and cumulative curve of open porosity of the stone (red) and the mortar (blue) (color figure online)

mercury porosimetry, the stone has an open porosity of 30.1%, and the mortar an open porosity of 26.8%. After taking into account the threshold intrusion problems of the mortar that occur in ink-bottle pores of cement-based pastes (Diamond 2000), it is more likely that the micro-CT technique is closer to the actual pore structure of the mortar. The difference between mortar and stone in terms of pore network and possible fluid flow is clearly demonstrated. Future formulations for repair mortar should therefore certainly include other binders than cement.

4 Conclusion

Tuffeau de Lincent is a locally used stone, with susceptibility for frost damage. The damage is due to a combination of extrinsic factors (freeze-thaw cycles) and intrinsic factors (the small maximum pore openings available for the expansion of water crystals). This, in combination with the low strength, makes the stone even more friable.

There were until recently several approaches for the design of repair mortars, which all tested the possible repair mortar through trial-and-error for appearance, chemical effects and physico-mechanical aspects. However, a general methodology leaving room for specific demands was still missing. In this frame, the auto-formulation tool was developed. The first prototype of this tool which contained only colour and strength as objective, gave acceptable results. Both colour and strength of the mortar agree more or less well with the stone. In terms of pore connectivity and pore sizes however, the mortar was not compatible with the stone. The pores in the mortar were only connected through very small pores or are closed

pores, which made the mortar nearly impermeable for water transport, and would increase the water retention in the already friable stone. The mortar used on-site was therefore also adapted to a lime-based mortar.

A mortar with a higher porosity and a better water (vapour) diffusion than the original stone should increase the lifetime expectancy of the stone. The auto-formulation tool was therefore improved and expanded later on, so that the tool is now developed to create mortars compatible in terms of elasticity, colour, and permeability with lime binders. The tool's mixing laws and empirical estimation methods were adapted so that it also allows the use of hydraulic limes as binder (Isebaert 2016).

Acknowledgements The authors would like to thank Jean-Christophe Scaillet from the Walloon government for the access on site, and Hughes Legrain from the 'Construction' Laboratory at EMRA for his support concerning the mercury porosimetry tests and Pieter Vandernieppen for his help with the micro-CT scans. Many thanks are also due to Fabrice Dagrain, Patrick Masson and Michael Baele for their assistance in the laboratory.

References

Amoroso, G., & Fassina, V. (1983). *Materials science monographs 11. Stone decay and conservation*. Elsevier. ISBN 0-444-42146-7.

André, M. F., et al. (2012). Quantitative assessment of post-restoration accelerated stone decay due to compatibility problems (St Sebastian's abbey church, Manglieu, French Massif Central). In *Manuscripts 12th International Congress Deterioration and Conservation of Stone*, NY, USA. http://hpef.us/conferences/stone-conference/manuscripts.

Beck, K., et al. (2003). Characterization, water transfer properties and deterioration in tuffeau: building material in the Loire valley-France. *Building and Environment, 38*(9–10), 1151–1162.

Beck, K., et al. (2008). Critères de compatibilité entre des mortiers à base de chaux et des pierres calcaires a forte porosité (tuffeaux blancs), Actes des 25^{e} Rencontres de l'AUGC, Bordeaux, France. http://www.iut.u-bordeaux1.fr/gc/augc07/index/Keyword/POROSITE.html.

Blauer, C., et al. (2010). Repair mortars for the sandstones of the cathedral of Berne. In Valek, J., Groot, C., & Hughes, J. J. (Eds.), *Proceedings HMC10 and RILEM TC 203-RHM FW* (pp. 909–916), Prague. http://www.rilem.org/gene/main.php?base=05&id_publication=82.

Brabant, L., et al. (2011). Three-dimensional analysis of high-resolution X-ray computed tomography data with Morpho+. *Micropscopy and Microanalysis, 17*(2), 252–263.

Bromblet, P. (2000). Evaluation of the durability and compatibility of traditional repair lime-based mortars on three limestones. *International Zeitschrift Bauinstandsetzen & Baudenkmalpflege, 6* (5), 513–528.

Bromblet P., et al. (2005). Approach for compatible mortars for restoration purposes: Stone repairs of the roman amphitheatre of Arles (France). In Groot, C. (Ed.), *Proceedings of International RILEM Workshop on Repair Mortars for Historic Masonry* (pp. 73–81). http://www.rilem.org/gene/main.php?base=05&id_publication=71.

Cnudde, V., & Boone, M. (2013). High-resolution X-ray computed tomography in geosciences: A review of the current technology and applications. *Earth-Science Reviews, 123,* 1–17.

Cnudde, V., et al. (2011). 3D characterization of sandstone by means of X-ray CT. *Geosphere, 7* (1), 54–61.

Cnudde, V. (2005). Exploring the potential of X-ray tomography as a new non-destructive research tool in conservation studies of natural building stones. Doctoral thesis, Geology Department, Ghent University. http://hdl.handle.net/1854/LU-471111.

Dagrain, F. (2011). Nouvelles techniques de caractérisation de la pierre naturelle dans le cadre de travaux de restauration. *Pierre Actual, 897,* 76–86.

Dagrain, F. (2001). Influence of the cutter geometry in rock cutting: An experimental approach. Master thesis. Civil Engineering Department, University of Minnesota, Minneapolis.

De Geyter, G. (1991). De tuffeau van Lincent en de Maastrichtersteen. *Bulletin van de Belgische vereniging voor Geologie, 99*(2), 177–183.

De Kock, T., et al. (2012). Multi-disciplinary characterization of gypsum crust on Lede stone. In *Manuscripts 12th Internatioinal Congress on the Deterioration & Conservation of Stone*, NY, USA. http://hpef.us/conferences/stone-conference/manuscripts.

De Kock, T., et al. (2017). Laminar gypsum crust on Lede stone: microspatial characterization and laboratory acid weathering. *Talanta, 162,* 193–202.

Dewanckele, J., et al. (2012). 4D imaging and quantification of pore structure modifications inside natural building stones by means of high resolution X-ray CT. *Science of the Total Environment, 416,* 436–448.

Diamond, S. (2000). Mercury porosimetry. An inappropriate method for the measurement of pore size distribution in cement-based materials. *Cement and concrete research, 30,* 1517–1525.

Dusar, R., et al. (2009). *Renovatie en Restauratie: Natuursteen in Vlaanderen* (pp. 395–400). Versteend verleden, Kluwer. ISBN 9789046523674.

Graue, B., et al. (2012). Requirements for replacement stones at the Cologne Cathedral—A systematic approach to general criteria on compatibility. In *Manuscripts 12th International Congress on the Deterioration and Conservation of Stone*, NY, USA. http://hpef.us/conferences/stone-conference/manuscripts.

Hayen, R. (2010). Herstelmortels breed uitgesmeerd. In Proceedings KIK/IRPA Versteend erfgoed—omgaan met herstelmortel en kunststeen. In Hayen, R., De Clercq, H. (Eds.), Brussels, pp. 4–19.

ICOMOS. (1964). *The Venice Charter. International charter for the conservation and restoration of monuments and sites*. http://icomos.org/en/charters-and-texts.

ICOMOS. (1994). *The Nara Document on Authenticity*. http://icomos.org/en/charters-and-texts.

Isebaert A., (2016). *Repair mortars for stone: Increased compatibility through optimised development*. Mons, Belgium: Université de Mons. Faculté Polytechnique ; Ghent, Belgium: Ghent University. Faculty of Sciences.

Kourkoulis, S. K. (Ed.). (2006). *Fracture and failure of natural building stones: Application in the restoration of ancient monuments*. Springer. ISBN 1402050763.

Léoskool, L., et al. (2012a). Compatible mortar for masonry restorations: Discrete optimization for equivalent strength and colour prescription. In *Proceedings ICDS12*, Lisbon, Portugal.

Léoskool, L., et al. (2012b). The recourse to cutting-based tomography for quantifying the surface strengthening of altered stones. In *Proceedings ICDS12*, Lisbon, Portugal.

Marie-Victoire, E., & Bromblet, P. (1999). A new generation of cement-based renderings: An alternative to traditional lime based mortars? In Bartos, P., Groot, C., & Hughes, J. J. (Eds.), *Proceedings in International RILEM Workshop on Historic Mortars: Characteristics and Tests* (371–393). Paisley, Scotland.

Macar, P., et al. (1947). Le tuffeau de Lincent, Centenaire de l'Association des Ingénieurs sortis de l'École de Liège, Congrès 1947. Section Géologie, A.I.Lg. (Ed.), pp. 326–328.

Masschaele, B., et al. (2007). UGCT: New X-ray radiography and tomography facility. *NIM A, 580,* 266–269.

O'Brien, P. F., et al. (1995). Role of mortars in the decay of granite. *The Science of the Total Environment, 167,* 103–110.

Papida, S., et al. (2000). Enhancement of physical weathering of building stones by microbial populations. *International Biodeterioration & Biodegradation, 46,* 305–317.

Pavia, S., & Bolton, J. (Eds.). (2001). *Stone monument decay study 2000*. An Chomhairle Oidhreachta/The Heritage Council.

Platroz, P., et al. (2006). Roches de France, Pro Roc, ISBN 978-2950899255.
Přikryl, R., & Smith, B. J. (Eds.). (2007). *Building stone decay: From diagnosis to conservation*. Geological Society Special Publications 271, ISBN 978-1-86239-218-2.
Ramge, P., & Kühne, H. C. (2012). Development of repair mortars for the restoration of natural stone in cultural heritage. In Alexander et al. (Eds.). *Concrete repair, rehabilitation and retrofitting III* (pp. 882–887). Taylor & Francis Group, ISBN 978-0415899529.
Steenmeijer, R. (2010). Kunststeen of natuursteen. Voorbeelden uit de praktijk. In Hayen, R., De Clercq, H. (Eds.), *Proceedings KIK/IRPA Versteend erfgoed—omgaan met herstelmortel en kunststeen* (pp. 33–38), Brussels.
Stefanis, N. A., & Theoulakis, P. (2010). Design of conservation mortars for the restoration of the Piraeus stones at the monuments of the Acropolis of Athens. In Valek, J., Groot, C., & Hughes, J. J. (Eds.), Prague, pp. 1181–1188. http://www.rilem.org/gene/main.php?base=05&id_publication=82.
Szemerey-Kiss, B., & Török, A. (2011). Time-dependent changes in the strength of repair mortar used in the loss compensation of stone. *Environmental Earth Sciences, 63,* 1613–1621.
Torney, C., et al. (2012). Plastic repair of natural stone in Scotland: Perceptions and practice. *Structural Survey, 30*(4), 297–311.
Trouvé, A. (1991). *La mesure de la couleur: Principes, technique et produits du marché* (p. 193). AFNOR-CETIM, Paris, 2-12-450811-3/2-85400-192-3.
Van Parys, L., & Dagrain, F. (2006). Scratching test applied for on-site determination of compressive strength on historical mortars. In Proceedings 7th International Congress on Theoretical & Applied Mechanics, Mons, Belgium.
Van Parys, L., et al. (2013). *Targetting colour and strength of a mortar through a genetic algortihm, HMC13*. Scotland: Glasgow.
Warscheid, T., & Braams, J. (2000). Biodeterioration of stone: A review. *International Biodeterioration and Biodegradation, 46,* 343–368.

Natural Hydraulic Lime Mortars: Influence of the Aggregates

P. Faria and V. Silva

Abstract Natural hydraulic lime specifications changed with the 2010 version of standard EN 459-1 and new natural hydraulic limes appeared in the market. The characteristics of mortars depend on many different parameters such as the type of binder, the type of aggregates, the use of fillers and of super plasticizers applied in the mortars formulations; also on mixing and curing conditions. In this paper mortars with a Portuguese NHL3.5 were formulated with binder:aggregate volumetric proportions1:3, varying the aggregates type and proportions between them. Two coarse sands, a medium sand, a river sand, a finer sand, a calcareous filler and a ceramic powder were used, being the two last mentioned aggregates by-products from industry. Standardized prismatic mortar samples and samples of mortar applied on a brick surface were prepared and conditioned in two different situations: following standard EN 1015-11 and at 65% relative humidity but with daily water spray during the first days. Mortars were characterized in the fresh state and at the age of 28 days. Results showed the influence namely of the curing, particularly in terms of water capillary, and of the fillers. They also showed that NHL3.5 mortars seem to be adequate for old masonries conservation and repair and, in some situations, they can be an alternative to air lime based mortars.

Keywords Natural hydraulic lime · Aggregate · Particle size · Mortar Characterization

P. Faria (✉) · V. Silva
Department of Civil Engineering, NOVA University of Lisbon, Caparica, Portugal
e-mail: paulina.faria@fct.unl.pt

V. Silva
e-mail: vmd.silva@fct.unl.pt

P. Faria
CERIS—Civil Engineering Research and Innovation for Sustainability, Lisbon, Portugal

J. J. Hughes et al. (eds.), *Historic Mortars*,
https://doi.org/10.1007/978-3-319-91606-4_14

1 Introduction

Traditionally mortars were prepared in situ in working sites but nowadays, at least the dry constituents are often prepared industrially. In situ mortars must be simple, without many different constituents, so they can be easily reproduced from batch to batch. The industrial preparation of the dry constituents can facilitate the introduction of different ones, namely of admixtures, several binders, different types of aggregates and with different particle size distributions. It can also turn possible the addition of by-products and industrial residues, which can contribute to the technical efficiency, sustainability and economy of the mortars.

Mortar aggregates are mainly sands but the type and particle size distribution of sands can be diverse and contribute to mortars characteristics. Residues can also be used as aggregates and fillers (Matias et al. 2013) and alter the mortars microstructure.

The 2010 version of standard EN 459-1 (CEN 2010), updated again in 2015 (CEN 2015), redefined the specifications and characteristics of limes with hydraulic properties. Some of the previously named natural hydraulic limes (NHL), following the ancient version of EN 459-1 (CEN 2001), are now classified as hydraulic lime HL as they contain additions. For that reason the characteristics previously presented for NHL mortars can no longer be extrapolated and compared to recent NHL mortars, due to great differences on the lime constitution, formulation and behaviour that can occur with these NHL binders. NHL being a natural product, problems of inconstancy of characteristics may be found in this binder (Charola et al. 2005). This should be verified. A new Portuguese natural hydraulic lime NHL3.5 appeared in the market and has been widely used in Portugal and elsewhere; following EN 459-1 (CEN 2010, 2015) it cannot have any addition, have to present at least 25% of calcium hydroxide and a maximum of 2% of sulphates. Recent studies have shown that mortars with this lime can present a behaviour in terms of capillary suction and drying comparable to those of air-lime based mortars (Faria et al. 2012a; Grilo et al. 2014a), very different from EN 459-1 (CEN 2001) NHL mortars. Those characteristics can contribute to a good behaviour particularly in repair applications. But different parameters (mechanical and physical) can be obtained when changing the aggregate, for instance with different sands or partial replacements of sand by ceramic wastes (Grilo et al. 2014a, b; Matias et al. 2013). Comparison can also be made with mortars formulated with other NHL, i.e. with NHL5 with different sands and water/binder ratios, characterized by Isebaert et al. (2015). These researchers point out that the W/B ratio can have less influence on the mortars characteristics, namely on pore size distribution and open porosity, than different aggregates. It is expected that these parameters directly influence mechanical and physical characteristics

Within this context, the present study began by trying to formulate a mortar that could be used to enwrap a net to confine and reinforce old masonry walls and also to try to evaluate which aggregates to use for mortars to re-point stone masonry; simultaneously an attempt was made to improve sustainable constructive practices.

Different mortars were formulated with this new NHL3.5 using various types of aggregates. Diverse mixtures of aggregates with different particle size distributions were also prepared. Fresh mortars were characterized in terms of composition, water/binder ratio, bulk density and flow table consistency. Samples were prepared applying the mortars in prismatic moulds but also directly on a brick surface, to reproduce the suction of a reference support on real applications, and maintained in two different curing conditions.

The aim of this work is to present the characterization of these NHL3.5-based mortars at young age and evaluate its compatibility to old masonry walls of existent buildings.

The evaluation of characteristics, particularly in terms of dynamic modulus of elasticity, flexural and compressive resistances, capillary water absorption, drying capacity and porosity (of the mortars applied on the moulds but also of the mortars applied on bricks to simulate the suction of the walls) will be discussed, mainly focusing at the role of the different aggregates.

2 Materials, Mortars, Samples and Curing

The binder used for the mortars preparation was a NHL3.5 produced by SECIL at a maximum temperature of around 900 °C (information from the producer). Chemical characteristics, also provided by the producer, are presented in Table 1.

The aggregates were: a current siliceous river sand R, a coarse siliceous washed sand G and calcareous filler Fl. A ceramic powder CP was also used in one of the mortars instead of the calcareous filler. One of the mortars was prepared with another coarse siliceous washed sand G2, a medium siliceous washed sand M and a finer siliceous washed sand F; this last mixture of aggregates have been used for experimental work within projects METACAL and LIMECONTECH, simulating an old mortar.

All the mortars were formulated with a volumetric proportion of 1:3 (binder: aggregate), with different aggregate mixtures (type and proportions between the aggregates) and are designated by the volumetric proportions of each aggregate. The particle size distributions of each of the aggregates and of the mixtures of aggregates of the mortars are presented in Fig. 1.

The dry constituents were manually homogenised, the quantity of water to obtain mortars with good workability was added in the first seconds of mechanical mixing in a mechanical laboratory mixing equipment. The mixing went on for three minutes. Flow table consistency and bulk density were determined for the fresh mortars, based on EN 1015-3 (CEN 1999a, b) and EN 1015-6 (CEN 1998). Mortar designations, proportions, water/binder ratios, flow table consistency, bulk density and workability evaluation are presented in Table 2.

Two types of samples were prepared: prismatic 40 × 40 × 160 mm^3 samples in metallic moulds, applied in two layers, each of one mechanically compacted with 20 strokes; 1.5 cm thickness of mortar over current hollow ceramic high absorption

Table 1 Chemical characterization of NHL3.5

Material	CaO	CO_2	SiO_2	Al_2O_3	MgO	SO_3	Fe_2O_3	K_2O	TiO_2	Na_2O	SrO_2	P_2O_5	MnO	Cl
NHL3.5	62.07	25.66	5.70	1.84	1.36	1.29	1.22	0.49	0.14	0.08	0.06	0.03	0.02	0.02

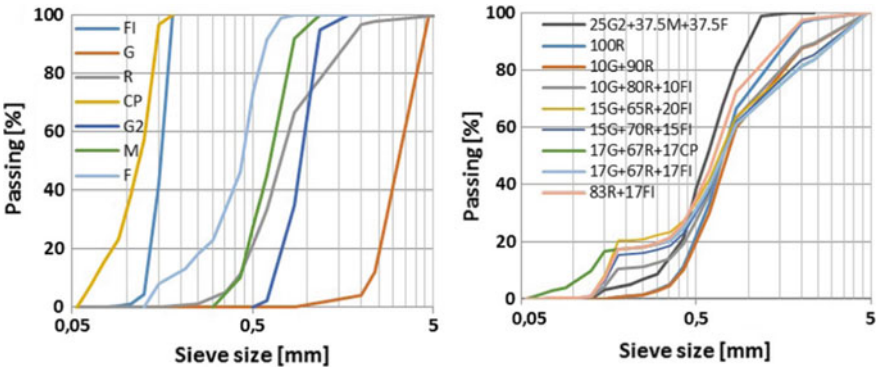

Fig. 1 Particle size distribution of each aggregate and of the mixtures of aggregates in the mortars

bricks with 20 × 30 cm^2 surface. For the preparation of these samples, the surface of the bricks to be rendered were previously sprayed with 10 g of water and the mortar was dropped from a constant high of 70 cm to simulate a constant energy of application. The samples of mortar on bricks were only prepared with some of the mortars. Prismatic samples were held in two different curing conditions N and A, while brick samples were only conditioned at curing A. For standard curing N, samples were held inside the moulds packed in polyethylene until demoulding, at the second day of curing; kept in polyethylene until 7 days of age (high relative humidity ambiance) and, until the age required for the test, kept at standard laboratory conditions at 65 ± 5% RH and 20 ± 2 °C temperature, following EN 1015-11 (CEN 1999a, b), considered unfavourable curing conditions (too dry) for NHL mortars. For curing A the mortar samples on the brick surface were daily sprayed with 7.5 g of water from the 2nd to the 5th day of age, de-moulded at the age of 2 days and also held at 65% RH and 20 °C until the age required for the test. The short period for spraying the samples was chosen to simulate minimum required in situ conditions; it is probable that different results could be obtained if the curing had water spray up to 28 days. In Fig. 2 curing conditions of different samples and curing stages can be observed.

3 Testing of the Harden Mortars

Mortars′ behaviour was characterized at the age of 28 days for dynamic modulus of elasticity, flexural and compressive strength, open porosity, capillary absorption and drying with prismatic samples kept on curing conditions N and A. Mortars behaviour was also characterized by visual observation, thermal conductivity, water intake under low pressure with Karsten tubes and mercury intrusion porosimetry (MIP) on the samples on bricks at the same age (curing condition A).

Table 2 Mortars' designation, proportion, water/binder ratio (W/B), flow table consistency, bulk density (BD) and workability evaluation

Mortar	Volume proportion		Weight proportion		W/B (−)	Flow (mm)	BD (kg/m^3)	Workability evaluation
100R	1:3	1:3	1:5.5	1:5.5	1.17	119	1483	Too dry; more water needed
100R (>W/B)	1:3	1:3	1:5.5	1:5.5	1.23	149	1502	Good
10G + 90R	1:3	1:0.3 + 2.7	1:5.5	1:1.1 + 4.4	1.17	163	1505	Good
10G + 80R + 10Fl	1:3	1:0.3 + 2.4 + 0.3	1:5.4	1:0.6 + 4.4 + 0.4	1.11	156	1510	Very good
15G + 65R + 20Fl	1:3	1:0.45 + 1.95 + 0.6	1:5.2	1:0.8 + 3.6 + 0.8	1.10	188	1556	Too much flow; less water needed
15G + 70R + 15Fl	1:3	1:0.45 + 2.1 + 0.45	1:5.3	1:0.8 + 3.9 + 0.6	1.04	158	1529	Very good
17G + 67R + 17Fl	1:3	1:0.5 + 2 + 0.5	1:5.3	1:0.9 + 3.7 + 0.7	1.04	180	1532	Very good
17G + 67R + 17CP	1:3	1:0.5 + 2 + 0.5	1:5.3	1:0.9 + 3.7	1.04	180	1535	Very good
83R + 17Fl	1:3	1:2.5 + 0.5	1:5.3	1:4.6 + 0.7	1.04	155	1526	Good
25G2 + 37.5M + 37.5F	1:3	1:0.75 + 1.12 + 1.12	1:5	1:1.3 + 1.9 + 1.8	1.05	168	1516	Poor workability; separation of water from the paste

Fig. 2 Prismatic samples inside the moulds and conditioned in polyethylene bags; mortars on brick and prismatic samples at laboratory controlled conditions

Dynamic modulus of elasticity was determined with a Zeus Resonance Meter based on EN 14146 (2004). Flexural and compressive strengths were determined based on EN 1015-11 (CEN 1999). Open porosity was determined by hydrostatic method based on EN 1936 (CEN 2006) for specimens from prismatic samples and, for specimens from samples applied over the bricks, by mercury porosimetry, based on specifications referred by Rato (2006). Capillary water absorption was determined based on EN 1015-18 (CEN 2002) and EN 15801 (CEN 2009). The capillary curve was defined; capillary coefficient, that expresses the initial absorption rate, and asymptotic value, that corresponds to the maximum absorption of the samples, was determined.

Drying capacity was determined following EN 16322 (CEN 2013b), based on former RILEM specification (1980), but at 65% RH. The drying curves of mortars with time in abscissa (showing the 1st phase of drying) and with the square root of time in abscissa (showing the 2nd phase of drying) are defined. The drying rate of the 1st phase of drying was determined as the negative slope of the initial linear section of the respective drying curve of each mortar; the drying rate of the 2nd phase of drying was determined by the negative slope of the linear segment of the respective drying curve. The drying index, that represents the difficulty to achieve a total drying, was determined over a period of 600 h of test.

Water absorption by Karsten tubes was determined by EN 16302 (CEN 2013a), based on former RILEM specification (1980) and presented in terms of absorption coefficient after 60 min of contact with water. Thermal conductivity was determined with ISOMET Heat Transfer equipment, with a contact probe with 6 cm diameter (Fig. 3).

4 Characterisation of the Harden Mortars

Mean values and standard deviation of dynamic modulus of elasticity, flexural and compressive strength and open porosity by hydrostatic method are presented in Table 3, for prismatic samples with curing N and A. Nevertheless NHL3.5 mortars

Fig. 3 Tests of dynamic modulus of elasticity and Karsten tubes

at 28 days may not be at their end-strength values; end values should be reached after 90 days, 180 days or even more, based on the study of Grilo et al (2014b). Depending on the curing conditions, mechanical strength may double the values obtained after 28 days of curing.

The capillary curves and the drying curves of some representative mortars are presented in Figs. 4, 5 and 6. Not all mortars are included to ensure visibility. Mean values and standard deviation of capillary coefficient, capillary asymptotic value, drying rates of the 1st and 2nd phases of drying and drying index are presented in Table 4, for prismatic samples with curing N and A.

Visual observation of the mortars applied on bricks did not present shrinkage; nevertheless the sample dimension was only 600 cm^2 (the 30 × 20 cm^2 surface of the bricks).

The curves from MIP for samples of some mortars applied on bricks with curing A are presented in Fig. 7. Mean values and standard deviation of thermal conductivity and of water absorption by Karsten tubes, results of open porosity by mercury intrusion and the most representative pore size of the mortars are presented in Table 5, for samples of mortar applied over bricks with curing A.

5 Discussion

Except the 100R mortar, all the mortars had workability to be applied as repair mortars, with mean value of consistency of 163 ± 15 mm. Those mortars correspond to water/binder ratios of 1.2–0.9. The mortars tested on brick had W/B = 1.0, except the 100R (>W/B) with W/B = 1, 2. Fresh mortars with similar composition, only changing the use of filler or ceramic powder, registered the same consistency and bulk density. The substitution of some coarser sand by river sand reduced the consistency and the bulk density of 83R + 17Fl mortar. For the mixture without fines (10G + 90R) a decrease on bulk density was registered, although presenting

Table 3 Dynamic modulus of elasticity (Ed), flexural (FSt) and compressive (CSt) strength, open porosity by hydrostatic method (P_{hydr}) − mean value and standard deviation

Mortar	Sample/curing	Ed (N/mm^2)		FSt (N/mm^2)		CSt (N/mm^2)		P_{hydr} (%)	
		Mean	St. dv.	Mean	St. dv.	Mean	St. dv.	Mean	St. dv.
100R	Prismatic samples—curing N	3098	101	0.41	0.06	0.94	0.01	26	0.3
100R (>W/B)		3541	54	0.70	0.07	0.70	0.08	25	0.1
10G + 90R		3052	42	0.39	0.03	0.82	0.07	27	0.1
10G + 80R + 10Fl		3890	36	0.55	0.06	0.86	0.59	26	0.1
15G + 65R + 20Fl		4007	78	0.58	0.03	1.38	0.06	27	0.1
15G + 70R + 15Fl		4219	201	0.61	0.06	1.57	0.09	25	0.3
17G + 67R + 17Fl		3760	77	0.73	0.09	1.46	0.14	25	0.2
17G + 67R + 17CP		3680	40	0.72	0.15	1.75	0.07	26	0.1
83R + 17Fl		3153	101	0.68	0.05	0.83	0.04	25	0.8
25G2 + 37.5M + 37.5F		3548	43	0.42	0.04	1.00	0.10	27	0.5
100R	Prismatic samples—curing A	2777	52	0.44	0.03	0.89	0.03	25	0.1
100R (>W/B)		3518	42	0.76	0.10	0.75	0.04	25	0.4
10G + 90R		3465	56	0.49	0.05	0.88	0.02	24	0.4
10G + 80R + 10Fl		3925	125	0.64	0.05	1.16	0.10	24	0.4
15G + 65R + 20Fl		4461	39	0.74	0.02	1.34	0.18	25	0.2
15G + 70R + 15Fl		4854	222	0.78	0.01	1.41	0.28	24	0.2
17G + 67R + 17Fl		3699	46	0.76	0.06	1.33	0.06	24	0.6
17G + 67R + 17CP		3286	67	0.73	0.10	1.37	0.14	24	0.2
83R + 17Fl		3421	61	0.62	0.11	1.16	0.07	24	0.4
25G2 + 37.5M + 37.5F		3841	165	0.56	0.01	1.11	0.02	23	0.4

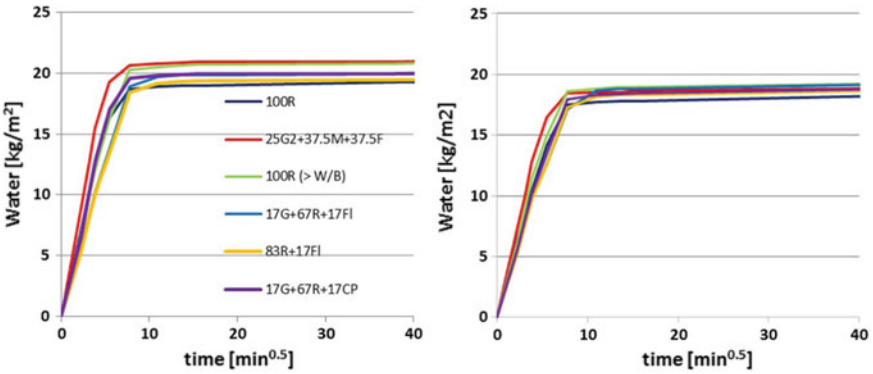

Fig. 4 Capillary curve of some mortars with curings (left) N and (right) A

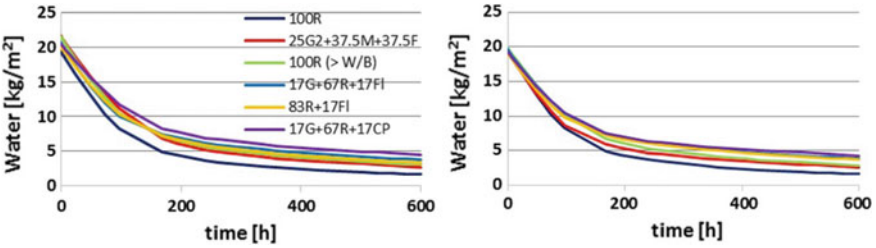

Fig. 5 Drying curves of some mortars by time, showing the 1st phase of drying with curings (left) N and (right) A

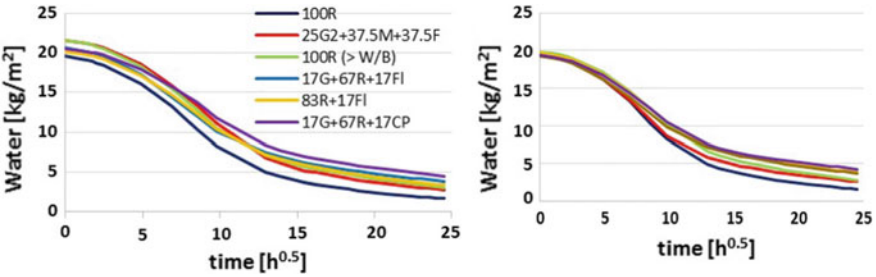

Fig. 6 Drying curves of some mortars by square root of time, showing the 2nd phase of drying, with curings (left) N and (right) A

an intermediate consistency. The fresh mortar evaluated with too much water (15G + 65R + 20Fl) presented the highest bulk density.

The mortars with higher flexural strength were generally the ones which had mixtures of coarser and river sands and filler or ceramic powder; nevertheless the mortar only with river sand but with not so low consistency also presented a high

Table 4 Capillary coefficient (CC), capillary asymptotic value (CAV), drying rates of drying phases 1 (D1) and 2 (D2), drying index (DI)—mean value and standard deviation

Mortar	Sample/cure	CC (kg/(m^2 $min^{0.5}$))		CAV (kg/m^2)		D1 (kg/(m^2 h))		D2 (kg/(m^2. $h^{0.5}$))		DI (−)	
		Mean	St. dv.	Mean	St. dv.	Mean	St. dv.	Mean	St. dv.	Mean	St. dv.
100R	Prismatic samples—curing N	3.01	0.12	19.6	1.6	3.09	0.14	1.34	0.05	0.25	0.03
100R (>W/B)		3.00	0.14	21.3	0.4	3.22	0.05	1.28	0.01	0.31	0.00
10G + 90R		3.65	0.20	21.5	0.5	2.85	0.23	1.46	0.10	0.26	0.01
10G + 80R + 10Fl		3.06	0.14	20.1	0.6	3.13	0.15	1.33	0.05	0.28	0.01
15G + 65R + 20Fl		2.91	0.23	21.6	1.5	3.08	0.32	1.35	0.11	0.31	0.02
15G + 70R + 15Fl		2.81	0.12	21.0	1.8	3.14	0.18	1.32	0.06	0.31	0.02
17G + 67R + 17Fl		2.55	0.10	20.3	0.5	3.24	0.14	1.27	0.04	0.25	0.01
17G + 67R + 17CP		3.18	0.11	20.3	1.1	4.12	0.46	1.01	0.10	0.38	0.04
83R + 17Fl		2.50	0.07	19.8	1.0	3.61	0.10	1.15	0.03	0.34	0.03
25G2 + 37.5M + 37.5F		3.59	0.05	21.5	1.6	3.45	0.38	1.21	0.12	0.30	0.00
100R	Prismatic samples—curing A	2.58	0.11	18.7	0.5	3.17	0.52	1.34	0.05	0.24	0.03
100R (>W/B)		2.78	0.13	19.4	1.6	3.77	0.07	1.31	0.05	0.33	0.02
10G + 90R		2.86	0.21	18.6	0.9	3.03	0.39	1.35	0.05	0.25	0.02
10G + 80R + 10Fl		2.40	0.25	18.8	0.7	2.77	0.15	1.29	0.03	0.25	0.02
15G + 65R + 20Fl		2.57	0.17	19.4	0.2	3.14	0.19	1.31	0.02	0.29	0.02
15G + 70R + 15Fl		2.86	0.21	18.6	0.9	2.94	0.24	1.24	0.03	0.28	0.00
17G + 67R + 17Fl		2.34	0.08	19.4	0.2	3.85	0.06	1.19	0.04	0.36	0.02
17G + 67R + 17CP		2.49	0.03	19.2	1.1	4.02	0.06	1.16	0.06	0.38	0.01
83R + 17Fl		2.34	0.15	18.9	0.4	3.71	0.07	1.14	0.07	0.36	0.02
25G2 + 37.5M + 37.5F		3.06	0.38	19.2	1.7	3.33	0.24	1.30	0.08	0.30	0.01

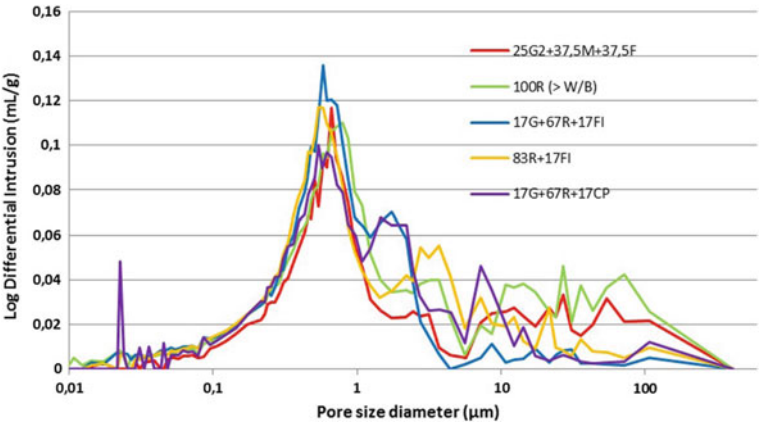

Fig. 7 Mercury porosimetry curves of some mortars applied on bricks after 28 days of curing with water spray during the first week

Table 5 Thermal conductivity (ThC), water absorption by Karsten tubes (AKt) – mean value and standard deviation -, open porosity by mercury intrusion (P_{MIP}) and pore size

Mortar	ThC (W/(m K))		AKt (kg/(m^2 $min^{0.5}$))		P_{MIP}	Pore size
	Mean	St. dv.	Mean	St. dv.	(%)	(µm)
100R (>W/B)	0.57	0.08	7.90	0.57	29	100
17G + 67R + 17Fl	0.86	0.09	5.69	0.50	22	2
17G + 67R + 17CP	0.83	0.09	5.60	0.63	23	2 and 100
83R + 17Fl	0.78	0.08	6.88	0.81	24	100 and 4
25G2 + 37.5M + 37.5F	0.76	0.17	4.31	0.40	21	100

flexural strength. Results of dynamic modulus of elasticity and compressive strength presented a similar tendency. Mortars with higher compressive strength were the mortars with mixtures of aggregates G, R and Fl or CP, with these last ones in higher amounts (15, 17 or 20%). The mortar with the lowest compressive strength was the one only with river sand (>W/B) which presented the highest flexural strength. This mortar also presented one of the highest open porosities, which can justify this low result of compression and show that its influence for flexural is not the same. Generally there is not a big difference for mechanical properties between the two curing conditions and the mortars tested with MIP presented the same tendency in terms of open porosity. The open porosity by MIP is in agreement with the thermal conductivity, which as expected is lower for mortars with higher porosity.

The MIP curves evidenced clearly the differences in microstructure of mortars applied on bricks with the same binder:aggregate ratio when the proportions of the different aggregates and particularly the type of aggregates changed. Without

jeopardizing the fact that the brick substrate may significantly change the microstructure of all the mortars due to water suction from the fresh mortar, those differences can at least partially explain the mechanical and physical properties of the mortars.

Grilo et al. (2014a, b) have tested NHL3.5 mortars (binder:sand 1:3 volumetric proportion and 1:5 mass proportion) after 28, 90 and 180 days of curing in standard curing (RH 65% and 20 °C temperature), humid curing (HR 95% and 20 °C temperature) and Portuguese marine environment (by the Atlantic coast). Flexural and compressive strength at humid and marine curing increased mainly from 28 to 90 days. In standard curing the strength did not increased much after 28 days and kept lower compared with the mortars at more humid curing conditions (Grilo et al. 2014b). The main hardening reaction has proven to be carbonation. The infilling of the porous structure is significantly justified by moisture presence in curing conditions (Grilo et al. 2014b). Therefore it can be highly expected that the mechanical strengths of the mortars analysed in the present study would benefit if the daily water spraying would have last longer (not only the first week), so that the strengths would increase at least until 90 days of curing. The daily spray for a longer period would most probably simulate natural environmental conditions for instance of Portugal or other countries by the coast, with humid nights even with relatively dry periods during daytime.

Comparing the flexural and compressive strength at 28 days of the present study with those presented by Grilo et al. (2014a) it can be observed that the influence of the particle size of aggregates can have an influence on mechanical strengths as significant as the type of curing.

For properties of the mortars related with water (absorption and drying) a tendency for a better behaviour is registered with curing conditions with initial water spray A. The use of higher water/binder ratio increased the CC and the CAV but turned faster the initial drying, although showed no benefit to complete drying capacity. Mortar without filler or ceramic powder (10G + 90R and 25G2 + 37.5M + 37.5F) presented the higher CC, although not so high CAV. The drying behaviour of the mortars without filler or ceramic powder was not distinguished from the others. Mortars with filler and ceramic powder with standard curing N present a decrease in the 2nd phase of drying in comparison with similar mortars with curing A.

The mortars chosen to be tested on the bricks presented the faster initial drying but more difficulty to achieve complete drying. In terms of water absorption coefficient by Karsten tubes after 60 min, the tendency of the mortars has direct correspondence with the open porosity by MIP.

The mortars analysed in this paper with type A curing (first week daily water spray) presented similar CC, CAV and DI values to those of air lime-based mortars with aggregates similar to 25G2 + 37.5M + 37.5F and binder aggregate proportion 1:3 (Faria et al. 2012b). They also registered much lower values of CC and CAV when compared to similar mortars but with a former NHL5 (in agreement with the previous version of standard EN 459-1) (Faria et al. 2012a), what must be enhanced. When CC and CAV are compared with mortars with NHL3.5 with

similar volumetric proportions binder:sand analysed by Grilo et al. (2014a) it can be observed that a well defined particle size distribution of aggregate seems not to have significant influence on the total of water absorbed (CAV) but may have an important role on decreasing the speed of capillary water absorption, decreasing CC. Simultaneously it may be expected that those parameters decrease with the time of curing, at least from 28 to 180 days (Grilo et al. 2014a).

6 Conclusions

Dynamic modulus of elasticity between 2800 and 5000 N/mm^2, flexural strength between 0.4–0.8 N/mm^2 and compressive strength between 0.7–2.0 N/mm^2 induce a proper mechanical behaviour for application in historic masonry repair (Veiga et al. 2010) of NHL3.5 mortars with binder:aggregate proportion 1:3 and different aggregates. Water absorption and drying behaviour of these mortars seems to be enhanced by spraying water during the first days of curing. But a longer period of water spraying, that could simulate better a daily humid curing period, for instance during the night, would most probably be more advantageous for this type of NHL mortars, mainly in terms of flexural and compressive strength. As it is probable that the mechanical and physical characteristics improve with the age of curing, the influence of the type and particle size of the aggregates should be tested after a longer period of curing (at least 90 days but, if possible, 180 days)

The use of fine aggregates, and namely of calcareous filler or ceramic powder, by-products of gravel production and of ceramic industries, seems to be advantageous, particularly in terms of water absorption and drying capability.

The results induce that these types of NHL3.5 mortars are mechanically, physically and ecologically adequate to be applied for old masonries conservation and repair.

Further studies are being carried out to evaluate the steadiness qualities of the NHL and the durability of mortars.

Acknowledgements The authors would like to thank the support of LNEC on project PRESERVE, to company MONUMENTA for the demand for starting this study about the influence of aggregates and to company Secil for the NHL3.5 and its chemical characterization.

References

CEN. (2001). EN 459-1:2001—Building lime. Part 1: Definitions, specifications and conformity criteria.

CEN. (2010). EN 459-1:2010—Building lime. Part 1: Definitions, specifications and conformity criteria.

CEN. (2015). EN 459-1:2015—Building lime. Part 1: Definitions, specifications and conformity criteria.

CEN. (1999). EN 1015-3:1999/A1:2004/A2:2006)—Methods of test for mortar for masonry. Part 3: Determination of consistence of fresh mortar (by flow table).
CEN. (1998). EN 1015-6:1998/A1:2006—Methods of test for mortar for masonry. Part 6: Determination of bulk density of fresh mortar.
CEN. (1999). EN 1015-11:1999/A1:2006—Methods of test for mortar for masonry. Part 11: Determination of flexural and compressive strength of hardened mortar.
CEN. (2002). EN 1015-18:2002—Methods of test for mortar for masonry. Part 18: Determination of water absorption coefficient due to capillary action of hardened mortar.
CEN. (2006). EN 1936:2006—Natural stone test methods. Determination of real density and apparent density, and of total and open porosity.
CEN. (2004). EN 14146:2004—Natural stone test methods. Determination of the dynamic modulus of elasticity (by measuring the fundamental resonance frequency).
CEN. (2009). EN 15801:2009—Conservation of cultural property. Test methods. Determination of water absorption by capillarity.
CEN. (2013a). EN 16302:2013—Conservation of cultural heritage. Test methods. Measurement of water absorption by pipe method.
CEN. (2013b). EN 16322:2013 - Conservation of cultural heritage. Test methods. Determination of drying properties.
Charola, E., et al. (2005). Pozzolanic components in lime mortars: Correlating behaviour, composition and microstructure. *Restoration of Buildings and Monuments, 11*(2), 111–118.
Faria, P., et al. (2012a). Compatible natural hydraulic lime mortars for historic masonries (in Portuguese). In *CIRea2012—International Conference Rehabilitation of Old Masonries* (pp. 29–38). NOVA University of Lisbon.
Faria, P., et al. (2012b), Lime-based mortars for ceramic tile application: the influence of the lime, the use of a metakaolin and the curing. In *International Conference AZULEJAR*. Aveiro University (CD).
Grilo, J., et al. (2014a). New natural hydraulic lime mortars. Physical and microstructural properties in different curing conditions. *Construction and Building Materials, 54,* 378–384.
Grilo, J., et al. (2014b). Mechanical and mineralogical properties of natural hydraulic lime-metakaolin mortars in different curing conditions. *Construction and Building Materials, 51,* 287–294.
Isebaert, A., et al. (2015), Pore-related properties of natural hydraulic lime mortars: an experimental study. *Materials & Structures*. https://doi.org/10.1617/s11527-015-0684-5.
Matias, G., Faria, P., & Torres, I. (2013). Viability of ceramic residues in lime-based mortars. In *3rd Historic Mortars Conference*, Glasgow.
Rato, V. (2006). *Influence of morphologic microstructure on mortars behaviour* (in Portuguese). PhD thesis, NOVA University of Lisbon.
RILEM. (1980). Commission 25 PEM, Test nº II.4—Water absorption under low pressure; Test nº II.5—Evaporation curve. *Materials & Structures 13*(75), 200–207.
Veiga, R., et al. (2010). Lime-based mortars: viability for use as substitution renders in historical buildings. *Architectural Heritage, 4*(2), 177–195.

The Influence of Calcitic Filler in Hydraulic Lime Mortars for Use in High Temperature and High Humidity Climatic Conditions: A Preliminary Investigation

Alan M. Forster, Nadia Razali, Phil Banfill, Ewan Szadurski and Clare Torney

Abstract The widespread adoption of alternative binders are playing an increasing role in carbon dioxide (CO_2) abatement in green construction and the repair of traditionally built structures. Natural Hydraulic Lime (NHL) has better environmental credentials than Portland Cement (PC) due in part to its lower calcination temperature and its ability to absorb CO_2 during carbonation. However, NHL is more sensitive to climatic conditions during the setting and hardening processes and this is especially pronounced in high humidity climates. It is well understood that high humidity environments create favourable conditions for the development of the products of hydration, but the carbonation reaction can reduce or become dormant due to high sustained moisture contents. Anecdotal evidence suggests that the addition of crystalline $CaCO_3$ into hydraulic lime mortar mixes can enhance the carbonation reaction due to 'seeding' of the crystal architecture. This research assesses the influence of $CaCO_3$ modification of NHL mortars subject to high humidity environments and investigates the subsequent effect on early development of various physical properties.

Keywords Lime mortar · Seeding · Calcitic materials · High humidity and temperature

A. M. Forster (✉) · N. Razali · P. Banfill · E. Szadurski
School of Energy, Geoscience, Infrastructure & Society,
Heriot-Watt University, Edinburgh, Scotland, UK
e-mail: a.m.forster@hw.ac.uk

C. Torney
Historic Environment Scotland, 7 South Gyle Crescent, Edinburgh, Scotland, UK

J. J. Hughes et al. (eds.), *Historic Mortars*,
https://doi.org/10.1007/978-3-319-91606-4_15

1 Introduction

Environmental conditions can significantly influence the set characteristics and performance of lime mortars. Relative humidity and temperature specifically, influence both hydration and carbonation set reactions with the formation of hydrates determining the mineralogical composition and the ultimate strength and stability of the matrix (Dotter 2010; Taylor 1997; Hewlett 2004). Hydraulic lime mortars placed in a high humidity environment are understood to exhibit lower rates of carbonation and may not readily attain their full set characteristics (Allen 2003) due to the potential for high and sustained moisture contents (Forster and Carter 2011). The wide scale adoption of non-Portland Cement alternative binders (including NHL) in emerging markets may be hindered by performance and behavioural uncertainty associated with high humidity conditions and equally so by the slow rates of initial set in such materials (Pavia 2008; Ball et al. 2009, 2011; El-Turki et al. 2007). Hydraulic lime mortars exposed to elevated temperatures and optimal moisture contents should follow similar hydration kinetics to that associated with belite (β-C_2S) cements (Hewlett 2004) and exhibit accelerated precipitation of products of hydration (Forster 2004; Desai et al. 2011). The importance of the carbonation reaction in hydraulic limes cannot be underestimated. Carbonation in simplistic terms is the conversion of $Ca(OH)_2$ into calcite via a chemical reaction with atmospheric CO_2. The extent and rate (kinetic) of the carbonation process are also affected by physical parameters of the masses (porosity/permeability) and by the practical curing and exposure conditions (e.g. CO_2 concentration, humidity, temperature, etc.) (Pacheco Torgal et al. 2012).

Evidence suggests that seeding of lime mortars encourages the early stage precipitation of calcite by accelerated carbonation reaction (Forsyth 2007). Lawrence (2006) concurs indicating that the seeding of lime mortars with 6% finely ground calcite has been shown to improve the rate of carbonation. The addition of calcitic aggregates into lime mortars has many historic precedents and these components are often found in many historic mortars (Hughes and Valek 2003; Gibbons 2003). The understanding of the perceived beneficial nature of these aggregates is little understood, however, their serendipitous addition could have inadvertently enhanced performance. In contemporary work, calcitic aggregate additives are used by specifiers and contractors to enhance the initial set in limes in high humidity environments. This is especially common on the West Coast of the UK, well known for high rainfall and low potential evaporation (Hall et al. 2010).

Seeding materials used in lime mortars can vary in physical form but are primarily, calcium carbonate in nature. There are three types of polymorph of $CaCO_3$; calcite, aragonite and vaterite, of which calcite is the most stable. Seeding is not understood mechanistically, however, several potential reasons have been postulated for its performance. It is evident that an increase in mass of the mortar is noted within the carbonation process as the diffused CO_2 transforms Portlandite into calcite (Dheilly et al. 2002). In addition it has been suggested that the presence of calcitic materials aids carbonation as it is typically a relatively porous particulate

and therefore facilitates CO_2 diffusion through the fresh mortar. Another hypothesised explanation is the establishment of crystal architecture that catalyses the precipitation of Ca^{2+} ions into growth of $CaCO_3$. This concurs with work by various investigators (Hewlett 2004; Forster 2004) into the influence of temperature, and super-saturation of Ca^{2+} ions in the liquid phase upon hydration kinetics. The rate of hydration of calcium silicates is restricted by an impermeable hydrate layer of Ca^{2+} ions that surrounds the grain potentially leading to a temporary period of dormancy. The addition of calcitic material may minimise the effect of the dormancy period leading to an accelerated deterioration of the Ca^{2+} ion layer as they are readily utilised in the formation of calcite. This is potentially responsible for the reactivation of the hydraulic phase dissolution and precipitation activity. The development of early stage products of hydration have been previously associated with an impedance to CO_2 diffusion in lime mortars (Radonjic et al. 2001), therefore inhibiting carbonation. It was later concluded by Ezziane et al. (2007) that the seeding processes can positively influence the mortar hydration and minimise disorders caused by the temperature rise.

2 Research Objectives

The aim of the research is to undertake an analysis of the influence of calcitic aggregate modifications in naturally hydraulic lime mortars and determine their subsequent effect on early strength development and other physical phenomena. This programme has ultimately been developed to aid specification of mortars in high temperature and high humidity environments such as the Tropics. The research objectives are;

i. To investigate the effects of mortar seeding on mortars' physical properties using laboratory testing techniques including tensile and compressive strength
ii. To investigate the effects of mortar seeding on chemical properties i.e. composition of binder/carbonation front using laboratory testing techniques
iii. To investigate through sorptivity testing if seeding additives affect the moisture handling characteristics of mortars.

3 Experimental Work

3.1 Materials and Characterisation

Control samples were manufactured using an NHL 3.5 (moderately hydraulic) lime binder and a well graded coarse sand. These materials were selected on the basis of being commonly used for the repair of the traditional built environment and being

relatively representative of historic mortars. Material characterisation was based on sieve analysis of the aggregate in accordance with BS EN 13139 (2002), to determine the grading profile, and powder X-Ray diffraction (XRD). XRD samples were analysed on a Thermo ARL X'TRA Diffractometer with a 2Theta range of 5°–70° at a rate of 1°/min to determine mineral composition of the anhydrous binder.

3.2 Aggregate

Well graded silicaceous sand (Cloddach sand, Perthshire) was selected as it is representative of materials commonly used for the repair of traditional masonry structures in Scotland. This aggregate ensured isolation of variables due to an absence of calcitic mineral components. The grading curve was ascertained in accordance with BS EN 13139 (2002). The bulk density of the aggregate was determined to be 1630 g/l. Three types of calcite were procured for use as seeding materials, namely; (i) precipitated calcium carbonate (ii) oyster shells and (iii) limestone chippings. Precipitated calcium carbonate (99.99% pure) was used as point of reference to ensure consistency. Oyster shells composed approximately 98% of $CaCO_3$, although the exact percentage would vary based on several factors such as the species, molecular impurities in the shell, and the number and frequency of proteins embedded in the shell. The 10 mm limestone chips are sedimentary in nature; composed largely of mineral forms of calcite and aragonite and were derived from Lancashire. The calcitic seeding materials were mechanically crushed, using a multi-frequency Siebtechnik Gyro Mill, fitted with a Tungsten Carbide pot and rings and sieved to attain a particle size in the range of 250–300 μm.

3.3 Binder

St. Astier natural hydraulic lime (NHL) (compliant with European norm BS EN 459-1 (2010) was selected for sample manufacture as it is one of the most commonly used binders in the UK and is therefore considered as reflective of site practice. NHL 3.5 (moderately hydraulic) was used for the control samples prior to seeding additives. The anhydrous NHL3.5 binder composition was established through technical data provided by the manufacturer and qualitative XRD analysis.

3.4 Sample Manufacture, Batching and Curing

Samples were prepared using a binder/aggregate ratio of 1:3 by volume. The mix proportion were selected based on the void ratio of the aggregate, and the

requirement of the lime binder to fill the voids between aggregate grains to produce a 'complete' mortar. Cloddach sand has a void ratio of approximately 33%, hence the ratio of 1 part binder to 3 parts aggregate. All materials were batched by weight to ensure accuracy. 6% of the total Cloddach sand weight within the grading range of 250–300 μm was isolated and substituted with seeding materials within the same grading range (250–300 μm).

The manufacturing regime in BS 459-2 (2010) was modified to integrate the relative bulk density (RBD) calculations for the NHL 3.5 binder, resulting in an alteration of the quantity of binder from the standard 450 g established in BS EN 196-1 (2005) to 189 g. This adjustment was undertaken to ensure the 1:3 ratio (by volume) was maintained for the manufactured samples. The mortar was prepared by the 'dry mixing' method undertaken by (Allen et al. 2003; Ball et al. 2009). The samples were batched adopting the proportions shown in Table 1, and mixed mechanically for 4 min in a bench top paddle mixer at low speed. The sides of the mixer bowl were scrapped after 2 min to ensure all dry powder was incorporated into the mix. Water was added and mixed for 5 min at low speed, and finally for 1 min at high speed. The consistency was determined by flow table and was found to be 165 mm ± 2 mm. Mixing and casting of mortars was undertaken in accordance with BS 459-2 (2010), with the exception that the 160 × 40 × 40 mm steel 3 gang moulds were substituted for 160 × 40 × 40 mm single use polystyrene 3-gang moulds. Polystyrene moulds offer several benefits; ease of use; reduced weight in the environmental curing cabinet; and the elimination of the need for releasing agent which may pose uncertainties regarding the interaction of the two surfaces. Upon casting into moulds, an automatic vibrating table was used to compact mortar samples, removing any trapped air (BS EN 459 2010). Table 1 indicates the quantities of constituents required for the preparation of 15 l mortars.

All specimens were placed in the TAS Environmental Curing Cabinet under controlled environment of 33 ± 1 °C and 90 ± 5% Relative Humidity (RH). The samples were de-moulded 7 days, after which they were placed within the cabinet. To ensure satisfactory carbonation, a CO_2 injection system was designed and installed, enabling a constant CO_2 level.

Table 1 Mortar manufacture constituents and flow value

NHL designation and RBD (g/L)	Constituent amounts of materials in mortar used in slump test			Flow value (mm ±2 mm)
	Mass of NHL (kg)	Mass of sand (kg)	Mass of water (kg)	
NHL 3.5 620 g/L	0.189	0.750	0.273	165

3.5 *Physical and Chemical Characteristic Testing*

Physical and chemical characteristics of the mortars were established using a number of testing methods. Control specimens were used to provide a datum for subsequent materials tests. The control and the seeded mortars were subjected to the following testing regimes.

3.5.1 Carbonation Depth

Mortar specimens were used to assess the carbonation depth by spraying a freshly exposed surface of the mortar with 1% phenolphthalein solution (Lo and Lee 2002). The solution is a colourless acid/base indicator, which turns pink when the pH is above 9, denoting the presence of $Ca(OH)_2$. This procedure indicates the boundary at which the progressing carbonated front meets the un-carbonated (unchanged) alkaline mortar.

3.5.2 Sorptivity

Sorptivity of the mortar specimens was evaluated using the 'sharp front' calculation method established by Hall and Hoff (2002). Tests were carried out on parallel piped specimens, after drying in an oven, at a temperature of 100 ± 10 °C. This ensured a constant weight. The specimens were coated with epoxy resin on the vertical faces, reducing the effect of water evaporation. Samples were placed on non-absorbent rods in a shallow tray of water to allow contact with the unsealed surface. The initial sample weight was recorded and subsequently re-recorded after being placed in the water at one, three, five, 10, 15 and 30 min; before weighing, the specimens', excess water was removed by lightly dabbing on a cloth. Sorptivity was determined from the slope of the graph of mass against $\sqrt{t}$ime according to equation established by Hall and Hoff (2002).

3.5.3 Tensile and Compressive Strength

Mortar specimens were tested at specific time intervals (7, 14, 28, 42 and 56 days) to assess strength development over time. This was carried out using a Lloyds Universal Testing Machine (Model M5 K) with a maximum load cell of 5 kN.

4 Results and Discussion

4.1 Carbonation Depth

Early stage (7 days) carbonation testing reveal little information on the effects of seeding additives as samples were held within moulds for the first 7 days of curing, with only a single face exposed and therefore subject to carbonation. Mid-study measurements (28 days) show all seeding materials to have a positive impact on carbonation depth compared with the un-seeded control samples. This positive carbonation effect was most noticeable in the Limestone seeded materials. The positive effects of the oyster shells are however short lived, with control samples exceeding carbonation of oyster shell seeded samples by 42 days. Limestone appears to be the only material that has any significant, prolonged impact on carbonation depth; the increase in carbonation depth achieved with calcium carbonate seeding at 42 days is likely to be within the error of measuring. All samples achieved full carbonation by 56 days (Fig. 1).

These results highlight the variation in effect of seeding materials on carbonation. These variations may be the result of differing compositions and/or physical forms of the seeding materials. Additionally, the small cross sectional area of the samples does not allow for the evaluation of long-term effects on carbonation; identifying how the reaction proceeds beyond 42 days.

4.2 Sorptivity

The water absorption in control and seeded samples was evaluated by determining sorptivity between 7 and 56 days (Fig. 2).

Results show that the control samples exhibited the greatest sorptivity compared to all modified mortars. This could suggest that seeding materials create a segmented pore structure relative to the control samples interconnected system. As all seeded material was crushed to the same sieve fraction, and directly substituted for aggregate particles of the same size, it is more likely that pore resistance to liquid water occurred as a result of an increase in the formation of products of hydration,

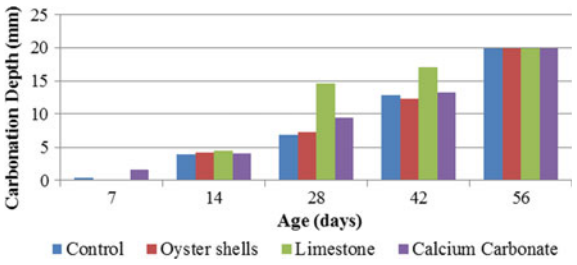

Fig. 1 Average carbonation depth of mortar samples

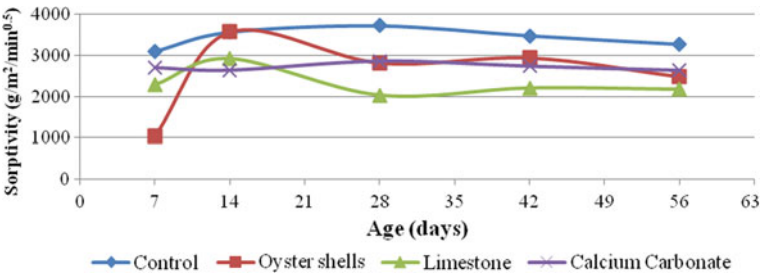

Fig. 2 Sorptivity of mortar samples

rather than from any direct impedance associated with the seeding grains themselves. That said, such effects would not typically be expected until after 28 days as hydration products in hydraulic limes form primarily from the hydration of slower acting β-belite rather than the faster acting alite or aluminium silicate components found in Portland Cement; sorptivity results exhibit relative stability by 28 days. Fluctuations in early stage sorptivity (7–28 days) are inconsistent with variations expected from the carbonation and hydration of typical hydraulic lime mortars. It may be the case that minor components within the seeding materials may have impacted upon the reactions in progress, however further trace element chemical analysis would be required to clarify this.

4.3 Tensile and Compressive Strength

Experimental results indicate a clear difference between the seeded specimens and the control samples with regards to the development of both tensile and compressive strength (Figs. 3 and 4).

All samples exhibited an elevated flexural strength at 7 days that subsequently decreased at 14 days. This could be potentially associated with high initial moisture contents in the samples; when the samples had subsequently dehydrated at 14 days

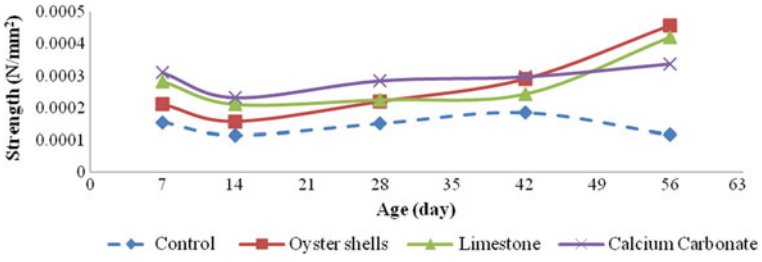

Fig. 3 Tensile strength of mortar samples

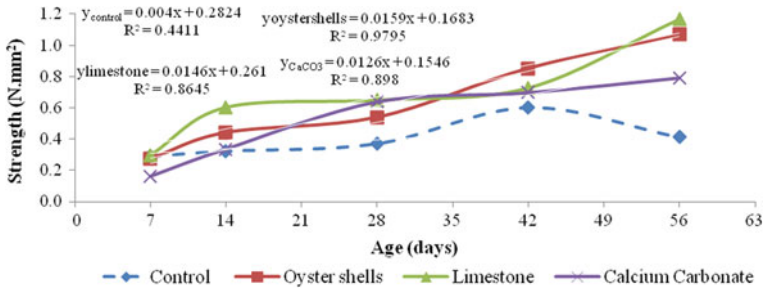

Fig. 4 Compressive strength of mortar samples

the flexural strength decreased. The seeded materials exhibited higher flexural strength than the control mortar throughout the test period, elevating significantly at 56 days; it is unclear why the control sample displayed a decline in flexural strength at 56 days, this may be a reflection of changes (an increase) in pore structure associated with carbonation although this does not correlate with the formation of hydration productions, which would also be expected within this time period (42–56 days).

Figure 4 shows the variation of the compressive strength for the range of mortars. The control specimen exhibited a significant loss of strength between, 42 and 56 days unlike the seeded mortars which continued to gain strength. The relative increase in compressive strength in the seeded material is most likely associated with the disproportionate reliance on carbonation in strength development first month prior to the hydration of belite. Providing 'nucleation sites' for the carbonation of portlandite will in itself promote strength development, as well as producing a hydration-promoting environment at later stages (i.e. a solution that is not supersaturated with Ca^{2+} ions and therefore does not inhibit hydration).

5 Conclusions

This work has highlighted the impact that calcitic seeding materials have on NHL 3.5 lime mortars. The effects of seeding materials undoubtedly vary with type, possibly due to variations in trace element chemistry and in physical form/crystallinity. In general, calcitic materials have a positive influence on the strength development and rapidity of carbonation of the hydraulic lime mortars exposed to high humidity and temperature environments. In line with the impact on strength development, seeding materials have shown a negative impact on sorptivity characteristics. This is most pronounced in the limestone seeding materials.

These results go some way in identifying the most appropriate calcitic media for seeding lime mortars. The relationship between mortars and seeding materials is clearly complex. Further analysis on the seeding materials themselves may help to

explain some of the discrepancies evident in this work. It is evident that the addition of limestone chips in the range of into moderately hydraulic lime used for high humidity environments will accelerated the set.

References

Allen, G. (2003). *Hydraulic lime mortar for stone, brick and block masonry*. Shaftesbury: Donhead.

Allen, G., Allen, J., Elton, N., Farey, N., Holmes, S., Livesey, P., Radonjic, M. (2003). *Hydraulic lime mortar for stone, brick and block masonry*. Dorset: Donhead.

Ball, R. J., El-Turki, A., & Allen, G. C. (2009). Influence of carbonation on the load dependant deformation of hydraulic lime mortars. In *11th International Conference on Non-conventional Materials and Technologies (NOCMAT 2009)*. Bath, UK.

Ball, R. J., El-Turki, A., & Allen, G. C. (2011). Influence of carbonation on the load dependent deformation of hydraulic lime mortars. *Materials Science and Engineering A, 528*(7–8), 3193–3199.

British Standards, I. (2010). BS EN 459-1: 2001 Building lime: Definitions, specification and conformity criteria. BSI Group, UK.

British Standards, I. (2010). BS EN 459-2: 2010 Building lime. Test methods. BSI Group, UK.

BS EN 196-1. (2005). Methods of testing cement: Part 1 determination of strength. BSI Group, UK.

BS EN 13139: 2002 Aggregates for mortars. BSI Group, UK.

Desai, S. N., Patel, S., & Patil, H. H. (2011). Elevated temperature curing of concrete with industrial wastes. *International Journal of Advanced Engineering Technology, 2*(4).

Dheilly, R. M., Tudo, J., Sebai bi, Y., & Quéneudec, M. (2002). Influence of storage conditions on the carbonation of powdered $Ca(OH)_2$. *Construction and Building Materials, 16*.

Dotter, K. R. (2010). Historic lime mortars: Potential of local climate on the evolution of binder morphology and composition. In B. J. Smith, C. Robin, & M. Gomez-heras (Eds.), *Limestone in the built environment: Present-day challenges for the preservation of the past*. Bath: The Geological Society Publishing House.

El-Turki, A., Ball, R. J., & Allen, G. C. (2007). The influence of relative humidity on structural and chemical changes during carbonation of hydraulic lime. *Cement and Concrete Research, 37*(8).

Ezziane, K., Bougara, A., Kadri, A., Khelafi, H., & Kadri, E. (2007). Compressive strength of mortar containing natural pozzolan under various curing temperature. *Cement & Concrete Composites, 29*.

Forster, A. M. (2004). *How hydraulic lime binders work: Hydraulicity for beginners and the hydraulic lime family*. Edinburgh: Love Your Building Publishing.

Forster, A. M., & Carter, K. (2011). A framework for specifying lime mortars for rubble masonry construction. *Structural Survey: Journal of Building Pathology & Refurbishment*, *29*(5), 373–396.

Forsyth, M. (2007). *Understanding historic building conservation*. Oxford: Blackwell Publishing.

Gibbons, P. (2003). *Preparation and use of lime mortar*. Edinburgh: Historic Scotland.

Hall, C., Hamilton, A., Hoff, W. D., Viles, H. A., & Eklund, J. A. (2010). Moisture dynamics in walls: Response to micro-environment and climate change. *Proceedings of the Royal Society A Mathematics, Physical & Engineering Sciences*.

Hall, C., & Hoff, W. D. (2002). *Water transport in brick, stone and concrete* (2nd ed.). London: Spoon Press.

Hewlett, P. (2004). *Lea's chemistry of cement and concrete* (4th ed.). Oxford: Butterworth-Heinemann.

Hughes, J. J., & Valek, J. (2003). *Mortars in historic buildings: a review of the conservation, technical and scientific literature*. Edinburgh: Historic Scotland.

Lawrence, R. M. H. (2006). *A study of carbonation in non-hydraulic lime mortars*. Ph.D. Thesis. University of Bath.

Lo, Y., & Lee, H. M. (2002). Curing effects on carbonation of concrete using a phenolphthalein indicator and Fourier-transform infra-red spectroscopy. *Building and Environment, 37*(5).

Pacheco Torgal, F., Miraldo, S., Labrincha, J. A., & De Brito, J. (2012). An overview on concrete carbonation in the context of eco-efficient construction: Evaluation, use of SCMs and/or RAC'. *Construction and Building Materials, 36*.

Pavia, H. S. (2008). A study of the workability of natural hydraulic lime mortars and its influence on strength. *Materials and Structures, 41*(2).

Radonjic, M., Hallam, K. R., Allen, G. C., & Hayward, R. (2001). Mechanism of carbonation in lime-based materials. In *Proceedings of the 8th Euro seminar On Microscopy Applied to Building Materials*, Athens (Greece), pp. 465–75.

Taylor, H. F. W. (1997). *Cement chemistry* (2nd ed.). London: Thomas Telford Publishing.

Viability of Ceramic Residues in Lime-Based Mortars

G. Matias, P. Faria and I. Torres

Abstract When we approach the subject of construction and rehabilitation of buildings we necessarily must think about external wall coatings as they are the elements more exposed to climate actions, mechanical and environmental conditions and, consequently, the first to be deteriorated and to need rehabilitation. Concerning to the replacement of old plasters and renders, air lime mortars are normally the ones that are more compatible with the existing elements, presenting, however, some limitations due to its slow setting time. As an alternative we may use natural hydraulic lime mortars. We know that brick dust and grains have been widely used in mortars in the past, improving its characteristics, and that actually there are many kinds of ceramic residues that are byproducts of industry and are normally carried into landfills. Within this context and associating the improvement of mortars characteristics to the necessity of sustainable construction practices, some mortars, formulated based on air lime or natural hydraulic lime, with the addition of ceramic residues, have been recently studied. The aim of this paper is to present the experimental work that has been developed concerning the behaviour of two types of these lime mortars with ceramic residues. Characteristics, particularly in terms of flexural and compressive resistances, capillary water absorption and water vapour permeability will be discussed. Comparison will be made between the characteristics of the mortars made with the two limes, and of mortars made with those limes with partial substitutions of siliceous sand by different types of ceramic

G. Matias (✉)
ITeCons—Institute for Research and Technological Development in Construction, Energy, Environment and Sustainability, Coimbra, Portugal
e-mail: ginamatias@itecons.uc.pt

P. Faria
UNIC, Department of Civil Engineering, Faculty of Sciences and Technology of NOVA, University of Lisbon, Lisbon, Portugal
e-mail: paulina.faria@fct.unl.pt

I. Torres
Department of Civil Engineering, Faculty of Sciences and Technology, University of Coimbra, Coimbra, Portugal
e-mail: itorres@dec.uc.pt

J. J. Hughes et al. (eds.), *Historic Mortars*,
https://doi.org/10.1007/978-3-319-91606-4_16

residues. It will be possible to draw same conclusions about the interest and viability of recycling the ceramic residues as aggregates, its contribution as pozzolan and filler, and also if natural hydraulic lime-based mortars can be a good alternative to air lime-based mortar for ancient masonry.

Keywords Air lime mortars · Natural hydraulic lime mortars · Ceramic residues

1 Introduction

First signs of lime mortars with ceramics incorporation appear in 3000 A.C. buildings, during the Babylonian Empire (Moropoulou et al. 2005). However, it is during the Roman Empire (2nd cent. BC) that brick shards introduction in mortars arises and the technique would ultimately be spread through all South Europe, North Africa and Asia. Catone and Vitruvius were, during that period, the main authors to characterize and register this type of solution (Baronio et al. 2006). They were applied with some different designations: "cocciopesto", "opus testaceum", "surkhi", "homra", "horasan", among others (Moropoulou et al. 2005; Böke et al. 2006; Bakolas et al. 1998; O'Farrell et al. 2006). Brick shards were introduced in mortars as dust, to act as pozzolans or filler, or in bigger granular sizes as a partial replacer of aggregates. Each fraction's introduction depended, essentially, on the type of mortar and its function—in plasters, smaller particles were used while in masonry mortars, for example, granular particles could be used (Moropoulou et al. 2005). It is possible to find, in Portugal, some signs of these types of mortars, in archaeological sites where Roman Empire ruins are found, such as Troia and Conimbriga.

From the functionality point of view, and considering some characterization works that have been already performed, air lime mortars and hydraulic lime mortars incorporating these materials have revealed improved behaviour, when compared with simple lime mortars. The apparent hydraulic behaviour of lime mortars with calcinated clays it is due to pozzolanic reactions developed, conditioned by aspects such as smaller particles' specific surface and the amounts of silica and alumina in amorphous state. When combined with calcium hydroxide contained in lime, silica and alumina from ceramic products generate silicates and aluminates which provide hydraulic properties to mortars. According to major authors, the amount of silica and alumina is one of the most essential conditions to reactivity. However, these materials should appear in amorphous state, which is mainly conditioned by clays calcination temperatures (Böke et al. 2006). It is believed that, for most of the argillaceous raw materials, ideal calcination temperatures goes around 800–1000 °C, depending on the author (Böke et al. 2006; Charola et al. 2005; Pereira-de-Oliveira et al. 2012; Toledo Filho et al. 2007). On the other hand, when used in a granular way, residues could develop cohesion mechanisms with the binder, whose behaviour is still not well known (Böke et al. 2006).

As a substitute of commonly used aggregates in mortars or as dust, the use of ceramics waste presents several advantages, from the economic, ecologic and energetic point of view. As dust, when pozzolanic reactions occur, this product might contribute to conventional binders' consuming reduction. In this way, it is possible to reduce energetic consumptions due to raw materials' calcination at high temperatures and also to reduce CO_2 emissions (Toledo Filho et al. 2007).

As an aggregate partial replacer, ceramic residues can contribute to the reduction of use of natural resources and prevent the dangerous environmental impacts caused by natural minerals' extraction. Generally, this proposal of industrial ceramic waste recovery will allow an actual solution for wastes that in most of the cases are disposed into landfills.

In this study, some air and hydraulic lime mortars were prepared, with residues from ceramic industries of the central region of Portugal. These residues were mainly obtained from brick, tile and decorative pot production. After milling, the residues, that according to producers were calcinated at temperatures between 900 and 1000 °C, were introduced into lime mortars as a replacer of the common aggregate with different proportions. This analysis allowed the understanding of the influence of each kind of residue in mechanical and physical behaviour of the mortars. It is presented a brief characterization of fresh state mortars. Mechanical strength, water vapour permeability and water absorption due to capillary action were also determined at distinct ages (28, 60 and 120 days).

With this work it is intended to extend the knowledge of viable solutions for old buildings repair mortars, as well as to create guidelines that will allow the generation of real and applicable products. This type of mortars could produce solutions to problems such as incompatibility between available recent products and old supports or existing mortars, not forgetting the environmental, economic and energetic causes, the engines for sustainability.

2 Experimental Procedure

2.1 Materials Characterisation

Mortars were made using hydrated powder air lime and natural hydraulic lime as binders, a river sand and ceramic residues.

Air lime, designated as CL 90 according to EN 459-1:2010 standard, was produced by Lusical (designed as H100). Its $Ca(OH)_2$ minimum content is 93%. Natural hydraulic lime was provided by Secil Martingança and it is classified according to EN 459-1:2010 as NHL3.5. This product has a declared $Ca(OH)_2$ content higher than 25% and less than 2% sulphates.

Ceramic residues collected from brick, tile and decorative pot industries were crushed, with a laboratory Retsch jaw crusher, with a 10 mm cribble. The material was characterized in what concerns to particle size distribution. Particle size

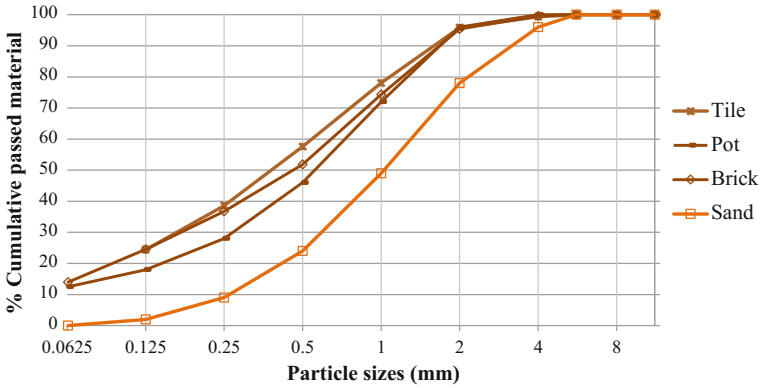

Fig. 1 Ceramic residue and sand particle size distribution

Table 1 Loose bulk density, ρb, of the materials

	Brick (B)	Tile (T)	Pot (P)	River Sand	CL	NHL3.5
ρ_β (Mg/m^3)	1.10	1.17	0.99	1.54	0.36	0.81

distribution of the ceramic residues and of the siliceous sand used as mortar constituents, determined according to EN 933-1:1997, is presented in Fig. 1. Loose bulk density was also determined to allow weight proportions' evaluation. The value obtained for the limes, the sand and for each residue's, determined according to EN 1097-3:1998, is presented in Table 1.

From the analysis of Fig. 1 it can be noticed that residues particle size distribution after crushing is quite similar to the one of river sand. They are distinguished essentially from the percentage of particles smaller than 0.063 mm that, in residues' cases, represent 10% of the sample. Smaller particles from river sand are practically residual.

In terms of loose bulk density of the dry materials, all residues presented quite similar values, lower than river sand and close to hydraulic lime value. Air lime bulk density has the lowest value obtained.

2.2 Mixtures Characterisation

Several mortars' compositions were prepared with the materials described above. Main volumetric proportion was 1:3 (binder:aggregate) and for each type of residue, 20 and 40% of the natural sand was replaced. Mortars with 20% of sand's substitution were designated with an L (Low) and mortars with 40% of sands substitution were designated with an H (High). Mortars with brick residues were attributed B suffix, mortars with tile shards, T, and mortars with decorative pot were

attributed a P. Natural hydraulic lime mortars were designated with an NH prefix. Besides indicated mixtures, reference mortars without residues were also prepared and they were referenced with an R. These mortars allowed the evaluation of each residue influence, as well as the influence of the substitution percentages.

All mixtures were prepared with water amounts that allowed a consistency in fresh conditions of [135:165] mm, range that allow this type of lime-based mortars workability. This parameter was determined according to EN 1015-3:1999 standard (flow table method). Water/binder proportions were also determined and results are presented in Table 2. Table 3 indicates volumetric and weight proportions applied.

From fresh mortars, based on EN 1015-11:1999/A1:2006, cylindrical specimens for water vapour determination and prismatic specimens for mechanical strengths and water absorption were prepared. Specimens were kept in the first 5 days at 20 °C and 95% relative humidity (RH). They remained for 2 more days in 20 °C and 65% RH and were demoulded. They remained in these conditions until the age of test. The incorporation of ceramic residues also acted as a pigment and the mortars became slightly coloured.

2.3 Strength Resistances

Flexural and compressive strength resistances were determined, for each specimen, according to EN 1015-11:1999/A1:2006 standard specifications. For this purpose, three prismatic specimens were moulded, for each sample and curing period, with 40 mm × 40 mm × 160 mm dimensions. Specimens were kept in standard conditions until 28, 60 and 120 days. Compressive strength resistance was determined with one of the halves resultant from flexural strength resistance tests. Flexural strength results are indicated in Fig. 2, and compressive strength results are presented in Fig. 3.

It was observed that neither air lime mortars' flexural or compressive strength resistance presented a significant increase through time, except for mortars with high percentages of tile and pot residues. All mortars with high percentage of residues revealed clearly higher strength resistances. In all cases, mortars presented higher strength resistance values than both reference mortars, R and HR and in some cases resistances at 60 days curing were superior to ones obtained at 120 days.

2.4 Water Absorption Due to Capillary Action

Water absorption due to capillary action was determined at 28, 60 and 120 days, according to EN 15801:2009 standard recommendations, more appropriate to slow curing mortars as air lime ones. One of the two resultant halves from flexural resistant specimens was used and weightings were carried out at 5, 10, 15, 30, 60,

Table 2 Water/binder ratio (w/b) and flow value (fv)

Mortar	R	LB	HB	LT	HT	LP	HP	NHR	NHLB	NHHB	NHLT	NHHT	NHLP	NHHP
w/b(m/m)	2.85	2.21	2.56	2.62	2.35	2.35	2.63	0.91	1.02	1.06	0.99	1.08	0.98	1.07
fv (mm)	147.6	150.8	152.9	151.3	153.2	151.4	151.0	151.8	143.1	141.8	164.6	162.3	154.8	148.9

Table 3 Volumetric and weight proportions

Mortar	CL	NHL3.5	Residues			Sand	Volumetric proportions	Weight proportions
			B	T	P			
R	1	–	–	–	–	3	1:3	1:12.2
LB	1	–	0.6	–	–	2.4	1:0.6:2.4	1:1.8:10.2
HB	1	–	1.2	–	–	1.8	1:1.2:1.8	1:3.6:7.7
LT	1	–	–	0.6	–	2.4	1:0.6:2.4	1:1.9:10.2
HT	1	–	–	1.2	–	1.8	1:1.2:1.8	1:3.9:7.7
LP	1	–	–	–	0.6	2.4	1:0.6:2.4	1:1.9:10.2
HP	1	–	–	–	1.2	1.8	1:1.2:1.8	1:3.9:7.7
NHR	–	1	–	–	–	3	1:3	1:5.7
NHLB	–	1	0.6	–	–	2.4	1:0.6:2.4	1:0.8:4.5
NHHB	–	1	1.2	–	–	1.8	1:1.2:1.8	1:1.6:3.4
NHLT	–	1	–	0.6	–	2.4	1:0.6:2.4	1:0.9:4.5
NHHT	–	1	–	1.2	–	1.8	1:1.2:1.8	1:1.7:3.4
NHLP	–	1	–	–	0.6	2.4	1:0.6:2.4	1:0.7:4.5
NHHP	–	1	–	–	1.2	1.8	1:1.2:1.8	1:1.5:3.4

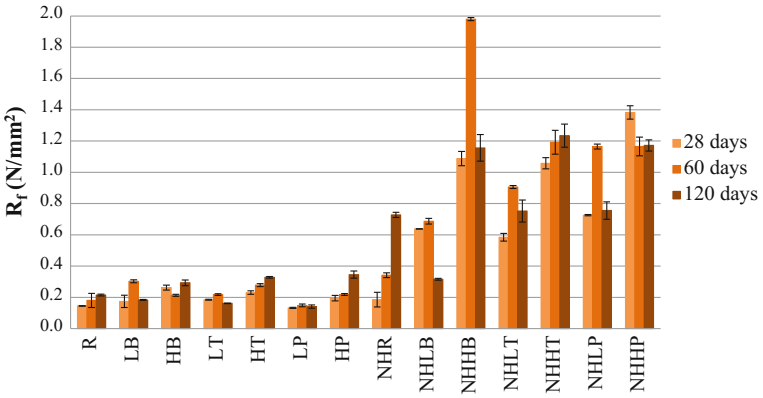

Fig. 2 Flexural strength at 28, 60 and 120 days of curing

90, 120, 180 min and each 24 h after first contact of the specimens with the water slide, until constant mass was reached. Water absorption coefficient, graphically determined, is represented in Fig. 4. Figures 5 and 6 show the 1st hour of the absorption curves, at 28 and 120 days of curing, respectively.

Generally air lime mortars obtained higher capillary coefficient values. However, these ones also generated more uniform values regarding to residue type and curing period. Hydraulic lime mortars' capillary coefficients resulted in discrepant results that did not allow any evident conclusions. Nonetheless, at 120 days curing,

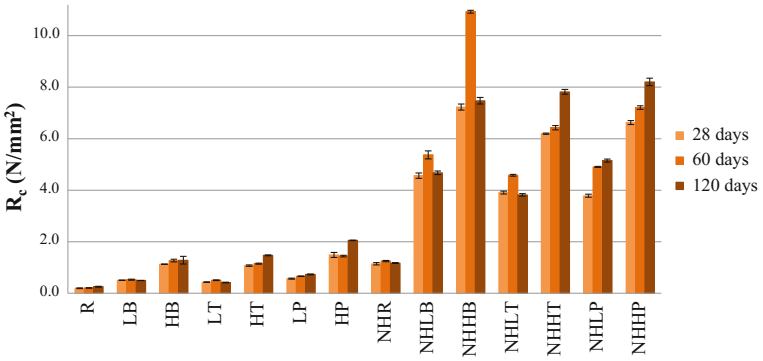

Fig. 3 Compressive strength resistances at 28, 60 and 120 days of curing

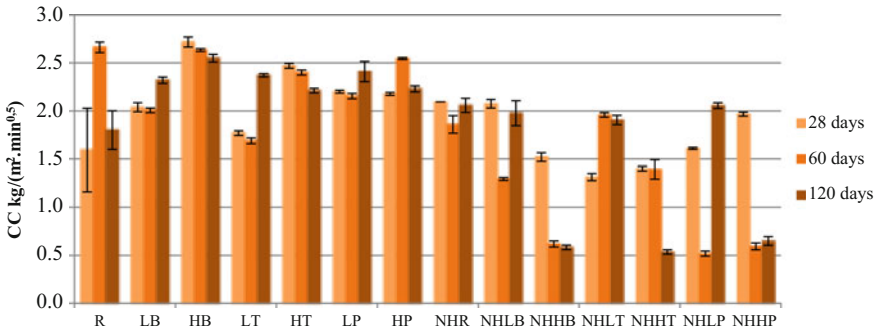

Fig. 4 Capillary coefficient at 28, 60 ad 120 days

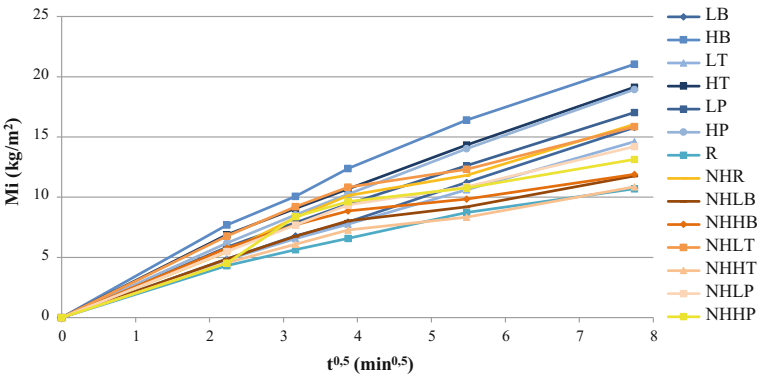

Fig. 5 Water absorption due to capillary action, 28 days curing (1st hour)

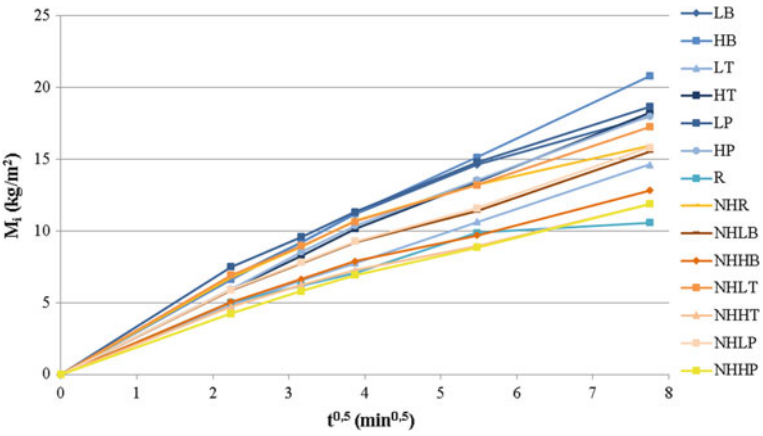

Fig. 6 Water absorption due to capillary action, 120 days curing (1st hour)

hydraulic lime mortars with high residues' percentage obtained the lower water absorptions by capillary. Air lime mortars, at this period, resulted in higher water absorptions.

In what concerns to water absorption during the 1st hour of test, represented in Figs. 5 and 6, high residue percentage air lime mortars shown higher water absorption velocities (with higher water absorption's curve bent) and air lime mortars with tile residues presented lower water absorption velocities. In general, hydraulic lime mortars revealed slower water absorptions. It was verified, however, that after 120 days, hydraulic lime mortars behaviour tends to approach to air lime ones, as their water absorption velocities suffer a slight increase.

2.5 Water Vapour Permeability

Three circular specimens were prepared for each mortar, with an approximated diameter of 100 mm and thickness of 17 mm. Following the procedure indicated by ISO 12572:2001 standard, wet cup method was selected. Tests were performed at 28, 60 and 120 days. Figure 7 shows the obtained results for water vapour permeability at indicated ages, as well as standard deviation associated to each result. Figure 8 presents the water vapour diffusion-equivalent air layer thickness values, S_d, which allows thickness evaluation of an equivalent air layer in terms of water vapour resistance.

With respect to the type of binder, evident water vapour permeability differences were observed. Water vapour permeability values obtained for air lime mortars with residues are always higher than those with NHL3.5 and residues. The mortars with

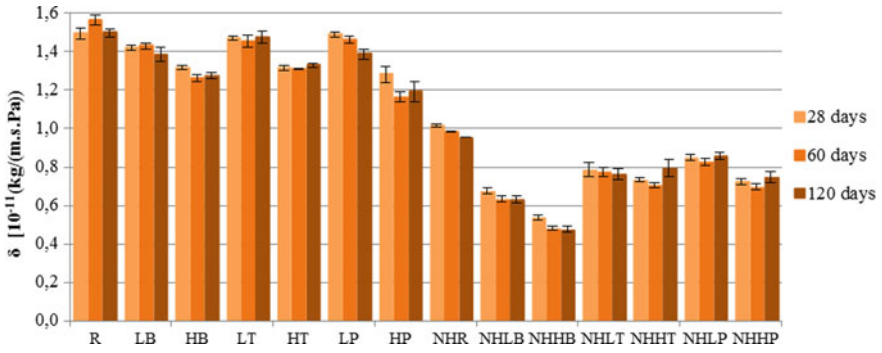

Fig. 7 Water vapour permeability

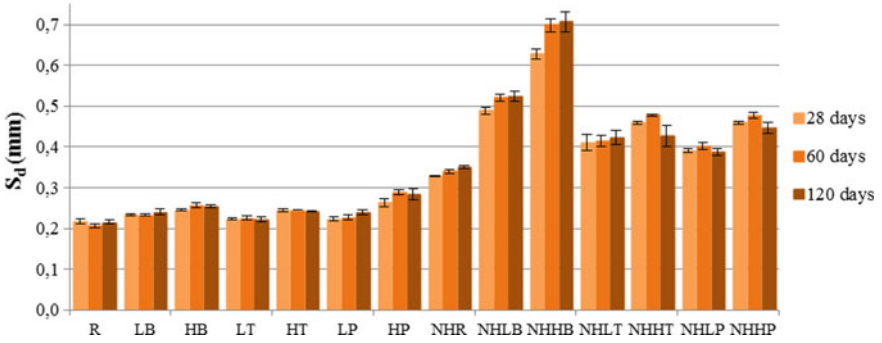

Fig. 8 Water vapour diffusion-equivalent air layer thickness

NHL3.5 and brick residues present the lowest water vapour permeability. The addition of ceramic residues decreases the permeability almost for all mortars but is more pronounced for mortars with brick residue and for higher percentage of substitution. Concerning to water vapour diffusion-equivalent air layer thickness, all air lime mortars obtained quite uniform values, significantly lower than ones obtained from hydraulic lime mortars.

In the case of the last ones it was possible to observe evident differences related to substitution's percentage: low residues' percentage mortars presented lower water vapour diffusion-equivalent air layer thickness values, as expected considering water vapour permeability results. Highest water vapour resistance mortar was the one with hydraulic lime and high brick residue's percentage. Also, in both water vapour permeability and air layer thickness, significant standard deviations were not detected.

3 Discussion

Regarding to mechanical behaviour, strength resistances of air lime mortars with high percentage of residues from tile and pot residues might be related to some kind of pozzolanic reactivity. The fact that all mortars with residue presented higher resistance values than the correspondent reference ones may also be an indicator of this type of reaction. These results may also be related with the substitution of common rounded aggregates by irregular and angular surface residues that could contribute to materials cohesion. It was not found any reason for the fact that some mortars obtained higher values at 60 days than at 120 days curing. The causes for these results should be explored in following studies to see if there are instable products that may be formed at around two months of age and then are transformed in other products (Grilo et al. 2014a, b). In fact, Gameiro et al. (2014) observed a similar behaviour for air lime and metakaolin mortars, and established a relation between mechanical strength reduction and calcium hydrate aluminate instability in the presence of free lime. After longer curing periods, this instability disappeared as free lime was consumed during carbonation and pozzolanic reactions.

The fact that mortars do not reach the standardized strength must be due to the use of different aggregates, water/binder ratio and mixture procedures and curing conditions. In the specific case of moisture conditions, Grilo et al. (2014a, b), Gameiro et al. (2014) verified that higher relative humidity (RH) conditions provided natural hydraulic lime mortars higher mechanical strengths, especially when pozzolanic reactions were involved. In this specific case, metakaolin partially replaced NHL. They observed that the exposition to a 90% RH during the curing period promoted lime hydration and pozzolanic reactions, with direct impact in the porous structure. Higher RH led to a reduction of pore size and, consequently, to the increase in mechanical strengths.

In terms of water absorption due to capillary action at the 1st hour of test, hydraulic lime mortars presented more satisfying values, for their slower water absorption. However, their behaviour tended to approach from air lime ones for longer curing periods (120 days). Generally, this parameter is directly related to water vapour permeability: higher water vapour permeability mortars resulted in higher water absorption due to capillary action. Thereby it is possible to relate water absorption with mortars' porous structure, as this occurs essentially due to smaller pores.

Regarding to water vapour permeability, all mortars with high percentage of residue revealed lower permeability values when compared to correspondent low residue percentage mortars. This behaviour might be related to higher amounts of residues' small particles, which leads to finer porous structures. The absence of significant differences through time might be an indication of the unchanged porous structures due to carbonation and hydration process.

When requirements for old buildings substitution mortars, applied as renders, plasters or repointing (Veiga et al. 2010) are analysed, water vapour diffusion-equivalent air layer thickness should present values inferior to 0.1 mm. In this

study, none of the mortars fulfils this requirement. However, air lime mortars obtained close values, whereby they might be considered adequate for the effect that is purposed. In what concerns to capillary coefficient, it is defined an interval from 1.0 kg/(m^2/$min^{1/2}$) to 1.5 kg/(m^2/$min^{1/2}$). Most hydraulic lime studied mortars, in different curing periods, presented quite close values and air lime mortars present slightly higher values. Mortars which revealed better capillary behaviour were the ones with tile residues. Veiga et al. (2010) also define adequate strength resistance values: flexural strength resistance should be between 0.2 and 0.8 N/mm^2. Air lime mortars obtained values quite close from the minimum value defined and low residue substitution hydraulic lime mortars presented higher values but very close to maximum flexural strength resistance defined. In this way, these two groups seemed to be the ones with a more adequate flexural strength behaviour for rehabilitation purposes. In what concerns to compressive strength resistance, ideal values might be between 0.4 and 3 N/mm^2. Air lime mortars with high residue substitution fulfil this requirement. Natural hydraulic lime mortars with low residue substitution are quite close the maximum limit defined. It should be taken into account that test methodologies might have some differences and, as so, direct results comparison must be careful.

4 Conclusions

In mechanical behaviour terms, air lime mortars with high residue substitution and natural hydraulic lime mortars with low residue substitution have shown a better performance for low strength repair requirements. Through the analysis carried out, it may be said that there is clear evidence of the existence of some pozzolanic reactivity.

In what concerns to physical behaviour, it was observed that water vapour permeability and water absorption due to capillary action are closely related to porous structure and small pores amount and it was concluded that residues' material properties might have an insignificant influence on water absorption properties. Generally, obtained results were quite satisfying when compared to reference documents consulted.

Globally, it is considered that studied mortars have a quite satisfying behaviour and the residues inclusion may improve the characteristics of common lime mortars. Some natural hydraulic lime mortars with residues may present too high resistance for some old buildings; however formulations of mortars with lower binder proportions may be tested and its characteristics might be adjusted to the characteristics of the existent buildings.

Having mortars with improved behaviour when formulated with ceramic residues, that are generally land filled, encourage the development of rehabilitation mortars with formulations based on these studies.

References

Bakolas, A., Biscontin, G., Moropoulou, A., & Zendri, E. (1998). Characterization of structural byzantine mortars by thermogravimetric analysis. *Thermochimica Acta, 321,* 151–160.

Baronio, G., Binda, L., & Lombardini, N. (2006). The role of brick pebbles and dust in conglomerates based on hydrated lime and crushed bricks. *Construction and Building Materials, 11,* 33–40.

Böke, H., Akkurt, S., İpekoğlu, B., & Uğurluet, E. (2006). Characteristics of brick used as aggregate in historic brick-lime mortars and plasters. *Cement and Concrete Research, 36,* 1115–1122.

Charola, E., Faria-Rodrigues, P., McGhie, A., & Henriques, F. (2005). Pozzolanic components in lime mortars: correlating behaviour, composition and microstructure. *Restoration of Buildings and Monuments, 11*(2), 111–118.

Gameiro, A., Santos Silva, A., Faria, P., Grilo, J., Branco, T., Veiga, R., et al. (2014). Physical and chemical assessment of lime–metakaolin mortars: Influence of binder: aggregate ratio. *Cement & Concrete Composites, 45,* 264–271.

Grilo, J., Faria, P., Veiga, R., Santos Silva, A., Silva, V., & Velosa, A. (2014a). New natural hydraulic lime mortars—Physical and microstructural properties in different curing conditions. *Construction and Building Materials, 54,* 378–384.

Grilo, J., Santos Silva, A., Faria, P., Gameiro, A., Veiga, R., & Velosa, A. (2014b). Mechanical and mineralogical properties of natural hydraulic lime-metakaolin mortars in different curing conditions. *Construction and Building Materials, 51,* 287–294.

Moropoulou, A., Bakolas, A., & Anagnostopoulouet, S. (2005). Composite materials in ancient structures. *Cement & Concrete Composites, 27,* 295–300.

O'Farrell, M., Sabir, B. B., & Wild, S. (2006). Strength and chemical resistance of mortars containing brick manufacturing clays subjected to different treatments. *Cement & Concrete Composites, 28,* 790–799.

Pereira-de-Oliveira, L. A., Castro-Gomes, João P., & Santos, Pedro M. S. (2012). The potential pozzolanic activity of glass and red-clay ceramic waste as cement mortars components. *Construction and Building Materials, 31,* 197–203.

Toledo Filho, R. D., Gonçalves, J. P., Americano, B. B., & Fairbairn, E. M. R. (2007). Potential for use of crushed waste calcined-clay brick as a supplementary cementitious material in Brazil. *Cement and Concrete Research, 37,* 1357–1365.

Veiga, M., Fragata, A., Velosa, A., Magalhães, A., & Margalha, G. (2010). Lime-based mortars: Viability for use as substitution renders in historical buildings. *International Journal of Architectural Heritage, 4,* 177–195.

Effects of Various Chemical Agents on Mechanical Characteristics of Weak Lime Mortar

Z. Slížková and M. Drdácký

Abstract Lime water treatment on a specific lime mortar was tested and evaluated for effectiveness, showing that after a sufficiently high number of applications (160 cycles, 54–80 days of a permanent consolidation treatment) some of the poor mechanical characteristics (compression and surface cohesion) were substantially improved. The lime water treatment was also compared with some other less labour-intensive technologies. The most efficient agents were dispersions of calcium hydroxide in alcohols, which are marketed under the trade name CaLoSiL by the German producer IBZ Freiberg. The major advantage with these agents is that they can be applied much more rapidly than tens to hundreds of lime water cycles and they deliver a higher amount of lime in each cycle. While lime water contains only small calcium ions, sized about 0.1 nm, calcium hydroxide particles in CaLoSiL are considerably larger (50–200 nm). This property makes the use of these nanolime dispersions limited to structural consolidation of porous material with a sufficiently large pore diameter. Nanolime dispersions applied to mortar where the majority of pores are around 100 μm in diameter is efficient enough to allow for a one-day application of CaLoSiL E15 (7 cycles), to reach significant strengthening. It appears from the results that lower concentrations of CaLoSiL (E 15) create a better distribution of the new binder and therefore lead to higher compression strength than the more concentrated CaLoSiL (IP 25). Diluted, 8% silicic acid ester, applied in two cycles, showed the same consolidation effect as CaLoSiL E 15 applied in 7 cycles. Surface cohesion of mortar was improved following most of the consolidation treatments tested, including multiple applications of ammonium oxalate and barium water. Addition of metakaolin to lime water did not provide any added strengthening benefit. However, the combination of silicic acid ester with nano-lime product (CaLoSiL IP 25) was shown to be effective.

Z. Slížková (✉) · M. Drdácký
Institute of Theoretical and Applied Mechanics AS CR, V. V. I, Telč, Czech Republic
e-mail: slizkova@itam.cas.cz

M. Drdácký
e-mail: drdacky@itam.cas.cz

J. J. Hughes et al. (eds.), *Historic Mortars*,
https://doi.org/10.1007/978-3-319-91606-4_17

Keywords Lime mortar · Historic render · Historic plaster · Consolidation Strengthening · Treatment · Consolidant · Nanolime

1 Introduction

Consolidation treatment is an important conservation intervention aiming to improve lost cohesion of porous materials. This action usually requires either activating the remaining binder, or introducing a new binder into the degraded layer of historic material. The different types of binders applied in a liquid state onto degraded materials for this purpose are referred to as consolidating agents (or e.g. consolidants, strengtheners, etc.). These products can be applied to the surface using various procedures (coating, spraying, pouring, poultice, injection) and tools (brush, sprayer, syringe, pipette etc.) and should be able to penetrate the degraded layer to a pre-determined depth. This paper addresses the consolidation of plasters and renders for a depth range of several millimetres at the surface. When the mortar absorbs the liquid product, the hardening process, specific for the product type, should start and induce consolidation of the degraded material.

The efficiency of the consolidation treatment depends on the product used, the mortar or stone characteristics, the application procedure, and the ambient conditions during and after the product application (Ferreira Pinto and Delgado Rodrigues 2007). The research presented in this paper aimed to test the effect of various consolidation agents applied to a poor lime mortar under laboratory conditions. First, compressive strength of the treated mortar was evaluated. Laboratory prepared specimens resembling the historical poor lime mortar were consolidated with various individual and combinations of consolidant products. The selection of the tested products was based on recent conservation practice and on scientific literature encompassing mortar and stone consolidation research (Millar 1897; Mora et al. 1977; Peterson 1982; Price 1984; Quayle 1996; Brajer and Kalsbeek 1999). The present paper focuses on the effects of lime water applied through different procedures and its performance in comparison with the strengthening effects of lime nanodispersions and other consolidating agents.

2 Experiment

The literature review indicated very slight effects of repeated wetting of degraded stone with lime water, with regards to both penetration and strengthening (Price et al. 1988). Therefore, the current experiment was developed with specific mortar test specimens designed and prepared in the shape of short tubes for compression tests, and thin plates for tension tests. The specimens were fabricated from a very poor (lean and weak) lime mixture and moulded in stainless casts (with no separation treatment of steel walls), and were well compacted. This enabled the

specimens to be pushed out from the cast immediately after moulding, and prevented the development of shrinkage defects. The tubular cast increased the surface-to-cross-section area ratio and intensified the measurable strengthening effect. The shape of the specimens and the absence of separation layers also improved the penetration of the agent and the maturing conditions. The material ready for impregnation was very porous and could be crushed easily between the fingers. Porosity of the reference lime mortar specimens determined by mercury intrusion porosimetry was 28% and a significant number of pores had a diameter of about 100 μm. The specimens were made of lime mortar prepared from powdered air lime hydrate and river quartz sand in a ratio of 1:9 by volume, and were left to harden for 6 months. Then the consolidating agents were applied, and after treatment, the specimens were left to mature for 60 days further.

The following consolidation substances were applied: distilled water, calcium hydroxide saturated solution in water ("lime water"), lime water + metakaolin, calcium hydroxide colloidal solutions in alcohols ("nanolime" CaLoSiL E15, CaLoSiL IP25), barium hydroxide 5% w/w solution in water ("barium water"), calcium sulphate saturated solution in water ("sulphate water"), ammonium oxalate solution in water (2.5% resp. 5% w/w), colloidal solution of silica in water (silica sol), silicic acid ester (SAE) solution in ethanol (ethyl silicate) and various combinations of lime and silica based consolidants. Calcium sulphate solution treatments should resemble the phenomenon that occurs where the gypsum crust developed on the historical surface dissolves during the consolidation treatment from repeated watering and redistributes in the treated mortar layer. The applied consolidation substances are listed in Table 1 together with data of the consolidation procedure.

Commercial nanolime products CaLoSiL E15 and IP25 were applied without any adjustment. Silica-based products Dynasylan 40 and Kostrosol 0830 containing comparatively higher levels of silica were dissolved obtaining SiO_2 concentrations more suitable for poor lime mortar consolidation. Dynasylan 40 was dissolved with ethanol (1:4 weight parts) and Kostrosol 0830 with distilled water (1:9 w.). The final silica content in these products adjusted for mortar specimens treatment was about 8% w. and 3% w. for Dynasylan and Kostrosol, respectively. Water solutions of calcium hydroxide, barium hydroxide, calcium sulphate and ammonium oxalate were prepared using chemical products p.a. (pro analysi) and distilled water. For the lime water modified with pozzolanic material, the commercially available metakaolin Mefisto L 05 (ČLUZ Nové Strašecí, CR) was used (2 g of calcium hydroxide, 2 g of metakaolin in l L of distilled water). All active substances contained in the consolidating agents prior to application on the mortars are presented in Table 1.

Each agent was applied by continually excreting it from a syringe onto the tubes fixed in a horizontal position on a rotating shaft (tubes, Fig. 1). The mortar specimens were fully saturated during each individual application, and the amount of liquid applied was monitored and recorded. Two different variations of the drying time interval were tested: first, 2 applications per day were performed and the tubes were allowed to dry completely before each new application; and second, 3

Table 1 Substances and consolidation treatment used in the experiment

Tested agent, active substance % w.	Commercial product (*d* = *diluted*)	Number of applications per 1 day	Total number of applications	Total amount applied (l/m^2)	Total time treatment (days)
Distilled water		2	50	55	25
Distilled water		2	160	180	80
Lime water, $Ca(OH)_2$ 0.16%	$Ca(OH)_2$ p.a.	2	50	52	25
Lime water, $Ca(OH)_2$ 0.16%	$Ca(OH)_2$ p.a.	3	58	58	19
Lime water, $Ca(OH)_2$ 0.16%	$Ca(OH)_2$ p.a.	2	160	156	80
Lime water, $Ca(OH)_2$ 0.16%	$Ca(OH)_2$ p.a.	3	160	155	54
Lime water + Metakaolin	+Mefisto L 05	3	58	55	19
Lime water + Silica sol	+Kostrosol 0830 *d*.	3	58 + 5	56 + 3.5	19 + 2
Sulphate water, $CaSO_4$ 0.26%	$CaSO_4.2H_2O$ p. a.	2	50	51	25
Sulphate water, $CaSO_4$ 0.26%	$CaSO_4.2H_2O$ p. a.	3	58	58	19
Barium water, $Ba(OH)_2$ 5%	$Ba(OH)_2.8H_2O$ p.a.	3	58	57	19
Ammonium oxalate water, 5%	$(NH_4)_2C_2O_4.H_2O$	3	58	27	19
Ammonium oxalate water, 2.5%	$(NH_4)_2C_2O_4.H_2O$	3	38	32	13
Nanolime, $Ca(OH)_2$ 1.5%	CaLoSiL E 15	12	40	30	3.5
Nanolime, $Ca(OH)_2$ 1.5%	CaLoSiL E 15	7	7	6.5	1
Nanolime, $Ca(OH)_2$ 2.5%	CaLoSiL IP 25	12	40	24	3.5
Silica sol, SiO_2 3%	Kostrosol 0830 *d*.	3	5	3.5	2
Silicic acid ester (SAE), SiO_2 8%	Dynasylan 40 *d*.	2	2	1.5	1
Silica sol 3% + Nanolime 2.5%		3/4	5 + 4	3.5 + 3.5	2 + 1
SAE 8% + Nanolime 2.5%		2/4	2 + 4	1.5 + 3.5	1 + 1

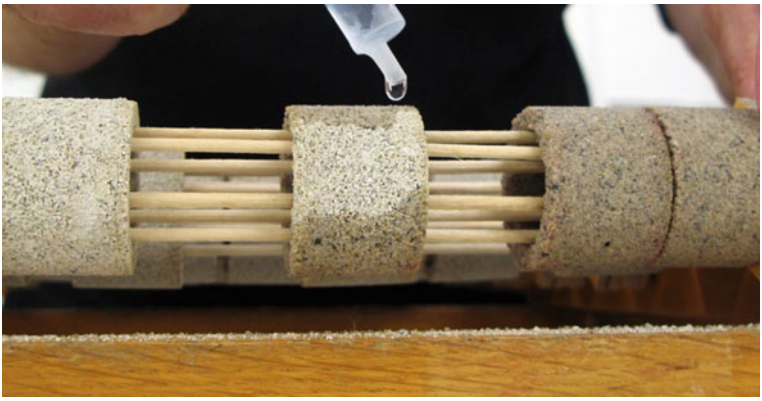

Fig. 1 Application of the consolidation agents in mortar specimens

applications per day were performed with each additional treatment completed on partially wet mortar. In lime water and distilled water tests, two schedules were adopted regarding the number of the applications—50 to 58 cycles and 160 cycles. Sulphate, barium, ammonium oxalate water and nanolime dispersions were applied in 38–58 cycles. Some consolidating treatments were performed to study the effect of agents after 2–7 applications made during 1 or 2 days (silicic acid ester, silica sol, lime nanodispersion). When combining two products, the second consolidating agent was applied 24 h after the first product application. Two months after the completion of the mortar consolidation treatments, compression strength tests were then performed.

3 Mechanical Tests Results

The short mortar tubes were loaded along the tube axis in compression (Drdácký and Slížková 2008, 2012; Moreau et al. 2010). Results are illustrated in the graphs depicted on Figs. 2, 3 and 4.

Fifty cycles of lime water with drying (twice per one day) as well as 58 cycles of lime water applied more often (three times per one day), led to an increase in the compression strength of the thin-walled tubes. However, this increase was so small that it may not be apparent when standard mortar beams are tested. The results further show that there is no apparent difference between lime water application with total drying or partial drying. There is a considerable increase in the compression strength of a poor lime mortar after 160 cycles (both 54 and 80 days of consolidation). The consolidation effect of lime water was substantially improved when it was combined with colloidal silica. 5 cycles of 3% solution of silica were applied at the beginning of this treatment set and then 58 cycles of lime water followed. This approach significantly increased the effect of lime water impregnation.

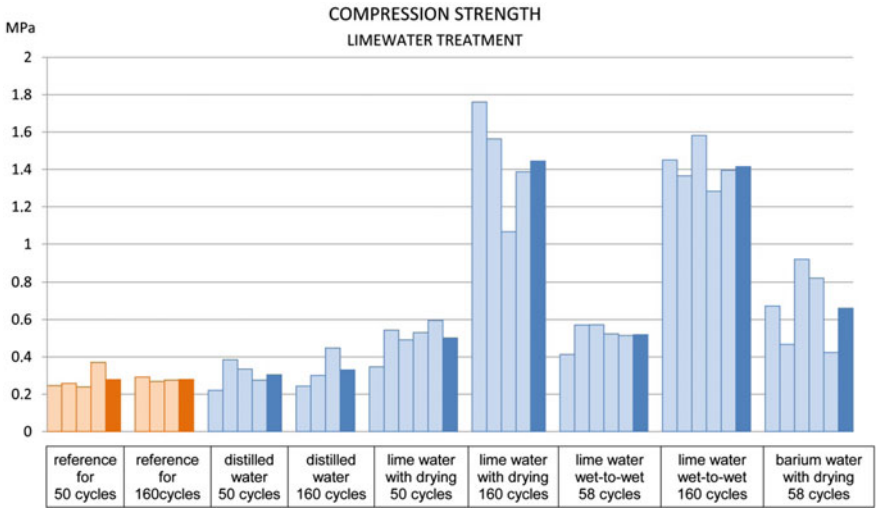

Fig. 2 Influence of water, lime water a barium water treatment on compression strength of specimens

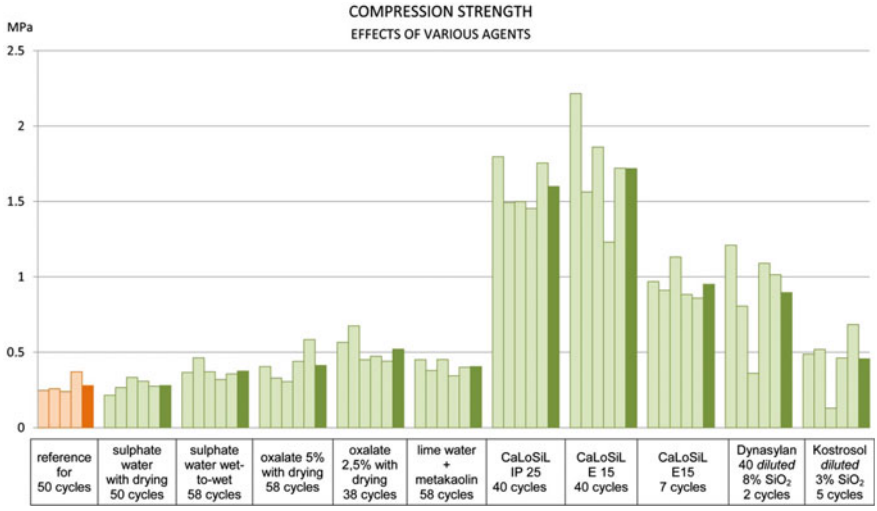

Fig. 3 Selected consolidation treatment influence on compression strength of specimens

On the other hand, the combination of lime water with metakaolin did not provide any benefit. Even though the pozzolanic activity of metakaolin used was high (1002 mg/g), the products of pozzolanic reaction of metakaolin and calcium hydroxide in lime water were not water soluble.

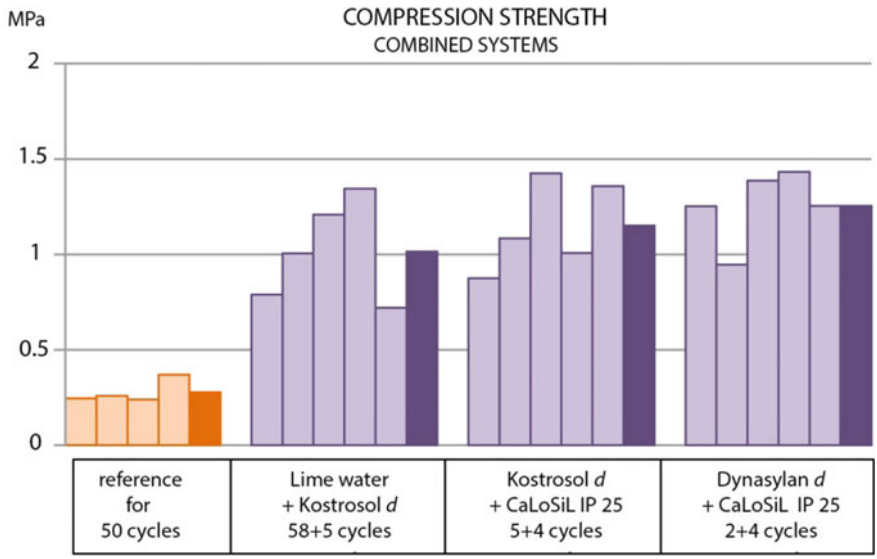

Fig. 4 Influence of consolidation treatment based on combination of two agents

No detectable improvement of the lime water modified with metakaolin indicates that both metakaolin and the reaction products with lime probably did not penetrate the porous structure of mortar specimens and therefore did not improve the compression strength. The lime present in the lime water was consumed during the pozzolanic reaction with metakaolin resulting in a consolidation treatment even lower effective than lime water without modification.

Good results were achieved with barium water, where solubility of $Ba(OH)_2$ in water allowed much higher concentration of resulting "barium water" (5% w.) compared to lime water (0.16% w.). Ammonium oxalate (2.5% concentration, 38 applications), showed strengthening similar to lime water after 58 applications. The lower concentrated solution (2.5%) penetrated better than the higher concentrated solution (5%) where accumulation of salt crystals in the mortar surface layer was evident.

Both the sulfate water treatment and the use of distilled water alone provided a negligible increase in compressive strength of the mortar. The mortar specimens are very weak due to the very low lime content of the mortar, so the known self-healing process of lime mortars by repeated watering would not occur when using distilled water alone in this case.

The most significant increase in strength was achieved using nanolime products CaLoSiL, which was applied in multiple cycles for comparison with lime water treatment. Very good results were found in mortars consolidated with CaLoSiL E 15, with 7 applications. Because ethanol evaporates quickly, the 7 cycles of the product were applied in one day. The least labourious (2 cycles) consolidation treatment was completed using diluted Dynasylan 40 (SiO_2 content in the applied

agent 8% w.). The combined treatment of silicic acid ester with low content of SiO_2 (diluted Dynasylan 40) following the application of nanolime product (CaLoSiL IP 25) was shown to be effective in terms of both time and strength increase. Comparing the effects of CaLoSiL E 15 and IP 25, the tests concluded that a higher concentration of the active substance does not always lead to higher strengthening. Consolidation with CaLoSiL IP 25 is likely to lead to reduced (less uniform) distribution of the new binder in mortar specimens, when compared to lower concentrated CaLoSiL E 15 treatments.

4 Water Drop Absorption Results

The water drop absorption rate is defined as the absorption time of a limited and finite amount of water by the surface of the material (RILEM II. 8b 1980). A laboratory pipette, filled with 0.01 ml of water was used in this experiment. The water drop was applied on the tube mortar specimen surface (Fig. 5) and the change in the behaviour of untreated (reference) specimen and the specimen treated with a specific consolidant was evaluated. This method is mainly used for measuring the water repellency of surfaces, however, in this case the method was also used for evaluation of possible reduction of open pores after the consolidation treatment. The time required for the total absorption of the water dropped onto the tube specimen surface from a height of 1 cm was recorded. A minimum of five measurements were performed for each consolidation treatment. The mean values of the absorption times for each individual treatment are reported in Table 2.

For each of the tested water solutions, the change in the absorption rate was only observed for specimens treated with 5% solutions (barium hydroxide and

Fig. 5 Test of the water drop absorption rate

Table 2 Results of water drop absorption and peeling test

Tested agent, active substance % w.	Total amount of applied consolidant (l/m^2)	Absorption time of water drop (s)	Peeling test ***A*** constant (mg)
Untreated reference specimen	0	<1	4.720
Distilled water	55	<1	3.439
Distilled water	180	<1	
Lime water, $Ca(OH)_2$ 0.16%	52	<1	3.790
Lime water, $Ca(OH)_2$ 0.16%	58	<1	2.474
Lime water, $Ca(OH)_2$ 0.16%	156	<1	0.053
Lime water, $Ca(OH)_2$ 0.16%	155	<1	0.250
Lime water + Metakaolin	55	<1	0.284
Lime water + Silica sol	56 + 3.5	<1	0
Sulphate water, $CaSO_4$ 0.26%	51	<1	0.326
Sulphate water, $CaSO_4$ 0.26%	58	<1	0.125
Barium water, $Ba(OH)_2$ 5%	57	358	0
Ammonium oxalate water, 5%	27	1.6	0
Ammonium oxalate water, 2.5%	32	<1	0
Nanolime, $Ca(OH)_2$ 1.5%	30	394	0
Nanolime, $Ca(OH)_2$ 1.5%	6.5	50	0.634
Nanolime, $Ca(OH)_2$ 2.5%	24	610	0
Silica sol, SiO_2 3%	3.5	<1	0.694
Silicic acid ester (SAE), SiO_2 8%	1.5	13	0.910
Silica sol 3% + Nanolime 2.5%	3.5 + 3.5	2	0
SAE 8% + Nanolime 2.5%	1.5 + 3.5	<1	0

ammonium oxalate). The change was found to be much higher for barium hydroxide because that agent was applied in higher amount (57 l/m^2) than the ammonium oxalate (27 l/m^2). Even though the porosity of mortar and the size of

pores were large, the amount of the barium water applied, and likely also its distribution within the specimen caused the water absorption rate to decrease significantly through the consolidated mortar surface.

The most significant reduction in water absorption due to a consolidation treatment was achieved with nanolimes CaLoSiL when the products were applied in 40 cycles. The CaLoSiL IP 25 applied in 7 cycles also caused noticeable change in the water absorption behaviour. A slight decreasing effect was found after consolidation with silica sol and CaLoSiL (5 + 4 cycles) and after silicic acid ester application. The reason of the reduction in the second case (SAE) is probably a change of the wettability of the treated mortar in consequence of the higher contact angle of water (>90°) on the slightly hydrophobic mortar specimen. It was proved in the presented experiment, that the water drop absorption test is a simple, fast method, giving reasonable information about the change of water behaviour when water is applied on untreated and treated surface.

5 Peeling Test Results

The peeling test, also known in the literature as the Scotch Tape test, has been used for assessing the surface consolidation or strengthening efficiency of treatments. In the past, no standard protocols or rules were established for these applications. Therefore factors which influence the results achieved when a tape is applied on mortar or stone surface were studied by authors of this paper and the peeling test procedure was established (Drdácký et al. 2012). Main application strategy of this procedure exploits repeated peeling in the same place on a surface in order to eliminate the effect of the natural decrease in the detached material from the subsurface layers, which might be incorrectly interpreted as a consolidation effect. When sticking and peeling is repeated several times, the amount of detached material starts to become almost constant and characterizes the cohesion of the material.

For the evaluation of the weight measurements of detached material amounts a nonlinear approximation model was adopted. This model type was necessary namely if the data converge to some positive, i.e. non zero value, which is typical for testing of consolidation effects on degraded mortars. Then the constant A could be considered as a value describing the cohesion quality of the near surface material layer. Three parameters—A, B and C—described the cohesion quality and they were computed using the following approximation:

$$m(n) = A + B * e^{-C*n} \quad (1)$$

where m(n) denotes the removed material's weight (mg). According to the peeling-test model, unperturbed material's cohesion manifests itself as a constant amount of removed material in peeling sequence, denoted as ***A*** in the formula. This weight corresponds to the fragments broken apart from the surface in the process of

affixing the strip on the surface. It assumes that this component would remain constant if the peeling is repeated again and again.

In the experiment, areas without gross defects and imperfections were selected and the tape, sized 10 mm × 45 mm, was placed on the measured surface. The tape was smoothed into place by finger. After approximately 90 s of application the tape was removed by seizing the free end and pulling it off steadily at rate of about 10 mm/s and at angle of 90°. Then the sampler was weighted with stuck material. The test was then repeated ten times at the same location. For the each consolidation treatment, 5 mortar specimens were tested and the mean value of computed constants ***A*** of the individual specimens was evaluated. Results for the all assessed treatments are listed in the Table 2.

The treatment with the least reduction in the amount of removed material in comparison to reference specimens represents the treatment with the lowest surface strengthening efficiency, which in this case was demonstrated by mortars treated with 50 and 58 cycles of lime water (20–47% reduction). A similar minimal reduction was found for distilled water (42%).

The remaining treatments tested which provided favourable results and considerable reduction in removed surface material are listed as follows: diluted silicic acid ester (81% reduction), diluted silica sol (85%), nanolime CaLoSiL E 15, 7 cycles (87%), sulfate water, 50 cycles (93%), lime water and metakaolin (94%), 160 cycles of lime water application (95–99% reduction). All other consolidation treatments caused 100% change, where any material was removed from the mortar surface during the test with the used tape. The efficiency of the consolidation treatments in relation to the surface cohesion was characterized well by the peeling test, however the results are different from the compressive strength results, which refer closer to the structural characteristics. Figure 6 shows the relation between both measured characteristics.

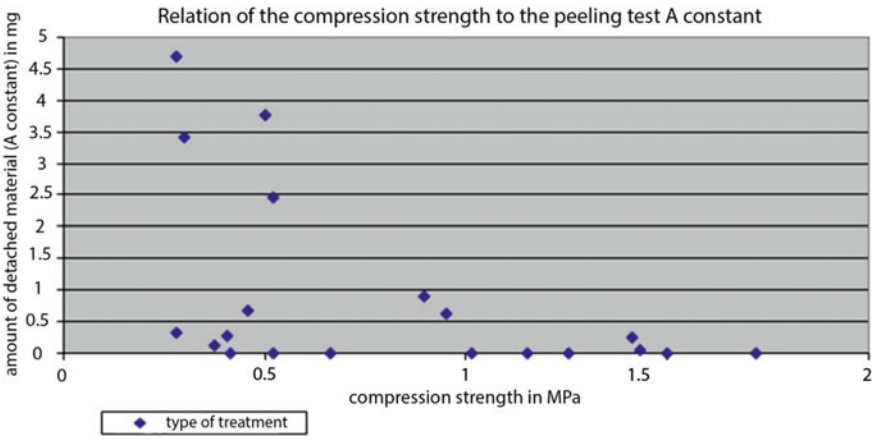

Fig. 6 Relation of the compression strength to the peeling test A constant

6 Conclusion

Lime water treatment of a specific lime mortar were shown to be effective after a sufficiently high number of applications (160 cycles, 54–80 days of a permanent consolidation treatment) and some poor mechanical characteristics (compression and surface cohesion) could be improved substantially. The lime water treatment was compared with some other technologies that are less labour-intensive. The most efficient agents were suspensions of calcium hydroxide in alcohols, which are marketed under the trade name CaLoSiL by the German producer IBZ Freiberg. Their major advantage is that they can be applied much more rapidly than tens to hundreds of lime water cycles and that they deliver higher amount of lime in a one cycle. The efficiency of suspensions in alcohol is signalled by a one-day application of CaLoSiL E15 (7 cycles), where there is a significant strengthening effect.

In terms of chemical composition, calcium hydroxide water solution (lime water) and also nanolimes (alcohol colloidal solutions) are supposed to be suitable for consolidation of calcitic porous materials, such a limestone, lime mortar and marlstone. Besides the different lime content and solvent, these lime agents differs in the particle sizes resulting in penetration ability. This should influence their application preference. While lime water contains calcium ion, sized about 0.1 nm, calcium hydroxide particles in CaLoSiL are considerably larger (50–200 nm). This property defines the use of nanolime dispersions for structural consolidation of porous material with a sufficiently large pore diameter. On the other hand, the content of calcium hydroxide in lime water is very low (1.7 g/l at 20 °C) and therefore in cases where it is necessary to add larger quantities of lime in a shorter time, or where repeated watering of the wall could be risky, CaloSiL products with higher lime content (5–25 g/l) could be the preferred agent. It seems from the results that lower concentration of CaLoSiL (E 15) provided a better distribution of the new binder in the mortar structure and higher compression strength than the more concentrated CaLoSiL (IP 25).

Like lime water and nanolime dispersions applied calcium hydroxide into mortar, silica sol and silicic acid ester introduced into the treated material amorphous silica. The amount of active substance (SiO_2) in the commercially available products is generally 100–500 g/l, which is a much higher content compared to lime based agents. Also when taking the required strength of mortar into account, diluted solutions of these products are more suitable for the consolidation of deteriorated mortar. Diluted, 8% silicic acid ester applied in two cycles was shown to be equally effective as CaLoSiL E 15 applied in 7 cycles. Silica sol, diluted down to 3%, was found be less effective, but in combination with lime water or CaLoSiL led to substantial improvement in strength. The combination of CaLoSiL and diluted silicic acid ester also appeared to be promising.

Surface cohesion of mortar was achieved with most of the tested consolidation agents including multiple applications of ammonium oxalate and barium water. In the second case, barium carbonate is the product of hardening (carbonation) of the

applied agent. When ammonium oxalate was applied in two different procedures, the lower concentrated solution (2.5%) gave better strength results.

5% concentrations of barium water and ammonium water in context with its multiple applications (58 cycles) caused a reduction in water drop absorption. As expected, the most significant reduction in water absorption due to consolidation treatment was found after 40 cycles of nanolimes CaLoSiL treatment. When CaLoSiL IP 25 was applied in 7 cycles it also caused noticeable change in the water absorption behaviour. A slight decreasing effect in the water absorption rate was found after consolidation mortar with silica sol and CaLoSiL (5 + 4cycles) and after the silicic acid ester application. In the second case the reason of the reduction was probably the residual hydrophobic character of the mortar specimens.

Success of the consolidating process is influenced by many factors. The basic characteristics and parameters need to be taken into account when designing optimal consolidation treatment, such as chemical, mineralogical composition, strength, size, shape of pores, porosity of treated material, further size of ions, molecules or particles of the active substance in the consolidation product, chemical composition and concentration of the active substance in the product, the drying rate and setting time of the new binder during and after expected ambient conditions.

Knowledge of these parameters is a good basis for the design of a consolidation treatment (type of consolidation agent, the concentration of active substance, method of application, the number of repeated applications during a consolidation process, the method of treating the substrate after impregnation). An important tool in the study of the behaviour of consolidants are trials on real objects as well as laboratory experiments using model substrates representing certain type of deteriorated material. The task is very complex and the reader should bear in mind that the tested mortar was cured in laboratory—there was no surface crust layer or paint present and there were no soluble salts in the treated material, which is not a common case in most practical situations. The research reported here did not aim to optimize the application of various agents, only to make a comparison under specific conditions. This should be understood in order to avoid misinterpreting the results.

Acknowledgements The authors gratefully acknowledge support from the Czech Grant Agency GA ČR grant 17-05030S.

References

Brajer, I., & Kalsbeek, N. (1999). Limewater absorption and calcite crystal formation on a limewater-impregnated secco wall paintings. *Studies in Conservation, 44,* 145–156.

Drdácký, M., Lesák, J., Rescic, S., Slížková, Z., Tiano, P., & Valach, J. (2012). Standardization of peeling tests for assessing the cohesion and consolidation characteristics of historic stone surfaces. *Materials and Structures, 45*(4), 505–520.

Drdácký, M., & Slížková, Z. (2008). Calcium hydroxide based consolidation of lime mortars and stone. In Delgado Rodrigues J, Mimoso JM (Eds.), *Proceedings of the International symposium "Stone consolidation in cultural heritage"*. LNEC: Lisbon, May 2008, ISBN 978-972-49-2135-8, pp 299–308.

Drdácký, M., & Slížková, Z. (2012). Lime-water consolidation effects on poor lime mortars. *APT Bulletin*, *43*(1), 31–36.

Ferreira Pinto, A. P., & Delgado Rodrigues, J. (2007). Stone consolidation: The role of treatment procedures. *Journal of Cultural Heritage, 9,* 38–53.

Millar, W. (1998). *Plastering (plain & decorative). 1897*. Reprint, Donhead Publishing Ltd.

Mora, L., Mora, P., & Philippot, J. (1977). *La conservation des peintures murales*. ICCROM

Moreau, C., Slížková, Z., & Drdácký, M. (2010). Consolidation of pure lime mortars with nanoparticles of calcium hydroxide. *Proceeding of the 2nd Historic Mortars Conference HMC2010 and RILEM TC 203-RHM 'Repair Mortars for Historic Masonry' Final Workshop* (pp. 1113–1121). CR: Prague.

Peterson, S. (1982). *Lime water consolidation, mortars, cements and grouts used in the conservation of historic building*. Roma: ICCROM

Price, C. A. (1984). *The consolidation of limestone using a lime poultice and limewater, adhesives and consolidants*. II C, London.

Price, C., Ross, K., & White, G. (1988). A further appraisal of the "lime technique" for limestone consolidation, using a radioactive tracer. *Studies in Conservation, 33,* 178–186.

Quayle, N. J. T. (1996). The Case Against Lime Water (or, the futility of consolidating stone with calcium hydroxide). *Conservation News, 59,* 68–71.

RILEM II. 8b (1980). Water drop absorption. RILEM 25-PEM, "Recommendations provisoires. Essais recommandés pour mesurer l'altération des pierres et évaluer l'efficacité des méthodes de traitement". *Matériaux et Construction 13*(75), 215–216.

Artisanal Lime Coatings and Their Influence on Moisture Transport During Drying

T. Diaz Gonçalves and V. Brito

Abstract Lime coatings such as whitewashes were originally used in historical buildings all across Europe and the rest of the globe, on lime plasters or directly on stone elements. Today, these coatings are increasingly used in conservation not only due to their unique aesthetic features but also for functional reasons. One of their main functional advantages is the ability to not hamper the drying of the substrate, which is very important because dampness is recurrent in historical buildings. The work presented here is aimed at improving the understanding of how and why lime coatings affect (or not) the drying of the porous building materials that usually constitute those substrates. We analysed experimentally the influence of one selected lime coating on the drying of five substrate materials with architectural relevance: one lime mortar and four stones, the well-known Ançã limestone, Maastricht limestone and Bentheimer sandstone, as well as a common Portuguese low porosity limestone. All the materials were characterized in relation to their capillary porosity and pore size distribution. Afterwards, the drying kinetics of the substrate materials, when coated or uncoated, was evaluated and compared. It was concluded that the lime coating not only does not hinder drying, but can even accelerate it. Indeed, at high moisture contents, the drying rate increases up to as much as 50%. This is likely to happen because the coating generates a larger effective surface of evaporation. In the article, we discuss the possible causes and implications of this phenomenon.

Keywords Lime coatings · Porous materials · Drying · Moisture transport Historical buildings

T. Diaz Gonçalves (✉) · V. Brito
National Laboratory for Civil Engineering (LNEC), Lisbon, Portugal
e-mail: teresag@lnec.pt

V. Brito
e-mail: vbrito@lnec.pt

J. J. Hughes et al. (eds.), *Historic Mortars*,
https://doi.org/10.1007/978-3-319-91606-4_18

1 Introduction

Lime coatings are common in historical buildings all across Europe and elsewhere. They were originally used for aesthetical and sanitary purposes, and also to protect the substrates. Numerous variations of composition and texture can be observed, in interiors and exteriors, over lime plasters or, in some cases, directly on stone elements (Holmes and Wingate 1997). Limewashes are the most typical of these coatings (Fig. 1, on the left). They were obtained from aqueous suspensions of hydrated lime, sometimes including also pigments or additives, which were applied by brush. But thicker lime coatings were also frequent (Fig. 1, on the right). These were obtained from lime pastes and were applied by brush or with a spatula or similar tool.

After the industrial revolution, lime coatings were gradually replaced by synthetic coatings. These, however, eventually proved unsuitable for historic buildings. The reasons were aesthetic, because lime coatings have unique gloss and texture, but also functional. One of the most critical issues stems from the huge influence that coatings have in the drying of the underlying elements. Indeed, coatings are at the interface between the construction and its environment, thereby controlling all the exchanges of moisture between them. The presence of moisture is usual in historic constructions which are based on thick solid walls made of porous hydrophilic materials and built in direct contact with the ground. When coatings hamper the evaporation of this moisture, they can exacerbate moisture problems. This has often been observed when lime coatings are replaced by synthetic coatings. One typical problem is an increase in the height that water reaches in walls with rising damp. In these walls, water rises by capillarity up to where the liquid flow through the base of the wall is balanced by the vapour flow through its surfaces. Therefore, when this vapour flow is reduced, for example by a coating, the water has to climb higher in the wall to restore equilibrium.

To overcome these limitations of ordinary synthetic coatings, industrial coatings specific for application on old buildings have been developed. Today, there are several types of such coatings available on the market (Brito et al. 2011). They

Fig. 1 Whitewashed façade at Terena village, Alentejo, south Portugal (on the left) and a thicker lime coating on stone masonry at Rendufe Monastery, Braga, north Portugal (on the right)

usually seek to reproduce the aesthetical characteristics and functional advantages of traditional lime coatings, while presenting higher durability. One of main functional advantages is the ability to not impede the drying of the substrate, which the new industrial coatings seek to achieve by means of high vapour permeability. But is this high vapour permeability the only factor behind the good performance of traditional lime coatings?

To find the answer to this question and, in general, to better understand how and why traditional lime coatings affect (or not) the drying of porous building materials, we have analysed experimentally the influence of one selected lime coating on the drying of five different substrates. These five substrates include one lime mortar and four natural stones which are representative of those found in old buildings. Further, they all have different porosity and pore size distribution. In the following sections, we describe the methods used in this work and discuss the obtained results based on a comparison between the performance of coated and uncoated materials.

2 Materials and Methods

2.1 Substrates

The experimental work was conducted using small cubes with around 24 mm edge of the substrate materials described in Table 1, lime mortar and four types of natural stone. The lime mortar was prepared following standard EN 1015-2. Moulding and curing were carried out as described in Diaz Gonçalves et al. (2012), following as close as possible standard EN 1015-11. The stone cubes were cut from larger blocks.

The capillary porosity of the materials is given in Fig. 2. This was measured at atmospheric pressure, after 48 h complete immersion, following the procedure II.1 of RILEM (1980).

The main pore radius of the materials is also presented in Fig. 2. For the lime mortar and the two Portuguese stones, these values were obtained from the pore size distribution curves presented in Fig. 3. Pore size distribution was determined by mercury intrusion porosimetry (MIP) with an Autoscan60 instrument from Quantachrome, following ASTM D4404-84 (ASTM International 2004) and always

Table 1 Substrate materials

Ref.	Designation	Description
A	Lime mortar	Air lime:sand (1:3) mortar
CA	Ançã limestone	Soft and porous stone from Coimbra, Portugal
CC	Grey limestone	Common Portuguese low porosity stone
M	Maastricht limestone	Light yellowish, soft and porous stone from the Netherlands
B	Bentheimer sandstone	Porous quartz-rich stone from Germany

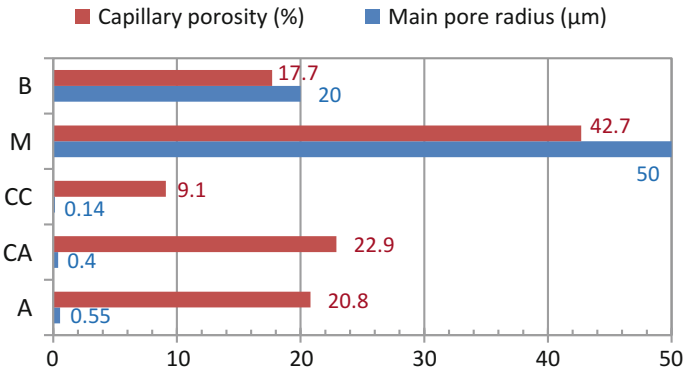

Fig. 2 Capillary porosity and main pore radius of the substrate materials

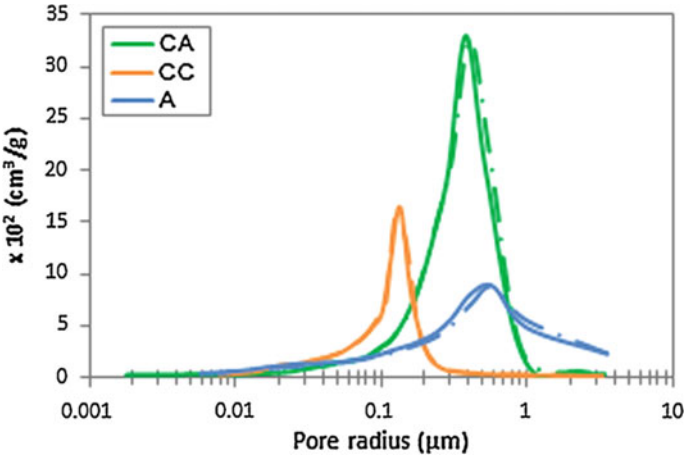

Fig. 3 Pore size distribution of the substrate materials

repeating the measurements. For the Bentheimer sandstone and Maastricht limestone, the main pore radius values reported by Dautriat et al. (2009) and De Clercq et al. (2007), respectively, are used. As seen, these two stones have much large pores.

The four lateral faces of the lime mortar and stone cubes were sealed with an epoxy resin. Afterwards, they were cleaned in a Branson 1200 ultra-sound cleaner.

2.2 *Lime Coating*

The lime coating was obtained by blending hydrated commercial lime powder (Lusical H100) with water. This lime is composed of calcium hydroxide $Ca(OH)_2$,

with no additives. A laboratory mixer of the type defined in EN 196-1 was used for that purpose. The lime was first mixed with water during 60 s at low speed, which was followed by manual incorporation of the material that adhered to the inner walls and, finally, by another 30 s mixing at the same speed.

The W/L ratio of the lime coating was established based on two main criteria: (i) maximization of the capillary porosity of the hardened paste; (ii) reasonable workability of the fresh paste. Five different W/L ratios were initially tested, 1.0, 1.2, 1.4, 1.6 and 1.8.

To evaluate the porosity of these five lime pastes, cubic specimens with 2.4 mm edge were moulded. They spent the first seven days in a conditioned room at 50% RH and 20 °C (in the first day inside a polyethylene bag), after which period they were demoulded and spent another fifteen days in a carbonation chamber at 21 °C, 65% RH and 5% CO_2. The capillary porosity was estimated as the percent ratio 100 V_w/V_s, where V_w is the volume of water absorbed after 48 h in partial immersion, and V_s the volume of the specimens. This volume was measured geometrically with a digital slide caliper. RILEM procedure II.1 of hydrostatic weighing could not be followed because the lime cubes disintegrated when totally immersed in water during 48 h. The pore size distribution was determined by MIP.

The capillary porosity of the hardened pastes has an inverted parabolic relationship with the W/L ratio (Fig. 4). This means that porosity increases up to certain percentage of mixing water. However, as we keep adding more water, it will eventually start decreasing. The reasons for this decrease are not totally clear and deserve further research. The increase in the W/L ratio involves also an initial increase of the main pore diameter, followed by stabilization (Fig. 5).

The initial increase of the capillary porosity with the W/L ratio is consistent with the results of Arandigoyen et al. (2005). However, their shorter range of W/L ratio does not allow detecting any further decrease in the capillary porosity, although a stabilization is devised at the higher W/L ratios.

Trial applications were then carried out to evaluate the workability of the pastes when applied as coatings. For W/L bellow 1.4, the lime pastes became very dry and

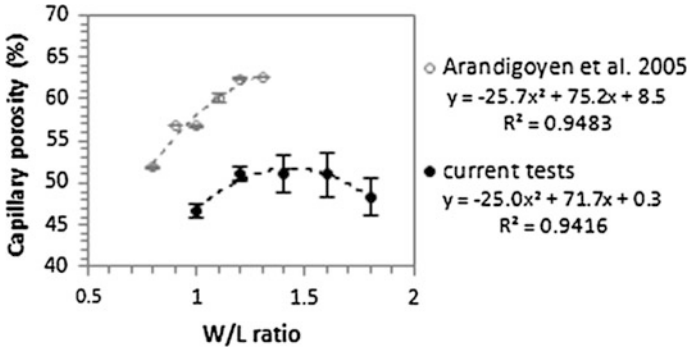

Fig. 4 Variation of the capillary porosity of the hardened lime pastes with their W/L ratio

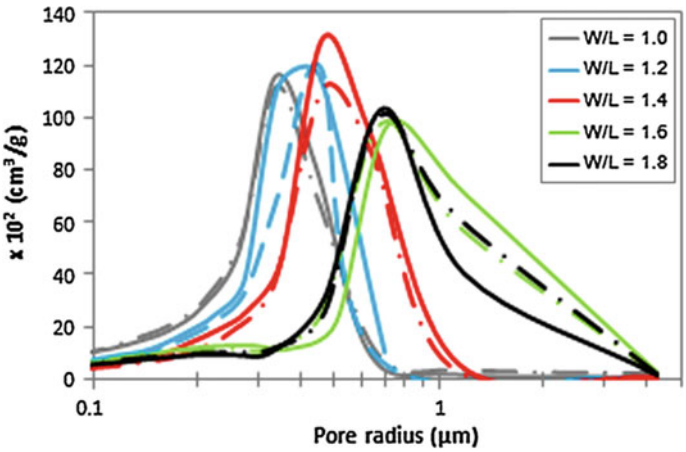

Fig. 5 Pore size distribution of the hardened lime pastes

a reasonable workability was not achieved. The lime paste with W/L = 1.4 was selected. Note that the porosity of the cubes should be considered only as a reference because the suction of the substrate may change it, and this change can be different for different substrate materials.

The lime coating was applied on mortar A using a paint-brush and on the remaining substrates using a spatula. The two different application techniques were necessary due to the different workability that the paste revealed on different substrates: workability was higher when the coating was applied on lime mortar substrate. Figure 6 shows that the consumption too varied with the substrate material. This means that the thickness of the coating may have changed too. However, no significant differences were visually noticeable.

2.3 Experimental Methods

The drying kinetics of the coated and uncoated substrate materials was evaluated by RILEM procedure II.5 (RILEM 1980). This procedure consists in saturating the specimens and then letting them dry through their top face, under controlled environmental conditions, while the loss of water is monitored by periodical weighing.

The specimens were oven dried at 40 °C until constant mass and placed in partial immersion in pure water for three days. Then, their bottom surface was sealed with polyethylene film. Drying took place in a conditioned room at 20 °C and 50% RH (Fig. 7). A minimum of four specimens of each kind was always used.

The results are expressed by the so-called evaporation curve (Fig. 8) whose slope corresponds to the drying rate. This curve is typically composed of two parts:

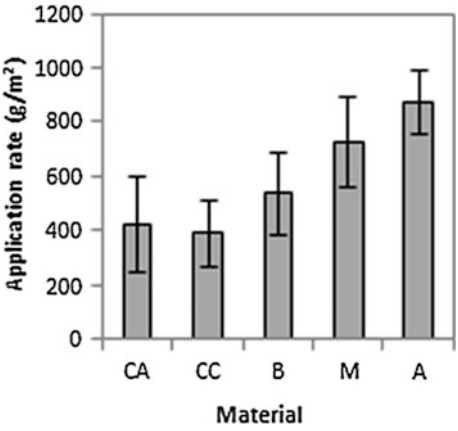

Fig. 6 Consumption of the lime coating on the five substrates

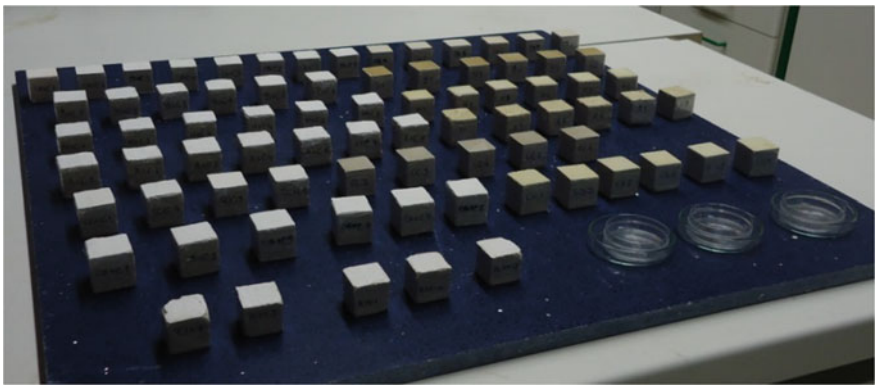

Fig. 7 Test set-up showing the 24 mm-edge specimens drying in the conditioned room, as well as water-filled petri dishes which were used to measure the evaporation rate of free water surfaces

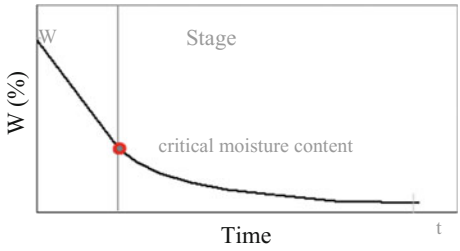

Fig. 8 Typical evaporation curve

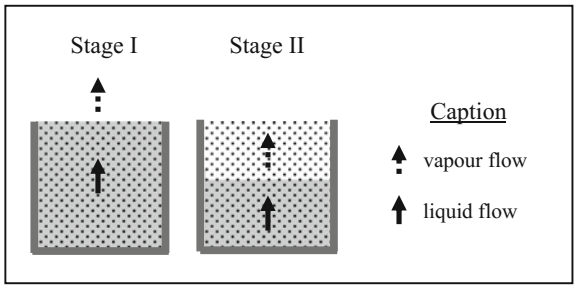

Fig. 9 Two main drying stages

an initial straight line segment, followed by a concave branch. The two parts correspond roughly to the two main stages that a porous material undergoes when drying from saturation (Fig. 9). Stage I, also called the constant drying rate period, occurs while the moisture content is high enough to sustain a saturated condition at the surface. Stage II, also called the falling drying rate period, starts when this moisture content is no longer sufficient to produce a liquid flow able to compensate the evaporative demand. In this second stage, the evaporation front recedes progressively into the material to maintain equilibrium between the liquid and vapour flows. The drying rate decreases accordingly, with reduction of the vapour pressure at the front and with the increase in the thickness of the dry layer that vapour has to traverse to reach the outer surface.

When there are several specimens of each kind involved, as it is the case here, the drying curve is not an appropriate way of expressing the results because there is necessity of a statistical treatment of those results. In these cases, it is better to use the drying index (*DI*), an empirical quantity that translates the drying curve into a single quantitative parameter (Eq. 1):

$$\mathrm{DI} = \frac{\int_{t_o}^{t_i} f(w_i) \times dt}{w_0 \times t_i} \tag{1}$$

$f(w_i)$ is the mathematical expression of the drying curve, given as a function of the moisture w_i (%), w_0 the water content at the beginning of drying and t_i (h) the total duration of the test. Note that the slower the drying the higher the DI.

Specimens of the hardened lime paste (PC) were always tested to serve as reference. The evaporation rate of free water surfaces was also measured during the tests, by the method described in Diaz Gonçalves et al. (2012), using full Petri dishes.

3 Results

The moisture content at the beginning of drying is not relevantly affected by the lime coating, as seen in Fig. 10. This means that the comparisons between coated and uncoated materials are free from distortions due to differences in the initial moisture content of the specimens.

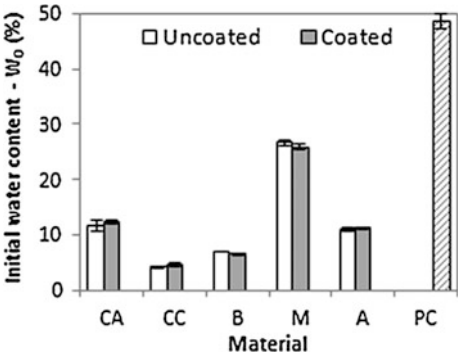

Fig. 10 Initial moisture content of the coated and uncoated materials and of the hardened lime paste

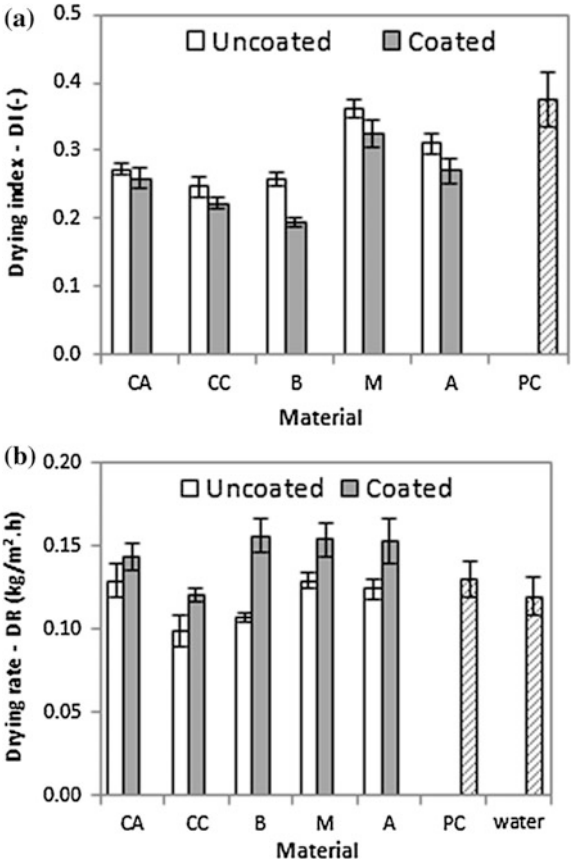

Fig. 11 Results of the drying test for the coated and uncoated materials, hardened lime paste and free water surface, in terms of **a** drying index and **b** stage I drying rate

The results of the drying test are given in Fig. 11 in terms of drying index and stage I drying rate. These results show that:

- The lime coating does not hinder the drying of the tested substrates. Strikingly, it even accelerates the process. This is clear both in terms of drying index (Fig. 11a) and, particularly, of the stage I drying rate (Fig. 11b). The greatest differences occur for the Bentheimer sandstone (B), whose drying index was reduced by 25% and stage I drying rate increased by 46%, respectively.
- The stage I drying rate is neither identical among the coated materials, nor between those and the hardened lime paste (Fig. 11b). This is contrary to what would be expected during a period where the evaporation front is always located at the surface, if the lime coating had always similar characteristics. It confirms, therefore, that substrates are able to change significantly the physical characteristics of the lime coating during its application and cure. This is in line with previous research results, for example, with those obtained within EU project COMPASS (EVK-CT 2001-00047).
- The drying rate of the materials, regardless of whether they are coated or uncoated, exceeds in several cases that of the free water surface (Fig. 11b).

4 Discussion

An overall acceleration of drying was observed for the five tested substrates after application of the lime coating (Fig. 11a). This overall acceleration can be due to the rise in the stage I drying rate (Fig. 11b). But why has this rate increased?

The reason is not obviously a high vapour permeability of the coating. That could justify, at the maximum, a drying rate as high as that of the uncoated substrate. Further, there is significant change of the stage I drying rate, and during this stage there is no vapour transport across the material because the wet front is at the surface.

It is, indeed, reasonable to assume that during stage I the wet front was at the surface of the specimens, either they were coated or not. This assumption would be unreasonable for a hydrophobic coating or one with larger pores than the substrate. Such coatings would be unable to absorb water from the substrate and, thus, the wet front would be located at the interface between the coating and the substrate (Petković et al. 2007). But our coating is hydrophilic and has pores within the range or smaller than those of the substrates. Indeed, this is the case with the lime paste cubes (Figs. 2, 3 and 5) and the suction of the substrate could, at the most, make these pores even smaller. So, we can safely admit that the wet front was at the surface during stage I.

A likely explanation for the higher drying rate that arises after application of the lime coating is that this coating increases the effective surface of evaporation, i.e., the dimension of the evaporating surface during stage I. Indeed, during this stage, the evaporation rate depends on the environmental conditions but also on the effective dimension of the evaporating surface. A larger effective evaporating surface obviously implies a higher drying rate for the material.

The effective surface of evaporation depends on the porosity of the material but also on other physical characteristics, such as the pore size distribution. The complex pore size distribution of the type of materials studied here gives rise to evaporating surfaces with irregular morphology, whose area may greatly exceed that of the projected surface. This explains also why the drying rate of the materials is, in some cases, even higher than that of a free water surface (Hammecker 1993; Jeannette 1997; Rousset-Tournier 2001; Diaz Gonçalves et al. 2012, 2014).

It is also interesting that the stage I drying rate of the lime coated materials is greater than that of the hardened lime paste itself (Fig. 11b). Indeed, all the coated materials were expected to have a drying rate very close to that of the hardened lime paste, because during stage I the drying front is located at the surface and this surface is always covered with the same lime paste. But Fig. 11b shows that this is not true. A first explanation is that each substrate is able to change, in a different way, the physical characteristics of the coating. The influence of the substrate could derive from the suction it exerts on the fresh coating. This suction varies with the capillary porosity and pore size distribution, and is probably also one of the factors behind the differences in workability (Sect. 2.2) and application rate (Fig. 6) observed among different substrates. A second explanation is that the transitional layer, where the coating interpenetrates the substrate, has also some effect in the stage I evaporation. This could occur because the menisci have to recede slightly into the material, so as to generate the capillary pressure gradient that drives the movement of liquid towards the surface. Since the coating is thin, the transitional layer could be reached by this small receding of the wet front.

The experimental results presented here suggest, therefore, that lime coatings are able to promote masonry drying in stage I conditions, i.e., at high moisture contents. High moisture contents can be found, for example at the base of walls with rising damp. Since the water rises up to where the evaporation flow through the surfaces balances the incoming liquid flow through the base of the wall, a faster stage I evaporation rate could allow reducing the height of capillary rise. It could also help reducing the temporal impact of moistening events, and eliminating the moisture trapped in a wall after the source is deactivated.

We think that this effect and the advantages that lime coatings thereby provide in terms of health conditions were probably intuited and experienced in practice by the ancient. Although the application of lime coatings on damp walls is problematic, the truth is that in most cases the moisture content of those walls has seasonal variations.

5 Conclusions

The main conclusion of this work is that the lime coating not only does not hinder drying, but can even accelerate it for a wide range of substrate materials. The acceleration in drying rate is particularly significant for stage I conditions, i.e., when the moisture content of the substrate is high enough so that the wet front is located

at the surface, as it often happens at the base of walls with rising damp. This beneficial effect on the stage I drying rate is not due to a high vapour permeability of the lime coating. It may be explained by a high effective surface of evaporation arising from the geometric complexity of its pore structure. We think the advantages that lime coatings thereby provide in terms of health conditions were probably intuited and experienced in practice by the ancient.

The magnitude of the increase in the stage I drying rate varies with the type of substrate, and may reach values in the order of 50%. It would be important, in future work, to understand better the mechanisms behind this influence of the substrate.

Acknowledgements This work was supported by national funds through the Portuguese Foundation for Science and Technology (FCT), under the research project DRYMASS (ref. PTDC/ECM/100553/2008). We are thankful to Veerle Cnudde and Timo G. Nijland for providing the Bentheimer sandstone. We would like to acknowledge also the support of Luís Nunes and José Costa in several aspects of the experimental work.

References

Arandigoyen, M., Pérez Bernal, J. L., Bello López, M. A., & Alvarez, J. I. (2005). Lime-pastes with different kneading water: Pore structure and capillary porosity. *Applied Surface Science, 252,* 1449–1459.

ASTM International. (2004). Test method for determination of pore volume and pore volume distribution of soil and rock by mercury intrusion porosimetry. ASTM Standard D 4404-84.

Brito, V., Gonçalves, T. D., & Faria, P. (2011). Coatings applied on damp building substrates: Performance and influence on moisture transport. *Journal of Coatings Technology and Research, 8*(4), 513–525.

Dautriat, J., Gland, N., Guelard, J., Dimanov, A., & Raphanel, J. L. (2009). Axial and radial permeability evolutions of compressed sandstones: End effects and shear-band induced permeability anisotropy. *Pure and Applied Geophysics, 166*(5–7), 1037–1061.

De Clercq, H., De Zanche, S., & Biscontin, G. (2007). TEOS and time: the influence of application schedules on the effectiveness of ethyl silicate based consolidants. *Restoration of Buildings and Monuments an International Journal (Bauinstandsetzen und Baudenkmalpflege eine internationale Zeitschrift), 13*(5), 305–318.

Diaz Gonçalves, T., Brito, V., & Pel, L. (2012). Water vapour emission from rigid mesoporous materials during the constant drying rate period. *Drying Technology: An International Journal, 30*(5), 462–474.

Diaz Gonçalves, T., Brito, V., Vidigal, F., Matias, L., & Faria, P. (2014). Evaporation from porous building materials and its cooling potential. *Journal of Materials in Civil Engineering, 27*(8), 04014222.

Hammecker, C. (1993). *Importance des transferts d'eau dans la dégradation des pierres en oeuvre (Importance of water transfers in the degradation of stones in the site)*, Thèse de doctorat (Ph.D. thesis). Strasbourg, France: University Louis Pasteur.

Holmes, S., & Wingate, M. (1997). *Building with lime: A practical introduction*. London: Intermediate Technology Publications. ISBN 1853393843.

Jeannette, D. (1997). Structures de porosité, mécanismes de transfert des solutions et principales altérations des roches des monuments. In R. A. Lefèvre (Ed.), *La pietra dei monumenti in*

ambiente fisico e culturale (pp. 49–77). Ravello: European University Centre for Cultural Heritage.

Petković, J., Huinink, H. P., Pel, L., Kopinga, K., & van Hees, R. P. J. (2007). Salt transport in plaster/substrate layers. *Materials and Structures, 40*(5), 475–490.

RILEM TC 25-PEM. (1980). Recommended tests to measure the deterioration of stone and to assess the effectiveness of treatment methods, Test No. II.1 "Saturation coefficient", Test No. II.5 "Evaporation curve", *Materials and Structures*, *13*, 204–207.

Rousset-Tournier, B. (2001). *Transferts par capillarité et évaporation dans des roches. Rôle des structures de porosité (Capillary transport and evaporation in rocks. The role of pore structures)*, Thèse de doctorat (Ph.D. thesis), University Louis Pasteur, Strasbourg, France.

Part III
Historic Contexts and Experimental Developments

The Development of Binders and Mortars in Sweden

J. E. Lindqvist and S. Johansson

Abstract Masonry with mortar joints and renderings were introduced in Sweden with the integration into the Catholic Church in the 11th and 12th century. The binders used were air lime to sub-hydraulic limes and in some cases hydraulic limes. The impurities give the mortars a greyish and light ochre colours. It was only on the island Gotland were limestone that could be used for production of bright white pure limes occurs. These types of binders were dominant until the 19th century. From the seventeenth century there is a difference in the development of mortars for use in water constructions compared to those used for building on land. Dutch engineers were involved in several important canal projects as well as the establishment of the city of Gothenburg in the 17th century. In the 18th century with the introduction of the mercantile economic theory it became important to handle also these constructions with national resources. Sweden aimed for mortars based of burned oil shale ash as artificial pozzolans. These were introduced in the 1770s and used until the early 20th century. These types of mortars were also to some extent used for masonry houses and military constructions. In the 19th century there was an increase of the built volume, requiring a faster and more industrial building process. This promoted an increased use of pozzolanic and hydraulic binders, not least Portland cement. In the late 19th early 20th centuries a wide variety of binders from pure air lime to highly hydraulic were used for house building.

Keywords Mortars · Binder · Sweden

J. E. Lindqvist (✉)
Swedish Cement and Concrete Research Institute,
Box 857, SE 501 15 Borås, Sweden
e-mail: janerik.lindqvist@cbi.se

S. Johansson
Byggkonsult Sölve Johansson AB, Batterivägen 12,
SE 461 38 Trollhättan, Sweden

J. J. Hughes et al. (eds.), *Historic Mortars*,
https://doi.org/10.1007/978-3-319-91606-4_19

1 Introduction

The present paper gives a short introduction to the development of binders and mortars in the geographical area that compares with present day Sweden, excluding the island of Gotland. The motivation for doing this compilation is that during the last two decades a large number of analyses of historic mortars were performed by the authors. This has resulted in a more complex view of the types of mortars that has been used in different times (Johansson 2007; Lindqvist and Johansson 2009).

A simplified division into four time periods is introduced in order to give an overview. The first period, 1050–1620, reaches from the introduction of mortars in Sweden to the onset of large scale masonry constructions in water and wet environments. The second period ends with the introduction of mortars with burned shale ash as pozzolan in 1770. The third period ends at the onset of building urban environments at a large scale. In this paper it is symbolized by the Lindhagen city plan for Stockholm presented in 1866. The last period ends with the Stockholm exhibition in 1930 which marks the final transition to modernism in Sweden. These periods mark changes in the building process and the choice of materials as well as mental changes. The changes seen in the Swedish practice has been closely related to and influenced by trends in other parts of Europe.

The knowledge concerning historic mortars and masonry has also been applied in practice. The pioneering work performed by Ingmar Holmström from the 1970s onwards has resulted in an amazing concentration of lime rendered and lime washed facades in the Old Town in Stockholm. In Sweden mortar analyses are often performed as a part of the investigation prior to repair actions and the results serves as a background in the choice of repair mortars.

2 The Period 1050–1620

Masonry with mortars and rendering was introduced when Sweden became a part of the Catholic Church in Western Europe. The first masonry churches were built around 1050. But it was not until hundred years later, in the mid twelfth century, that masonry buildings became common. A very large number of churches were built. It was a part of a European wave of building churches and convents that had a background of combined religious revival, a growing population together with good economic times. The technology, as well as the religion was provided by the church. Swedish masonry constructions were both in function and technology similar as in other parts of the Catholic world. The specialists, masons and builders, were taken in from other parts of Europe. It was, considering the resources available at the time, an enormous building boom and it was not until the late 19th century it was exceeded. The convent of Gudhem, which remains as a ruin, can serve as an example (Fig. 1). This was built in the 12th century and later rebuilt in the mid-13th

Fig. 1 The ruin of Gudhems convent from the 12th century

century by builders from continental Europe. The binders used for the masonry mortars were sub-hydraulic. The construction of palaces and fortress reached some volume first in the 13th century.

At this time the possibilities for long transport of building materials was limited and it was mainly local limestone that was used. Deposits in Sweden of pure limestone that could be used for the production of bright white mortars occurs mainly on the island of Gotland, and a few occurrences of pure white marble on the mainland. Most of the limestones used had a composition that would produce a range of materials from pure lime to weakly hydraulic limes with greyish and light ochre colours. Most of the mortars had compositions in-between these two groups, which have been defined as sub hydraulic mortars (Lindqvist and Johansson 2009). The mortar mixes were often binder rich and inhomogeneous. An example of mortar compositions based on the use of microscopical and chemical characterisation methods (Lindqvist and Sandström 2000; NT BUILD 437) are given in Table 1. The cementation index is calculated according to Eckel (1928). These results are based on analyses of acid soluble CaO and SiO_2 and the actual cement index is probably slightly higher.

During this time period no marine constructions were constructed in Sweden using masonry. Wood construction dominated for this type of construction at the time.

Table 1 Examples of mortar compositions. The cementation index is given according to Eckel (1928)

Time	Type of mortar	Aggregate/binder	Cementation index
1100	Masonry	1.74	0.15
1150	Render	3.09	0.07
1150	Masonry	3.44	0.07
1180	Masonry	3.40	0.14
1300	Render	0.77	0.03
1500	Masonry	0.50	0.03
1500	Render	2.17	0.17
1500	Masonry	1.68	0.15
1500	Masonry	2.66	0.09
1600	Masonry	1.83	0.13
1688	Masonry	1.68	0.05
1770	Render	2.84	0.06
1750	Render	2.15	0.08
1750	Render	7.56	0.16
1800	Render	1.59	0.17
1860	Render	2.85	0.04
1890	Render	4.95	0.27
1900	Render	7.39	0.54
1930	Render	5.56	0.39
1930	Render	6.07	0.43

3 The Period 1620–1770

The first half of this period was characterized by conservatism in the choice of materials. The changes that were introduced were rather motivated by the revival of old techniques than the introduction of new. The type of mortars and binder used in the previous period were used also during this period, but the most binder rich mortars became less common. During this period several Swedish architects travelled to other parts of Europe to gather knowledge concerning mortars and masonry. A result was the introduction of mortars with brick dust and clay. The pozzolanic effect of the brick dust used was generally minor. Brick dust used as a pigment also became common. The economy was poor in Sweden during the 18th century and as a result hybrid mortars with clay and lime were frequently used. Also forging-slag was used occasionally.

The construction of polders in the Netherlands which started in the early 17th century as well as the extension of Amsterdam in three stages during the first half of the 17th century had a huge impact internationally. This had a great influence on masonry constructed in water also in Sweden. The City of Gothenburg was founded in 1621, constructed after the city plan of Amsterdam by Dutch engineers. Dutch engineers were also involved in other projects including the Hjälmare Canal and the

first lock in Stockholm. Little or nothing remains of the original constructions today. It is thus not possible to determine from analyses if trass mortars were used for these constructions.

4 The Period 1770–1866

There was, based on mercantile economic theory, an increasing urge to make use of the national resources rather that imported ones. This was also a time for large scale canal constructions in Sweden. These factors led to development of new types of mortars aimed for use in wet environments. This was an international trend and led generally to the development of hydraulic binders (Elsen et al. 2013). The Swedish research community at that time chose to develop mortars with artificial pozzolans based on burned shale ash (Johansson and Lindqvist 2013). These mortars were first introduced in 1770. These shale ash mortars were mainly used for masonry constructions in water and wet environments such as locks in canals. Shale ash mortars were, however also used, although to a more limited extent, in house building and military masonry constructions. The mortars mainly used for house building was the same as during the previous period. During the latter part of the period hydraulic binders, such as the Parkers Cement, were imported from England to western Sweden (Johansson 2007). These mortars were mainly used in house building.

5 The Period 1866–1930

In 1848 Napoleon III gave Hausmann the commission to reconstruct Paris. In an amazing building process that lasted seventeen years the old Paris was replaced by the new Paris, "the City of Light". This was not only a new structure of the city but it was also a psychological revolution in the urban identity as described by Shelly (Shelly 1997). This made a huge impact internationally as well as in Sweden and served as a model for the new city plan for Gothenburg and the Lindhagen Plan for Stockholm both in 1866. This required a more rapid and more industrialized building process. One effect of this demand was that the pozzolanic and hydraulic materials developed in the previous period was used to a large extent also in general house building. The use of ordinary Portland cement was introduced during this period. In 1873 was the first cement plant was established in Southern Sweden. In 1887 was the first plant for precast concrete elements established. The choice of mortars during late 19th and also the early 20th century were characterized by a wide variation. It could range from pure lime mortars to mortars with burned alum shale and cement mortars in masonry and joints on one and the same building. The Allhelgona Church from 1891 in Lund can serve as an example of selection of materials and the more industrialized building process (Fig. 2). The binder in the masonry mortars are pure

Fig. 2 The Allhelgona church from 1891 is a typical example of its time

lime or weakly hydraulic while cement mortar has been used for jointing. Windows and friezes are precast concrete. The importance of masonry in water constructions decreased with the introduction of reinforced concrete.

6 Conclusions

When repairing or restoring historic masonry and renderings a general rule is to adopt the new to the old. This assuming that the existing technical solution has performed in a good way. The large variation of mortar and binder types used in historic times makes it important to know the type of mortars used originally in order to decide about the choice of repair mortars.

It is also obvious the development of masonry techniques and materials in Sweden is closely linked to trends and ideas in the surrounding world. There is also a strong connection between identity, ideas and mentality in society and the type of buildings and constructions from different times, and thus also the choise of

building materials. This raises questions concerning why and what we preserve. One reason to preserve a construction is that it can provide an understanding of the connection between the development of ways of thinking and the built environment. A construction can then be considered as an historic archive and therefore alterations from the original may then reduce the information contained.

References

Eckel, E. C. (1928 new print in 2005). Cement limes and plasters. Donhead.

Elsen, J. (2006). Microscoy of historic mortars—A review. *Cement and Concrete Research, 36,* 1416–1424.

Elsen, J., Van Balen, K., & Mertens, G. (2013). Hydraulicity in historic lime mortars: A review. In J. Válek, J. J. Hughes, & C. J. W. P. Groot (Eds.), *Historic mortars characterisation, assessment, conservation and repair series: RILEM bookseries*, Vol. 7 (pp. 125–139). Springer.

Johansson, S. (2007). Hydrauliskt kalkbruk Produktion och användning i Sverige vid byggande från medeltid till nutid. Göteborg studies in conservation 20.

Johansson, S., & Lindqvist, J. E. (2013). Historic mortars with burned alum shale as artificial pozzolan. In J. Válek, J. J. Hughes, & C. J. W. P. Groot (Eds.), *Historic mortars characterisation, assessment, conservation and repair series: RILEM bookseries*, Vol. 7 (pp. 77–88). Springer.

Lindqvist, J. E. (Corresponding author). (2009). Testing of hardened mortars, a process of questioning and interpreting. A publication from RILEM TC 203-RHM Repair Mortars for Historic Masonry. *Materials and Structures*, *47*, 853–865.

Lindqvist, J. E., & Johansson, S. (2009). Sub-hydraulic binders in historical mortars. Workshop RILEM TC RHM repair mortars for historic masonry hosted by TU-Delft. In C. Groot (Ed.), *RILEM proceedings pro067 repair mortars for historic masonry*, (pp. 224–230).

Lindqvist, J. E., & Sandström, M. (2000). Quantitative analysis of historical mortars using optical microscopy. *Materials and Structures, 33,* 612–617.

NT BUILD 437. (1995). Concrete, hardened and mortar: Calcium oxide and soluble silica contents.

Shelly, R. (1997). *Parisian views* (p. 267). MIT Press London.

Development of a Small-Scale Lime Kiln and Experimental Assessment of the Produced Quicklime

Jan Válek, O. Skružná, V. Petráňová, D. Frankeová and J. Jiroušek

Abstract A small-scale lime kiln was designed and built in order to evaluate lime binders produced in the past. The design does not copy any specific historic model but it is made to replicate two main historic procedures: intermittent wood and mixed-feed burnings. The prototype is equipped with sensors and the burning process is monitored by a set of thermocouples in three height levels, an air flow gauge on the primary air inlet and a gas analyser of fumes (CO, CO_2 and O_2) passing through a chimney. The obtained data are used for an assessment of the whole burning process and its optimisation. The paper presents data about four experimental wood burnings of air lime and summaries the newly gained experience regarding the operation of the kiln. In order to assess the quality of the produced lime several samples of quicklime were taken from three main positions according to heat distribution in the kiln. These samples were analysed and compared with samples obtained from five different modern industrial shaft kilns which use oil, gas and coal as fuel. The micro-structure of quicklimes was evaluated focusing on the influence of calcination temperature and its duration. SEM, MIP and BET analyses were used to evaluate the morphology, size of crystallites, porosity, pore size distribution and surface area of the produced quicklimes. The obtained characteristics were compared to the reactivity of lime and the quality of the products was discussed.

J. Válek (✉) · O. Skružná · V. Petráňová · D. Frankeová · J. Jiroušek
The Czech Academy of Sciences, Institute of Theoretical and Applied Mechanics, Prosecká 76, 190 00 Prague 9, Czech Republic
e-mail: valek@itam.cas.cz

O. Skružná
e-mail: skuzna@itam.cas.cz

V. Petráňová
e-mail: petranova@itam.cas.cz

D. Frankeová
e-mail: frankeova@itam.cas.cz

J. Jiroušek
e-mail: jjirousek@itam.cas.cz

J. J. Hughes et al. (eds.), *Historic Mortars*,
https://doi.org/10.1007/978-3-319-91606-4_20

Keywords Experimental lime kiln · Traditional lime burning · Properties of quicklime · Soft burnt lime

1 Introduction

Traditional lime burning is not a uniform technology and many historic methods exist. A typical example of traditional lime production is burning in a flare kiln. A common construction method for burning in a flare kiln is that a rough vaulted dome is built from larger pieces of limestone creating a combustion chamber. Smaller fragments of limestone are placed above the dome in sizes respecting assumed heat distribution within the kiln space. This way of lime burning is known since the Roman period (Adam 1994) and is technologically connected with the use of long flame burning fuels; the most widespread being wood. Wood-fired kilns were originally used for lime burning in many European countries and in less populated and developed regions with sufficiency of wood they survived up to the mid-19th century. About this time lime production technology started to become industrialised and only exceptional cases of traditional lime burning in flare kilns survived until today. In some places with a lack of firewood, other fuels had to be used. Olive kernels, bushes, dried grass and pine cones were utilised in Greece, Italy and Tunisia (Adam 1994). In some areas technological progress was faster, and as lime consumption increased so did the demands on its production, which required an ever-increasing quantity of fuel. Wood soon became scarce in these areas and the lime industry had to adapt to the use of coal, which impacted on the established technologies. Lime kilns using coal as fuel had to be adapted to the different operation modes and over time they gradually developed further and transformed from periodic to continuous operations. The use of coal or charcoal for lime burning is known from London, where the nuisance of smoke from coal burning was already noted as a problem in the early 14th century (Bowyer 1973).

Traditional lime burning is supposed to affect the final product. Hughes et al. (2002) concludes that lime burnt in an experimental mixed feed vertical shaft kiln is a different product in comparison with commercial product from the same raw material. Advantage of burning in a flare kiln is the separation of fuel from the charge. Wingate (1985) suggests that wood firing could produce some of the best quality lime. Also Eckel (2005) mentions, that lime is more evenly burnt and whiter when burnt separated from the charge. This suggests that lime burnt in a traditional flare kiln has a potential to be a high quality product. On contrary, there are some drawbacks when lime is burnt in a flare kiln. Eckel (2005) points out that stone nearest to the dome is liable to be overburnt (hard burnt and sintered).

Quicklime is divided into three categories according to the degree of burning: soft, medium and hard burnt. The bulk density of lime increases from approximately 1.5 g/cm^3 (soft) to over 2.1 g/cm^3 (hard) and reactivity (t_{60}) decreases from

<3 min for soft lime to >9 min for hard burnt lime (Oates 1998). Sintering of lime starts on its surface and is caused by calcination at high temperatures and prolonged residence time. Sintering of quicklime has a negative effect on its reactivity. In the case of large pieces in the dome it is a question whether sintering takes place on the sides even though the core is not fully dissociated or not. A complementary question is about the relation of the size of stone and the progress of the sintering. The liability to sintering also depends on limestone parameters and composition. Limestone with an extremely small portion of impurities exhibits high hard burn potential, i.e. is liable to sintering (Hogewoning 2008a). According to Hogewoning (2008b), sintering potential of limestone can be divided in three groups on the basis of Lime Saturation Factor (LSFII), expressed as the ratio of CaO to the amount of CaO that can be combined with impurities present in limestone, see formula (1).

$$LSFII = \frac{\mathrm{CaO} \times 100}{(2.8 \times \mathrm{SiO_2}) + (1.18 \times \mathrm{Al_2O_3}) + (0.65 \times \mathrm{Fe_2O_3})} \quad (1)$$

Tests on quicklime are usually carried out as a quality control assessing the suitability of a product and monitoring its compliance with a specification, e.g. European standard EN 459. For building limes fineness, reactivity, yield and bulk density are the typical tests. Very important part of testing and interpretation of the test results is sampling process. The quality of quicklime is influenced by the composition of the raw material and the production process as mentioned before. Obtaining a representative sample is therefore important when two different products are to be compared. In addition to this, storing and handling quicklime can also affect the test results. Negative effects of absorption of water (air slaking) and CO_2 (carbonation) on reactivity of lime are known (Oates 1998) and these two parameters should be determined and checked when samples of quicklime are tested.

2 Design and Development of a Small Scale Lime Kiln

The experimental lime kiln, shown on Fig. 1, was built to investigate the influences of traditional burning on the quality of lime and for the production and subsequent research of lime binders made with historically used raw materials (Válek 2015). In addition to the research reasons, it was constructed as a prototype enabling small-scale production of lime binders by traditional methods. A single batch wood-fired burning of limestone can be replicated in the kiln—this is what it was designed for—but the kiln can also be used to burn limestone in a mixture with fuel, known as mixed feed burning. Other elements of the design satisfied requirements for the durability of the kiln and ease and safety of operation.

Fig. 1 Prototype of a lime kiln

2.1 Construction

The actual kiln design is shown in Fig. 2. It consists of a cylindrical shaft with an inner diameter of 0.8 m and a height of 1.3 m above a cast-iron grate. The inner walling is made of refractory circle bricks on clay mortar. The brick cylinder is sheathed in a 50 mm layer of heat-resistant mineral wool insulation. On the outside, the kiln is enclosed by vertical timber boarding. The space between the exterior wooden shell and the insulation is filled with crushed limestone grit with grains fraction 0/4 mm. Air is fed into the kiln primarily through an inlet measuring 20 × 20 cm and passing through the ash pit and the grate. A secondary air inlet is situated in the burning chamber door. The crown of the kiln is formed of a 60 mm thick cast-concrete slab made of natural cement and gravel. The slab is cut into segments allowing its thermal expansion and the segments can be removed for inspection of the backfilling. A conical hood with flue can be optionally fitted onto the kiln to monitor combustion products and regulate the draught. The draught can be also regulated by opening or closing two main air inlets.

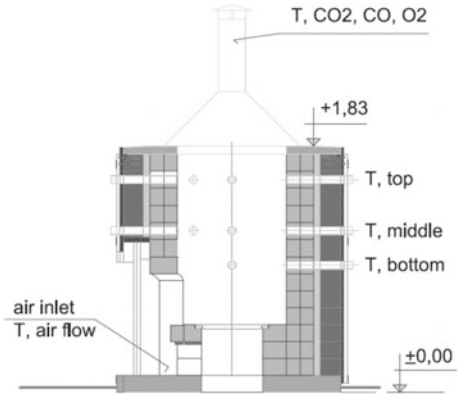

Fig. 2 Cross section of the lime kiln prototype

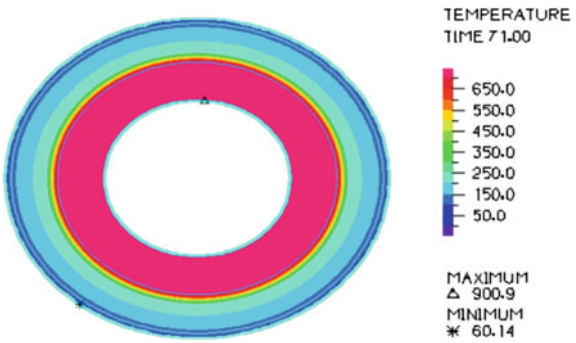

Fig. 3 Model of a temperature transport through a kiln wall

The kiln is designed and constructed using materials and technologies that can be regarded as generally available and which copy the traditional design in some points, e.g. bricks are laid on clay mortar, backfill is used as an elastic layer allowing expansion and movements of the inner walling. In order to decide about the insertion of a thermal insulation a model of temperature distribution in a kiln wall after 50 h of heating to 950 °C was computed, see Fig. 3. The effect of thermal insulation is clearly visible reducing the temperature by 200 °C. The model also predicted the maximum temperature on the external surface of the kiln. This confirmed the possibility to use timber boarding and provided information regarding the safety during operation. In practice, the burning lasts shorter time and the external surface does not reach temperatures higher than 35 °C.

2.2 Monitoring

Monitoring of the burning process was introduced for the evaluation of the kiln design and its operational modes. Heat distribution in the kiln can be monitored during the whole process with the aid of S-type thermocouples that are inserted into the built-in protection sleeves in three horizontal profiles and three vertical cross-sectional axes, see Fig. 4. The temperatures are usually monitored around the perimeter of the shaft, but the temperature profile from the middle to the perimeter can also be determined in three selected sleeve positions. This is enabled by insertion of an additional protection sleeve made of heat resistant steel (DIN X10CrAlSi25, grade 1.4762) with openings (four 12 mm holes drilled across diameter and placed 100 mm apart). Moving a thermocouple inside this sleeve allows measurements of temperatures in a horizontal profile within the kilns space in 100 mm steps. Emission gasses and the calcination process is monitored by an

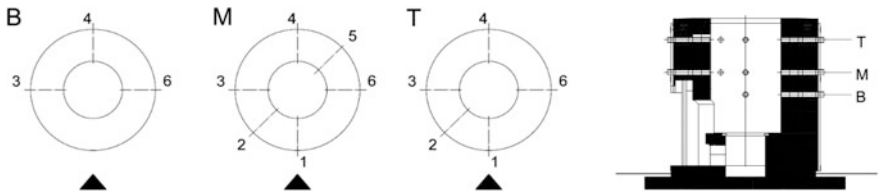

Fig. 4 Positions of kiln wall bushings for thermocouples' placements. Three horizontal levels are coded B—bottom, M—medium, T—top, the vertical profiles are numbered

MRU gas analyser Optima 7 with IR CO_2 sensor and O_2 and CO electrochemical sensors. In addition, the airflow velocity at the primary air inlet and the temperature, relative humidity and atmospheric pressure of the surrounding environment can be monitored. This relatively extensive monitoring is undertaken in order to describe the calcination processes and allow a subsequent optimisation of this process using known traditional measures, e.g. covering the top of the kiln with daub, draught regulation, insertion of stakes, etc.).

2.3 Filling the Kiln for Wood-Fired Burning

The first step is to build a vaulted dome. The internal space under the dome is the burning chamber and the dome holds all limestone feedstock above it. In many ways its proper construction is key for the successful burning. It is typically built from relatively large angular sharp-edged limestone pieces that have a good grip and also irregular surface that allows air, fumes and flames passing through the voids it creates. The stones are arranged in the vault vertically, with the narrower end at the bottom. After ensuring that the dome structure is well built and stable the rest of the kiln can be filled up with limestone to its upper rim. Altogether, just under one tonne of limestone fits in this experimental kiln. The size of the dome stones ranges from 100 to 250 mm. Then stones measuring around 80–125 mm are placed in the kiln, with fractions measuring around 20–40 mm placed in the 'cooler' areas. For this kind of calcination it is very important that the fuel burns with a long flame that passes through the entire limestone batch. When filling the kiln it is essential to know or predict areas where the heat does not spread easily by natural draught. These are usually at the base of the vault in the bottom part of the kiln, around the perimeter of the kiln and above the stoke-hole. Therefore, the batch is placed in the kiln in various sizes in a manner that corresponds to the expected spatial temperature distribution, ensuring that the burning efficiency is as high as possible. The stone should get gradually smaller from halfway up the kiln and to the sides.

2.4 Wood-Fired Burning Procedure and Variability of the Progress

The burning process follows four main stages: drying, heating, limestone decomposition and cooling. Duration of the drying stage is based on estimation and is typically a relatively short. During this first stage, the fire is kept low in order to avoid a shock heating and cracking of limestone. The aim of the second stage is to reach 900 °C within the kiln space. In average ambient conditions and stoking rate of 16 kg/h these two stages together span from 12 to 20 h (considering the kiln is fully loaded). Duration of the following decomposition stage depends on the size of charged limestone. For the stone sizes presented above minimal 12 h are allowed to ensure full decomposition of limestone. This residence time is estimated based on known tabulated values (e.g. Oates 1998). When the limestone decomposition is finished, no more fuel is added and the kiln is let to cool down. The final stage lasts approximately 24 h and lump quicklime is drawn from the kiln when temperature is below 60 °C.

Table 1 presents selected characteristics regarding the fuel consumption and environmental conditions of four experimental burnings. In order to be able to compare the burnings the following two parameters were selected: time to reach 900 °C on any of the thermocouples and fuel consumption from the beginning to the point of reaching 900 °C. A high scatter of these two parameters points at the fact that the burning process was dependent on some influential factors. Amongst them were environmental conditions and some other parameters. The ambient environment was partially monitored; other parameters like the type of wood and its moisture content were noted; but there were also other factors that were more difficult to be determined, like the way the stone pieces were placed in the kiln, or to be controlled, like the effect of wind and climatic changes.

In practice, the burning process is often related to the draught in the kiln. The higher the draught is the more intensively fuel burns and thus the calcination process progresses faster. The draught depends on the air pressure difference between the bottom (air inlet) and top (fume outlet) parts of kiln, which exists due to temperature differences and other factors. The complexity of the factors that affect the burning is illustrated by the following examples noted during the trial burnings. In the case of the second burning, the wood burnt very slowly and the draught was minimal for the first 24 h. This was possibly due to the passing thunderstorms and rapid changes in climatic conditions, like descending air currents, which affected the duration of the whole burning process and the corresponding fuel consumption per hour. On contrary, the best draught occurred during the fourth burning and that led to the intensification of burning and calcination.

For each burning the fuel consumption was driven mainly by the draught and thus the amount of oxygen which was let in by the primary and secondary inlets. For each burning condition a certain stoking pattern was established; usually 8–15 kg in a 30 min span. Figure 5 shows the fuel stoking rate during the third burning.

Table 1 Fuel consumption up to reaching 900 °C and environmental conditions of experimental burnings (*n.m.* not measured; *VT* Vitošov limestone; *CS* Koněprusy limestone)

Burning	Stone	Heating to 900 °C				Environmental conditions					
		Position	Time (h)	Wood (kg)	Wood (kg/h)	p_{atm} (Pa) @ 320 m AMSL		T (°C)		rh (%)	
						Min	Max	Min	Max	Min	Max
I	VT	M2 wall	12.7	284	22.4	97,182	97,379	11	28	27	53
II	VT	M2 wall	30	528	17.6	96,630	97,130	10	28	30	71
III	CS	T4 centre	16.8	368	22.0	n.m.	n.m.	4	22	52	72
IV	CS	M4 centre	8.8	237	26.9	98,025	98,796	6	14	66	77

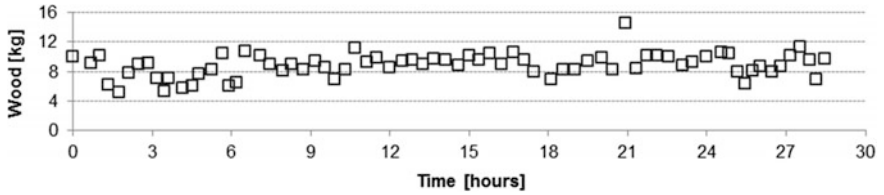

Fig. 5 Fuel stoking during the third burning

The highest temperatures were reached in the centre of kiln right above the firing space. Hotter zones were also established in draught channels within the stone. These channels were typically in the centre of kiln but their position was also influenced by the wind direction, the way stone was placed in kiln and its sizes, and the way the kiln top was covered. The fume hood with a 1.5 m tall chimney was placed on the top of kiln to measure emissions and to unify the burning conditions during the experiments. The distribution of temperatures recorded during the third burning is shown in Fig. 6. All thermocouples but one (T4) were placed so that they protruded about 5 mm inwards to the kiln space. T4 was recording in the centre of the kiln and was placed in the sleeve number 4 at the top level. It should be noted that thermocouples recorded the temperature of air, not the stone, in a certain spot. The recorded value was affected by the temperature of passing air and gases, conduction of heat by the surrounding solids and radiation. The thermocouples that responded to the wood stocking by dropping and rising temperature usually showed the higher temperatures. They were influenced by passing air. On contrary, the more stable ones typically showed the lower temperatures. The thermocouples placed at the periphery of the feedstock showed the lowest temperatures within the kiln. Temperatures identified within the stone by moving thermocouples from the sides about 10 cm inwards were about 150–200 °C higher during the calcination phase. That is why almost 90% of limestone was fully calcined even though the most of the thermocouples placed on the perimeter did not reach 900 °C by the time the burring was stopped. This estimation of burning efficiency was based on weighing the stone charge before and after calcination and was also confirmed by the amount of material left on a sieve after slaking. It was also interesting to note that the highest temperature during this third burning was almost reaching 1200 °C. During the fourth burning the highest temperature reached even 1270 °C. Considering the relatively small scale of this operation, low capacity of the burning chamber and short burning times it can be suggested that in traditional wood-fired kilns temperatures around 1300 °C and possibly higher were commonly reached; although only locally in the hottest zones.

Figure 7 shows the level of oxygen, temperature of fumes and air flow velocity. All three values fluctuated due to stoking. The fumes temperature measured in the

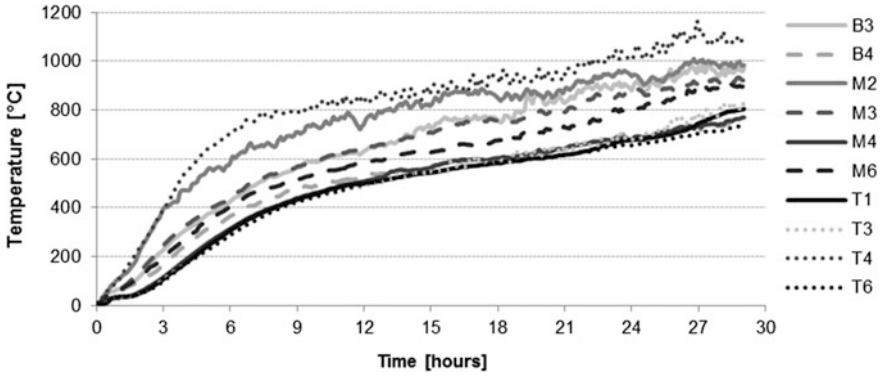

Fig. 6 Example of temperature distribution in the experimental kiln during the third burning

chimney at app. 1 m above the kiln top gradually increased and after approximately 15 h flames started to reach the thermocouple after stoking. There are visible small peaks on the temperature chart due to this effect. The level of oxygen (O_2) in the chimney also corresponded to the stoking regime. When a new fuel was added burning of released combustible gases consumed almost all oxygen. However, the monitored values demonstrate that overall wood burnt in the atmosphere with oxygen surplus. A certain balance between the primary and secondary air inlets had to be maintained to optimise the process of wood burning. The air flow values, shown in Fig. 7, were determined in the primary air inlet only and in average the flow velocity there was about 0.8 m/s through an area of 0.04 m^2. The temperature in the burning chamber as of the whole kiln also gradually increased with time and this affected the dynamics of burning.

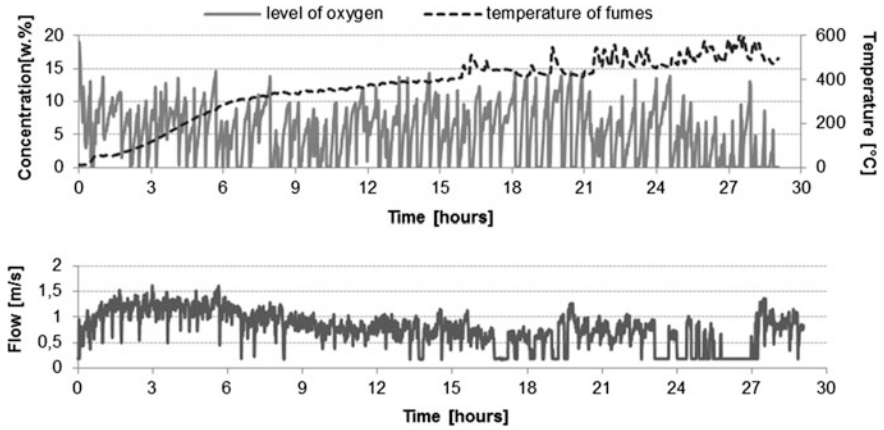

Fig. 7 Third burning. Examples of characteristics monitored during the third burning

2.5 Kiln Efficiency

Kiln efficiency and fuel cost have been always important issues for lime production. The kiln efficiency can be calculated based on formula (2) used by Practical Action (1997) advice adopted from Boynton (1980). The formula expresses the ratio between the theoretical heat required to decompose limestone and the heat provided in relation to the final quicklime (CaO) gain. The L_s value in the numerator considers chemical composition and variety of imperfections of the burning process (recarbonation, underburning etc.). In the denominator there is the total heat provided by the fuel burning.

$$E = \frac{H_c \times L_s}{C_f \times M_f} \tag{2}$$

where E is kiln efficiency; H_c is theoretical heat of calcination per tonne for pure quicklime (CaO), in this case taken as 3200 MJ/t; L_s is available CaO content in produced quicklime; C_f is calorific value of fuel (MJ/kg); and M_f is mass of fuel per tonne of quicklime (kg/t). The calorific value of wood was considered as 16.6 MJ/kg for both pine and oak, both having moisture content around 7%.

The kiln efficiency E calculated for the selected four burnings is expressed in Table 2. Available CaO content in lime was calculated from the chemical content of limestone multiplied by the burning efficiency, which was determined as a percentage ratio of achieved and expected theoretical weight losses due to calcination. Regarding the burning process, it should be mentioned that the first burning was not completely finished due to problems with the stability of the dome. The second burning was strongly affected by the adverse environmental conditions (thunderstorms). The third and fourth burnings can be considered as standard. Based on these trials the kiln efficiency ranges between 21 and 26%. A target efficiency, stated by the Practical Action Technical Brief (1997) for a forced draught vertical kiln, is 50%. The kiln efficiency value is low for single batch kilns as they operate on intermittent bases. During a traditional wood-fired periodic burning there are substantial heat losses due to the heating of the air, of which there is always an excess amount, and heating the kiln itself. Moreover, the batch burning does not allow any pre-heating of stone as is common in kilns operating in continuous modes. The calculated kiln efficiency is suitable for comparing calcinations performed in this specific kiln and can be also used for comparisons with equivalent facilities.

Table 2 Heat provided and kiln efficiency of four experimental burnings

Burning	Stone	Heat provided				Heat required to decompose $CaCO_3$					Efficiency
		Total fuel (kg)	Total duration (h)	Rate (kg/h)	Heat (MJ)	Limestone (kg)	CaO (%)	Burning efficiency (%)	Available CaO (%)	Heat (MJ)	E (%)
I	VT	397	18	22.1	6590	856	97	65	63.2	1732	26
II	VT	664	36	18.4	11,022	941	97	80	77.8	2344	21
III	CS	635	28.5	22.3	10,541	894	99	90	89.1	2549	24
IV	CS	720	27	26.7	11,952	917	99	90	89.1	2615	22

3 Experimental Assessment of Traditionally Produced Quicklime

The experimental replication of lime production in a wood-fired flare kiln was carried out at the above mentioned facility. The aim was to characterise the produced quicklime and a special focus was given to the degree of burning. The replication of traditional burning process also aimed at understanding of influences of production technology on the final product. The traditionally produced quicklimes were compared with industrially produced quicklimes. Two types of raw materials were used in the experiment and both were calcined in the traditional and industrial kilns. Each raw material calcined in the traditional and industrial kiln came from a single bench blast.

3.1 Raw Materials

Two type of high-calcium limestones were selected for the experiment. Vitošov (Vit) was a finely (0.05–0.25 mm) crystalline limestone with homogenous structure, see Fig. 8. Koněprusy (CS) was a well compacted micritic limestone with bioclasts and extraclasts, see Fig. 9. The average size of its particles was about 0.8 mm. Open porosity of both limestones was below 1%. Average chemical composition of the limestones, based on XRF analysis of powder samples drilled during bench blast preparation, and calculated Lime Saturation Factor (LSF II, see formula 1) are presented in Table 3. Koněprusy limestone had the LSFII factor in order of 10^4 and thus should be more liable to sintering than the Vitošov limestone.

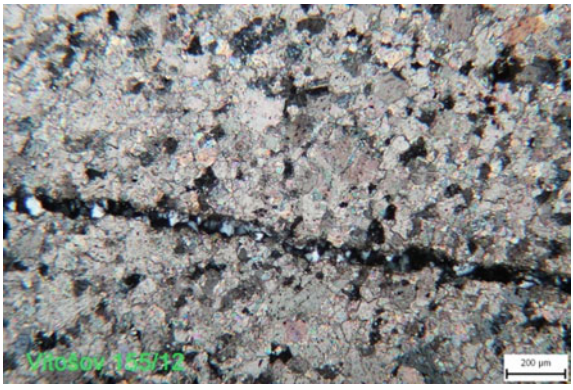

Fig. 8 Microphotograph of limestone from Vitošov (Vit), XPL. The fissure in the middle is secondarily filled with quartz. Field of view 2 mm across

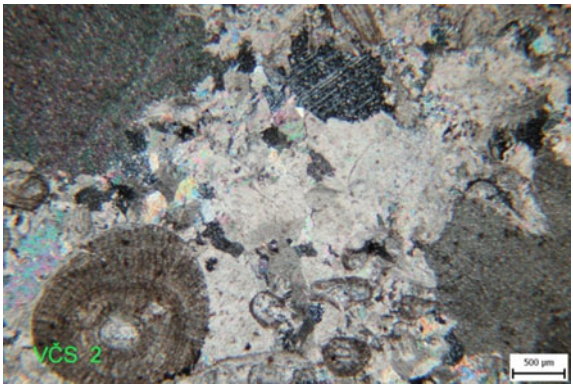

Fig. 9 Microphotograph of Koněprusy limestone (CS) showing larger (300–1000 µm) micritic extraclasts and bioclasts XPL. Field of view 5 mm across

Table 3 Composition of limestone (in wt%) determined by XRF, loss on ignition (LOI) and LSFII

	Origin	CaO	MgO	SiO_2	Al_2O_3	Fe_2O_3	MnO	LOI	LSF II
Vit	Vitošov	54.5	0.2	0.63	0.17	0.17	0.02	40	2626
CS	Koněprusy	55.5	0.33	0.04	0.04	0.03	0.006	42.9	31,058

3.2 Lime Production and Sampling

Altogether, thirteen 20 kg samples of quicklime were collected and initially evaluated. The overview of the collected samples is presented in Table 4. There were five samples from five different commercial kilns operating in continuous regime and nine samples from the traditional flare kiln obtained during four batch burnings. Samples are characterised by their way of production (first letter **C**-commercial, **T**-traditional) followed by the type of limestone (Vit-Vitošov, CS-Koněprusy), by a number referring to kiln/burning and in the case of traditional quicklime also the position in kiln is distinguished by additional number where 1 denotes a sample from the bottom part of the vaulted dome, 2 denotes a spot sample from the middle of the kiln and 3 denotes a sample from the top part of the kiln, app. 20 cm under the top feedstock surface.

Samples of quicklime (CVit 1-3 and CCS 1) were obtained from four different continuous vertical shaft kilns of two different lime producers. These kilns operate on the same principle using parallel flow of hot gasses and altering burning and non-burning shafts during operation. They apply regenerative preheating of all combustion air. Sample CCS2 was obtained from a production using classical mix-feed shaft kiln. Traditional samples of quicklime (TVit and TCS) were obtained during the experimental calcinations. Production-related characteristics of the collected samples are presented in Table 4. The temperature range and residence time are approximated to characterise the main calcination conditions. Typical temperature profile of the Maerz kilns and other production details are published by the producer.

Table 4 Denomination of samples and their production-related characteristics

	Calcination temperature (°C)	Residence time (h)	Fuel	Feedstock stone size (mm)	Spot sample acquisition
CVit1	~1150	10.5	Recycled oil/gas	40–70	Continuous production
CVit2	~1250	10.5	Recycled oil	20–40	Continuous production
CVit3	1050–1150	12	Coal/gas	20–80	Continuous production
TVit I-2	900–1000	6	Wood	30–120	Flare kiln—middle
TVit II-1	900–1050	8.5	Wood	150	Flare kiln—vault
TVit II-2	900–950	7.5	Wood	30–120	Flare kiln—middle
CCS 1	900–1000	12	Liquid fuel	40–100	Continuous production
CCS 2	900–1300	24	Solid fuel	60–100	Continuous production
TCS I-1	900–1150	16	Wood	150	Flare kiln—vault
TCS I-2	900–1150	14	Wood	30–120	Flare kiln—middle
TCS I-3	900–1150	13	Wood	30–50	Flare kiln—top
TCS II-1	900–1250	18	Wood	150	Flare kiln—vault
TCS II-3	900–1200	11	Wood	30–50	Flare kiln—top

3.3 Comparative Analysis of Samples

Interpretation of analytical results of quicklime samples is challenging due to several reasons. The first one is the representativeness of a sample to the produced batch. Lime kilns in general do not have uniform distribution of temperature during calcination process, raw material is naturally heterogeneous and the process of limestone decomposition is a function of burning temperature and stone physical size. Due to the above mentioned points and some additional influences the parameters of quicklime can differ significantly even so the samples are from the same calcined batch. In addition, quicklime typically reacts fast with air humidity and thus samples should be protected immediately after sampling and stored in conditions that do not allow hydration and subsequent carbonation. Last point to mention is that when comparing physical properties of quicklimes only fully calcined samples are comparable.

Some of the obtained samples were not fully calcined; some contained high portion of calcium hydroxide (they were partly hydrated). These samples were excluded from the detailed analytical studies described below that aimed to focus on the comparative assessment of well-burnt lime.

3.4 Analytical Techniques

Acquired samples of about 20 kg of quicklime were stored in plastic buckets closed with a lid and wrapped with a cling foil. Powdered CaO was prepared from app. 1 kg of lump lime with a pestle and mortar and passed through 2 mm sieve immediately before the further testing. The homogenised powder was used for reactivity test carried out according to EN 459-2. The presented values are average of two measurements. The composition was evaluated by thermogravimetric analysis (TGA/DTG) in the 20–1000 °C temperature range with a heating rate of 10 °C/min in a nitrogen atmosphere with SDT Q600 (TA Instruments).

Lump samples were used to study the CaO structure in low and high temperature zones (e.g. samples from the top and vault positions). Pore size distribution, surface area and skeletal density of lump samples were characterised by mercury intrusion porosimetry (MIP) by AutoPore IV with maximum pressure 33,000 psi; nitrogen gas adsorption (BET) at 77.5°K by ASAP 2020; and helium gas pycnometry (GP) by Accupyc II 1340, respectively. Morphology and structure of lump samples were qualitatively described in scanning electron microscope (SEM), Mira II LMU (Tescan) equipped with secondary electron (SE), back scattered electron (BSE) and energy dispersive X-ray (EDX) detector (Bruker). The samples were coated with a thin gold layer (app. 15 nm) to obtain better conductivity necessary for scanning in a high vacuum mode. The SEM set up was: 15 kV high voltage and 15 mm working distance in case of EDX analysis. The absorbed current reached the value 1.4 nA and the time of collecting of X-rays was 60 s. For quantification of elements was used a standard-less elemental analysis.

4 Results

The experimental study focused on properties of well-burnt quicklime samples and the results are summarised in Table 5.

4.1 Thermal Analysis (TA)

Thermal analysis identified that all quicklimes were partially hydrated (4–8%) and also partially carbonated (around 1%). The DTG peak of calcium carbonate

Table 5 Properties of analysed quicklime samples

	TA		MIP	BET	GP		Reactivity	
	Ca $(OH)_2$ (%)	$CaCO_3$ (%)	Porosity (%)	Surface area (m^2/g)	Density (g/cc)	Bulk density (g/cc)	$t_{60°C}$ (min)	T'_{max} (°C)
CVit 3	4.3	1.0	50.9	2.89	3.19	1.57	0.3	78.0
TVit II-1	7.1	1.0	50.9	1.65	3.15	1.55	5.3	72.7
CCS 1	3.0	1.0	54.5	2.08	3.30	1.50	0.4	79.1
TCS I-1	5.9	0.9	49.2	1.55	3.23	1.64	2.4	79.5
TCS I-2	7.4	1.1	49.9	1.36	3.18	1.59	2.5	78.9
TCS II-1	5.8	1.1	52.2	1.41	3.20	1.53	3.0	78.7

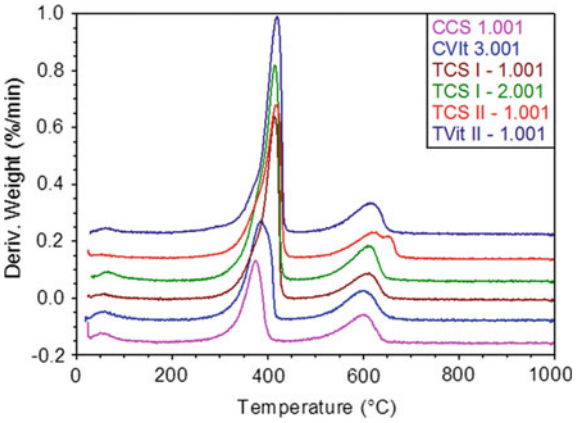

Fig. 10 Derived weight changes of selected lime samples when heated from 20 to 1000 °C. $Ca(OH)_2$ peak is about 400 °C, $CaCO_3$ peak is just above 600 °C

dissociation was accounted to re-carbonation as it appears in a relatively low dissociation temperature, just above 600 °C, see Fig. 10. All limes were thus assumed to be well burnt. The level of hydration was relatively high and might affect the reactivity and also other structure related properties. However a certain level of hydration and re-carbonation has to be expected due to the production processes and this is especially the case of traditional production when quicklime is left in kiln to cool down in natural conditions. A certain contribution of sample handling and storing to the elevated hydration of quicklime cannot be excluded.

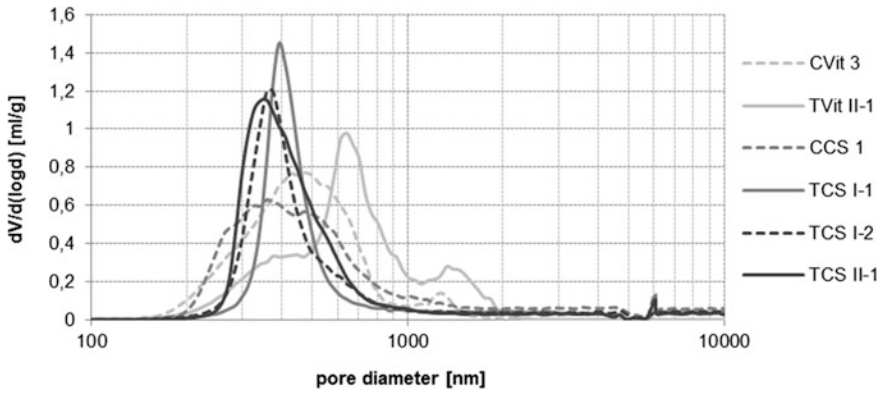

Fig. 11 Pore size distribution of lime samples determined by MIP

4.2 Mercury Intrusion Porosimetry (MIP)

Open porosity of quicklime samples was from 49 to 54.5%, see Table 5. This values indicate that all the tested samples fit to a category of soft burnt, which according to Oates (1998) ranges between 45 and 55%. Figure 11 presents pore size distributions and for most of the samples the main pore size was within the range of 200–600 nm. The exception was sample **T**Vit II–1 which was taken directly from the surface of stone placed in the vaulted dome. This could indicate lime sintering effect on the surface. The effect of quicklime hydration on the pore size distribution was not significant enough to be determined.

4.3 Gas Adsorption and Density

Density, bulk density and specific surface area (BET) of quicklimes are compared in Table 5. The two commercially produced limes had higher surface area values which also corresponded to a more rapid reactivity. The density values were similar for all six samples and according to Oates (1998), the analysed samples could be classified as soft burnt by their density.

4.4 Reactivity

Reactivity of the selected quicklimes is presented in Fig. 12. The commercial quicklimes were the most reactive and in general the samples from the dome had slower reaction. However, only the sample **T**Vit II-1 from the dome was classified

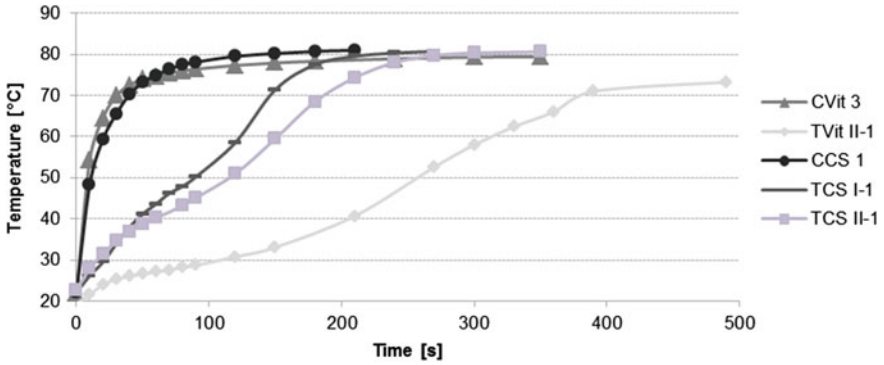

Fig. 12 Reactivity of quicklime samples

Table 6 Typical reactivity of commercial limes and production targets

	CVit 1	**C**Vit 2	**C**Vit 3	**C**CS 1	**C**CS 2
t_{60} (min)	3–4 min	6–8 min	<1 min	0–1 min	5–15 min
Production	Soft burnt lime	Hard burnt lime	Soft burnt lime	High react. low CO_2 content	Slow react. low CO_2 content

as a medium burnt lime based on the reactivity test. The rest was soft burnt according to the criteria of Oates (t_{60} of a medium burnt lime is 3–9 min). The industrial production targets certain degree of burning, see Table 6. The reactivity, degree of burning and further processing, depends on technological requirements of final customers. Both commercial samples involved in the experiment were produced with the intention to be fast reactive reaching temperature of 60 °C in less than 60 s.

4.5 SEM Observations

Samples of quicklime observed in SEM were all evaluated in three positions; region of surface exposed during the calcination in kiln, region 2–3 mm below the surface and region about 5 mm below the surface. These positions were all on the same line perpendicular to the surface. Images presented in Fig. 13 are all from the surface region. There were differences in the size of crystallites and interspatial voids but in principle the structure was very similar for all evaluated samples. Just comparing the set of the six samples, the smallest particles of CaO were about 400 nm and the largest ones were about 2000–3000 nm. One should note, that this quantification is

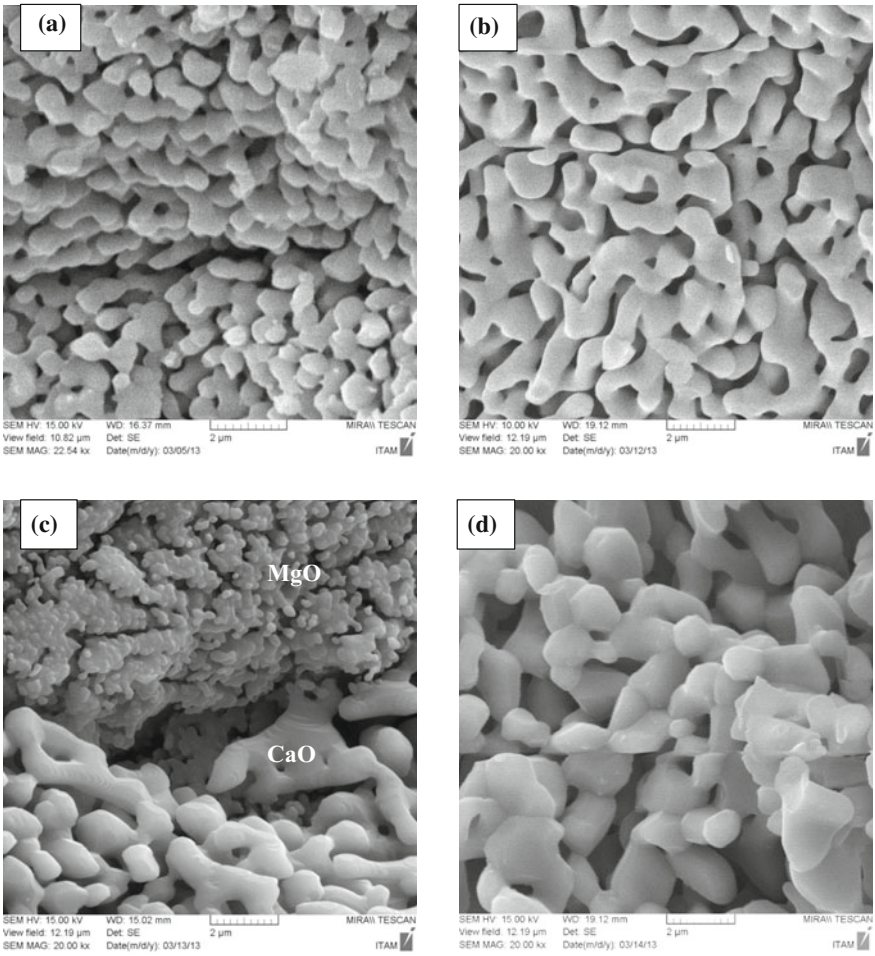

Fig. 13 Images from SEM (**a** CVit 3, **b** TVit II-1, **c** CCS 1, **d** TCS II-1); all images in the same scale; field of view 12.19 μm across

valid only for the six samples and it describes a very small area. On Fig. 13c there is also visible an MgO structure with much finer particles. Figure 14 left shows morphology of quicklime sample **T**CS I-1 that was obtained from the vaulted dome where larger crystallites of CaO (5–10 μm) were identified in the surface region. Just a few mm below are particles about 5x smaller than that of those observed on the surface, see Fig. 14 right.

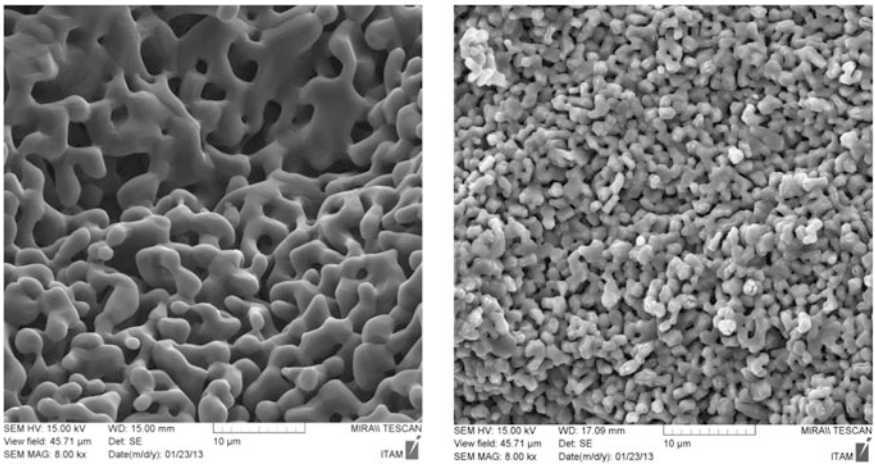

Fig. 14 Sample **T**CS I-1. Image of CaO crystallites near surface showing partially sintered particles (5–10 µm) on the left. Image from the same sample but just 3 mm below the surface showing CaO crystallites in the range of 1–2 µm, on the right. Field of view 45.7 µm across

5 Discussion

Lime was burnt in a way that replicated the traditional calcination process in a wood-fired flare kiln. Due to the experiment, it was possible to identify the key technological points which are significant for this traditional burning process: building the vaulted dome, distributing the stone within the kiln, optimal wood stoking and burning regime. The burning process was extensively monitored and described by quantitative values. In addition, some qualitative observations were noted. For example: colour of flames, relation of draught and rate of wood burning, temperature increase and its relation to the moment when flames appear at the top of kiln etc. The influence of environmental conditions on the burning process was noted, however, it was not possible to conclusively relate the monitored parameters, selected to describe the ambient environmental conditions, to the effects observed during burnings. A practical recommendation could be that certain climatic conditions should be avoided. For example rapid unpredictable changes in air currents due to thunder storms. The rate of burning depended on draught conditions in the kiln. With a good draught one tonne of limestone could be successfully calcined within 24 h in a kiln of this type. This time span also corresponds to known one day lime kilns that operated at the end of the 19th century in Moravia (Vápenice) and Slovakia (Skýcov). It is interesting to note that temperatures above 1250 °C, i.e. cement clinkering temperature, were reached by wood burning in this relatively small kiln. This means that mineral phases that are formed in this high temperature region, like C_3S, could have been produced in the past depending on limestone composition. Their proportion was probably negligible due to the facts that such

high temperatures were localised, high calcium limestones were historically preferred and particles that did not slake required additional treatment.

The temperature differences in the experimental kiln show that the same batch of lime is burnt in a very nonhomogeneous temperature field with a difference of 500 °C between the hottest and coolest zones. Considering the heat concentration to the central zone of the vaulted dome and also fact that typical historic flare kilns were much larger and thus probably reaching even higher temperatures in and above the combustion chamber leads to questions regarding the quality of lime from the hottest zones. It is known that the goal of every burning was to reach maximum burning efficiency in terms of converting limestone to lime. Longer residential times and relatively high temperatures suggest a possibility that lime from the vaulted dome could have been often hard burnt.

The laboratory assessment of the traditionally produced quicklimes attempted to answer two main questions; (i) was the quicklime produced in a wood fired flare kiln comparable with the modern commercial production and (ii) was the lime exposed to the high temperatures in the vaulted dome hard burnt? The evaluation of quicklime contributed to the assessment of the calcination procedure in the designed kiln. The results indicated that the chosen size of stone and the selected calcination regime was appropriate in terms of the reached temperatures. It also pointed out at some deficiencies in terms of heat distribution in the kiln.

The preliminary assessment of quicklime samples from commercial and traditional production led to a further selection and only well-burnt samples were analysed. It was interesting to note that a certain portion of underburnt, re-carbonated and hydrated parts was present in samples from the traditional kiln as well as from the modern industrial kilns. The complete process of lime production is the largest difference between the current industrial and traditional productions. Both, the modern and traditional processes have their own ways how to sort quicklime according to its quality. Modern processes allow a better control of the calcination conditions and quicklime can be sorted based on analytical results. Traditional processes relied on skills, experience and manual handling. The evolved knowledge and crafts of lime burning was linked to a further processing of lime and its application. The way lime was slaked and processed further in a traditional way allowed for selection of a good quality product in relation to its application.

The well-burnt traditionally produced quicklimes were not significantly different from the commercially produced ones in their main physical characteristics. There were two parameters, surface area and reactivity, that pointed at the difference between the commercial and traditional limes. The reactivity of the selected commercial limes was higher as it was a special intention of the producers; they also produce limes with lower reactivity. The traditionally produced limes could be regarded as soft burnt and the selected limes had reactivity between 2 and 5 min. In fact a very fast reactivity could be a problem for slaking lime in a traditional way. If the reaction is too fast, access of water to particles of CaO may not be sufficient (hand mixing is not fast and efficient enough) and the temperature can, due to the exothermic reaction, locally exceedingly rise and the slaked lime particles consequently aggregate together.

Temperature in the kiln reached over 1200 °C in the space above the combustion chamber when the sample **T**CS I-1 was calcined and the stone there was exposed to temperatures above 900 °C for 16 h. Some sintering effect was identified on the surface of stones placed directly above the combustion chamber however, given the size of stone, the sintered layer was relatively thin and the spot sample from this location could still be classified as a soft burnt lime. The sintering effect progressed from the surface inwards. These are interesting facts suggesting that the sintering (hard burning) was in practice dependent also on the size of calcined stone. The proportion of surface to total volume is decreasing with increasing diameter and thus a sintered surface into the depth of few μm has a relatively low effect on a decimetre large stone block.

A quantitative comparison of characteristics of quicklimes produced in industrial and traditional kilns is difficult as there are too many variables like natural variability of limestone, temperature variation and calcination conditions, re-carbonation, hydration etc. that cannot be determined. A statistically significant amount of data on representative samples would have to be analysed to relate the quicklime properties with influences of a specific kiln and production technology. In addition studying properties of lump quicklime is difficult as the pore structure related properties change across the particle. Particles of the same material but different sizes calcined in the same conditions thus have different pore structure.

6 Conclusions

The study demonstrated that a small-scale custom made lime production is in principle possible. The designed prototype was proved to be functional and lime was successfully produced. The experimental burnings and their monitoring allowed to describe the temperature distribution in the kiln including also the effect of formation of draught channels within the feedstock. The temperature difference within the kiln space was reaching 500 °C. The data obtained by monitoring confirmed the importance of placement of stone to the kiln in terms of their size and inter-particle voids. The size should correspond to the expected heat spread and should be in relation to the temperature reached during calcination and its duration. The inter-particle voids are important for the transfer of heat by hot air and fumes. The positioning of stones affected permeability and formation of draught channels. The experimental burning confirmed the importance of placement of stone within the kiln known from historic and ethnographic studies dealing with traditional lime burning. The practical experiment demonstrated that the environmental conditions significantly influence the burning process. However, the established monitoring of atmospheric pressure and ambient air humidity and temperature could not be fully related to the observed effects. Other, more influential factors existed that were not monitored. These were probably air currents and local wind conditions. The experimental burning demonstrated that the burning efficiency, i.e. the rate of converted quicklime, could under standard conditions reach 90% or possibly even

higher. The process was however energy demanding and the kiln efficiency was about 25%. High fuel consumption is typical for the traditional burning in open-top kilns without any heat recuperation. A practical conclusion is that the higher production costs would have to be justified by other reasons, like production of unique materials for conservation and restoration projects.

Based on the assessment of the produced quicklime the following conclusions can be drawn:

- According to the evaluated lime samples, the lime produced in the experimental wood-fired kiln could be classified as a soft burnt lime.
- Well-burnt quicklime produced in the experimental lime kiln was of a good quality and similar in properties to some currently produced commercial soft burnt limes.
- In the region of the vaulted dome, where the stone was exposed to temperatures reaching over 1200 °C, a sintering of quicklime occurred. The study indicates that in the case of the four experimental burnings, this effect was quite localised and mostly affected only a relatively thin surface layer.
- Wood-fired lime differs from the modern one in characteristics which relate to their technology of calcination and subsequent processing. The product is affected by specific conditions in the kiln that can differ based on external influences. In order to compare lime produced in traditional and modern kilns a long-term statistical study would be required.

Future studies will focus on an improved quantification of the identified effects and also on the relation of the production technology to the quality of lime and its use.

Acknowledgements The study was supported by the research project "Traditional lime technologies and their present use" (DF11P01OVV010) and its follow up project "Lime materials for restoration and conservation of authentic elements of historic buildings" (DG16P02H012) provided by the Czech Ministry of Culture within its NAKI research programme. Companies Vápenka Vitošov and Vápenka Čertovy Schody are thanked for providing limestone and quicklime samples. Dr. Pavel Beran is thanked for the thermal model of the kiln.

References

Adam, J. P. (1994). *Roman buildings—Materials and techniques*. Abingdon: Routledge.

Bowyer, J. (1973). *History of building*. London: Orion Books.

Boynton, R. (1980). *Chemistry and technology of lime and limestone*. New York: Wiley.

Eckel, E. C. (2005). *Cements*. Donhead: Limes and Plasters.

Hogewoning, S., Wolter, A., & Schmidt, S. (2008a). Dependence of hard burn potential on limestone properties (Part 1). *Zem Kalk Gips, 61*(6), 54–60.

Hogewoning, S., Wolter, A., & Schmidt, S. (2008b). Dependence of hard burn potential on limestone properties (Part 2). *Zem Kalk Gips, 61*(7), 84–93.

Hughes, J. J., Swift, D. S., Bartos, P. M. J., & Banfill, P. F. G. (2002). A traditional vertical batch lime kiln: Thermal profile and quicklime characteristics. Masonry opportunities for the 21st Century, ASTM STP 1432, Eds. West Conshohocken: American Society for Testing Materials.

Oates, J. A. H. (1998). Lime and limestone, chemistry and technology, production and uses. Weinheim: Wiley-VCH.

Practical Action Technical Brief. (1997). How to calculate the energy efficiency of your lime burning process, practical action, document from www.practicalaction.org.

Válek, J. (2015). *Lime technologies of historic buildings. Preparation of specialised lime binders for conservation of historic buildings*. Praha: ÚTAM.

Wingate, M. (1985). *Small-scale lime-burning, a practical introduction*. Intermediate technology publications.

Lime Burning Tradition in a Field Kiln of the Jämtland Model in Sweden

K. Balksten, C. Persson and J. Eriksson

Abstract This study focuses on the local lime tradition in the region of Jämtland, in central Sweden. Local lime was used when building the medieval stone churches and since they are in a need of restoration there is subsequently a need for understanding the use of local lime. The geology of Jämtland contains several layers of limestone in the folded mountains. There is a broad spectrum ranging from pure Silurian limestone to clay containing Ordovician limestone, giving all kinds of lime from pure air lime to strong hydraulic lime. The preserved historic mortars have mostly been made with the hydraulic lime. Several old field kilns have been preserved in the forest landscape as prehistoric monuments, showing the model of the local lime burning tradition. This paper discusses the process of identifying the historic lime kiln constructions and their burning technique. It also describes the process of slaking this hydraulic binder in order to produce a lime mortar with workability and compatibility required from a restoration mortar. Newly-produced samples of lime mortar have been compared with historic ones in thin section microscope for further understanding.

Keywords Lime mortar · Slaked lime · Lime burning · Lime kiln
Workability

1 Introduction

Oviken old church in Jämtland, Sweden was constructed with local limestone and lime mortar during several centuries. Now that there is a need of restoring the church a discussion regarding the use of local lime took place. In order to restore

K. Balksten (✉)
Department of Art History Conservation, Campus Gotland,
Uppsala University, 621 67 Visby, Sweden
e-mail: kristin.balksten@konstvet.uu.se

C. Persson · J. Eriksson
Department of Conservation, Gothenburg University, 405 30 Gothenburg, Sweden

J. J. Hughes et al. (eds.), *Historic Mortars*,
https://doi.org/10.1007/978-3-319-91606-4_21

with traditional materials and methods the general demand of authentic local lime binder has increased. The project was initiated by the Swedish Church, involving the local museum with a Conservation Officer and an Archeologist plus a research team from Gotland University and Gothenburg University specialized in lime burning and lime mortars.

This paper shows the process of producing local lime in a small scale for a single object; from analyzing the historic mortars, finding local limestone suitable for burning and slaking, inventory of field lime kilns, burning lime, slaking and mixing mortars. Similar projects have taken place in Sweden recently on Visby City Wall and Läckö Castle (Balksten and Thelin 2014; Mebus and Balksten 2015; Sandström Malinowski 2016).

Jämtland is a county in central Sweden where the Scandinavian mountains form the landscape. There is limestone originating from both the Ordovician and the Silurian period around the lake Storsjön. In the same village there have often been small quarries in more than one limestone layer with the effect that there are lime mortars with very different properties existing on the old stone churches.

The oldest stone buildings constructed with local lime are the churches of Hackås and Norderön from 1170–1180th. Field kilns were then used in Jämtland with continuity until the 1920s (Åsling 2000). There is a unique situation in Jämtland since several old field kilns from the 19th century still remains around in the forests, see Fig. 2. Several of them were built and never burned, for unknown reasons. 143 remaining lime kilns are registered as ancient monuments in the area (Fornminnesregistret). The positions of some of them are marked with yellow dots in Fig. 1.

2 Lime Burning Project of Oviken

The project started in Oviken old church with archive studies and analysis of the old mortars available at the church and its surrounding wall. The archives held information about the building history of the church and also about different materials that have been used during different restorations (Persson 2010).

The old mortar samples, as well as the newly-produced ones, were analyzed as thin sections with a Zeiss TM Polarization Microscope.

The remaining lime kilns in the area were studied and compared to other field kilns in Sweden. Local limestones were burned, first in a small lime kiln at Gothenburg University and then in a field kiln at Gotland University in order to locate a proper stone for burning in a field kiln of the local Jämtland type. A small field kiln with two fire passages was built with limestones from two quarries in May 2011, and burned during 80 h with birch wood (Persson 2012).

During a workshop in July 2011 the lime was slaked, mixed with sand and used as a mortar for restoring a part of the wall surrounding Oviken old church, see Fig. 3. Both dry slaking and wet slaking methods were used according to a method developed by Eriksson and used for Ordovician lime from south of Sweden

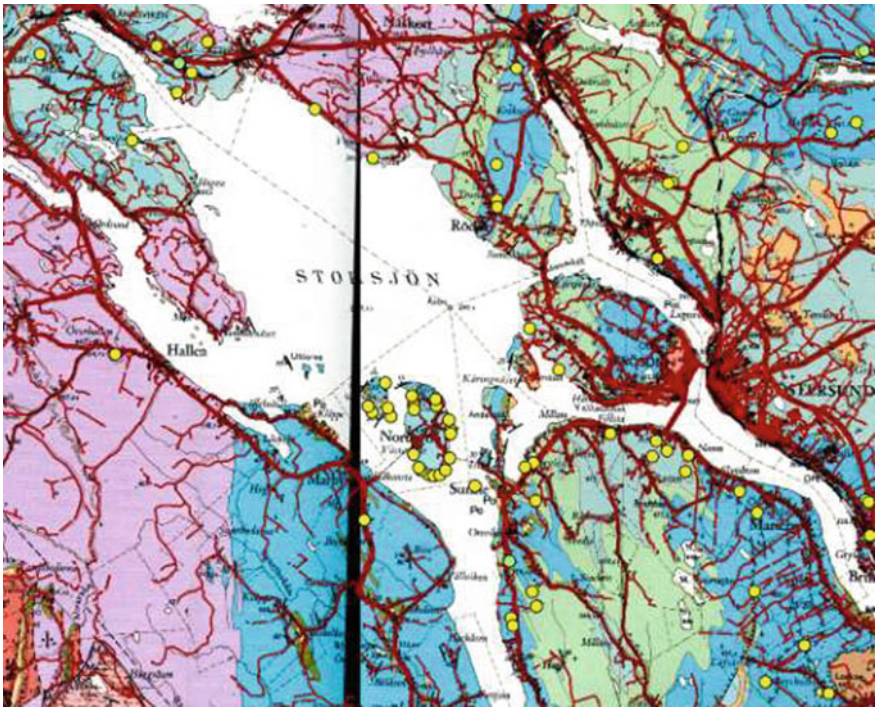

Fig. 1 Bed-rock map of Jämtland combined with the remains of lime kilns found in Jämtland marked with yellow dots (SGU 1980/Fornminnesregistret, Persson 2012) (Color figure online)

Fig. 2 **i** Illustration of a field kiln of Jämtland model (Åsling 2000). **ii** Unburned field kiln built in the late 19th century still standing in the forests of Åse. Now it is covered with moss but originally the stones were visible and not covered. **iii** Lime kiln from Havsnäs Jämtland in the1920s

(Eriksson 2015). When being slaked, the burned limestone was placed inside in an oil drum (Eriksson et al. 2012), see Fig. 9, giving the effect that the lime is slaked under a small pressure. When mixing mortars for test surfaces, an electric stirrer specialized for mortar were used. The mortars were then applied being pressed or thrown with a trowel; the more fat mortars had to be pressed while the more lean mortars could be thrown. Their surface texture was made as similar to the old

Fig. 3 Mortars are applied with a trowel onto the wall. Old mortars can be distinguished by color and texture, here as the white and yellowish surfaces in the picture

surfaces as possible. The workability of the mortars was the most essential property in the study and the discussion and dialog between the masons and scientists was essential when evaluating the results.

3 Limestone and Mortars of Jämtland

Old mortars from the area were analyzed by thin sections in order to show different parameters such as type of lime, type of sand and mixing ratio between lime and sand. The mortars came from Oviken old church and its surrounding wall and from Sunne church ruin, nearby. The mortars were most likely from the 15th to the 17th century, due to where they were found in and on the walls. They were extremely fat (rich of lime) made from lean lime (Balksten and Lindqvist 2016), from local lime stone found nearby the buildings. The lime stone in the area is un-pure and gives what today is defined as hydraulic lime [Shaikh et al. (1989)].

Because of the complex geology in Jämtland and the formation of folded mountains the limestone layers are found in many different small deposits in the area around Storsjön as well as in the mountains. The limestone existing in Jämtland is of many different characters; from the early and middle part of the Ordovician period and from the oldest part of the Silurian period, see Fig. 5. There are all kinds of limestones ranging from almost pure limestone (98% $CaCO_3$) that gives air lime mortar to limestone containing clay minerals (more than 85% $CaCO_3$) giving strong hydraulic mortar. The stone from the Silurian period is called Berge limestone and consist of more $CaCO_3$ than other limestone in the area. The stone from the Ordovician period studied in this project is called Isö limestone and often consists of approx. 90% $CaCO_3$. Ancient remains and ruins of historic lime kilns are preserved in the forests (Fornminnesregistret) and can be found all over the landscape showing that most kind of Berge and Isö limestone have been burned at one time. A stratigraphic table of limestone from Jämtland (Shaikh et al. 1989) shows the large variation of limestone available such as the Silurian *Berge,* and the

Fig. 4 Old lime mortars in Oviken. The oldest mortars from 17th century are extremely lime rich (20:1 lime/sand by volume) with a yellowish color. What occurs as sand particles to us might be just impurities from the limestone and the slaking process (Balksten and Lindqvist 2016). To reproduce such mortars we need to experiment more with slaking and storing of the specific lime. The surface has traces of lime wash and aging

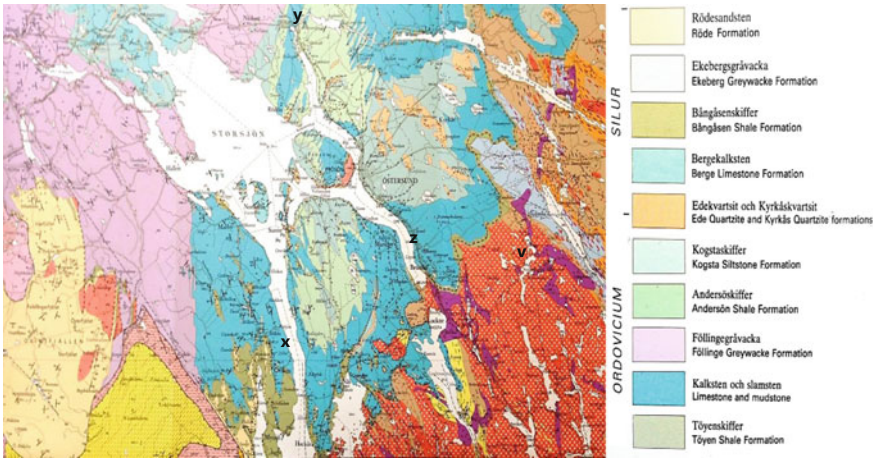

Fig. 5 Part of the bed-rock map around Storsjön in Jämtland showing the complex geology of the region. Notice the blue and turquoise colors showing the presence of limestone. The letter **v** marks Sunne church, **x** marks Oviken church, **y** marks Näversjöberg and **z** marks Marieby (Sveriges geologiska undersökning 1980)

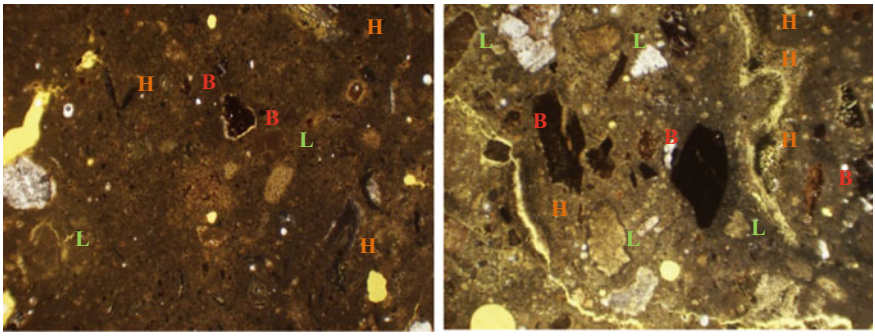

Fig. 6 Examples of thin sections made from old lime mortar samples from the old church wall in Oviken (see Fig. 4) and the church ruin in Sunne, Jämtland. The shown width of each image is equivalent to 4.5 mm. Both of the analyzed mortars are extremely rich of lime, showing almost no sand particles at all. The binder is not pure $CaCO_3$, it contains some other elements, or impurities. The thin sections show that the lime contains some darker hydraulic components, marked with H, lime lumps L and burned clay minerals B

Fig. 7 Field kiln built in 2011. It has two fire places, like some of the kilns found in the region had

Fig. 8 Lime kiln during the first, second and third day. On the third day the flames started to become blue all over the top of the kiln, giving a signal that the lime was burned long enough

Ordovician *Furulund, Slandrom, Dalbyn, Furudal, Folkeslunda, Seby, Segerstad, Holen, Isö, Länna* and *Latorp*.

The limestones burned in this project were chosen for several different reasons. The types of limestone available in the surroundings of Oviken were the interesting

Fig. 9 Lime slaking under pressure in an oil drum

ones to study. It is the Isö limestone from the Ordovician period that exists in the Oviken region. Analysis of limestone samples from the surroundings of Oviken shows a $CaCO_3$ content of 79–92%, the samples also contains clay minerals, see Table 1 (Shaikh et al. 1989). The limestones in this study were taken from open quarries in use were such certain types of limestone were available; *Näversjöberg* north of Storsjön and *Marieby*, east of Oviken.

Analysis by thin sections showed that the old mortar samples from Oviken and Sunne were composed of lime containing hydraulic components and a very small amount of sand. These types of mortars, made from local lime with high lime content, are characteristic for the medieval lime mortar tradition of Sweden (Johansson 2006; Balksten 2010; Balksten and Mebus 2012). Such extremely fat mortars were used all over Sweden until the mortar tradition of the late 18th century

Table 1 Chemical composition (79–92% $CaCO_3$) in the Isö limestone of Oviken

Sample nr	85082	85083	85084
SiO_2	3.9	12.3	4.4
Al_2O_3	1.02	3.80	1.28
TiO_2	0.08	0.22	0.04
Fe_2O_3	1.35	1.87	0.86
MnO	0.27	0.16	0.23
CaO	51.0	43.6	50.3
MgO	0.45	0.69	0.48
K_2O	0.29	1.06	0.37
Na_2O	0.05	0.06	0.03
P_2O_5	0.08	0.06	0.14
CO_2	40.5	34.9	40.4
F	0.01	0.02	0.02
S	0.46	0.49	0.01
Sum	99.46	99.23	98.56

Samples taken from the early Ordovician layer (Shaikh et al. 1989)

took over (Pasch 1826). Thin sections are made from soft yellow colored lime mortar samples which are extremely hard and fat, see Fig. 6. They both contain hydraulic reactions; reference material can be found in Johansson (2006) in analysis made by Jan-Erik Lindqvist and Torbjörn Seir and in Ingham (2011).

The lime kiln built in this project was made with a mix of limestone from both Näversjöberg and Marieby. Since the reconstruction of the historical proportions of the kiln was the essential task, the stones were arranged in size-order rather than separated in different types of limestone. The lime kiln was placed in a small slope, built with two fire passages. It was then burned with birch wood during 72 h. The temperature in the field kiln was expected to stay at approximately 800–1000 °C but the temperature was not measured. The expected temperature is based on the experience of highly skilled craftsmen and practical knowledge from the burning field kilns and small lime kilns in Sweden during 20th century where temperature have been measured with traditional methods such as looking at the color of a piece of iron that is inserted into the kiln. Figures 7 and 8 show the kiln during building and burning. For illustrations on how to build a field kiln of the type, Bernerman (2015) is recommended.

The lime was slaked using two different slaking methods; wet slaking with a small surplus of water and dry slaking with the amount of water that the stone would absorb when it was soaked in water for some seconds. The time was decided by the size of the stones, the absorption capacity was tested for each type of limestone. A stone was placed in water for a short time (10–20 s) until it ceases to bubble. It was then divided in two pieces, making it possible to see if the water had reached the center of the stone. The search for the right consistency of the lime defined the amount of water that was used during the slaking process.

The lime that was slaked was tested in situ with the aim to get stiff lime putty from the wet slaking method and dry lime powder from the dry slaking method. Some of the participants in the study had very long practical experience of lime slaking in leading the slaking process to produce lime with good workability. The lime must not be too stiff or too wet, it should be easy to mix with sand and it shouldn´t need too much sand in order to make a mortar, according to the analysis of the old mortar samples from the church. Because of the fact that the lime was difficult to slake, hot water (80 °C) was used in the slaking process of wet slaking in order to make it start faster and to be able to control that the slaking was completed. Many years of testing has shown that unslaked particles become more frequent in wet slaking if cold water is used for limestone that is difficult to slake. For the dry slaking cold water was used. The lime was slaked inside an oil drum under small pressure (made by placing heavy stones on top of the lid) to avoid unslaked particles, see Fig. 9. These slaking methods have been developed during many years of lime slaking of a similar Ordovician limestone in Västergötland, in Sweden at Gothenburg University (Eriksson et al. 2012). By slaking the lime under pressure it can be used faster without risking unslaked particles that will be slaked after being used. Both types of quick lime are extremely sensitive when it comes to adding too

much water during the wet slaking process, giving mortars with inconsistent and hard-worked qualities when it comes to workability. The amount of water used in wet slaking for similar kinds of limestone is known to cause extended time for the hardening process followed by lower resistance to degradation (Pasch 1826). Traditional wet slaking in Sweden (Sjöbladh and Engeström 1750) means using a larger surplus of water to slake the lime in the open atmosphere to achieve lime putty. In this project this technique was only tried on a few individual stones, but since the limestones of Marieby and Näversjöberg proved to be difficult to slake, the method of slaking under pressure developed by Eriksson (2015) was instead applied, see Fig. 9.

The lime was then used to prepare mortar together with local sand with a particle size of 0–3 mm in different mixing ratios. The sand was chosen from a quarry nearby, looking as similar as possible concerning color, shape and size distribution, compared to the content of old sand in the historic mortars. Several test-surfaces were made on the wall surrounding the cemetery in order to find a consistency with good workability, mixing ratio and structure similar to the old preserved mortar samples.

The limestone was put in a steel basket with holes and dipped in water for 18 s until it ceases to bubble. In the wet-slaking method hot water is placed in the drum in which the burned lime is poured into. When dry-slaking, the basket is put inside the empty drum. In both cases a lid is placed on top and a stone is placed on top of the lid in order to create a pressure, which minimizes the loss of energy. This method was created both from practical research and experience by Eriksson (2012), Eriksson et al. (2015).

The workability of the lime mortars was different from lime that the craftsmen, who came from other regions in Sweden, were used to. Even a very lime rich mortar didn't give the impression to be a very fat mortar. In the 19th century those kinds of lime were defined as "lean lime" rather than hydraulic lime (Pasch 1826; Henström 1869) even though their chemical composition suggests that they will give hydraulic lime. When occurring as wet slaked they could be stored for a few days but not more than two weeks. They were what the Swedish mason call "short" meaning they were not smooth nor gluing to the underlying surface. They were all quite difficult to work with. The surface had to be worked with light hand with a trowel, not with a wooden board. Otherwise the lime was "bleeding" to the surface and a lime film was too easily created. They were also extremely sensitive for time and consistency of the mortars when the surface could be worked on. All test mortars had to dry out and become stiff before they were worked on, otherwise they would not harden properly to become durable. In Table 2 a comparison between the two types of lime is presented. All mixing ratios are presented in volume between lime and sand. The local sand needed a lot of lime in order to give what felt as lime rich mortar.

The analysis as well as the practical tests show two very different types of lime after burning, slaking and hardening, see Fig. 10. As always it is essential that the

Table 2 A comparison between the slaked lime of Marieby and Näversjöberg

Marieby wet-slaked	Marieby dry-slaked	Näversjöberg wet-slaked	Näversjöberg dry-slaked
A yellowish lime, in color very similar to the original mortars of Oviken Mixing ratio 1:1 by volume felt like it was mainly sand. The mortar needed more lime in order to be able to work with. It was difficult to apply by throwing the mortar with a trowel since it was in one way sticky and attached to the trowel too much but in another way not sticky when attaching to the underlying wall Tests with mixing ratio 2:1 or 1.5:1 proved to work much better but in order to work the surface it was essential to wait for the mortars to set and not to use any pressure on the tools since the lime then would end up as a lime film on the surface Also 10:1 and 20:1 were tested of this kind of lime since analyses of old lime mortars showed such an extreme mixing ratio. Both were possible to work with but since they cracked a lot as they dried out it was essential to wait for the cracks to appear before working the surface with a light hand	Same color as wet-slaked It was not as sticky as the wet-slaked lime. Mixing ratio 1:1 gave a mortar impossible to work with so from the start more lime had to be added. Mixing ratio 1.5:1 gave a mortar that proved to be easier to apply. It was not possible to work the surface with any wooden tools. Steel trowels had to be used for working the surface when the mortar had set and one had to be very light on the hand to avoid a lime film on the surface	A brownish lime, darker than the Marieby lime This lime gave more fat mortars than the Marieby lime. Mixing ratio 1:1 was possible to work with. It could not be described as sticky but it hardened faster when applied to the wall. Already after a day it became very hard To make a good adhesion between the wall and the mortar, stiff mortar was brushed into the surface of the stone before a layer of mortar was thrown on. Without this procedure the mortar would roll off the wall immediately	The dry-slaked Näversjöberg lime is very similar to the wet-slaked Näversjöberg lime in the mortars It also needed the ground layer for adhesion, it hardened fast once applied to the wall. When working the surface one had to be very light on hand in order to avoid a lime film on the surface

Fig. 10 Burned limestone from Marieby; dry-slaked Näversjöberg lime in a special constructed steel basket; wet-slaked Marieby lime. The lime from Näversjöberg is almost a bit purple-grey when it is slaked compared to lime from Marieby that is yellow-brown (Color figure online)

craftsmen are experienced with fat lime mortars and comfortable with waiting on the setting time for each kind of mortar before working the surface. The Näversjöberg lime tended to act more hydraulic than the Marieby lime even though both kinds are made from the Isö limestone. The mixing ratio were frequently discussed and even small samples were made with 20:1 and 10:1 mortars in order to find out if it was possible to reproduce such fat mortars. However a later study of historic lime putty found in year 2014 (Balksten and Lindqvist 2016) taught us that slaking and storing of lean lime can have the effect that part of the binder transform into a function as aggregates as they partly harden. As we used a modern developed slaking technique to create a well slaked lime under small pressure, possibly we got a binder more active and fat, with a minimum of lime lumps, compared to the binder used in the original mortars we found and analyzed. If so, it can describe why we did not manage to create 20:1 mortars with good workability of the lime produced in this project. This question could be an object for further research and help us give an increased understanding for historic mortars.

In a region such as Jämtland where there have been limekilns in so many different deposits of limestone it is extremely difficult to find limestone giving exactly the same properties as the original mortars locally used. Adding the fact that old mortars are extremely different from mortars in modern mortar tradition concerning mixing ratio, there are other difficulties finding restoration mortars that are very similar to the historic ones since modern craftsmen are unsure of how to deal with fat lime mortars.

The tested mixes were extremely sensitive for too high water content, both when it came to applying the mortar and especially when it came to working the surface structure. All the tested lime mortars would easily bleed lime towards the surface if worked on before they had become stiff. Shrinking cracks occurring in the drying phase had to become visible before the render could be smoothened with a steel trowel with a light hand. The test surfaces showed that it is essential not to be in a hurry when building a render since every layer must be able to harden before another layer can be applied, and every layer must be worked on after it has set (Fig. 11).

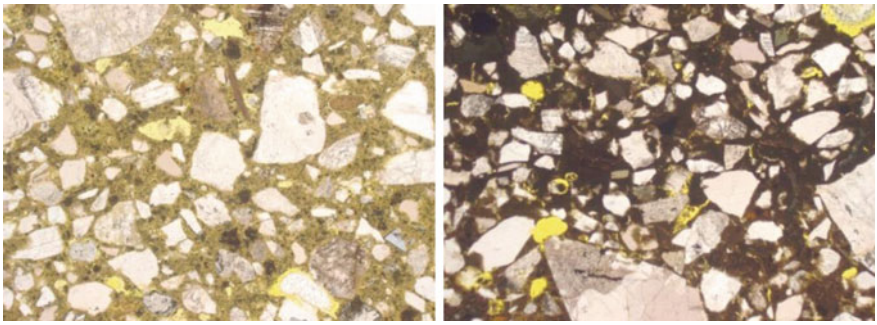

Fig. 11 Thin section of mortar samples made from dry slaked Marieby lime 1:1 and dry slaked Näversjöberg lime 1:1 to sand 0–3 mm. The shown width of the images is equivalent to 2.6 mm. A polarization Microscope, Zeiss TM, was used

4 Conclusions

To produce local lime in Jämtland was not too difficult since there is a known history and ancient ruins of the lime kilns developed for this certain region and its conditions concerning limestone and firewood. If there are a few people available with lime burning experience, as we have for instance due to the continuous lime production of Gotland (Mebus and Balksten 2015), the process of producing lime in a field kiln is rather simple. The difficulties in this project started with finding a proper stone that could provide a lime mortar with similar qualities as the original mortar of Oviken; firstly since Jämtland is a very difficult region with complex geology but also since most kinds of limestone have been used for burning historically. Many generations have developed their technique from local conditions during centuries and most of their knowledge was lost during the mid-20th century if not earlier. Today the knowledge must be recaptured and all the details from choosing stone, setting a lime kiln, burning technique and burning time, slaking technique and storing of slaked lime, sand quality, mixing ratio, mortar mixing technique to application method and surface working method have to be tested in order to find a proper restoration mortar for each type of masonry with remaining original mortars (Balksten 2005, 2007). Adding that the restoration mortar should have good workability as well as a long durability it requires a large quantity of tests and time for evaluation.

All types of lime produced in the project had interesting qualities and could give mortars with acceptable workability and color and structure similar to the old mortars. But it takes time to get used to how they work and how to control them in practice. In Sweden many impure limestones were burned historically (Johansson 2006) but in the 1940s only the pure lime compatible for lime-cement mortars became the ones that was burned (Balksten and Mebus 2012). This change has mediated the loss of knowledge among several generations of masons. Subsequently, our generation must learn to control mortars with properties far from

what they are used to if we want to restore our historic buildings with traditional and authentic materials and methods. As researchers and craftsmen nowadays work side by side in Sweden the conditions are rather optimistic.

References

Åsling, N. G. (2000). Kalk och kalkbruk i jämtländska bygder. [*Lime and lime mortar in the Jämtland region.*] Alsens hembygdsförening.

Balksten, K. (2005) Kalkputs—Porstrukturens betydelse för beständighet. [*Lime render—Importance of pore structure for durability*] Licentiate Thesis, Gothenburg: Chalmers Tekniska Högskola. ISSN 1652-943X. (http://urn.kb.se/resolve?urn=urn:nbn:se:uu:diva-220085).

Balksten, K. (2007). *Traditional lime mortar and plaster—Reconstruction with emphasis on durability*. Gothenburg: Chalmers. Doctorate Thesis. ISBN 978-91-7291-990-7. (http://urn.kb.se/resolve?urn=urn:nbn:se:uu:diva-220119).

Balksten, K. (2010), Understanding historic mortar and their variations—a condition for performing restorations with traditional materials. In *Proceedings of Historical Mortar Conference HMC-2010*. Prag, Tjeckien.

Balksten, K., & Mebus, U. red. (2012). Bruk av ruiner. [*The use of ruins*] Visby: Fornsalens förlag. ISBN 9789188036841. (http://urn.kb.se/resolve?urn=urn:nbn:se:uu:diva-220106).

Balksten, K., & Lindqvist, J. -E. (2016). Two-hundred year old lime putty from barrels found in the ground explaining the character of fat historic lime mortar. In *Proceedings of Historic Mortar Conference HMC-2016*. Santorini, Greece.

Balksten, K., & Thelin, C. (2014). Construction and materials of Visby medieval city wall—risk of damage. In *9th International Masonry Conference 2014*. Guimarães, Portugal.

Bernerman, M. (2015). Kalkbränning i fältugn. [*Lime burning in field kiln*] Thesis for Bachelor Degree. Gothenburg: University of Gothenburg (http://hdl.handle.net/2077/40723).

Eriksson, J. (2015). Bruk av kalk och sand: ur ett hantverkligt perspektiv. [*Use of lime and sand—from a craftsman perspective*] Gothenburg: University of Gothenburg, Acta universitatis Gothoburgenis. (http://hdl.handle.net/2077/38155).

Eriksson, J. et al. (2012). Erfarenheter av bränning och släckning av Kinnekullekalksten. [*Experiences of burning and slaking limestone of Kinnekulle*] Mariestad: Hantverkslaboratoriet, University of Gothenburg. ISBN 9789197938259.

Fornminnesregistret. (2011). www.raa.se/cms/fornsok, 2011-05-26.

Henström, A. (1869). Praktisk handbok i lantbyggnadskonsten. [*Practical hand book for buildings for peasants*] Örebro: Beijer.

Ingham, J. P. (2011). *Geomaterials under the microscope*. London: Manson Publishing.

Johansson, S. (2006). Hydrauliskt kalkbruk: produktion och användning i Sverige vid byggande från medeltid till nutid. [*Hydraulic lime mortar: production and use in Sweden in buildings from middle age to our time*] Doctorate Thesis. Göteborg: Chalmers. ISBN 91-7291-822-5.

Mebus, U., & Balksten, K. (red) (2015). Visby ringmur—kulturarv som rasar och återuppbyggs. [*Visby City Wall—Cultural heritage falling and being rebuilt*] Visby: Riksantikvarieämbetet. ISBN 978-91-7209-705-6 (http://kulturarvsdata.se/raa/samla/html/8220).

Pasch, G. (1826). Årsberättelser om vetenskapernas framsteg, afgifne af kongl. Ventenskaps-academiens embetsmän d.31 mars 1827. [*Annual stories about scientific progress*] Stockholm: P.A. Norstedt & söner.

Persson, C. (2010). Ovikens gamla kyrka—Förundersökning av putsen på kyrkan och bogårdsmuren. [*Oviken old church—Investigation of render on the church and its surrounding wall*] Östersund: Jamtli. Rapport-Jamtli 2010:5. ISSN 1654-2045.

Persson, C. (2012). Jämtlands byggnadskalk—Erfarenheter från ett kunskapsuppbyggnadsprojekt. [*Building lime of Jämtland—Experiences from en knowledge project*] Östersund: Jamtli. Rapport-Jamtli 2012:46. ISSN 1654-2045.

Sandström Malinowski, E. (2016). Historiska bruk på Läckö slott: fasadrestaurering och forskningsinsatser 2002–2009. [*Historic mortars on Läckö Castle: restoration and research 2002-2009*] Göteborg: Institutionen för kulturvård, Göteborgs universitet. (http://hdl.handle.net/2077/49953).

Shaikh, N. A. et al. (1989). Kalksten och dolomit i Sverige. Del 1 Norra Sverige. [*Limestone and Dolomite in Sweden. Part 1 Northern part of Sweden*] Sveriges Geologiska Undersökningar. Rapporter och meddelanden nr 54. Uppsala: SGU. ISBN 91-7158-457-9.

Sjöbladh, C. G., & Engeström, J. (1750). Beskrifning, huru kalk skal tilredas ifrån thes första Bränning och til then warder färdig til sitt bruk. [*Description how lime shall be produced from burning until it becomes mortar*] Original ur Calle Brobäcks Gotlandicasamling, Maj 2007.

Sveriges geologiska undersökning. (1980). *Berggrundskarta över Jämtlands län.* [*Bed-Rock map of Jämtland*] Uppsala: SGU.

The Compatibility of Earth-Based Repair Mortars with Rammed Earth Substrates

M. I. Gomes, T. Diaz Gonçalves and P. Faria

Abstract Earth constructions are susceptible to degradation due to natural or human causes. The degradation of the exterior surface of earth walls is very common, either due to lack of maintenance or to the use of incompatible materials, and often requires the application of a repair mortar. This work experimentally analyses the performance of earth-based repair mortars applied on rammed earth surfaces. The mortars are based on earths collected from rammed earth buildings in south Portugal or on a commercial earth. Eight repair mortars were formulated, with the unstabilized earths or including low binder content. For the stabilized mortars four types of binder were tested: hydrated air-lime, hydraulic lime, Portland cement and natural cement. The repair mortars were applied on two types of standard defects purposely made on rammed earth blocks, representing the most current common defects found on exterior rammed earth surfaces: a standard superficial defect and a standard deep defect. The performance of the mortars, their compatibility with the substrates and the visual effectiveness of the intervention were evaluated. It was concluded that the same mortars behaved differently when applied on different rammed earth supports. However, the best performances occurred always for the mortars made from unstabilized earth identical to that of the rammed earth substrate. Indeed, the use of stabilizers systematically worsened the behavior of the repair mortars, regardless of the type of binder used for that purpose.

M. I. Gomes (✉)
Department of Civil Engineering, Lisbon Engineering Superior Institute (ISEL), Lisbon Polytechnic Institute (IPL), Lisbon, Portugal
e-mail: idaliagomes@dec.isel.pt

T. Diaz Gonçalves
National Laboratory for Civil Engineering (LNEC), Lisbon, Portugal
e-mail: teresadiazgon@gmail.com

P. Faria
Department of Civil Engineering, NOVA University of Lisbon (FCT NOVA) and CERIS, Lisbon, Portugal
e-mail: paulina.faria@fct.unl.pt

J. J. Hughes et al. (eds.), *Historic Mortars*,
https://doi.org/10.1007/978-3-319-91606-4_22

Keywords Rammed earth substrate · Wall defect · Earth repair mortar
Compatibility between materials

1 Introduction

Faced with the energy crisis in the decades 70/80, industrialized countries have been forced to rethink the viability of technical solutions that were revealed greedy in energy terms. The construction sector has not escaped this re-examination and ways to reduce energy consumption, both in terms of materials used and the construction techniques, began to be focus of research. The European Union is committed to meet targets in the medium term, with less than: 50% of energy consumption, 40% of waste and 30% of raw materials consume (WCED 1987).

In a society where questions related to sustainable development and ecology start to matter, the use of locally sourced, non-processed building materials, such as natural earth, is a possible path for a greener economy. Other advantages of earth as a building material are its abundance, low cost and ease of recycling.

Because of the previous reasons earth as a building material became a focus of interest.

Houben and Guillaud (1996) reported that in the French region of Dauphine rural dwellings built with raw earth represent up to 90%. Another example is in California, which almost 200,000 adobe houses were estimated in 1980 and where the use of this technique has been growing at the rate of 30% per year.

In Portugal, the number of new rammed earth constructions is increasing, as is the number of old rammed earth or adobe masonry buildings being restored for modern uses.

Although building with earth is one of the oldest and traditional constructive methods, most of earth building elements characteristics and properties remain poorly understood and investigated. The lack of specific training of technicians in this area makes that there is not a domain in this field, since most of the know-how in terms of building practices or maintenance, has tended, in some regions, to disappear. However, it is necessary to understand these construction methods, the characteristics of the materials used and the causes of degradation in order to be able to give adequate response to the need of interventions of rehabilitation or conservation. In fact, in most of new construction and even rehabilitation the specific characteristics of the earth material or the building system are often not taken into account, which sometimes leads to errors and premature appearance of anomalies in buildings.

During the life time of a building it suffers diverse natural and accidental actions and frequent repair actions are needed. Therefore repairs in rammed earth walls may be necessary as a result of problems occurring during their life time, after a continuous environmental exposure when they are not covered, as well as problems arising due to inappropriate repair techniques or even to the original building technique (Keable 1996; Walker et al. 2005; Faria 2005; Houben and Guillaud 2006; Le Tiec and Paccoud 2006; Gomes and Faria 2011; Angulo-Ibáñez et al. 2012; Hamard et al. 2013; Miccoli et al. 2014).

The degradation of the exterior surface of earthen walls is very common, either due to a lack of maintenance which eventually conducts to direct exposure to the environment, or to the application of incompatible renders or other materials. Restoring the functionality and aesthetics of these walls often requires the application of a repair mortar.

Aiming at the development of appropriate repair mortars for rammed earth constructions, eight repair mortars were produced with four types of earth and tested on three types of rammed earth substrates. This study is important, insofar as the authors are not aware of other studies in which earth mortars are applied to a substrate, allowing a direct assessment of the compatibility between them. The substrates consisted of rammed earth blocks manufactured in the lab for that purpose with earth collected from old rammed earth buildings. Standard defects—superficial irregularities and deep voids—were created on the surface of these blocks, representing those commonly found in the exterior surfaces of rammed earth walls (Gomes and Faria 2011). The eight repair mortars were based on either the same earth as the substrate or a commercial earth. The commercial earth was used in its natural state or after stabilization with a small amount of hydrated air-lime, hydraulic lime, Portland cement or natural cement.

The earth-based mortars were applied onto two types of standard defects—a standard superficial defect and a standard deep defect—in order to evaluate their behaviour as repair mortars. The repair of deep defects was made in two different ways—the voids were filled only with mortar or with a mortar and coarse gravel (added to reduce the mortar's thickness).

The present article describes and discusses this work which is part of a more general project that included artificial ageing tests to assess the adequacy of earth-based mortars as repair mortars for rammed earth materials.

2 Materials

Four types of earth were used in this study. Three of them (earths Av, PD and VC) were collected from non deteriorated parts of walls of unstabilized rammed earth buildings located in the Alentejo region of Southern Portugal. These three earths were chosen because they represented different grain size distributions and types of clay. Av is more sandy than PD and VC, which are more clayey. The fourth (earth RE) is a commercial earth, composed mainly of clay. The four materials are fully characterized elsewhere (Gomes et al. 2012a, b).

The uniformity of the particle size distribution (PSD) was ensured as it is a important factor when studying such material. A uniform PSD allows for a more efficient compaction because the grains can align in a way that minimizes the empty spaces between them (Keable 1996; Walker et al. 2005). It is commonly accepted that the more compact the material, in principle, the lower the porosity and the higher the mechanical resistance; hence a greater durability (Keable 1996; Walker and Australia 2001; Walker et al. 2005). Morton (2004) also notes that buildings

with earthen well-graded materials can be remarkably durable, while poorly graded mixes never perform well.

2.1 Rammed Earth Blocks

The rammed earth blocks were produced with the site-collected earths Av, PD, and VC. The preparation of the material is detailed in Gomes et al. (2012c). It was first disaggregated with a rubber hammer so (not to break the aggregates) and then dry sieved, rejecting the material that passed through the 12.5 mm sieve (½" ASTM).

2.2 Mortars

The compositions of the eight repair mortars are presented in Table 1. As seen, the mortars with clayish earths include sand. The sand is composed mainly of quartz and has a grain dimension in the range 0.6–2.0 mm. Its addition had the main objective of reducing the shrinkage of the mortar which otherwise would be very high due to the clay content of the earths. The MRE mortars include also 15% of powder hydrated air-lime (CL), hydraulic lime (HL), Portland cement (PC) or natural cement (NC).

Table 1 Composition of the eight mortars

Group of earth based mortars	Designation of the mortar	Weight proportions (clay:sand)	Volumetric proportion (clay:sand)	Stabilizant (%)[a]			
				CL[b]	HL[c]	PC[d]	NC
Local earth Av	MAv	1:0	1:0	–	–	–	–
Local earth PD	MPD	1:1.9	1:1.5	–	–	–	–
Local earth VC	MVC	1:2.4		–	–	–	–
Reference-earth	MRE	1:3.8	1:3	–	–	–	–
Reference-earth with hydrated air-lime	MRE_CL15			15	–	–	–
Reference-earth with hydraulic lime	MRE_HL15			–	15	–	–
Reference-earth with Portland cement	MRE_PC15			–	–	15	–
Reference-earth with natural cement	MRE_NC15			–	–	–	15

[a]Percentages by weight in relation to the reference earth
[b]EN 459-1 CL 90-S; [c]EN 459-1 HL5 and [d]CEM II/BL 32.5 N

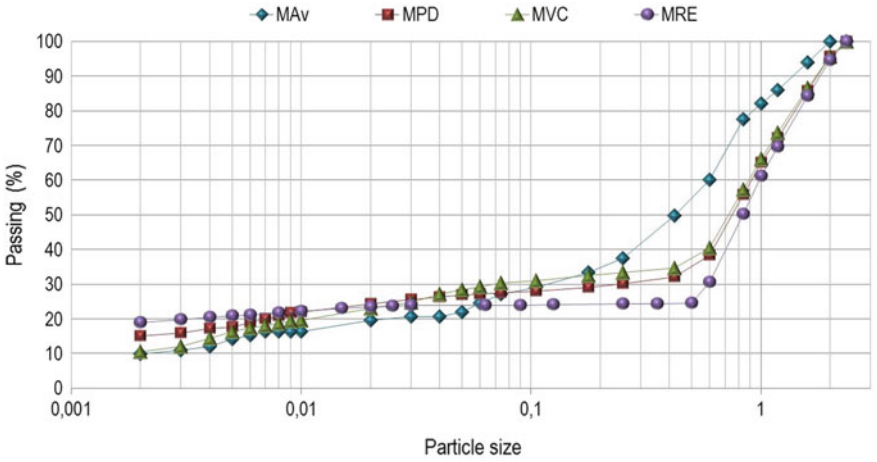

Fig. 1 Particle size distribution of the mortar materials, MAv, MPD, MVC and MRE

The earth was prepared as follows: (i) the three earths (Av, PD, VC) collected from the buildings were wet sieved through a 2 mm sieve (Nº10 ASTM); the material that passed through the sieve, after decanting, was dried in a ventilated oven at 40 °C; it was ground and homogenized; (ii) the commercial earth (RE) was ground to disaggregate the material before the sample was homogenized.

Figure 1 shows the particle-size distribution of the unstabilized materials for the mortars, MAv, MPD, MVC and MRE.

To fill some of the standard deep defects coarse gravel with dimensions between 20 and 40 mm was also used to reduce the thickness of the mortar.

3 Experimental Methodology

3.1 Rammed Earth Blocks

Ten rammed earth blocks, with dimensions 30 cm × 20 cm × 28 cm, were manufactured with each type of collected earth (BAv, BPD and BVC). The two types of current defects: superficial loss of material (2 cm depth) and deep voids (semi sphere with 10 cm diameter), were recreated on the blocks: The blocks were kept in a controlled environment at 20 °C and 50% RH for 20 months. Details of their manufacture can be found in Gomes et al. (2012c).

3.2 *Preparation and Characterization of the Earth-Based Mortars*

For the mixing of the mortars, EN 196-1 was followed as closely as possible. A mechanical mixer was used composed of a 3 L stainless steel vat and a paddle mixer driven by an electric motor.

The methodology used for mortars MAv, MPD and MVC was as follows: (i) manual homogenization of the material; (ii) introduction of water into the mixer, followed by introduction of the dry material; (iii) mixing at low speed for 90 s; (iv) a 90 s halt (in the first 15 s the mortar adhering to the walls of the vat was removed with a rubber spatula and added to the remaining mortar); (v) mixing at low speed for another 60 s.

For the MRE mortar it was necessary to increase the mixing time because a good homogenization would not be achieved otherwise due to the large clay content. Thus, after (ii) the mortar was manually mixed for an extra period of 2 min and (iii) was prolonged to 150 s.

The consistence by flow table, EN 1015-3 (Table 2), was used to determine the amount of water in the mortars. The quantity of water was added so that the flow values were adjusted to the target interval of 160–176 mm which corresponds to earth-based mortars with excellent workability (Gomes et al. 2012c).

It was also important to limit the shrinkage of the mortars (Gomes et al. 2012c). The linear shrinkage of raw earth materials is commonly evaluated by Alcock's test (also called the shrink-box test). Linear shrinkage should not be more than 3% in accordance with the New Zealand Standard (SNZ 4298, 1998). Interestingly, linear shrinkage does not appear to be representative of total shrinkage therefore volumetric shrinkage was also determined (Gomes et al. 2012a, b).

Table 2 Water/dry material ratio, flow table consistency, linear and volumetric shrinkage of the eight earth-based mortars

Mortar designation	Water/dry material ratio	Flow (mm)	Shrinkage (%)	
			Linear	Volumetric
MAv	0.13	174	≈0	≈0
MPD	0.20	177	1.00 ± 0.18	1.25 ± 0.23
MVC	0.21	177	1.35 ± 0.36	1.46 ± 0.15
MRE	0.31	170	0.90 ± 0.12	0.95 ± 0.08
MRE_CL15	0.30	170	1.36 ± 0.31	6.21 ± 0.27
MRE_HL15	0.29	172	0.57 ± 0.38	5.49 ± 0.50
MRE_PC15	0.29	180	0.37 ± 0.06	3.19 ± 1.00
MRE_NC15	0.29	159	1.72 ± 0.06	6.11 ± 0.54

3.3 Application Technique of the Repair Mortars

After the analysis of anomalies in current rammed earth walls (work described in Gomes and Faria 2011), it was found that the disintegration of superficial material and, consequently, the lack of surface thickness are recurrent in this type of construction. This type of degradation can reach only a superficial level or, in certain cases, lead to occasional formation of deeper wells. These two degradation patterns (specific surface erosion and cavities) were typed, yielding the standard defects: superficial and deep. They were reproduced in the blocks to allow testing repair mortars (see Fig. 2). These standard defects allow simulate, in a standardized way, the most common anomalies found on the exterior walls of rammed earth buildings (Keable 1996; Walker and Australia 2001; Walker et al. 2005; Toumbakari et al. 2010; Gomes and Faria 2011).

The three mortars MAv, MPD e MVC that correspond to local earths were applied only in the blocks made from the same earth. Consequently, the commercial earth mortars (MRE) are intended for general use and, therefore, were applied on the three types of rammed earth blocks. For each mortar three applications were always carried out, either to the standard superficial defect or for each type of deep defect filling.

Before applying the mortars the rammed earth surfaces were prepared as follows:

(i) the repair area was brushed to remove loose particles and dust;
(ii) the surface was wet by spraying for 30, 20, 10 min and 30 s before applying the mortar to avoid a sudden drying out of the mortar, thereby preventing a large initial retraction.

The application technique of the repair mortars in the superficial defects was as follows (Fig. 3):

(i) the mortar was thrown vigorously against the support with a trowel, always from the bottom to the top;
(ii) the mortar was tightened and repointing was performed particularly in the corners, with a trowel;
(iii) the surface of the mortar was made regular with a wooden or metal ruler;
(iv) the surface of the mortar was smoothed with a sponge.

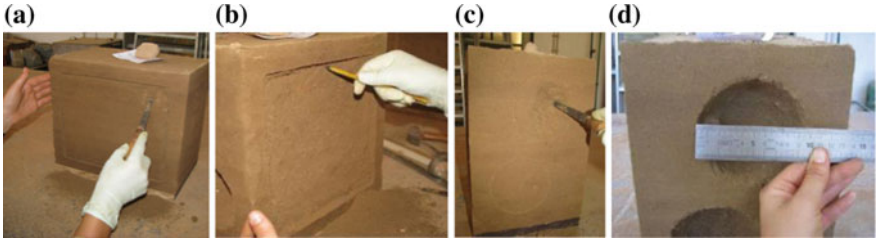

Fig. 2 Realization of the standard defects: **a**, **b** superficial; **c**, **d** deep

Fig. 3 Application of the mortar MRE_CL15 on a standard superficial defect of the PD rammed earth

Fig. 4 Application of the mortar MRE on a standard deep voids defect of the Av rammed earth

In the case of the deep defects the mortar was applied using the following procedure (Fig. 4):

(i) the mortar was launched vigorously against the support with a trowel followed by tightening; the thickness of this first mortar layer was of 0.5–1 cm;
(ii) in the case of using coarse gravel to partially fill the holes of the defects these were applied after this first layer of mortar;
(iii) the interval of 15–20 min between the application of mortar layers was respected so that the previous layer had time to achieve enough resistance;
(iv) the application of the last layer of mortar was careful, especially in the zone of connection with the support; repointing was carried out where necessary;
(v) the surface was made regular with a wooden or metal ruler;
(vi) finally the surface was smoothed with a sponge.

Immediately after application of the mortar the initial shrinkage begins; this is inhibited by adhesion to the support. This shrinkage leads to the development of shear stresses in the plane of contact between the mortar and the support. This can cause detachment and/or tensile stress in the mortar which can cause cracking. Because of this it was necessary to repoint some cracks. Cracks appeared in the mortars approximately 2–3 h after application, on both types of standard defects and on both types of deep hole defect repairs (with and without coarse gravel). The repointing was undertaken 4 h after application.

4 Results and Discussion

The performance of the repair mortars, in terms of workability, was evaluated in a fresh state. All the mortars were found to have a good workability. When hardened, the mortars were evaluated 10, 30 and 90 days after their application on the blocks. However, no changes were detected between the 10 and 90 days, which means that most of the shrinkage occurred before then.

Tables 3 and 4 summarize the observed anomalies which were: micro cracks; medium cracks, large cracks, and loss of adhesion between the mortar and the support rammed earth blocks BAv, BPD and BVC. The classification of cracking in the mortar was based on the respective opening, adopting the French standard NF P 84-401 (Veiga 1998), which details the following specifications for cracks within stabilized renders and plasters: micro cracks—width less than 0.2 mm; medium cracks—width between 0.2 and 2 mm and large cracks—width greater than 2 mm.

Table 3 Main decay patterns of the repair mortars applied on the standard superficial defect

	BAv	BPD	BVC
MAv	Micro cracks[a]	–	–
MPD	–	Micro + medium cracks[b]	–
MVC	–	–	Micro[a] cracks
MRE	Medium cracks	Medium cracks[b]	Micro[a] + medium cracks
MRE_CL15	Micro + medium cracks loss of adhesion	Medium cracks	Micro + medium[b] cracks
MRE_HL15	Micro + medium cracks	Micro + medium cracks[b]	Micro + medium cracks[b]
MRE_PC15	Medium cracks loss of adhesion	Medium cracks[b]	Medium cracks
MRE_NC15	Micro + large cracks[b] loss of adhesion	Micro + medium cracks	Micro + medium cracks[b]

[a]Only contour cracks
[b]Cracks only in the mortar

Table 4 Main decay patterns of the repair mortars applied on the standard deep defect

	BAv	BPD	BVC
MAv	Medium cracks[a]	–	–
MPD	–	Micro + medium cracks[a]	–
MVC	–	–	Micro + medium cracks[a]
MRE	Micro[b] + medium cracks[a]	Not visible	Micro[a] + medium cracks[b]
MRE_CL15	Micro + medium cracks[a]	Micro[a] + medium cracks	Micro[a] + medium cracks
MRE_HL15	Medium cracks[a]	Micro[b] + medium cracks[a]	Micro[b] + medium cracks
MRE_PC15	Medium cracks[a]	Medium cracks	Medium cracks
MRE_NC15	Medium cracks[a] loss of adhesion	Micro[b] + medium cracks[a]	Micro[b] + medium[a] + large[b] cracks

[a]Only contour cracks
[b]Cracks only in the mortar

Analyzing the anomalies observed for the eight families of mortars (Tables 3 and 4), it is seen that:

(i) the unstabilized mortars MAv, MPD and MVC applied on blocks of the same type of earth showed the best performance, presenting just contour cracks;
(ii) the performance of the stabilized MRE-based mortars (Fig. 5) was always worse than that of the unstabilized MRE mortars: cracking was more intense and was sometimes accompanied by detachment of the repair mortar;
(iii) loss of adhesion between the mortar and the support was verified only for the Av substrate which has a low clay content;
(iv) the incorporation of gravel did not prevent or reduce the occurrence of anomalies in the mortars applied on the deep standard defect (Fig. 6).

Unstabilised mortars had only few cracks and did not detach from the substrate. This is due to their lower shrinkage rate (Table 2) and to the fact that they have

Fig. 5 Mortar MRE_NC15 applied in block BAv on standard superficial defect: left, detachment of the mortar; center, cracks; and right, detail of large cracks

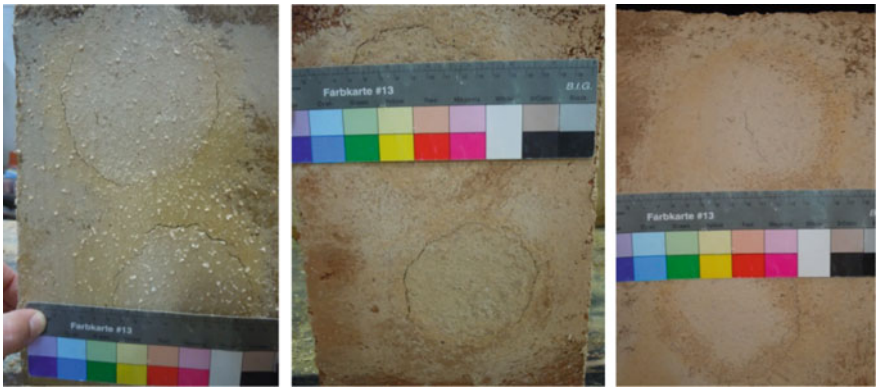

Fig. 6 Medium cracks on the mortar MRE_CL15 applied on the standard deep void defects in the blocks: left, in BAv; center, in BPD; and right, in BVC

mechanical characteristics closest to those of the substrate. The similarity between the mortar and the substrate is particularly relevant for the MAv, MPD and MVC mortars which were applied on blocks of the same type of earth and, in fact, were the ones with better behaviour. This assertion is corroborated by Morton (2004), who assertains that the compatibility of materials is a favourable criterion in their durability. He also states that constructions are more vulnerable to progressive decay at the interface between different materials, e.g. when other denser materials are applied to the surface.

The stabilized mortars behaved worse, particularly in the case of the BAv substrate where detachement of the whole repair occurred in several cases (Fig. 5). This was probably due to the lower adesion provided by this relatively high sand content susbtrate.

On the deep standard defects, the incorporation of coarse gravel did not improve the performance of the repair mortars. However, it facilitated their application because it decreased the amount of mortar used. It also made the application quicker because the repair was achieved with fewer mortar coats.

These results validate that in practice, it will be more appropriate to repair unstabilized rammed earth walls by means of unstabilized mortars, preferably based on earth similar to that of the substrate. The repair philosophy must be that of: "*minimum intervention to ensure long-term stability and optimum performance of the structure without causing physical disruption*" (Maniatidis and Walker 2003, p. 72).

Many studies indicate that the addition of cement is not recommended for earth construction repairs (Ashurst and Ashurst 1995; Warren 1999), representing a colossal mistake that can bring major problems in long-term (McHenry 1984; Walker and Australia 2001; Guelberth and Chiras 2003). Also Jiménez Delgado and Guerrero (2006) and Walker et al. (2005) advise against the use of cement rich renders for non stabilized earth walls. McHenry (1984), Boussalh et al. (2004) and Walker et al. (2005) also mention that the modern and contemporary solutions, in

particular cement mortars, are inappropriate for earth buildings, since they are very rigid and do not promote the exchange of water vapour present in the earth walls.

Warren (1999) refers that the most common mistake of ignorance is the application of cementitious mortars in earth structures; these materials fail to make the connection with the earth structure since they have completely different properties. Cimentitious renders suffer from the disadvantage of resistance to water vapor permeability and rigidity; as a result, detachment between materials start to appear (Norton 1997) and the repair becomes ineffective.

Cementitious mortars provide only temporary protection for earth structures; above all, in medium to long term they have the potentially to be destructive. Their physical and chemical properties do not allow them to adhere to the earth materials; furthermore and they aggravate problems with moisture. Despite all these indications the use cement mortars in repairs is still a common practice; it is also possible to found indications of using cementitious coatings in earthen structures in two standards (SAZS 724 2001 and New Mexico Code 2006).

5 Conclusions

The durability of the earth when used as construction material must be ensured to guarantee its acceptance for contemporary constructions and be recognized as effective in existing buildings. However, this is also one of the areas in building construction that have major gaps in knowledge. It is important to assure not only the durability of repair mortars to make interventions with longer life cycles, but also their compatibility with the support, since the first premise cannot put in question the second.

Mortars behaved differently when applied on different rammed earth supports. Supports with higher percentages of clay are more prone to cracking the stabilized mortar, even with low percentage of binder; clay particles have higher water absorption than the sand particles; water present in the fresh mortar is thus more easily absorbed by the clay present in the support, which accelerates the drying process of the mortar and contributes to increased cracking thereof.

Supports with lower percentages of clay, in general, present more tendencies for detachment of stabilized mortars; this fact is probably due to the lower adherence provided by this type of rammed earth, which is sandier.

The best performance occurred with the mortars composed of unstabilized earth identical to the rammed earth substrate. An application of protective render or plaster can be used to reinstate the wall thickness and repair and micro and medium cracks when they appear.

The incorporation of low amounts of the non earth binders, used as stabilisers, systematically worsened the behavior of the repair mortars, regardless of the type of binder. This indicates that in practice, it will be more appropriate to repair unstabilized rammed earth walls by means of unstabilized mortars, preferably based on

earth similar to that of the wall itself. This also has additional conservation benefits as it enables the repair of the structure on a like for like materials basis.

The success of a repair mortar application is strongly influenced by the support where it is applied. The use of low amount of mineral binders as stabilizers in repair mortars has not proven beneficial, since systematically led to a worse performance in terms of cracking or detachment of the mortars, regardless the type of binder used. Thus in practice it seems that for unstabilized rammed earth walls repair is more appropriate to use unstabilized earth mortars, preferably based on the same earth of the substrate.

Acknowledgements M. I. Gomes was supported by a doctoral grant from the Fundação para a Ciência e a Tecnologia (FCT). This work was carried out at the National Laboratory for Civil Engineering (LNEC), in Lisbon. The authors are grateful to the people who collaborated in the experimental work, in particular LNEC technicians José Costa, João Junior, Luis Nunes, and Bento Sabala. We wish to thank the following companies for their aid: Sorgila company, Lusical and Secil, Georg Hilbert and Aubiose.

References

Angulo-Ibáñez, Q., Mas-Tomás, Á., Galvañ-LLopis, V., & Sántolaria-Montesinos, J. L. (2012). Traditional braces of earth constructions. *Construction and Building Materials, 30,* 389–399.

Ashurst, J., & Ashurst, N. (1995). *Practical building conservation: Brick, terracotta & earth* (Vol. 2). Hampshire, England: English Heritage Technical Handbook. Gower technical press.

Boussalh, M., Jlok, M., Guillaud, H., & Moiset, S. (2004). Manuel de conservation du patrimoine architectural en terre des vallés présahariennes du Maroc. Noûs. CERKAS-Centre du Patrimoine Mondial de l'UNESCO-CRATerre—Centre de Recherché et d´Application.

EN 196-1, (2005). Methods of testing the cement—Part 1: Determination of mechanical strength. Brussels: CEN—European Committee for Standardization.

EN 1015-3. (1999). Methods of test for mortar for masonry. Part 3: Determination of consistence of fresh mortar (by flow table). Brussels\ A1: 2004\ A2: 2006: Brussels: CEN—European Committee for Standardization.

Faria, P. (2005). Rendering of earth walls. In *Earth Architecture in Portugal*. 1st Edição. Lisboa, Argumentum. 68–73.

Gomes, M. I., & Faria, P. (2011). Repair mortars for rammed earth constructions. In V. P. Freitas, H. Corvacho, & Lacasse (Eds.), *Proceedings of the 12th International Conference on Durability of Building Materials and Components* (Vol. 2, pp. 689–696). Faculdade de Engenharia da Universidade do Porto, Portugal, 12–15 April.

Gomes, M. I., Gonçalves, T. D., & Faria, P. (2012a). Análise experimental de argamassas de terra com cais e fibras naturais. *Proceedings of the 4th Congresso Português de argamassas e ETICS - APFAC*. Coimbra, Cd Proceddings.

Gomes, M. I., Gonçalves, T. D., & Faria, P. (2012b). Earth-based repair mortars : Experimental analysis with different binders and natural fibers. In C. Mileto, F. Vegas, & V. Cristini (Eds.), *Proceedings of the 1st International Conference on Rammed Earth Conservation* (pp. 21–23). Valencia, Spain.

Gomes, M. I., Gonçalves, T. D., & Faria, P. (2012c). Evaluación de la influencia del contenido de agua en la trabajabilidad del mortero de tierra. *APUNTES, 25*(2), 8–27.

Gomes, M. I., Gonçalves, T. D., & Faria, P. (2012d). Unstabilised rammed earth: characterization of the material collected from old constructions in south Portugal and comparison to normative

requirements. *International Journal of Architectural Heritage, Taylor & Francis, 8*(2), 185–212.
Guelberth, C. R., & Chiras, D. (2003). *The natural plaster book: Earth, lime and gypsum renders for natural homes*. Gabriola Island, Canada: New Society Publishers.
Hamard, E., Morel, J.-C., Salgado, F., Marcom, A., & Meunier, N. (2013). A procedure to assess the suitability of plaster to protect vernacular earthen architecture. *Journal of Cultural Heritage, 14*(2), 109–115.
Houben, H., & Guillaud, H., (2006). Earth construction: A comprehensive guide Technology. London: Technology Intermediate Publications (1st edition 1994), ITDG Publishing.
Houben, H., & Guillaud, H. (1996). Earthen architecture: Materials, techniques and knowledge at the service of new architectural applications. The Courier. No. 159, Dossier Investing in People Country Reports: Mali.
Jiménez Delgado, M. C., & Guerrero, I. C. (2006). Earth building in Spain. *Construction and Building Materials, 20*(9), 679–690.
Keable, J. (1996). *Rammed earth structure: A code of pratice*. London: Intermediate Technology Publications Ltd.
Le Tiec, J.-M., & Paccoud, G. (2006). Pisé H_2O. De l'eau et des grains pour un renouveau du pisé en Rhône-Alpes (CRATerre.). Villefontaine, France.
Maniatidis, V., & Walker, P., (2003). A Review of Rammed Earth Construction. Review Literature and Arts of the Americas DTi Partne (May).
McHenry, P. (1984). *Adobe and rammed earth buildings: Design and construction*. Arizona: The university of Arizona Press. Wiley-Interscience.
Miccoli, L., Müller, U., & Fontana, P. (2014). Mechanical behaviour of earthen materials: A comparison between earth block masonry, rammed earth and cob. *Construction and Building Materials, 61,* 327–339.
Morton, T. (2004). Earth structures, renders and plasters: Experiments in historical techniques and weathering. In Dachverband Lehm e.V. (Eds.), *4th International Conference on Building with Earth, LEHM* (pp. 272–275). Weimar, Germany, 29–30 October 2004. ISBN: 3000148647.
New Mexico Code. (2006). New México Earthen Building Materials Code 14.7.4, New Mexico: Santa Fé, NM: Construction Industries Division (CID) of the Regulation and Licensing Department. Available at: http://www.nmcpr.state.nm.us/nmac/parts/title14/14.007.004.htm.
Norton, J. (1997). *Building with earth* (2nd ed.). Warwickshire: Pratical Action.
SAZS 724. (2001). Standards Association Zimbabwe. Standard Code of Practice for Rammed Earth Structures, Harare: Standards Association of Zimbabwe.
SNZ, 4298. (1998). Materials and workmanship for earth buildings. Standards New Zealand. New Zealand.
Toumbakari, E.-E., Ntziouni, A., & Rigopoulou, V. K. (2010). Cement-stabilized earth mortars for application in archaeological sites and prehistoric momuments. In J. Válek, C. Groot, & J. J. Hughes, (Eds.), *2nd Historic Mortars Conference and RILEM TC 203-RHM Final Workshop* (pp. 1209–1217). Prague, Czech Republic, 22–24 September: RILEM Publications SARL.
Veiga, R. (1998). *Behavior of mortar coating walls. Contribution to the study of its resistance to cracking (in Portuguese).* Ph.D. thesis, Faculty of Engineering of University of Porto.
Walker, P., Keable, R., Martin, J., & Maniatidis, V. (2005). *Rammed earth: Design and construction guidelines*. Watford: BRE Bookshop. ISBN 1 86081 734 3, 146.
Walker, P., & Australia, S. (2001). *HB 195: The Australian earth building handbook*. Sydney, Australia: Standards Australia International Ltd. ISBN. 0733740006, 151.
Warren, J. (1999). *Conservation of earth structures*. British Library: Butterworth Heinemann.
WCED. (1987). *Report of the World Commission on environment and development*: *Our common future*, 83.

Heat and Moisture Simulations of Repair Mortars: Benchmark Experiments and Practical Cases in Conservation

Roel Hendrickx and Hilde De Clercq

Abstract Simulation tools are increasingly used for assessment and design of buildings, for new construction as well as for historical buildings. HAM (heat, air and moisture) simulations of porous materials can be very useful to assess the behaviour of repair mortars because hygrothermal conditions govern many decay mechanisms and are one of the keys to compatibility. This paper demonstrates some of the possibilities for mortars in a number of practical cases, using Delphin as a HAM simulation code. The first is a 2D assessment of the hygric interaction between mortar and brick. Next there are a series of 1D simulations of multi-layered porous systems. Pragmatic methods to obtain the necessary material parameters are proposed. Issues like local alterations of transport properties and interface resistances are briefly discussed. The possibilities of simulations of the behaviour of salt solutions are introduced. In a last case, a procedure to assess the risk on frost damage is demonstrated. Finally some possible or desirable future developments are pointed out: incorporating climate change, combining HAM with other simulation methods and stochastic treatment of material parameters.

Keywords Repair mortar · Simulations · HAM

1 Introduction

Although simulations to assess energy efficiency, stability, acoustical comfort, etc., of newly built constructions are common practice, their use in the field of conservation of architectural heritage is far from being systematic. Nevertheless some

R. Hendrickx (✉) · H. De Clercq
Royal Institute for Cultural Heritage KIK-IRPA, Brussels, Belgium
e-mail: roel_hendrickx@yahoo.com

Present Address:
R. Hendrickx
Steenweg op Antwerpen 27 bus 4, 2300 Turnhout, Belgium

J. J. Hughes et al. (eds.), *Historic Mortars*,
https://doi.org/10.1007/978-3-319-91606-4_23

experience has been gained in the past decade at universities and research institutions.

Simulation codes used in building design and assessment can generally be divided into 3 categories:

1. lumped models, which are based on equilibrium equations of nodes. These nodes can represent interior parts of a building such as rooms or zones, or the exterior (Hagentoft 2001). Several properties can be ascribed to nodes, such as a capacity, and their temperature and moisture content is variable. In analogy to electrical circuits, nodes are connected to each other with a certain resistance. Lumped models are often used to estimate the exchange of energy between building parts and the external environment and are useful to simulate energy efficiency aspects. EnergyPlus and TRNSYS are widespread software packages, known as Building Energy Simulation (BES) tools, but they don't cover moisture transport.
2. Computational Fluid Dynamics (CFD) models enable to calculate the flow of a liquid or a gas in a confined space within certain boundary conditions. It is especially useful to assess air movement in large spaces, which has an important influence on heat and vapour transfer, user comfort, etc. ANSYS Fluent is the most widespread software package.
3. Heat, Air and Moisture (HAM) models are capable to calculate transport phenomena in porous materials, ranging from very open insulation materials to impermeable layers. Mathematically they can be subdivided in two classes according the strategic approach applied to solve problems: using the Finite Elements Method (FEM) or the Finite Volume Method (FVM). Unlike the lumped models, a material is represented spatially by a mesh of cells in 1D, 2D or 3D, which should be sufficiently precise.

HAM tools are particularly interesting to study degradation phenomena of historical mortars and porous materials in general, because they make a link to some important weathering causes or mechanisms of degradation, e.g. frost action, mould growth, hygrothermal cycling, etc.

This article illustrates and discusses a number of possibilities, which have been explored in consultancy projects. An introduction into the physical principles behind the simulations can be found in some essential handbooks (Hagentoft 2001; Hall and Hoff 2002; Hens 2012).

2 Different HAM(S) Codes and Their Possibilities

The available HAM codes differ strongly in user-friendliness, possibilities and flexibility. Giving a full overview is beyond the scope of this paper, but we can briefly discuss 3 of them, which are currently used: Delphin, HAMFEM and WUFI. Apart from these 3, it is also possible to use open source packages stemming from

soil hydrology, e.g. Hydrus, which is available for free in the 1D version (Šimunek et al. 2008). However, when considering typical phenomena for buildings, such as wind-driven rain on vertical elements and radiative heat exchange with the surroundings in the short wave (sun) and long wave (IR) range, such open access tools generally have limited possibilities.

Delphin has been developed at TU Dresden (with extensions from Syracuse University). Most of the results mentioned below, were obtained using this software. It allows HAM calculations (in 1D, 2D and axisymmetric 3D cases), as well as pollutant dispersion and to a certain extent also salt transport (Nicolai 2007). The possibilities to characterise materials are very complete, including curves for water retention, liquid and vapour permeability, moisture-dependent heat conductivity, etc. A graphical interface can be used to produce input files and a post-processor to treat the data (graphically) is available. Climate files with hourly data for a number of German cities are included as well as a database with many parameter sets of building materials.

HAMFEM was developed at KU Leuven (Belgium) and is mainly intended for academic research purposes (Janssen et al. 2007). No graphic interface or a manual are provided. HAMFEM is not commercialised, but it is available on request, however without structural support. Hence it requires considerable skills from the user. The possibilities are comparable to those of Delphin, however excluding salt transport or pollutant dispersion. Contrary to Delphin, HAMFEM allows 3D calculations (in an orthogonal grid). There is a limited library with material parameters.

WUFI, developed at the Fraunhofer Institute, Germany, is a more user-friendly package, but more limited in simulation possibilities. It has an extensive graphical interface, simple input menus and an extensive database of materials parameters and climatic conditions from all over the globe. There are however important restrictions in the material parameters: liquid transport is calculated as a diffusion phenomenon using an approximate logarithmic diffusion coefficient (Krus 1996). Although this method simplifies the calculations, the accuracy is evidently less. The liquid water conductivity is the critical material parameter for adequate simulations, for mortars as well as for other porous media, and there are several possible approaches. WUFI calculation results are not included in this paper. Nonetheless, the merits and possibilities of this package for a non-expert user-group are considerable and it probably allows to assess many practical cases, at least on a comparative basis.

3 Obtaining Accurate Material Parameters

3.1 Defining a Minimal Set of Necessary Parameters

The two basic properties needed to simulate moisture transport are: (1) the capacity of a material to hold or retain moisture and (2) the property of a material to allow for liquid water and vapour to flow through it. The first property is most completely expressed by a water retention curve, which contains the capillary suction which a porous material exerts as a function of its liquid content. In normal conditions mortar, stone and brick are hydrophilic and they tend to absorb water into their pores. The smaller the pores and the dryer the material, the higher the suction it exerts on water. The maximum of the curve is either the total porosity accessible to water or the capillary saturated porosity. The capillary saturated porosity (or more briefly "capillary porosity") is the fraction of pores which is filled in the first relatively rapid phase of absorption in a typical 1D free absorption experiment (Figs. 1 and 2).

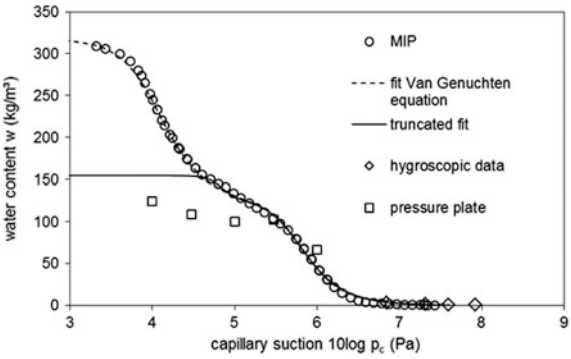

Fig. 1 Water retention curve of Savonnières limestone. The dotted curve has the total accessible porosity as maximum; the truncated curve is limited to the capillary porosity; p_c is capillary suction

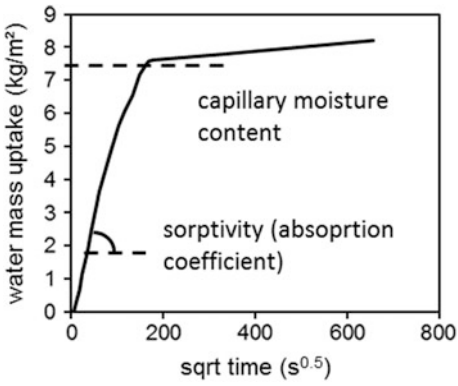

Fig. 2 Example of an absorption curve of a bedding mortar of the veterinary school of Anderlecht

Mortars and stones with an important portion of very small pores—especially below 0.1 μm—have hygroscopic properties: they adsorb water molecules from the vapour in the air. It is known that cementitious mortars, pozzolanic mortars and special types of repair mortar like zinc oxide mortars, have an important amount of nano-pores (<100 nm). The amount of moisture taken up by a mortar under influence of relative humidity, can be expressed in a "sorption isotherm" or "hygroscopic uptake curve" (water content as a function of relative humidity). Like in liquid water uptake, a strong effect of hysteresis may be observed in hygroscopicity. This is usually not taken into account in HAM simulations. However the phenomenon on itself should be taken into account, and this can be done by including measured points into the moisture retention curve, as is demonstrated with the 4 hygroscopice data points at the right end of the graph presented in Fig. 1. In this case, the horizontal axis is converted from relative humidity (RH) to capillary suction, using Kelvin's law: $p_c = -R_v T\rho_w \ln(RH)$ with R_v the gas constant of water vapour and ρ_w the density of liquid water.

The permeability of mortars varies strongly with moisture content as well. When a mortar is fully saturated, the permeability is a constant (K_{sat}) and the flow can be described by Darcy's law. However in the situation of a real building a mortar is almost never saturated and the permeability is much lower, often several orders of magnitude, and can be expressed as $K(w)$ or $K(\theta)$ with w the moisture mass density in the mortar (kg/m^3) or θ the volumetric moisture fraction (m^3/m^3), depending on the type of expression.

Apart from these two parameters, which govern liquid transport, it is important to know the permeability for water vapour, especially if we want to simulate drying behaviour. It can be expressed as a vapour resistance number μ, which decreases when a mortar is moist. Thermal characteristics like conductivity and heat capacity are of course also important, but in practical cases it is sufficiently accurate to use literature data, based on the nature of the mortar and its density.

3.2 *Obtaining the Right Sample Specimens in Practical Situations: Size Matters*

There are 3 options for obtaining the absorption and drying data of which 2 require sampling:

1. drilling cores through part of the wall or the whole wall;
2. taking small prisms with a hammer and chisel, or
3. doing in situ Karsten absorption tests without any sampling.

Table 1 illustrates the descending degree of damage to the wall, which unfortunately corresponds to a decrease in quality of the obtained data. There are several reason for this loss of quality. Firstly, small specimens lead to more important side effects, which may in turn lead to overestimating or underestimating the sorptivity

Table 1 Criteria for sampling or on-site testing for the determination of absorption (and drying) properties

	core drilling	prisms	Karsten
damage to wall			
quality of data			
value of wall			

(see some comments in (Hall and Hoff 2002)). Secondly, irregular shapes of the small specimens lead to practical difficulties in measuring the correct dimensions and variations of the cross section over the height. An finally, large inclusions (e.g. lime lumps) and heterogeneity of the mortar lead to large scatter of the results.

This means that the optimum method of sampling is case-specific: it should be based on the historical and artistic value of the building and on practical considerations. In the case of listed monuments, there is always communication with the heritage authorities prior to sampling.

Although a number of standards are available for absorption tests, most of them cannot be followed rigorously when the specimens taken from a historical building are small and irregular (CEN 2009). The resulting absorption curve yields the sorptivity of the materials and moisture content corresponding to capillary saturation (Fig. 2). The drying test, which can be executed right after the absorption test when the capillary moisture content is reached, yields an initial drying rate and a critical moisture content, at which the first rapid and linear drying phase ends (Fig. 3).

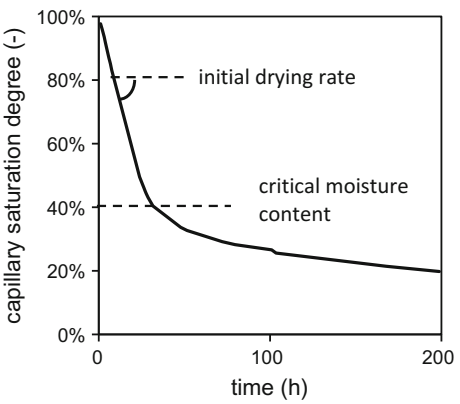

Fig. 3 Example of a drying curve, indicating the initial drying rate and critical moisture content

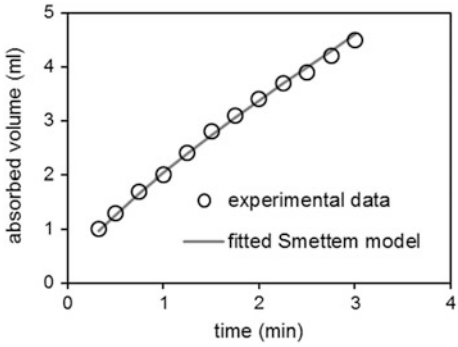

Fig. 4 Fit of experimental data of a Karsten test, to a model for a soil disk infiltrometer by Smettem. Measurement taken on a brick at the cathedral of Antwerp

Vapour permeability (or the vapour resistance number) can be measured in dry cup or wet cup tests (CEN 2001). It is however a parameter of much less importance than liquid permeability, because most of the drying of mortars occurs at the surface. Moreover, it is possible to make a reasonable estimation when the nature of the mortar is known, based on literature data. In previous projects, we found values for the vapour resistance number (μ) up to 40 for cement mortars and about 13 for an NHL mortar or a lime-pozzolan mortar (values obtained for 1:3 binder: sand ratio mortars).

As Table 1 clarifies, the Karsten tube test is the only non-destructive manner to measure the liquid transport parameters. In its original form however, the test only yields a comparative value (Δ_{5-15}) which has no direct physical meaning (RILEM TC25-PEM 1980). Recent investigations have demonstrated that it is possible to calculate the sorptivity from the data if some extra measurements are taken and if the results are fitted to an existing analytical model developed for a soil disk infiltrometer (Hendrickx 2012) (Fig. 4). The procedure has been validated with simulations (Fig. 5) and a series of experimental results. One of the peculiarities of the method is that the capillary moisture content has to be calculated from the diameter of a visible wetted zone, or estimated.

Apart from the major advantage of being non-destructive, quick and easy, the Karsten test has some important drawbacks: there are no direct data about drying and mortar joints are much more difficult to measure than bricks, because of their limited size. The diameter of the effective contact zone with the tube is usually between 20 and 22 mm, which is larger than an average joint. This means that raw data are always contaminated by effects of the surrounding brick(s).

3.3 The Water Retention Curve Calculated from the MIP Results

Strictly speaking, the water retention curve, i.e. the equilibrium water content as a function of the capillary suction, depends on the history: the moisture content is

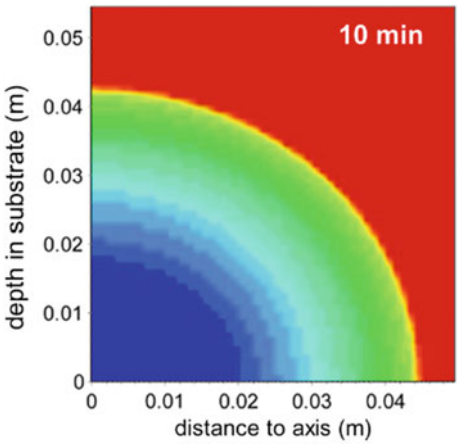

Fig. 5 Axial section of a 3D simulation of water uptake in a brick during a Karsten test after 10 min of contact. The colour indicates the moisture content from zero (red) to saturation (blue) (Color figure online)

usually lower in the wetting stage than in the drying stage. Moreover the maximum depends on whether or not there is an external pressure applied or if there is a vacuum in the pores. The most reliable method to determine a drying water retention curve is by using a pressure plate. But in many practical cases, it is possible to obtain sufficient correspondence to experimental data with one curve, which is calculated from the pore size distribution (PSD), e.g. using the procedures laid out in (Roels 2000). The PSD can be obtained using mercury intrusion porosimetry (MIP). The procedure relies on the law of Young-Laplace, which relates capillary suction to a pore size, assuming perfect wetting behaviour (i.e. a contact angle of 0°) between water, air and the pore wall.

Figure 1 illustrates how the MIP data are used to construct a water retention curve, in this case a fitted equation of a shape suggested in (Van Genuchten 1980). MIP data have the total porosity as a maximum, whereas the practical maximum is rather the capillary moisture content. Hence, the curve is simply truncated, meaning physically that the largest pores (in this case >8 μm) are not supposed to be filled and are not considered. Alternatively, a scaling of the whole curve would have been an option in this case, possibly resulting in a better agreement to the pressure plate results.

3.4 The Permeability Curve Based on the Mualem Model and a Procedure for Calibration

An extensive overview of how to construct a permeability curve, is given in (Scheffler and Plagge 2010). One of the least complicated methods for a mortar or stone is to use the data of the PSD and to assume that the pores consist of a bundle of tubes with circular section, having a certain tortuosity τ. Due to frictional effects

small size tubes have higher resistance to flow than large ones. A straightforward model (Eq. 1.1) is the one by Mualem, as mentioned in (Van Genuchten 1980).

$$K_{rel}(\theta) = \theta^{\tau}\left(\frac{\int_0^{\theta} 1/p_c(\theta)d\theta}{\int_0^{\theta_{sat}} 1/p_c(\theta)d\theta}\right)^2 \tag{1.1}$$

The tortuosity τ can be taken equal to ½, by default for soils, but it is larger for mortar, stone and brick: values between 1.5 and 4 are stated in (Poupeleer 2007). A first approximation can be based on a relation between porosity Ψ, vapour resistance number μ and τ: $\tau = \Psi\ \mu$. An example of a permeability curve obtained using this formula for a brick is plotted in Fig. 6 together with a curve which has been obtained experimentally and which has been calibrated. The latter was based on a diffusivity method as proposed in (Carmeliet et al. 2004).

The second necessary step is a calibration of the obtained permeability curve. The deviations in the near saturated zone in Fig. 6 may seem small on a logarithmic scale, but they can lead to large errors. The pragmatic approach which has been adopted in a number of simulations carried out at KIK-IRPA consists of an iterative optimisation using two simulations:

1. a simulation of the absorption experiment, used to adjust the permeability at capillary saturation. A higher saturated permeability leads to faster absorption and higher sorptivity.
2. a simulation of the drying experiment, used to adjust the shape of the relative permeability. The critical moisture content during drying depends on how permeable the material is when it is not any longer saturated. This means that the non-saturated part of the curve (e.g. the left part in Fig. 8) can be shifted upward to fit with a higher measured critical moisture content or vice versa.

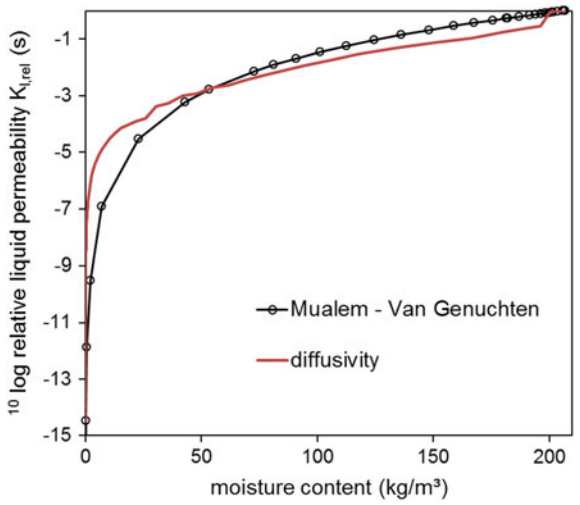

Fig. 6 Relative permeability curves for a ceramic brick, obtained with 2 methods

4 Simulations of a Benchmark Experiment

Wetting and drying behaviour of a brick-mortar or a brick-stone system is highly relevant for the assessment of repair mortars. In order to simulate this, a 2D model is necessary if one wants to account for the depth in the wall and the differences of the 2 materials. This case was worked out as a benchmark simulation using parameters of a brick, a lime mortar and a cement mortar which are representative for Belgian monuments. In Fig. 7 the simulation results of absorption and subsequent drying are shown for a situation where both materials are first wetted during 2 min and then allowed to dry at normal atmospheric conditions during 2 h. This is representative for a short but intense rain shower with heavy wind followed by a 2 h of drying.

5 Surface Alteration, Contact Resistance and Cracks

5.1 Natural Surface Alteration

When simulating the wetting and drying behaviour of masonry, one should consider the fact that the outer millimeter(s) of an aged façade might behave differently than the bulk of the material. Bricks do not actually have a "skin" when produced, but they do develop a less permeable outer layer (Van Hunen 2012). This layer is sometimes referred to as a patina, and may be rich in dust, soot and deposits of water-soluble components like gypsum. Groot measured the drastic decrease of absorption of the brick surface upon ageing by removing a brick from the wall and measuring the absorption from both sides. The decrease of absorption was found to be up to 50% for 19th century buildings and up to 70% for 18th century buildings (Groot and Gunneweg 2005). Like limestone and sandstone, mortars may also

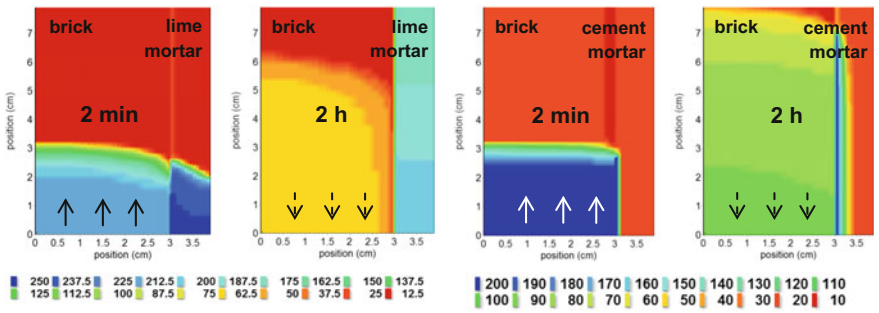

Fig. 7 Simulation results for absorption and subsequent drying through the bottom face of a brick—lime mortar system (left) and a brick—cement mortar system (right). The brick has a thickness of 3 cm, the mortar 1 cm; the y-axis represents the depth in the wall. The colour code indicates moisture content expressed in kg/m^3

develop gradients in composition near the surface, due to leaching of constituents and the formation of other compounds, e.g. the development of a gypsum crust.

When measurements of the non-aged and the altered behaviour are available, the properties of a surface layer can be modelled either by adding a "true" contact resistance (with no thickness) or by changing the properties of the material over a limited depth, e.g. 1 or 2 mm. The first option can also be implemented as a drop in capillary suction, as proposed in a physical model by (Hall and Hoff 2002). In a HAM code like Delphin, a hydraulic resistance or vapour resistance can be added on one side of a volume element in the grid. When the choice is made to adapt the properties of a thin layer, a reduction of the permeability is feasible.

5.2 Alterations in Substrates Due to the Action of Chemical Agents

Water-repellent agents tend to leave the pore size distribution more or less unchanged: their effect is a strong increase of the contact angle from almost 0° (hydrophilic) to values of at least 100° (hydrophobic). This changes both the water capacity and the permeability of building materials (Van Hees et al. 1998). In a recent investigation, Derluyn simulated the behaviour of a 3 mm thick water-repellent layer by drastically reducing the water capacity (Derluyn 2012). In an ongoing experimental programme, we found that the absorption of mortars prepared with water-repellent admixtures is very low, but never zero. Such mortars can be measured and modelled successfully, although the measurements may take a long time. It was also found that the vapour resistance is not necessarily high. This point is often mentioned by producers as a positive argument.

5.3 Contact Resistances at Interfaces and Internal Cracks

The physical presence of contact resistances between two materials has been demonstrated by many authors. They can be due to the discontinuity of the pore system, or to imperfect contact. A review is given in (Hall and Hoff 2002), who also cite a simple experiment by Freitas where a stack of brick slices is found to absorb much more slowly than a single piece of brick. The specific case of the contact resistance between a mortar and a brick is discussed in (Derluyn et al. 2011). They found substantial interface resistances depending on whether or not the brick was prewetted: higher for the case with a dry brick (2.5E10 m/s) than for the case of a pre-wetted brick (1.25E10 m/s). This indicates the importance of early liquid transport between mortar and joint.

Several authors have investigated influences of the liquid transport from mortar to brick in the fresh state of the mortar. No significant contact resistance was

noticed, because the liquid phase is a continuous phase in that stage (Hendrickx et al. 2010). Simulations (using HAMFEM) without any contact resistance during the 1st 2 h of contact could be validated experimentally. It can be assumed that the interface resistance between mortar and brick is formed during hardening, when hydration products are formed and the pore structure of the mortar changes. The same goes for the interface between a bedding mortar and a repointing mortar (Van Hees et al. 2002).

6 Simulations Including the Action of Salts

6.1 Principles

There is an important interest to include salt transport and phase changes into HAM simulations, but the complications are very considerable and to our knowledge none of the existing codes deals with the full complexity. Nicolai developed an extensive framework within the Delphin code, which has been used since some time but hasn't been validated experimentally (Nicolai 2007). The changing factors which affect liquid and moisture transport are:

- increased viscosity and density of the solution with respect to pure water, which lead to a scaling of the permeability;
- heat sources and pits due to enthalpy of crystallisation and dissolution;
- decreased relative humidity in the pore system due to the presence of salts;
- change in water retention due to a changed surface tension and maybe also contact angle;
- increased osmotic pressures, which tend to draw water towards zones with higher salt concentrations;
- decreased effective permeability in zones where salt crystals clog the pores.

Most of these factors are taken into account in Delphin release 5.6.8, which we have used for a series of simulations. There has been some debate about the importance of osmotic pressure in desalination processes: indeed a porous material which contains a saline solution with a molal concentration of 5 mol NaCl per kg of water, exerts an osmotic suction on pure water of about 3E7 Pa, which is of the same order of magnitude as the capillary suction of sub-micron pores (Voronina and Pel 2013). It depends on the equilibrium $RH_{eq,\ salt}$ of the salt solution as:

$$p_{osm} = \frac{RT}{V_w} \ln(RH_{eq,salt}) \tag{1.1}$$

where V_w is the molar volume of water, R the gas constant of water vapour and T temperature.

This is implicitly dealt with in Delphin by the adaptation of relative humidity. The effective relative humidity is defined as: $RH_{eff} = RH_{cap}RH_{eq,salt}$. According to

this equation the relative humidity in the presence of salts is reduced, which leads to an increase of the total suction exerted on the pore liquid. If p_c is the capillary suction in the presence of pure water and p_c' the one in the presence of a salt solution, Kelvin's law allows the following:

$$p_c' = \frac{RT}{V_w} \ln(RH_{cap} RH_{eq,salt}) = p_c + p_{osm} \tag{1.2}$$

6.2 *Example of Salt-Accumulating Renders Simulated with Delphin*

One particular case of a salt-related problem with mortars is the action of salt accumulating renders. Usually these are applied in a layered system, with the aim of forming a drying front in the central layer which has a high porosity and relatively high strength, so that it can accommodate salt crystals without being severely damaged. In an ongoing experimental programme we measured the properties of the separate layers and of the substrate, so that the whole process could also be simulated. The experiment consisted of the absorption of a saline solution from the bottom of the substrate until capillary saturation of the substrate, followed by a drying phase through the top surface during 1 month in dry conditions.

Figure 8 shows the simulated results and the experimental values. The salt concentration was measured with ion chromatography on drilled powders. Except for the early salt crystallisation in the top layer, the simulations are quite accurate. It should be noted that the top layer was cracked and that salts formed in the cracks instead of in the bulk, which explains why they are absent in the experimental measurements in which cracks were excluded.

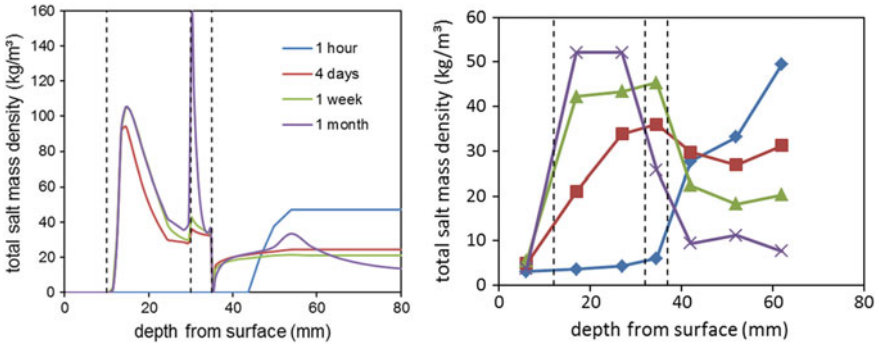

Fig. 8 Simulated (left) and measured (right) salt distribution over a 3-layered salt accumulating render system applied on a brick during a drying experiment

Figure 8 contact resistances and alterations in the substrate were considered. Contact resistances were fixed on 10^5 m/s. The alteration of the substrate consisted of a water-repellent effect in the first 2 cm of the substrate, presumably due to the migration of admixtures when the renders were applied. The existence of this effect came to evidence from the comparison of the absorption data to the normal results of the substrate.

From the results above, it can be concluded that moisture transport in highly complex situations—including salts and very specific mortar types—can be simulated with reasonable success, but they require advanced methods and labourious experimental work. At this stage, more work for validation is essential.

6.3 Other Simulation Codes

In the simulation code of Derluyn, a similar reduction of relative humidity is implemented. As opposed to Delphin, the code uses the FEM-principle, which allows for (small) deformations of the grid (Derluyn 2012). It incorporates stresses in the solid matrix and the formation of cracks within a poromechanical approach. Some empirical functions are incorporated to govern the crystallisation kinetics. Her model was validated by a series of 1D absorption and drying experiments using sodium sulfate and sodium chloride solutions.

Espinosa and co-workers developed a code called AStra, mostly intended to simulate corrosion-enhancing mechanisms in concrete. This includes the transport and phase changes of salt, as well as the mechanism of acid attack (Espinosa et al. 2007).

7 Evaluation of Risk—Frost Damage

Together with salt crystallisation, frost action is one of the most common decay phenomena for mortars. As can be seen in Fig. 7, mortar joints tend to retain a large amount of moisture on the long term, as opposed to bricks, which usually dry faster. When an almost saturated mortar is subjected to freeze-thaw cycles, there is an important risk of damage. In the framework of a renovation and rehabilitation project for the former veterinary school in Anderlecht, the application of internal insulation was considered to improve the energy performance of the building. However, it is known that this decreases the temperature and increases the moisture content of the façade. Several types of simulations were performed to estimate the risk for frost damage. Table 2 shows the simulated liquid moisture distribution results for a continuous mortar joint. The plotted data are results of the 6th year in a long-term simulation, using the same climatic data repeatedly, in order to reach an equilibrium.

Table 2 Simulated moisture distribution over a continuous mortar joint during the 6th year for 2 cases: the original situation (top) with plaster on the inside and pointing mortar on the outside, and the insulated situation (bottom) with a 12 cm calcium silicate board on a glue mortar layer and finished with a vapour-open plaster. The colour code stands for liquid moisture content expressed in vol.%

model	liquid moisture distribution
	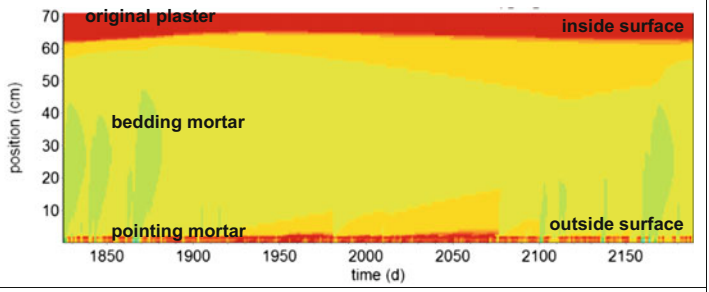
	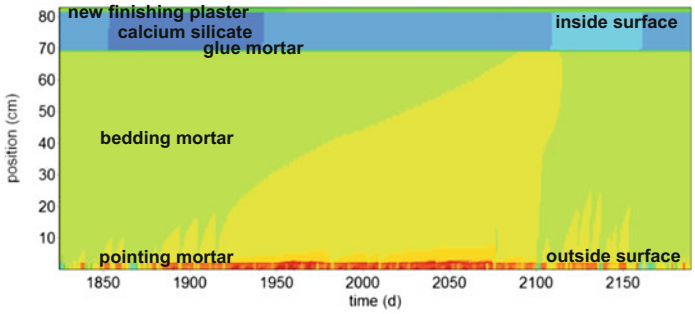
	

The first simulated situation is the actual one, consisting of a bedding mortar over almost the whole thickness, with an original inside plaster (top of the model) and a pointing mortar on the outside (bottom of the model). The second simulation is the insulated case, with a 12 cm calcium silicate board on the inside, applied with a glue mortar and finished with a vapour-open plaster. The increase in moisture content is clearly demonstrated, although it is not very strong in de pointing mortar, which is most exposed to frost.

In a second step, the obtained information of moisture content and temperature were used for a quantitative estimation of the risk for frost damage. For this purpose, we considered a point in the joint mortar at a depth of 3 mm from the outside of the wall and assumed that the number of freeze-thaw cycles which occur at a moment when the moisture content is high, would be the best indicator for risk. An important question is: which degree of moisture saturation is needed to cause damage? In Table 3, three levels of saturation were taken into account as threshold

Table 3 Calculated number of frost-thaw cycles in a mortar joint at 3 mm of depth for 3 different cases of build-up of the wall and for 3 different levels of moisture content

	Cycles	>30% sat	>50% sat	>70% sat
Existing	61	13	4	2
Ensulated with calcium silicate	67	30	9	6
Insulated with porous plaster	65	19	5	3

values: 30, 50 and 70% of capillary saturation. The calculation was done for the existing situation as well as for the strongly insulated case (calcium silicate) and the less insulated case (porous plaster). From the numbers in the table it is clear that the number of cycles increases with the level of insulation and that the number of cycles decreases if we consider a higher threshold of saturation. The conclusion was that the application of the calcium silicate probably aggravates the risk on frost damage substantially, while the increase expected for an insulating plaster is minimal (Table 3).

8 Synthesis and Future Developments

HAM simulations are a versatile tool to analyse the decay of historical mortars and masonry in general. Of all available simulation tools for building industry, they most closely reflect the factors that influence the most common damage mechanisms. Considering the complexity of the process, the best option is to choose for high-end codes which were developed for research purposes at universities (Delphin, HAMFEM). On the other hand, more simplified commercial codes can probably also lead to interesting comparative results (WUFI). The advantage of the codes which are mentioned are that they have built-in modules to assign realistic climate data as boundary conditions.

A series of practical cases were briefly demonstrated: the 2D interaction between mortar and brick, the transport of liquid over interfaces, a case with salt solutions and an assessment of risk for frost damage. Some of these cases could be experimentally validated, others are more academic or reflect future situations.

Most future scenarios for the climate in Western Europe in the 21st century predict an increase in temperature and an increase in hot extremes, heat waves and heavy rain events. In general precipitation is expected to decrease in summer and to increase in winter (IPCC 2007). HAM simulations can be used easily to assess the influence of these changes, by adapting the climate data in the software. For the case of Belgium, relevant results for the near future can be obtained by using the recorded climate data of 2009, which was a warm year, with a rather dry summer.

Another useful development is the combination of lumped models with HAM. This will be especially useful when the inside climate is essential, e.g. when a church will be heated and the response of the walls is critical, e.g. when salts are

present. Several research groups are working on possibilities to integrate them or to use an external coupling (Cóstola et al. 2009).

Another very important issue, which was left out of this paper, is the large variation of material parameters, such as water retention and permeability. Because this variation can lead to very different results depending on the input, each simulation result should actually be a stochastic quantity with some probability density function. In order to evaluate this, an ongoing research project in the framework of the IEA ECBCS Annex 55 is working on procedures to use batches of input files (based on Monte Carlo data) to generate such results (Van Gelder et al. 2012; Janssen 2013). Although the computational effort is considerable, this approach is very promising and will probably gain in importance.

Acknowledgements Andreas Nicolai is kindly acknowledged for his support concerning Delphin simulations. Hans Janssen, Rosa Espinosa and Liesje Van Gelder provided useful information about their work.

References

Carmeliet, J., Adan, O., Brocken, H., Černý, R., Hall, C., Hens, H., K. Kumaran, M., Pavlik, Z., Pel, L., Plagge, R., & Roels, S. (2004). Determination of the liquid water diffusivity from transient moisture transfer experiments. *Journal of Thermal Envelope and Building Science, 27*. https://doi.org/10.1177/1097196304042324.

CEN. (2001). *EN-ISO 12572: 2001 (en): Hygrothermal performance of building materials and products—Determination of water vapour transmission properties*.

CEN. (2009). *EN 15801: 2009 Conservation of cultural property—Test methods—Determination of water absorption by capillarity*. Brussels: CEN.

Cóstola, D., Blocken, B., & Hensen, J. (2009). External coupling between BES and HAM programs for whole-building simulation. *Eleventh International IBPSA Conference, Glasgow*, (pp. 316–323). July 27–30, 2009.

Derluyn, H. (2012). *Salt transport and crystallization in porous limestone: Neutron—X-ray imaging and poromechanical modelling* (Ph.D. thesis). ETH Zürich.

Derluyn, H., Janssen, H., & Carmeliet, J. (2011). Influence of the nature of interfaces on the capillary transport in layered materials. *Construction and Building Materials, 25*(9), 3685–3693.

Espinosa, R., Franke, L., Deckelmann, G., & Gunstmann, C. (2007). Gekoppelter Wärme- und Stofftransport einschließlich der Korrosionsprozesse in porösen Baustoffen mit dem Simulationsprogramm AStra. *Bauphysik, 29*(3), 187–193.

Groot, C., & Gunneweg, J. (2005). Totaalonderzoeksproject Aanpak vochtproblematiek massief metselwerk. Deelonderzoek kwaliteitseisen restauratiebaksteen, Delft http://repository.tudelft.nl/search/ir/?q=kwaliteitseisen+restauratiebaksteen&faculty=&department=&type=&year= Publication OR1 of this link (version March 16).

Hagentoft, C.-E. (2001). Introduction to building physics, Lund, ISBN 9144018967 (422p).

Hall, C., & Hoff, W. D. (2002). Water transport in brick, stone and concrete, London: Taylor & Francis, ISBN 0–419-22890-X (318p).

Hendrickx, R. (2012). Using the Karsten tube to estimate water transport parameters of porous building materials—the possibilities of analytical and numerical solutions. *Materials and Structures, 46,* 1309–1320.

Hendrickx, R., Roels, S., & Van Balen, K. (2010). Water transport between mortar and brick : the influence of material parameters. In J. Valek, C. J. W. P. Groot & J. J. Hughes (Eds.), *Historic mortars. Characterisation, assessment and repair RILEM*, ISBN 978-94-007-4634-3, pp. 329–342.

Hens, H. (2012). Building physics. Heat, air and moisture. Fundamentals and engineering methods with examples and exercises. Berlin: Ernst and Sohn, ISBN 978-3433030271 (330p).

IPCC. (2007). Climate change 2007 : An assessment of the intergovernmental panel on climate change.

Janssen, H. (2013). Monte-Carlo based uncertainty analysis: Sampling efficiency and sampling convergence. *Reliability Engineering and System Safety, 109,* 123–132.

Janssen, H., Blocken, B., & Carmeliet, J. (2007). Conservative modelling of the moisture and heat transfer in building components under atmospheric excitation. *International Journal of Heat and Mass Transfer, 50*(5–6), 1128–1140.

Krus, M. (1996). Moisture transport and storage coefficients of porous mineral building materials: Theoretical principles and new test methods, Fraunhofer IRB, Stuttgart, ISBN 3-81674535-0 (106p).

Nicolai, A. (2007). *Modeling and numerical simulation of salt transport and phase transition in unsaturated porous building materials* (Ph.D. thesis). Syracuse University.

Poupeleer, A.-S. (2007). *Transport and crystallization of dissolved salts in cracked porous building materials* (Ph.D. thesis). KULeuven.

RILEM TC25-PEM. (1980). Recommended tests to measure the deterioration of stone and to assess the effectiveness of treatment methods (in french). *Materials and Structures, 13*(75), 175–253.

Roels, S. (2000). *Modelling unsaturated moisture transport in heterogeneous limestone* (Ph.D. thesis). KULeuven.

Scheffler, G., & Plagge, R. (2010). A whole range hygric material model: Modelling liquid and vapour transport properties in porous media. *International Journal of Heat and Mass Transfer, 53*(1–3), 286–296.

Šimůnek, J., Van Genuchten, M. T., & Šejna, M. (2008). Development and Applications of the HYDRUS and STANMOD Software Packages and Related Codes. *Vadose Zone Journal, 7*(2), 587–600.

Van Gelder, L., Janssen, H., & Roels, S. (2012). Retrofitting cavity walls—an example of a Monte Carlo simulation to evaluate risks and energy savings. In *5th International Building Physics Conference*. May 28–31, 2012, Kyoto cd-rom (abstract p. 112).

Van Genuchten, M. T. (1980). A closed-form equation for the prediction of the hydraulic conductivity of unsaturated soils. *Soil Science Society of America Journal, 44*(5), 892–895.

Van Hees, R. J. P. et al. (Eds.) (1998). *Evaluation of the performance of surface treatments for the conservation of historic brick masonr*y (Research Report No 7). European Commission, ISBN 92-828-2366-0.

Van Hees, R. P. J., Pel, L., & Lubelli, B. (2002). Towards compatible repair mortars for masonry in monuments. In E. Galan & F. Zezza (Eds.), *5th International Symposium on the Conservation of Monuments in the Mediterranean Basin—Protection and Conservation of the Cultural Heritage of the Mediterranean Cities*, *Seville, Spain* (pp. 371–375) Lisse: Swets and Zeitlinger (2000).

Van Hunen, M., (2012). Het geveloppervlak van dichtbij bekeken. Eigenschappen en waarde van de huid. In M. Van Hunen, (Ed.), *Historisch metselwerk. Instandhouding, herstel en conservering* (pp. 275–287). Zwolle: W Books.

Voronina, V., & Pel, L. (2013). The influence of osmotic pressure on poulticing treatments for cultural heritage objects. *Materials and Structures, 46,* 221–231.